# University of Southampton

Faculty of Engineering and Physical Science

School of Engineering

**Modelling Water Quality Dynamics with Remote Sensing Images:  Tonle Sap Lake, Cambodia, the Largest Freshwater Lake in South East Asia**

by

Mukarramah Yusuf

Thesis for the degree of Doctor of Philosophy

September 2021

# University of Southampton

## Abstract

Faculty of Engineering and Physical Sciences

School of Engineering

Thesis for the degree of Philosophy

Modelling Water Quality Dynamics with Remote Sensing Images:  Tonle Sap Lake,
Cambodia, the Largest Freshwater Lake in South East Asia

by

Mukarramah Yusuf

Eutrophication is one of the problems the world needs to tackle to achieve one of the targets of the United Nations' Sustainable Development Goal 6: to improve water quality by 2030. Albeit a global problem that has been studied for many years, there is a huge gap in the reporting of eutrophication incidences and associated research work between the Global South and Global North countries. However, the available evidence suggests that nutrient loads and hence eutrophication may be increasing in the Global South. Nevertheless, assessing these trends with confidence can be challenging, especially in the Global South, because long-term (i.e. multi-decadal) water quality monitoring data, which is important for the formulation of science-based environmental policy, is very scarce. The utilisation of freely accessible satellite images to monitor long-term (i.e. multi-decadal) trends in water quality indicators is a potential solution to this challenge, as has already been used by the Great Lakes in North America and UNESCO.

This thesis aims to explore the potential of employing satellite-based methods to evaluate water quality trends in large water bodies in the Global South, using the Tonle Sap Lake, Cambodia, as a case study. The work focuses on retrieving spatial and multi-decadal (1990-2019) temporal trends of two water quality parameters: (i) Total Suspended Sediment (TSS) and (ii) chlorophyll-a (Chl-a) concentration of the Tonle Sap Lake using satellite-based techniques.

Tonle Sap Lake is the largest freshwater lake in South East Asia, whose hydrology is an integral part of the Mekong River, an international river that flows through 6 countries. The lake experiences an unusual flow reversal from and to the Mekong River every six months, supporting a wide range of valuable ecosystem functions.  Specifically, the Tonle Sap Lake and its flow reversal play an important role in the economic, ecological, and socio-cultural life of Cambodia and, indeed, the broader South East Asia region. With the Mekong Basin undergoing rapid development and with the threat posed by ongoing climate change, there is a real concern that alterations of the Tonle Sap's flow regime, changes in annual water level, open water area, and

suspended solid delivery from the Mekong River may adversely impact these critical ecosystem services. However, little is known about the current and recent historical eutrophication status of Tonle Sap Lake, and water quality monitoring efforts are woefully inadequate.

For this study, a field campaign undertaken in February 2019 collected new ground-based measurements of TSS concentrations, chl-a concentrations, and surface reflectances of land covers/water surfaces, which have allowed regression relationships to be developed that link the surface reflectances from Landsat OLI imagery to these critical water quality parameters. These regression relationships were then used to estimate trends in TSS and chl-a during the period 1990-2020 at each of five locations across the lake, these locations representing discrete environments within the lake that may be affected by drivers of change in different ways.

The satellite-based retrievals of TSS and chl-a concentrations were analysed, together with water level data from a gauging station located at Kampong Luong on the shores of the lake, to develop data-driven conceptual models of the response of TSS and chl-a to seasonal and inter-annual variations in the lake hydrology during the study period. These models highlight that TSS concentrations vary in opposite phase with the seasonal water cycle, with maximum values of TSS concentration induced by wind-generated waves resuspending fine-grained sediments from the bed of the lake during the dry season. In contrast, seasonal and inter-annual variations in chl-a have a more complex response, being influenced not only by water levels but likely also by the nutrients associated with suspended sediments. Thus the lowest values of chl-a concentration typically occur during the low water period, while the highest chl-a concentrations occur during the period of high water as the lake begins to flow out towards the Mekong River (October to December).The data-driven conceptual models also highlight variability in the TSS and chl-a concentrations driven by inter-annual variability in the magnitude of the Tonle Sap Lake's annual flood.

Overall, the new conceptual models based on the satellite retrievals cast new light on the seasonal and inter-annual variations in TSS and chl-a, and their inter-relationship, during the last 30 years. An important conclusion of the research presented herein is that, contrary to some studies that have speculated on the risks of deteriorating water quality, the Tonle Sap Lake is in a mesotrophic condition, with little evidence of any statistically significant long-term (i.e. multi-decadal) trend in chl-a concentrations.

# Table of Contents

Table of Contents

# Table of Tables

# Table of Figures

Table of Figures

Table of Figures

# Research Thesis: Declaration of Authorship

Print name: Mukarramah Yusuf

Title of thesis: Modelling Water Quality Dynamics with Remote Sensing Images:  Tonle Sap Lake, Cambodia, the Largest Freshwater Lake in South East Asia

I declare that this thesis and the work presented in it are my own and has been generated by me as the result of my own original research.

I confirm that:

1.  This work was done wholly or mainly while in candidature for a research degree at this University;
2.  Where any part of this thesis has previously been submitted for a degree or any other qualification at this University or any other institution, this has been clearly stated;
3.  Where I have consulted the published work of others, this is always clearly attributed;
4.  Where I have quoted from the work of others, the source is always given. With the exception of such quotations, this thesis is entirely my own work;
5.  I have acknowledged all main sources of help;
6.  Where the thesis is based on work done by myself jointly with others, I have made clear exactly what was done by others and what I have contributed myself;
7.  None of this work has been published before submission

Signature:   ....................................................... Date: 8 September 2021

# Acknowledgements

Firstly, I would like to thank my main supervisor, Prof. Stephen E Darby, for his years of support and guidance during this Ph.D. project. Thank you for the humanity in your attitude.

I also acknowledge remote sensing guidance from Prof. Jadu Dash.

And I will always remember the help from the lab staff of the School of Geography and Yanjie Zhao for their help during the fieldwork in Cambodia.

And thank you to Bee for sharing her knowledge and experience in the remote sensing field.

And lastly, a great thank you to my husband for being alongside me in this constantly going up and down journey.

# Introduction

## 1.1     Water Quality and Eutrophication

Lakes cover less than 4% of the land surface of Earth, but their relatively small area is critical in underpinning a wide range of services on which humans depend: food security, human health, urban and rural settlements, energy production, industrial development, economic growth, and biodiversity (UN Water, 2020b). A critical factor in regulating these services is not just the quantity of water but also its quality. One of the targets of the United Nations in its Sustainable Development Goal 6, is to improve water quality by 2030.

Water quality refers to the physical, chemical, or biological properties of a water body (Omer, 2019). Physical properties of water quality include temperature, turbidity, taste, and odour. Chemical characteristics involve parameters such as pH, nitrogen, dissolved oxygen, and alkalinity. The presence or absence of bacteria and phytoplankton are importantly biological indicators of water quality.

Unfortunately, water quality degradation is occurring on many parts of the planet as a result of pollution. Around the world, about 30% of the global population lack the basic quality water sources needed to meet their sanitation needs, while 60–70% of the global population live in areas with absolute water scarcity or under severe water stress (Macedonio et al., 2012). Water pollution involves the process of contamination by substances that change the physical, chemical, or biological properties of water in ways that eventually lead to a damaging consequence for living organisms. This contamination is often a direct result of human activities (Evans et al., 2019; A. Li et al., 2019; Q. Wang & Yang, 2016).

One particularly detrimental problem that frequently arises from water pollution is the process of eutrophication. Eutrophication occurs when water bodies become enriched with nutrients that trigger harmful cyanobacterial blooms, which, if sufficiently severe, can result in anoxia that leads to the creation of a dead zone in waterbodies. Nutrient sources that typically are associated with this problem include sewage and animal wastes, atmospheric deposition by legumes, as well as runoff from agricultural lands that have been treated with fertilizer (Anderson et al., 2002).

Eutrophication has been studied extensively. For example, a search in Web of Science with the search terms 'lake' and 'cyanobacteria' or 'eutrophication' or 'bloom' from the published literature from 1970 – April 2021 gives some 20,000 results (with an increasing annual trend as seen in Figure 0-1), but there is still a limitation of the global picture about the extent of

eutrophication in freshwater lakes, in part because the extent of eutrophication in developing countries is less well defined (see below). Nevertheless, the extent to which eutrophication is a significant problem around the globe is clear: a two-decade-old survey by the International Lake Environment Committee Foundation between 1988 to 1993 showed that 54%, 53%, 48%, and 41% of lakes are eutrophic in Asia, Europe, North and South America, respectively, with 28% of lakes in Africa also being classified as eutrophic (Chorus & Welker, 2021). There are also concerns that these problems may be further exacerbated by climate change.  Climate change will affect the availability, quality, and quantity of water (UN Water, 2020a). For example, increasing temperatures will likely accelerate evaporation that in turn could lead to a decrease in water availability. Rising temperatures have also been found to boost cyanobacterial blooms in shallow lakes (Kosten et al., 2012).
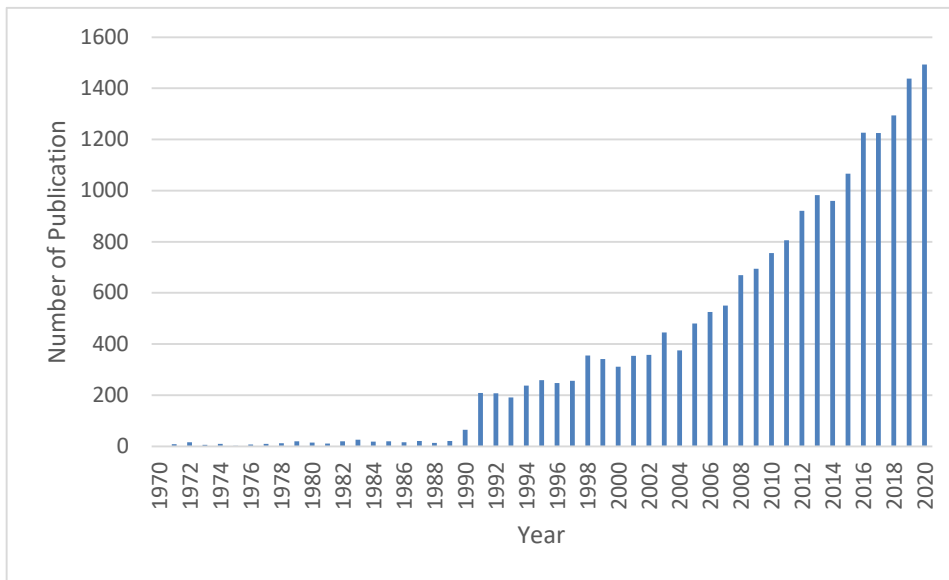


Figure 0-1 Number of recorded publications on 'eutrophication' and 'lake' in Web of Science

Eutrophication in freshwater lakes has typically most frequently been reported in the Global North (half of the above results from Web of Science are from just 32 countries, see also Figure 2-1). In the Global North the problem is well acknowledged, the concentrations of nutrients in streams to the lake are (usually) well regulated, and restoration efforts are often well managed (e.g., Søndergaard *et al.*, 2007; Ferreira *et al.*, 2011; Teubner, Kabas and Teubner, 2018). The knowledge is advanced for temperate lakes which dominate the lakes in these countries, for example, it is well established that phosphorus is the limiting nutrient for most lakes, and that harmful blooms can be predicted using bloom data from the past to prevent harmful events occurring (Tromas et al., 2017).

On the contrary, in the Global South, compared to the number of literature that has reported major episodes of eutrophication in China's lakes, rivers, and coastal zones  (e.g., Le *et al.*, 2010; Li

*et al.*, 2011; Paerl *et al.*, 2011; Wang *et al.*, 2012, 2018, 2019, 2021; Guan *et al.*, 2020), there have been relatively fewer reported incidences of eutrophication and less associated research work. It is unclear whether this reflects a systematic under-reporting of a problem or whether water quality in developing nations has not (yet) been so strongly impacted by human activities as in more developed economies.

In the Global South, water quality monitoring networks and capacity are lacking relative to more economically developed nations, and monitoring data, notably long-term (i.e., multi-decadal) data, is very scarce. However, circumstantial evidence may be used to infer that the potential sources of eutrophication may be increasing in this region.

For example, the UN has reported that only 28% of municipal and industrial wastewater is treated in lower-middle-income countries, compared to about 70% of it in higher-income countries (UN Water, 2017). With rapid development, a growing population that depends on intensified agriculture (UN Water, 2018), and becoming the main exporters of polluting industries such as fashion (Anguelov, 2015; Niinimäki et al., 2020), there is reasonable cause to consider that nutrient pollution is likely to be both prevalent and increasing. Indeed, recent studies show that nations in the Global South together contribute the most to global anthropogenic nitrogen and phosphorus (Mekonnen & Hoekstra, 2018; Uwizeye et al., 2020).

Environmental monitoring provides the basis for the formulation of science-based environmental policy. Further, continued monitoring also allows the evaluation of policies, whether they have had their intended effect and have been cost-effective (Lovett et al., 2007). However, traditional water quality data collection methods are time-consuming, the data produced is occasionally unreliable, and often has gaps both spatially and temporally. These difficulties arise as a result of the specific challenges faced in these regions including access to remote locations and problems of technical and institutional capacity. On top of that, the processes of environmental monitoring are very costly. For example, the US alone spends around 40 billion dollars annually to control water pollution (Fig 1, Keiser, Kling and Shapiro, 2019). In Global South countries, the highest barrier to water quality data monitoring and collection is probably their economic unaffordability, which has been seen as a cause of clean water scarcity (Rijsberman, 2006).

As a potential solution to the economic cost problem, satellite images are now accessible globally at no cost through platforms such as NASA's Landsat archive and the European Union's Copernicus programme. Satellite technology has allowed the indirect estimation of various water quality parameters on a global scale over long periods of time and is now proving useful in coastal waters, estuaries, lakes, and reservoirs, which are relevant to water quality managers (Andres et al., 2018). For example, within the Great Lakes in the USA, which frequently experience

cyanobacterial blooms, a number of operational satellites have been used to estimate physical and biological parameters on a daily to monthly basis (Auer et al., 2014). Recently, UNESCO's International Hydrological Programme (IHP) launched the World Water Quality Portal (http://sdg6-hydrology-tep.eu/) that provides data on five key indicators of the state of water quality: turbidity and sedimentation distribution, chlorophyll-a, Harmful Algal Blooms (HAB), organic absorption and surface temperature. The UN proposed the use of remote sensing to conduct global water quality monitoring while considering its limitations, for example the number of water qualities that are predictable is limited, compared to traditional water quality monitoring. Spatial, spectral and radiometric resolutions currently sometimes limit the precision of the estimated water quality parameters, but future satellite-borne remote sensing platforms are expected to have higher resolution and will therefore expand the opportunities for water quality assessments of inland waters (Water, 2016).

## 1.2     Research Objectives

The overall goal of this research is to explore the potential of employing satellite-based methods to evaluate Water Quality trends in large water bodies in the Global South, using the Tonle Sap Lake, Cambodia, as a case study. This goal will be achieved by evaluating spatial and multi-decadal (1990-2019) temporal trends of two water quality parameters: (i) Total Suspended Sediment (TSS) and (ii) chlorophyll-a (chl-a) concentration of the Tonle Sap Lake, employing satellite-based techniques. The specific objectives are to:

1) Develop a quantitative method for estimating TSS and chlorophyll-a from Landsat satellite images;
2) Estimate the spatial variability of, and temporal trends in, the concentration of Total Suspended Sediment and chlorophyll-a within the Tonle Sap Lake, Cambodia, over the 30-year period from 1990 to 2019;
3) Establish a conceptual model of the environmental controls on spatio-temporal variations in TSS and chlorophyll-a concentration in the Tonle Sap Lake;

The detailed research gaps that these objectives collectively address are elaborated in Chapter 3, whereas Chapter 2 provides a detailed contextual review of water quality trends and their drivers in freshwater lakes.

## 1.3     Thesis Structure

This thesis is structured in the following way. Chapter 2 provides a literature review that firstly outlines the mechanisms and consequences of eutrophication, before subsequently describing the typical sources of water pollutants, focusing on nutrients leaching to water bodies. The chapter then goes on to explore the cycle of nitrogen and phosphorus as key nutrients that trigger eutrophication and phytoplankton blooms, including the vital role of sediment as a nutrient carrier. This is followed by explanations of how chlorophyll-a concentration in water can be used as a surrogate indicator of phytoplankton biomass.

Chapter 3 provides an overview of the case study lake system used in this research. This chapter firstly describes the geographical setting of Tonle Sap Lake, Cambodia, and outlines its unique hydrological system. It follows by highlighting how Tonle Sap Lake plays a hugely significant role in regulating ecosystem services within and beyond Cambodia. The chapter also describes environmental threats to the Tonle Sap Lake, including eutrophication. With its extremely large size and limited in-country technical capacity, remote sensing can potentially provide solutions to the challenge of monitoring water quality in Tonle Sap Lake.

Chapter 4 is a methods chapter that initially provides a discussion of the potential use of remote sensing technology to monitor water quality parameters. It first details existing studies that have employed satellite data to monitor water quality, before evaluating the differences between commonly used satellites and justifying the decision to use Landsat in this research. This chapter subsequently explains the data collection protocols employed in the research for the purpose of calibration and validation. Field sampling and data acquisition sites are detailed, and sampling instrumentations discussed. The procedures for sample preparation and analysis are outlined, and the field data presented. The rest of the chapter elaborates the development and validation of chlorophyll-a and TSS prediction algorithms for the Tonle Sap Lake area, including an explanation of how 5 specific locations of interest within the lake were chosen for focused analysis.

Chapter 5 presents the results of TSS and chlorophyll-a concentration estimation for Tonle Sap lake over a period of 30 years at the five focus study sites. Firstly, an overall picture of spatial and temporal variations is provided. Then the results of Mann Kendall trend analyses, applied to determine whether there have been long-term (i.e., multi-decadal) trends in water quality, are outlined. The chapter also presents an overview of the variations in TSS and chlorophyll-a concentrations over seasonal time scales.

Chapter 6 firstly defines three categories of year experienced in the Tonle Sap Lake: flood, drought, and normal years. Then a conceptual model of TSS and chlorophyll-a dynamics is derived

based on consideration of the satellite-based variations in TSS/chlorophyll-a concentration against changing lake water levels in the flood, drought, and normal years.

Chapter 7 provides a discussion that seeks to synthesise the different components of the thesis together and to identify the potential drivers affecting the trends in TSS and chlorophyll-a concentrations, as identified from the satellite-based analyses, in the Tonle Sap lake. The thesis concludes by summarising the main findings and implications of the research, as well as by identifying directions for possible future research opportunities.

# Chapter 2    Eutrophication Processes and Drivers in Freshwater Lakes

## 2.1  Definition

Aquatic primary producers need nutrients for their life. However, if the concentration of nutrients present in water bodies exceeds the amount required for primary production, eutrophication may occur. Eutrophication is defined as "the enrichment of water by nutrients, especially compounds of nitrogen and phosphorus, causing an accelerated growth of algae and higher forms of plant life to produce an undesirable disturbance to the water balance of organisms present in the water and to the quality of the water concerned" (European Commission, 1991).

Eutrophication would usually happen happen as a natural part of lake succession (Harper, 1992) and, when it does, this type of eutrophication is termed natural eutrophication. In contrast, cultural eutrophication refers to situations in which excess nutrients are sourced from human activities. The process of natural eutrophication takes from a few years for shallow water bodies to millions of years for deep crater lakes created by movements of the Earth's crust (Open Learn, 2016). In comparison, cultural eutrophication typically occurs over much shorter periods of time (Carpenter, 2009) and brings adverse impacts associated with the rapid decline in water quality.

Eutrophication has been studied for many years and is recognised as a worldwide problem. Lakes were the first water bodies where eutrophication effects were observed, mainly because of their use as water resources for drinking water supply (e.g., Dillon and Rigler, 1974). Indeed, eutrophication has most frequently been reported in deep lakes, located in the Northern hemisphere (United States, Canada, and Western Europe) and Australia. However, nowadays, eutrophication occurs not only in lakes but also in rivers (e.g., Stringfellow et al., 2009), water reservoirs (e.g., Smith et al., 2002), and estuaries (e.g., Bricker et al., 1999). Examples of eutrophication may now be found in all regions, including temperate (e.g., Boynton et al., 1996), tropical (e.g., Starling et al., 2002), and even arctic (e.g., Douglas and Smol, 2000) environments. Studies indicate that lake eutrophication started in industrialized countries from around the 1930s. One instance is the eutrophication of Lake Bourget (France), which first took on a eutrophic state around 1933 (Giguet-Covex et al., 2010; Jenny et al., 2013). However, (Dubois et al.(2018) pointed out that long-term reconstructions of nutrient concentrations in Holocene sediment records (see the references therein) show evidence ofeutrophication resulting from early agriculture that date back several thousand years. First human impacts and responses of aquatic systems: A review of palaeolimnological records from around the world.

As a result of an observation project undertaken by the OECD on a number of lakes in Europe and North America (Vollenweider & Kerekes, 1982), the severity of eutrophication can be categorised into five eutrophic levels, ranging from oligotrophic (nutrient-poor) to hypertrophic or hypereutrophic (nutrient-rich) (see Table 2-1). Even though this classification scheme is accepted and widely applied, local variations in the physical, chemical, and biological conditions of lakes mean that some countries, even those who have membership of the OECD, have established their own national standards. For example, America through the U.S Environmental Protection Agency (USEPA, 2001), Australia and New Zealand with Australian and New Zealand Environment and Conservation Council water quality guidelines (ANZECC, 2000), and several European countries.

Table 2-1 Trophic status by OECD. Modified from (Istvánovics, 2009) and (EPA, 2008)

| Trophic category | Total Phosphorus (µg /L) | Mean chl-a (µg /L) | Max chl-a (µg/L) |
|---|---|---|---|
| Ultra-Oligotrophic | <4 | < 1.0 | < 2.5 |
| Oligotrophic | <10 | <2.5 | <8 |
| Mesotrophic | 10-35 | 2.5- 8 | 8 - 25 |
| Eutrophic | 35-100 | 8-25 | 25-75 |
| Hypereutrophic | >100 | >25 | >75 |

There are still efforts to redefine the chlorophyll-a reference values to precisely fit the conditions of particular lakes, such as lakes in Alpine regions with watershed area that have less industrialisation, intensive urbanisation, or agriculture (Poikāne et al., 2010). The OECD criteria are not matched with Brazilian tropical lakes where there is no relationship between the trophic status and the ratio of maximum or mean biomass (Huszar et al., 1998). Further, in terms of tropical lakes, it has been argued that a trophic index for temperate lakes should not be used, as there has been no clear relationship established between Secchi depth, chlorophyll-a, or Total Phosphorus (TP) and trophic status for tropical lakes (as has been defined in temperate lakes) (Huszar et al., 2006).

Overall, recent developments have seen an advanced and better understanding of the drivers of eutrophication: physical and chemical, as well as enhanced insight into the biological receptors of

the eutrophication process (e.g., Chen et al., 2020), especially for temperate lakes. However, despite the number of studies conducted since eutrophication was first established as a problem (see Figure 0-1), eutrophication remains a major concern worldwide, and there is a limitation of the global picture about the extent of eutrophication in freshwater lakes because the extent of eutrophication in many developing countries is unknown.

A search in Web of Science with 'lake' and, 'cyanobacteria', 'eutrophication' or 'bloom' from published literature from 1970 – April 2021 gives some 20,000 results with an increasing trend (see Figure 0-1). In comparison, the same search keywords for coastal areas return 25,000 results, and 'malaria' returns 90,000 results.
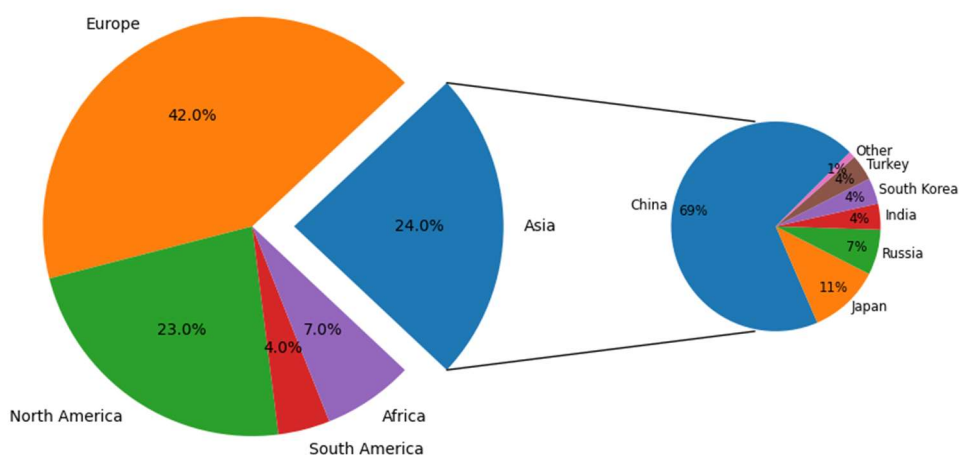


Figure 2-1 Percentage of publications on 'eutrophication' and 'lake' in Web of Science, by country

However, there is a substantial regional gap in terms of publishing institutions (Figure 2-1). As much as 17% of these publications are undertaken by Chinese institutions alone. Almost a half is from European countries and around 20% from North America. Institutions from Japan, Australia, Brazil, and African countries each contribute only around 2%, and the very small remaining percentage is shared by other Asian, South American and African countries. Some studies from South East Asia include studies on Lake Maninjau (Setiawan et al., 2019; Syandri et al., 2020) and Lake Toba in Indonesia (Lukman et al., 2019; May et al., 2021), Lake Lanao in Philippines and Tasik Chini in Malaysia (May et al., 2021; Sharip et al., 2014; Sharip & Jusoh, 2010).

## 2.2   Eutrophication: Mechanisms and Consequences

The detrimental effects of nutrients in water bodies arise as a consequence of the associated abnormal (accelerated) growth of algae and aquatic plants. This growth stimulation in turn arises from elevated nutrient levels (Anderson et al., 2002). Such accelerated growth is problematic

because nutrient-stimulated algal blooms can cover almost the entire surface of the water and prevent other plants in the water from getting enough sunlight to photosynthesise. Meanwhile, excess growth of aquatic plants can also deplete dissolved oxygen levels within the lake, in part because the process of decomposition of dead plants is undertaken by aerobic bacteria that require oxygen to work. The depletion of dissolved oxygen can reach such an extent that no organism can survive (Codd et al., 2005; Paerl et al., 2001); a condition known as the anoxic state (Mason, 2002), creating a dead zone in the water body (e.g., in Joyce, 2000). In stratified lakes, hypoxia in the hypolimnion (the cooler bottom layer when stratification happens) leads to an internal phosphorus load being released by the sediment (Mortimer, 1971), which in turn amplifies the eutrophication of the system (Dodds, 2006).

Even before the hypoxic state is reached, other adverse impacts associated with lake eutrophication are felt, in particular, fishing operations or boating may become difficult due to the dense growth of the plants in the water (F. Khan & Ansari, 2005). Furthermore, algal blooms can turn the lake to an unhealthy greenish look, and the decay of dead plants can produce an unpleasant smell so that eutrophic lakes or reservoirs may lose their aesthetic and tourism values (Liddle & Scorgie, 1980). Floral and faunal diversity can be influenced as well by increased nutrient loading, for example, the loss of submerged aquatic vegetation may result in a loss of zooplankton and invertebrate diversity (Morgan, 1970) or homogenising macroinvertebrate to pollution-tolerant species (You Zhang et al., 2019).

Some algal blooms produce dangerous toxins, including the two most toxic cyanobacteria *Microcystis spp.* and *Anabaena spp.* (Codd et al., 2005; WHO, 2003). In tropical Asia, Africa, and Central America *Microcystis* is the most frequently occurring bloom genus throughout, and in various locations in tropical Australia, America, and Africa, *Cylindrospermopsis* and *Anabaena* blooms have occurred (Mowe et al., 2015).

The presence of potentially toxic algae poses serious health risks to water supply, irrigation, and recreational use (WHO, 2003) and degrades the ecological status of water bodies (Carvalho, Miller, Scott, et al., 2011). The toxins may poison humans, pets, and livestock (Codd et al., 1999). The health effects of Microcystin include damaging the liver, promoting tumours, and causing skin irritations and allergic reactions of varying severity (WHO, 2003). A concentration of 10 µg chlorophyll-a/litre with a dominance of cyanobacteria can cause a relatively low level of adverse health effects, such as gastrointestinal illness and skin irritations.  Moderate effects, such as the potential for long-term illness, can be achieved from water with a concentration of 50 µg chlorophyll-a/litre. And the potential for acute poisoning can occur when the whole-body has contact with cyanobacterial scum (WHO, 2003).

Serious cases of human and livestock poisoning and deaths have been recorded in a number of countries worldwide (Codd et al., 2005; Mowe et al., 2015). This includes the mass mortality of sheep, cattle, horses, pigs, and dogs after drinking from cyanobacterial scum in lake water in Europe and Australia. Fatalities have occurred several times in Brazil, and the most notable one is the deaths of 52 out of over 100 affected people in one episode of algal bloom poisoning in 1996 (Codd et al., 2005).

### 2.2.1 Point and Non-Point Sources of Pollutants

Anthropogenic activities have dramatically increased nitrogen and phosphorus export from the landscape to rivers, lakes, and estuaries (Bennett et al., 2001; Huang et al., 2020; May et al., 2021; Penuelas et al., 2013; Vitousek et al., 1997). In fact, the planetary threshold for nitrogen, i.e., the amount of $N_2$ removed from the atmosphere for human use, has been exceeded, while for phosphorus, it is soon approaching its planetary boundary (quantity of phosphorus flowing into the ocean) (Rockström et al., 2009; Steffen et al., 2015).

During the 1960s and 1970s, phosphate and nitrate from agriculture and detergent use were mainly linked to nutrient enrichment (Schindler, 1974). However, a recent study (Hamilton et al., 2018) shows that the two biggest nitrogen and phosphorus contributors for eutrophication are crop production and animal husbandry.

There has been a shift in diet trends within the global population nowadays such that there is now more animal-sourced protein-rich food. The drivers to this increasing meat consumption include high income per capita and natural endowments such as land availability and a favourable climate to established farms (Milford et al., 2019). In 2016, in the wealthier economies such as the USA, meat consumption is around 110 kg per capita per year, while in developing countries such as Indonesia, people consume only a quarter of it (30 kilograms per capita per year) (Whitnall & Pitts, 2019).

Meat consumption contributes to nitrogen and phosphorus pollution in a number of ways. First is the need for a vast amount of synthetic nitrogen fertilizer and manure application as the result of the mass production of feed. Animal wastes are significant sources of both nitrogen and phosphorus (Toth et al., 2006; Van Faassen & Van Dijk, 1987). Using a global database for 2011, Uwizeye *et al.* (2020) estimate that in feed production, the total synthetic fertilizer and biological nitrogen fixation used to produce livestock feed is 76 Tg/year (Teragram = $10^{12}$ gram). That alone has already reached the planetary boundary for nitrogen, which is 62–82 Tg/year. In total, livestock farms and their whole supply chain system contribute ~65 Tg/year of nitrogen pollution, equivalent to one-third of current human-induced nitrogen emissions. These emissions contain

~39% (29 Tg/year) of global anthropogenic nitrate ($NO_3^-$) released to the surface and groundwater. Moreover, most of the nitrogen emissions from the livestock supply chain take place in Global South regions i.e., South Asia (23 Tg/year), East and Southeast Asia (18 Tg/year), Latin America and the Caribbean (7 Tg/year).
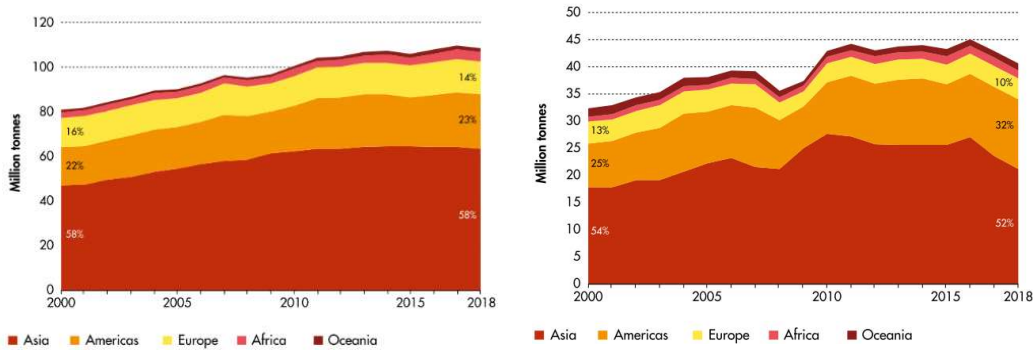


Figure 2-2 Chemical fertiliser use by nutrient and region. Left: nitrogen-based fertiliser, Right: phosphorus-based fertiliser. After (FAO, 2020).

Fertilisers are used both in food and feed production. FAO (2020) reported increased fertiliser use in all regions of the world between 2000 and 2018 (Figure 2-2). In 2018, total agricultural use of chemical fertilisers, specifically nitrogen type (N) and phosphorus type ($P_2O_5$) fertilisers, was 109 million tonnes and 41 million tonnes, respectively. Together with potassium-based fertiliser, over an 18-year (2000 to 2018) period, there has been an increase of 40% in the global use of these fertilisers.

FAO (2020) also reported that Asia used more than half of fertilizers in 2018 (55% of the world total). The next most intensively used regions include the Americas (27%), Europe (12%), Africa (4%), and Oceania (2%). This ranking of the regions is the same, both for nitrogen and phosphorus. China is the largest user of any fertiliser in Asia (accounting for 73% of all fertilisers in Asia (Farmer, 2018)) and in the world. After China, the primary users of chemical fertilizers in the world are India, the United States of America, and Brazil (FAO, 2020). Of these biggest four, only America is in the Global North.

Nitrogen and phosphorus pollution is not only related to food or feed production, but also is generated in a range of non-food sectors, with around one-third of the global nitrogen and phosphorus emissions being sourced from non-food products (Hamilton et al., 2018). Among non-food production, clothing is the major nitrogen pollution contributor (Anguelov, 2015; Hamilton et al., 2018). The wastewater from reeling (winding thread on spools) contains ammonia while dyeing and finishing both result in total nitrogen and phosphorus and release high concentrations

of suspended solids (Hossain et al., 2018; S. Khan & Malik, 2014). There is no comprehensive analysis yet about the amount of nutrient pollution from the fashion industry, but for an illustration, one tonne of silk dress is equivalent to 350.45 kg nitrate ($NO_3^-$) emissions, of which the reeling process accounts for 87.9% of the total emission (F. Chen et al., 2020).

Anguelov (2015) reported that China is the leading country in the overall apparel industry, followed by India, Nepal, Macao, Turkey, Bangladesh, Srilanka, Vietnam, Myanmar, Cambodia, and Tunisia. He stated that according to data from 1995 to 2008, several countries (Bulgaria, Turkey, and Cambodia) have become more reliant on apparel production. Cambodia (the focus nation of this research), in particular, dedicates the majority of its manufacturing capacity to apparel. With many garment producers being located in developing countries, it is important to note that most of the wastewater emitted by these industries is not treated. Using the example of Bangladesh, one of the biggest garment exporters, dyeing factories in Dhaka dump their wastewater directly to the Dhaleshwari River without any treatment. Sadly, there are no academic publications that elaborate on the extent of the water pollution that the garment industry is responsible for within Bangladesh. CNN have reported that local people compare their now black water river with the clean river from which they were able to catch fish around 30 years ago. Coloured runoff on the road around the dyeing factories during the rainy season is now a normal scene (Regan, 2020).

Another major source of nutrient pollution is wastewater. Over the past 25 years, domestic wastewater has been a key contributor to nutrient increases in the aquatic environment (Kroeze et al., 2013) and has become a key component of both the global nitrogen and phosphorus cycles (Galloway et al., 2008; Reinhard et al., 2017). Household sewage contains phosphates ($PO_4^{3-}$) from human sources, detergents, food waste, food additives, and other products (Farmer, 2018). This sector contributed 54% to the total global anthropogenic phosphorus load to freshwater systems from both diffuse and point sources, which is estimated at 1.5 Tg/yr. More than half of this total load is derived from Asia, followed by Europe (19%) and Latin America, together with the Caribbean (13%) (Mekonnen & Hoekstra, 2018). With its current population accounting for more than half of the world's population, it is not surprising that Asia is the biggest polluter.

Phosphate was introduced to synthetic detergents in 1948 (Köhler, 2006), and since the widening of eutrophication in European lakes in the 1960s, detergents have been blamed as the primary source of phosphate in freshwater. However, at least in the EU countries, it is found that phosphate from detergent only accounts for 10% of the total anthropogenic phosphorus load to rivers and lakes, while human waste accounts for 24% (Köhler, 2006). Meanwhile, nitrogen in

human excreta accounted for roughly 15–20% of the total anthropogenic production of reactive nitrogen per year (Larsen et al., 2016).

These sources of pollutants to water bodies can be categorised into two types: point and non-point sources. Runoff from agricultural areas is one of the major non-point sources (Egli, Bally, & Uetz, 1990; Ongley, 1996). In developing countries, wastewater from urban areas is mainly considered as a non-point source as it is diffuse, as distinct from wastewater of households and industries in developed nations, which flows mainly from treatment facilities that can be regarded as point sources (Jenny et al., 2016). Non-point sources also include runoff from construction sites, abandoned mines, atmospheric deposition over a water surface, and activities on land that generate contaminants, such as wetland conversion, construction, and the development of land or waterways (S. R. Carpenter et al., 1998; Novotny & Olem, 1994). Deforestation is another non-point source. Burning, as a typical deforestation method, converts the standing stock of phosphorus in plant matter to phosphorus in ash which is rapidly dissolved, leached, and transported into rivers over timescales of a year or two (Schlesinger, 2005).

Discharges from point sources are relatively simple to measure and regulate because they tend to be continuous, with little variability over time, and often can be monitored in a single place. More consideration has been given to non-point sources of pollution because they are much more difficult to measure and regulate as they are often hard to detect, intermittent, and linked to seasonal or irregular activities. In the USA, for example, the top impairment for the rivers and lakes comes from non-point sources, while typical point sources such as municipal sewage only rank 7th. Similarly, in Europe, it is found that almost 50–80% of the total nitrogen load and roughly half of the total phosphorus load are contributed by non-point sources (Zheng et al., 2014).

In developed countries, point sources are strictly regulated and monitored. For example, the European Environment Agency monitors the phosphorus in lakes as part of its programme of monitoring nutrients in freshwater. Monitoring provides data for decision-making at the management level and to evaluate the effectiveness of policies that are being executed. For example, the most recent report from the European Environment Agency (EEA, 2021) revealed that the average total phosphorus concentration in lakes decreased 0.8% over the period 1992-2018 (0.0003 mg/L). This (albeit modest) decrease is most likely due to improvements in wastewater treatment and the reduction of phosphorus in detergents. Meanwhile, for nitrate in rivers, concentrations are levelling off in recent years. Another example is that the U.S. Environmental Protection Agency conducted its National Lake Assessment (NLA) for 1835 U.S. lakes between 2007 – 2012 (USEPA, 2016) to evaluate their biological, chemical, physical, and

recreational condition. From the survey, it was found that 40% of lakes have excessive levels of total phosphorus and 35% have excessive levels of total nitrogen, while cyanobacterial toxins were detected in 39% of the lakes.

However, in the Global South, nutrient monitoring is still lacking. Farmer (2018) suggests that the collection of domestic wastewater in many countries in South and East Asia may be limited and, where collected, treatment is often basic at best, despite their high densities of population. In Brazil, 70% of municipalities do not have a wastewater treatment plant, whereas the remaining 30% of municipalities only covers 43% of the population's wastewater collection and treatment (Chrispim et al., 2019). This is the fact for Brazil, which, in a study comparing six countries in South America, was found to be the country with the strictest regulations among the others (Noyola et al., 2012).

In developing and emerging economies such as those countries located in Africa and Asia, within the global trend towards overconsumption of calories and protein-rich food, the average daily per capita protein intake is significantly lower than the global average consumption (Kearney, 2010). However, the per capita nitrogen discharges in Africa and Asia are comparable with those in the developed economies as the result of insufficient sanitation and wastewater management (X. Wang et al., 2019).

Several studies (Hendriks & Langeveld, 2017; von Sperling & de Lemos Chernicharo, 2002) have suggested that one of the problems in wastewater treatment regulations found in Brazil and most developing countries is that the emissions standards in the regulations tend to be set at a generic level, which does not necessarily recognise the specific conditions of the water bodies encountered in the country. Another problem is that even where there are regulations, the level of compliance is often very low (von Sperling & de Lemos Chernicharo, 2002), even in strict countries like China (Zheng et al., 2014).

Take another example in Indonesia, with industrial tofu production. It is mostly domestic and does not have a waste treatment facility (Seroja et al., 2018). A recent study (Wijaya & Soedjono, 2018) found that the waterway around one of the tofu home industry areas has an ammonia level of 129.3 mg/L. There exist environmental regulations for normal nitrate concentration on surface water which takes WHO standard (WHO, 2004), i.e., up to 3 mg/L. However, there is never an inspection on the implementation of the regulations. The same study found an orthophosphate concentration of 95.5 mg/L, while in natural, unimpacted freshwater, total phosphorus concentrations are below 0.025mg/l (Farmer, 2018).

In the Global North, studies on nutrient pollution in lakes and other water bodies have already included the cycle and different species of nitrogen and phosphorus, which have been found to contribute differently to the eutrophication process itself, and the phytoplankton as biological receptors of the eutrophication. This topic is elaborated in the subsequent sub-sections.

### 2.2.2 The Freshwater Nitrogen Cycle

Ammonia bound in rocks and sediments is the largest nitrogen inventory of the earth, but it has a minor role in annual biogeochemical nitrogen cycling (Kuypers, Marchant, and Kartal, 2018). The largest freely accessible global nitrogen inventory is dinitrogen gas in the atmosphere (Bernhard, 2010). However, instead of this atmospheric nitrogen, most organisms need more reactive nitrogen compounds such as ammonia ($NH_3$), nitrates ($NO_3^-$), or nitrites ($NO_2^-$) for their growth.

Nitrogen reaches freshwaters through a number of pathways: by atmospheric deposition on the catchment or directly on the water body (by the nitrogen-fixing cyanobacteria), by leaching from diffuse sources within the catchment (fertiliser and manure application), by sediment erosion of nitrogen-rich soils, and by direct inputs from point sources such as sewage treatment works (Grizzetti et al., 2015; Wetzel, 2001).

Nitrogen in aquatic environments comprises dissolved inorganic nitrogen, dissolved organic nitrogen, and particulate nitrogen that is almost entirely organic (Worsfold et al., 2008). Dissolved inorganic nitrogen is the dominant form of nitrogen that is mainly assimilated by aquatic organisms. Dissolved inorganic nitrogen is derived from combinations of ammonium ($NH_4$), nitrite ($NO_2^-$), and nitrate ($NO_3^-$). Nitrogen transforms into different species through a cycle of processes: nitrogen fixation, nitrification, anammox, denitrification, ammonification. This is illustrated in Figure 2-3 and reviewed in more detail below.
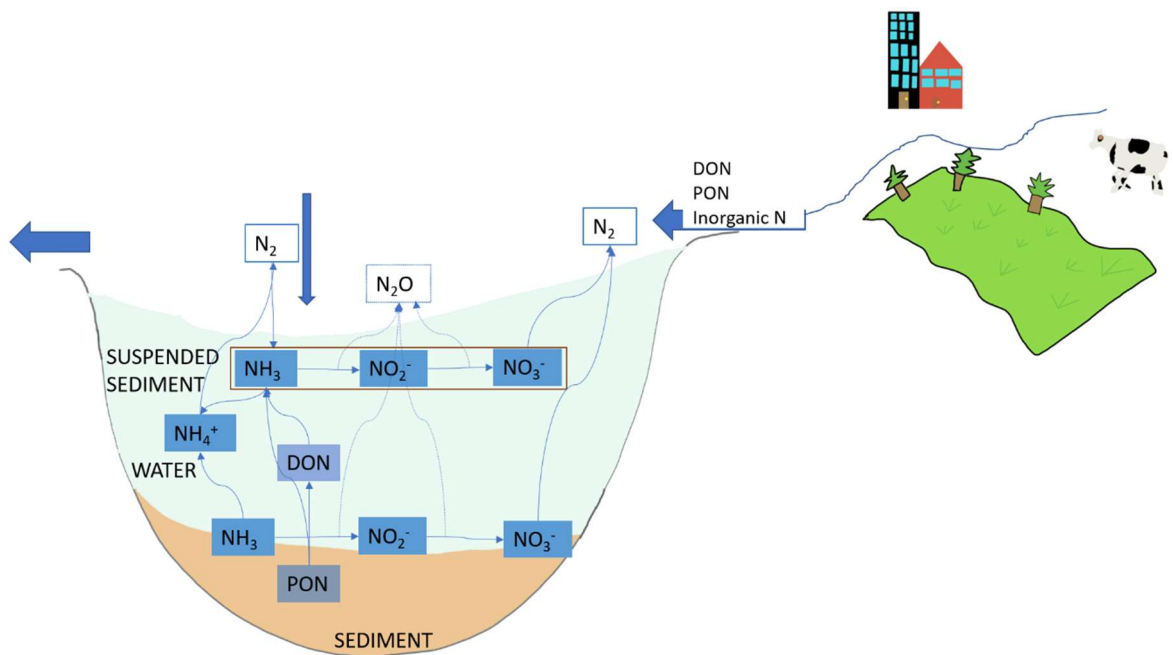
Figure 2-3 The Freshwater Nitrogen Cycle

**Nitrogen Fixation**

The process of converting $N_2$ into biologically available nitrogen (i.e., ammonia) is called nitrogen fixation. Naturally, nitrogen fixation is carried out by prokaryotes. Prokaryotes are single-cell organisms without a nucleus. But only those that have enzyme nitrogenase, a catalysator of the conversion of atmospheric nitrogen ($N_2$) to ammonia ($NH_3$), can perform nitrogen fixation (Wagner, 2011). The most significant nitrogen fixers on the land are symbiotic bacteria associated with leguminous plants, and in the water environment the most significant fixers are cyanobacteria (Bernhard, 2010; Britannica, n.d.; Kuypers et al., 2018).

Nitrogen can be fixed abiotically by lightning or specific industrial processes such as the Haber-Bosch process (Bernhard, 2010), by which nitrogen fertilizers are produced. It is estimated that round 120 million tonnes of $N_2$ from the atmosphere per year are converted into reactive forms by human processes, mainly the manufacture of fertilizer for food production and the cultivation of leguminous crops (Rockström et al., 2009). In the form of fertilizer used, this nitrogen fixation has an increasing trend, as discussed in the previous section.

**Nitrification**

Nitrification is the process that converts ammonia ($NH_3$) to nitrite ($NO_2^-$) and then to nitrate ($NO_3^-$). Nitrification is an important process in nitrogen removal from the aquatic system, as once nitrate is produced, it can be converted to $N_2$ gas which is then returned to the atmosphere (see

Denitrification below). Excessive nitrate is harmful—the limit of nitrate in drinking waters recommended by the WHO is 11.3 mg/L.

Most nitrification occurs aerobically and is carried out solely by prokaryotes. Nitrification consists of two distinct steps, each of which is carried out by distinct types of microorganisms. The first step involves the oxidation of ammonia ($NH_3$) to nitrite ($NO_2^-$), which is carried out by microbes known as ammonia-oxidizers. The second step in nitrification is the oxidation of nitrite ($NO_2^-$) to nitrate ($NO_3^-$), carried out by nitrite-oxidizing bacteria. Ammonia-oxidizers and nitrite-oxidizers are ubiquitous in aerobic environments. Nitrification occurs in natural environments such as soils, estuaries, lakes, and open-ocean environments (Bernhard, 2010). These processes release the green-house gas Nitrous Oxide ($N_2O$).  In the aquatic environment, these bacteria are known to grow suspended in the water column and to be attached on and within the surface sediment. The nitrification itself occurs in the water column and on sediment (Pauer & Auer, 2000), but it is found that the nitrifying bacteria tend to attach to the sediment; hence high suspended sediment concentrations from erosion or bottom sediment resuspension will accelerate the nitrification process (Xia et al., 2009).

Nitrification consumes a large amount of oxygen, which could be up to 27-30% of the total oxygen consumption (Clevinger et al., 2014), or could account for almost all of the oxygen demand (Dai et al., 2006). Nitrification will continue to happen until the dissolved oxygen in the water reaches 0.3 mg/L (Wetzel, 2001). Nitrification can cause or accelerate hypoxia in water (Clevinger, 2013), which subsequently could lead to phosphorus release from the sediment (as discussed in Section 2.2.3).

**Anammox (anaerobic ammonia oxidation)**

In 2002, Thamdrup and Dalsgaard (2002) discovered a new type of ammonia oxidation occurring under anoxic conditions. Before that, all nitrogen oxidation was thought to be carried out under aerobic conditions (Bernhard, 2010). Although it was first observed in seabed sediments, a similar oxidation process was also found in many freshwater systems, including in eutrophic lakes (e.g., Yoshinaga *et al.*, 2009; Qin *et al.*, 2018).

Anammox bacteria oxidize ammonia by using nitrite as the electron acceptor to produce gaseous nitrogen under anoxic condition, hence removing bioavailable nitrogen and returning it to the atmosphere, as the denitrification process does (Kuypers et al., 2005; Ward et al., 2009). Due to its last product, anammox could help mitigate eutrophication to some level. Anammox can contribute to 50% of nitrogen loss in the ocean, but has not yet been well studied in the freshwater environment, although it is acknowledged as an important path in the biogeochemical cycle in the ocean (Crowe et al., 2017).

**Denitrification**

Denitrification is the process that transforms nitrate into dinitrogen gas. Denitrification is an anaerobic process, occurring mostly in surface sediments and anoxic zones in lakes and oceans (Bernhard, 2010; Potter et al., 2010; Solomon et al., 2009). During denitrification, nitrate ($NO_3$) can be reduced to $N_2$ via the formation of nitrite ($NO_2^-$), nitric oxide (NO), and nitrous oxide ($N_2O$), which are considered as green-house gases. The permanent loss of $N_2$ to the atmosphere through denitrification contributes substantially to nitrogen loss in lakes (Seitzinger et al., 2006) in both temperate (James et al., 2011) and tropical (Lewis Jr, 2002) regions.

Zhu *et al.* (2021) observed that in shallow lakes (a depth of <~10 m), the sediment denitrification rate is negatively correlated with lake depth. This is due to turbulent energy being more likely to reach the sediment beds in shallower lakes, oxygenate the water column and subsequently promote oxygen penetration into sediments. This will increase the availability of substrates and oxygen for nitrification, which provides more nitrate for further denitrification. In mountain lakes, denitrification rates are determined by high atmospheric nitrogen deposition that increases nitrate availability (Palacin-Lizarbe et al., 2020).

Denitrification is the main mechanism of nitrogen retention (the difference between N inputs and N outputs to the system), alongside sedimentation and nitrogen uptake by aquatic organisms (Seitzinger et al., 2006). It can account for up to 96 percent of nitrogen removal in sediment (Nizzoli et al., 2020), hence could balance the external nitrogen loadings (James et al., 2011) and mitigate the negative impacts of excessive nitrogen in eutrophic lakes. However, denitrification rates are suggested to decline with increasing trophic status. This is due to the fact that under the more eutrophic conditions, nitrogen assimilation by phytoplankton will reduce water column $NO_3^-$ concentrations and its availability for denitrifying bacteria in the sediment (Nizzoli et al., 2020).

**Ammonification**

In ammonification, prokaryotes release inorganic nitrogen (i.e., ammonia) from organic nitrogen (see sub-section below). The resulting ammonia then becomes available for plants and other microorganisms for growth (thereby contributing directly to the potential for eutrophication), or may subsequently be oxidized to nitrate through nitrification (Back, 1997; Bernhard, 2010; Kemp & Mudrochova, 1972; Kuypers et al., 2018).

**Organic Nitrogen**

The organic nitrogen comprises dissolved organic nitrogen and organic particulate nitrogen. The organic particulate nitrogen is organisms' excreta and dead bodies. Remineralisation by bacteria

transforms particulate organic nitrogen into dissolved organic nitrogen, which can be further transformed into ammonia. Particulate organic nitrogen can also go through ammonification and directly transform into ammonia. Dissolved organic nitrogen typically constitutes the largest part (between 10 and 70% ) of the total dissolved N in freshwaters (Willett et al., 2004). Dissolved organic nitrogen can also be assimilated directly by aquatic organisms. However, the understanding of the bioavailability of dissolved organic nitrogen is only well developed for the marine environment (Worsfold et al., 2008).

### 2.2.3     The Freshwater Phosphorus Cycle

Phosphorus is sourced from the Earth's crust. Though phosphorus is the eleventh most abundant element, the estimated phosphorus reserves are calculated to be 15,000 million tons, which can only last for 90 years (Vaccari, 2009). Phosphorus enters the biosphere by weathering or mining. The annual global mining and weathering flux are in a similar magnitude, i.e.,  18.5 Tg (Teragram) and  15–20 Tg (Teragram), respectively (Bennett et al., 2001).

Figure 2-4 illustrates the cycle of phosphorus in lakes. There are three sources from where phosphorus enters lakes: atmospheric precipitation, groundwater, land runoff, and flowing waters (Wetzel, 2001). Atmospheric precipitation, mainly dust sourced over the land from soil erosion, is found in highly fertilised agricultural areas. Phosphorus loading from atmospheric precipitation and groundwater is low, around 20 µg/L and < 30 µg/L (unpopulated areas), respectively (around 100µ/L in the urban-industrial areas). Land runoff and flowing waters receive a very large amount of phosphorus from domestic sewage and agricultural regions.
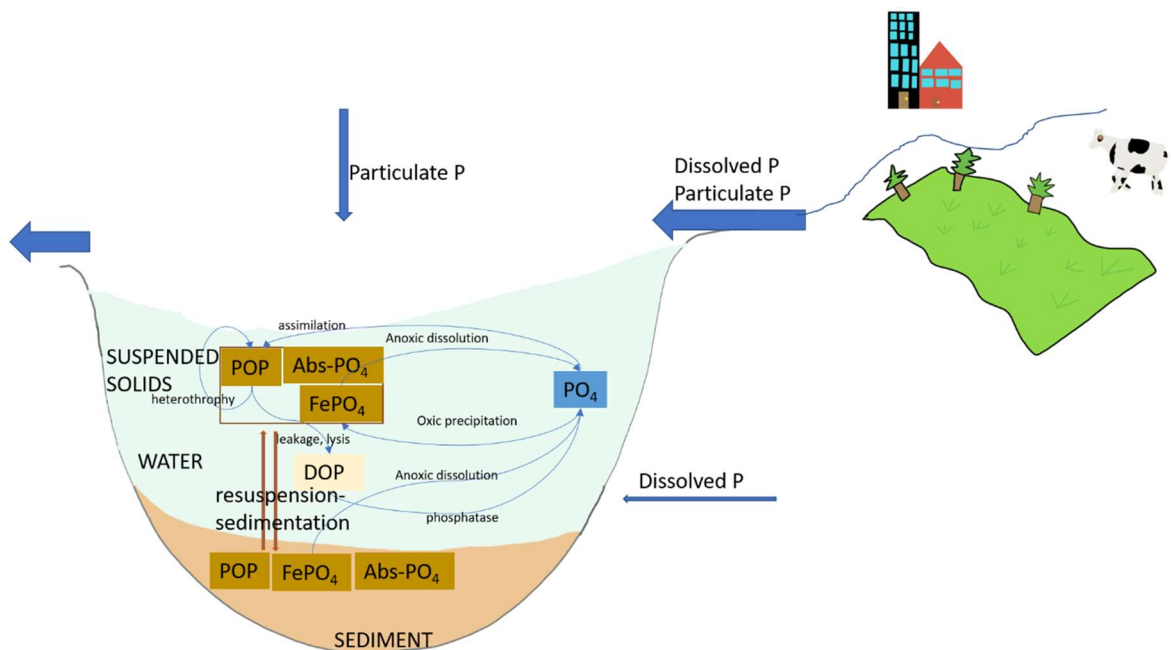
Figure 2-4 The Phosphorus Cycle in Lakes. Modified from (Dodds & Whiles, 2002, 2010, 2020; Forsberg, 1989).

The phosphorus that is moved from soils to aquatic environments is transferred in two forms: soluble phosphorus and particulate phosphorus. In most cultivated lands, the 60 to 90% (Sharpley, 1999) of phosphorus transported in surface runoff comprises inorganic particulate phosphorus absorbed onto the clay minerals (iron and aluminium-oxides) within the soil (Daniel et al., 1994; Sharpley et al., 1994), or as precipitates of calcium, iron or aluminium phosphates or weathering apatite in soil, and particulate organic form in detritus (Broberg & Persson, 1988). The organic phosphorus component is usually less than the inorganic part. The smallest portion comprises dissolved phosphate (Harper, 1992), but dissolved phosphate nevertheless can be about 3.5 times more bioavailable than particulate phosphorus (Joosse & Baker, 2011). However, surface runoff from areas such as grassland, forest, or non-cultivated soils is generally dominated by dissolved phosphorus because runoff from such environments usually has little suspended sediment. The dissolved phosphorus is released from manure, soil, and plant material when an interaction between rainfall or irrigation water and a thin layer of surface soil and plant material happens before leaving the field as surface runoff (Sharpley, 1999).

Landcover also determines the type of phosphorus in the soil and correlates with phosphorus contained in the surface runoff. For example, in forest soils, 70 percent of total phosphorus is organic, while in cropped soils, 75% of the total phosphorus is inorganic (Daniel et al., 1994). Most dissolved phosphorus is immediately available for biological uptake. For planktonic algae and bacteria, even though there is also direct uptake of some organic phosphates, the inorganic form,

particularly orthophosphate ($H_2PO_4^-$, $HPO_4^{2-}$ or $PO_4^{3-}$), is regarded to be the only directly available phosphorus source (Boström et al., 1988). The ratio of assimilation is 106:16:1 for carbon, nitrogen, and phosphorus, respectively.

Organisms such as algae, bacteria, and zooplankton have phosphatase enzymes that liberate orthophosphate from dissolved organic phosphorus (Jansson et al., 1988). When phosphorus becomes scarce, the excretion of extracellular phosphatases increases because the enzymes function to increase the availability of phosphate to cells (Dodds & Whiles, 2002, 2010, 2020). Hence phosphate enzymes can be used as phosphorus deficiency in algal or plankton communities (Jansson et al., 1988). In oligotrophic waters, dissolved organic phosphorus accounts for a significant percentage of the total dissolved phosphorus pool, and the regeneration of orthophosphate from dissolved organic phosphorus may become a potentially important source of phytoplankton nutrients (Auer et al., 2014).

Heterotrophy, i.e., consuming other plants or animals to gain energy and nutrients, recycles particulate organic phosphorus back to particulate organic phosphorus, and also inorganic phosphorus (Dodds & Whiles, 2002, 2010, 2020). This is because many animals cannot use inorganic phosphorus directly, but instead they must consume organic phosphorus in the form of lipids and/or nucleic acids to meet their needs. Organisms excrete excess phosphorus as phosphate (inorganic phosphorus) or organic phosphorus in both oxic and anoxic environments.

Inorganic phosphorus (i.e., phosphate) interacts strongly with iron; therefore iron is important in determining the availability of phosphorus in many aquatic systems. The precipitation of phosphate with ferric iron ($Fe^{3+}$, an oxidized form of iron) occurs only in oxic conditions. The binding of ferric iron and phosphate is known to dissociate under anoxic conditions. The dissociation could occur on the anoxic bed sediment surface or anoxic hypolimnion (Dodds & Whiles, 2002, 2010, 2020). However, in shallow lakes it is found that the dissociation is related more to the eutrophic level, not the presence of $O_2$. In oxic or anoxic conditions, lake sediments with higher trophic levels will release more phosphate (Welch & Cooke, 2005).

The particulate part of phosphorus that enters lakes can be directly deposited in the sediment. And the dissolved phosphate that is assimilated in organic matter by primary producers will eventually sink to the bottom of the lake in an organic form (Søndergaard, 2007). Phosphorus found in the sediment can transform several times, bound to a variety of organic and inorganic sediment components (Søndergaard et al., 2001).

Even after the reduction of the external loading of phosphorus to lakes, lakes can still experience eutrophication for a long period due to the gradual release of phosphorus from lake sediments, a

process named internal loading. Buried phosphorus can be released back to the water column when phosphorus-loaded sediments are resuspended. There are numerous mechanisms leading to phosphorus release to the water column from such resuspensions of underlying sediments. Phosphorus bound in precipitates and inorganic materials may be desorbed and dissolved. Microbial mineralization of organic matter also releases phosphate. Or phosphate diffuses from sediment pore waters.

The inorganic phosphorus released from sediments varies, but studies have shown that it can contribute up to 80% of the total phosphorus input in some temperate lakes and may become the main driver of primary production, especially when the bottom waters become anoxic in the summer (Penn et al., 2000; Søndergaard et al., 2003).

In shallow lakes, suspended solids within the water column can be caused by wind-induced wave disturbance, currents, and turbulent fluctuations (Bengtsson & Hellström, 1992; Bloesch, 1982; Kristensen et al., 1992). Besides resuspension, low redox potential, elevated pH, and temperature are factors causing phosphorus to be released from the sediment (Forsberg, 1989; Søndergaard et al., 2003).

Lake sediments can be highly variable in their potential to retain and release phosphorus. This is due to the different capacity to bind and release phosphorus of varying chemical composition and the attendant variations in controlling parameters such as iron, aluminium, manganese, calcium, clay, and other elements that may all influence sediment-water interactions (Forsberg, 1989; Søndergaard et al., 2003).

The information on phosphorus species and their cycle, along with the potential of sediment controlling phosphorus cycling in lakes and the consequences of harmful algal blooms, is helpful for controlling lake water quality. For management, for each lake, there are efforts to reveal the potential of sediment controlling phosphorus cycling and the consequence of harmful cyanobacteria blooms. Such studies are relatively extensive in developed nations, but rarely found in developing countries.

## 2.3 Phytoplankton as a Biological Receptor of Eutrophication and Chlorophyll-a as a Proxy for Phytoplankton Biomass

Primary producers in the aquatic environment are broadly divided into three groups: (i) periphyton, which grows on substrates such as mud, (ii) phytoplankton, which is suspended in the water column, and; (iii) macrophytes that are visible (Hoverman & Johnson, 2012). In many lakes in Europe and North America, it has been found that during the 20th century, the input of

phosphorus and nitrogen from urban communities and agriculture has triggered a shift from a clearwater state with submerged macrophytes as the most significant primary producer, to a turbid state in which phytoplankton are now the dominant primary producer (Søndergaard, 2007 and references therein).

In the three-domain biological classification system (Woese et al., 1990), i.e., Eucarya, Bacteria and Archaea, phytoplankton consists of organisms from two of those three domains (Colin S Reynolds, 2006). The first domain is the Eucarya domain, into which most phytoplankton fall. This domain includes chlorophyte (green algae), chrysophytes (golden/brown algae), bacillariophyte (diatoms), and a few other phyla. The second domain is the Bacteria domain, which is biochemically bacterial in nature but performs plant photosynthesis. Falling into this category are cyanobacteria, formerly known as blue-green algae.

As bacteria, cyanobacteria have the ability to fix nitrogen from the atmosphere (although there are some cyanobacteria that do not perform nitrogen-fixation), which usually happens when nitrogen in the waterbodies is deficient.  It has been observed that cyanobacterial toxin concentrations increased a few days after significant $N_2$ fixation rates were observed in Lake Mendota, USA (Beversdorf et al., 2013). The fixed nitrogen can be sufficient enough to allow phytoplankton biomass to continue to be produced in proportion to phosphorus, even after the reduction of external nitrogen loading (Schindler et al., 2008). Bacteria also have higher optimal growth temperatures, thereby aiding the proliferation of cyanobacteria in warm temperatures, such as would be found in contemporary tropical environments. This is the primary concern when climate change is brought into consideration across the world's lakes.

The subsequent sections below elaborate the correlations between nutrients and physical environment with phytoplankton abundance and community diversity, indicating how chlorophyll-a can be used as a proxy when measuring phytoplankton biomass.

### 2.3.1      Nutrients Shape Phytoplankton Abundance and Community Diversity

Phytoplankton form the base of the aquatic food web. Phytoplankton are autotrophs, organisms that can make their own food by synthesizing organic matters from inorganic materials, using energy from sunlight or a chemical source to drive the process. The chemical sources needed are macronutrients (nitrogen, phosphorus, silica) and micronutrients (iron, aluminium, etc.). Thus nutrients, particularly macronutrients, will limit the aquatic primary production and ultimately shape the ecosystem.

**Limiting Nutrients**

A nutrient tends to be limiting when the ratio of nitrogen to phosphorus of nutrients available to primary producers is below the Redfield ratio of 16:1 (molar), which is the average ratio of nitrogen and phosphorus in algae. Phosphorus was believed to be the limiting nutrient for many lakes. Very early studies (Dillon & Rigler, 1974; Sakamoto, 1966) show a significant correlation with phosphorus and phytoplankton biomass which was measured as chlorophyll-a (see Section 2.3.3 for chlorophyll-a as a proxy for phytoplankton biomass). These findings supported the mainstream idea that most lakes are phosphorus limited.

However, later it was found that nitrogen can be the primary or at least co-limiting nutrient for phytoplankton production in several lakes in the world, including in locations in North and South America, as well as Europe (e.g., Elser, Marzolf and Goldman, 1990; Diaz and Pedrozo, 1996; Van der Molen *et al.*, 1998). It has also been found that even if a lake is phosphorus limited, nitrogen limitation of phytoplankton can also occur for short periods (Carvalho, Miller, Spears, et al., 2011; Maberly et al., 2002). There is an argument that tropical lakes are more likely to be nitrogen-limited than phosphorus limited, as distinct from lakes in the temperate regions (Huszar et al., 2006), or at least more widespread in the tropical area (Maberly et al., 2020). But studies on this topic are not numerous and most studies on lakes in tropical regions assume that these lakes are also phosphorus limited.

The limiting nutrient does not only define the abundance of the phytoplankton but also strongly affects the structure of algal communities in a waterbody (Andersen et al., 2020). For example, under phosphorus limiting conditions, the phytoplankton assemblage tends to be occupied more by chlorophytes and diatoms, in both marine and freshwater systems. However, under nitrogen limiting conditions, cyanobacteria are often the dominant algal group. One of the explanations is related to the point that some cyanobacteria species can fix atmospheric $N_2$ gas. Cyanobacteria can increase nitrogen-fixation rates to partially compensate for nitrogen scarcity when nitrogen limiting conditions occur (Andersen et al., 2020). As a result, the abundance of cyanobacteria tends to increase after the onset of nitrogen limitation, leading to an increase in cyanobacterial toxin (Beversdorf et al., 2013). This supports the idea that in eutrophic lakes, even after a reduction of external nitrogen loading, the nitrogen fixed by cyanobacteria can still be sufficient to allow phytoplankton biomass to continue to be produced in proportion to phosphorus (Schindler et al., 2008).

**Nutrient Preference**

Phytoplankton may exhibit preferences for particular nutrient species. For example, it was found that cyanobacteria and chlorophytes showed a preference for ammonium ($NH_4$) (Andersen et al., 2020; Berg et al., 2003; Domingues et al., 2011; Gardner et al., 2017), presumably because ammonium is more bioavailable than nitrate ($NO_3$) (Q. Chen et al., 2020). Meanwhile, diatoms showed an equal preference for $NH_4$ and $NO_3$, and occasionally a greater preference for $NO_3$, not only in coastal, but also in freshwater environments (Andersen et al., 2020; Donald et al., 2011, 2013; Glibert et al., 2016).

Furthermore, nutrient preference is also found at the species level. For instance, nitrogen enrichment experiments have detected that cyanobacteria blooms dominated by *Microcystis aeruginosa* are highly responsive to ammonium additions rather than the additions of nitrate and urea ($CH_4N_2O$). Alternatively, cyanobacteria blooms dominated by *Planktothrix agardhii* respond to all the additions of nitrate, ammonium, and urea (Chaffin & Bridgeman, 2014).

Meanwhile, the growth of diatoms depends on the presence of dissolved silica (another micronutrient), whereas the growth of non-diatom phytoplankton does not (Conley et al., 1993). Diatoms assimilate dissolved silica ($Si(OH)_4$) in order to build frustules. Diatom frustules accumulate rapidly in the bottom of diatom-dominated lakes because their specific gravity is far greater than that of non-siliceous algae (Colin S Reynolds, 1984 in Goto et al., 2007).

Due to these nutrient preferences, the available nutrients, and their forms, alongside the physical conditions (explained in section 2.3.2), can create seasonal diversity in the phytoplankton community. Further, knowledge of algae response to nutrients and other environmental changes has been utilised in efforts to model shifts in community composition over seasonal time scales in particular environments (e.g. Fragoso Jr et al., 2008), or to use particular indicator species or combinations of species in assessing water quality (Bellinger & Sigee, 2015). However, a note of caution is warranted: the prevalence of such studies on nutrient speciations and their complex correlations with phytoplankton are dominated by studies in the Global North, meaning that considerable gaps in our understanding of these processes still exist in tropical lakes.

**Algal Blooms**

Algal blooms refer to the fast growth and accumulation of phytoplankton and are stimulated under conditions when available nutrients in the water exceed what the primary producers need. Hence, the onset of an algal bloom is widely used as an indication of eutrophication. Cyanobacteria and several species of diatoms (e.g. Ferris & Lehman, 2007; Grami et al., 2011) are bloom-forming algae. Cyanobacteria is receiving the most attention because many cyanobacteria

(e.g., *Anabaena*, *Microcystis*, *Cylindrospermopsis* spp.) can produce toxins that are harmful not only to aquatic life, but also to humans (see Section 2.2).

Smith (1983) reported a dramatic tendency of cyanobacteria to bloom when the nitrogen and phosphorus ratio is below 29 or 23 in Canadian lakes (Orihel et al., 2012), although a low nitrogen and phosphorus ratio does not always translate to a cyanobacteria bloom (e.g., Lv et al., 2011). Low silica to nitrogen and silica to phosphorus proportions are sometimes important factors as well (Dokulil & Teubner, 2000).  Organic nutrients (especially nitrogen) demonstrate the potential of supporting the growth of harmful algal bloom species. As seen, correlations between nutrients and phytoplankton are different between place to place. Thus, there is no assurance that the knowledge found in these lakes will apply to other lakes as well.

### 2.3.2    Physical Environments Shape Phytoplankton Abundance and Community Composition

In oligotrophic environments, algal community structures are driven by intense competition for nutrients (Tsiola et al., 2016). However, when nutrients are abundant in a eutrophic environment, the species interactions can shift from competition for nutrients to competition for light, for instance (Burson et al., 2018; H. Wang et al., 2020). For African tropical lakes, it has indeed been found that light may become the primary limiting factor (Ndebele-Murisa et al., 2010). The physical forcing variables like wind and temperature that modify the physical structure of lakes, for example, can affect the phytoplankton community in a few days (Pannard et al., 2007).

Cyanobacterial blooms are also known to be favoured by a number of physical factors, including meteorological and climate-related variables. These factors are mainly seasonal, including warmer temperatures, windiness, light, the strength, frequency, and duration of thermal stratification of the water column, and slow-moving water (Adrian et al., 2009; Bernhardt et al., 2008; Elliott, 2010; Foy et al., 1976; Gerten & Adrian, 2002; Mischke, 2003; Sherman et al., 1998; Winder & Sommer, 2012). In shallow tropical lakes, drought and tropical cyclones may also stimulate cyanobacterial blooms (Brasil et al., 2016; M. Zhu et al., 2014). Chemical conditions such as high alkalinities and associated high pH have also been found to favour cyanobacteria blooms (Sellner et al., 1988; Shapiro, 1984).

A phytoplankton functional classification, named the CSR (*competitor*, *stress* tolerator, and *ruderal*) model, has been proposed to classify phytoplankton based on differences with regards to their strategies for resource competition (nutrients, light, temperature) and metabolic rates, as well as their morphological features (for instance, settling velocity). The CSR functional group classification was originally developed for terrestrial plants and then adapted for phytoplankton

(Bernhardt et al., 2008 and references therein). The CSR system could help predict the type of abundant phytoplankton based on the available environmental parameters.

Diatom, cyanobacteria, and green-algae fall within the R ('disturbance tolerant ruderals'), S ('stress-tolerant') and C ('competitors') groups, respectively (Huszar & Reynolds, 1997; Colin S Reynolds et al., 2002; Colin S Reynolds, 2006). The R group has high maximum growth rates and higher metabolic losses, strong phosphorus and weak nitrogen competitors, lower tolerance to low light availability, low-temperature optima, silica requirements, and high sinking velocities. The environments favouring the R group tend to have high nutrient availability and intense turbulence. Meanwhile the S group has low maximum growth and metabolic rates, weak phosphorus and strong nitrogen competitors, higher tolerance to low light availability, low settling velocities, high-temperature optima, and higher shading effects (i.e., filamentous cyanobacteria). Environments favouring the growth of the S group tend to have low nutrient concentrations and low turbulence. Finally, the C group stands as an intermediate group between the two extremes: ruderal phytoplankton species (i.e., diatoms), and stress-tolerant species (i.e., cyanobacteria followed by dinoflagellates).

Additionally, latitude has been found to be uncorrelated with phytoplankton, with few phytoplankton taxa being exclusively found in temperate or tropical latitude. For example, *Aulocoseira (Melosira) granulata* is widely distributed and abundant in Europe, North America, and other temperate locations, but is also abundant and important at tropical latitudes in South America, Africa, and Southeast Asia (Lewis Jr, 1996).

### 2.3.3 Chlorophyll-a as a Proxy for Phytoplankton

Chlorophyll-a is a coloured pigment that functions as a sunlight receptor to use in photosynthesis. It is found in plants and all phytoplankton groups. There are several types of chlorophyll: chlorophyll-a, b, c, d, and e. Among all the various kinds of chlorophyll, chlorophyll-a has been used in numerous prior studies as a proxy for phytoplankton biomass. The first main reason for this is that chlorophyll-a is found in all phytoplankton groups. Phytoplankton contains different sets of chlorophylls; for example, cyanobacteria have chlorophyll-a, b, and d, and chlorophyte contains chlorophyll-a and b (Björn et al., 2009). The second major reason for the use of chlorophyll-a as a proxy for phytoplankton biomass is because there are uncertainties with the measurement of other chlorophyll types (UNESCO 1966). And finally, chlorophyll-a exhibits the strongest reflection of energy in the green light spectrum as compared to other chlorophyll types (Milne et al., 2015).

Chlorophyll-a concentrations are typically determined using spectrophotometry. Spectrophotometry is a method to measure how much light a chemical substance absorbs at a specific wavelength. The method is based on the principal that each compound absorbs or transmits light over a certain range of wavelengths (LibreTexts, 2020). For chlorophyll-a in chlorophytes, for instance, the spectrophotometer beams light through the sample solution and measures absorbance of the 677nm wavelength (Brown, 1969). Generally, chlorophyll-a absorbs most strongly in the violet-blue and orange-red part of the light spectrum, with absorption maxima located at c. 433 nm (blue) and c. 686 nm (red) (Hunter et al., 2008), as shown in Figure 2-5.

Chlorophyll-a concentrations also can be measured by a fluorometer that records the light fluorescence of chlorophyll-a at a specific length. Specifically, when photosynthetic tissues/organisms are illuminated by photosynthetically active radiation (PAR), which is light between approximately 400–700 nm wavelengths, these tissues emit red to far-red light. Chlorophyll-a fluorescence intensity of red to far-red light is found to be inversely proportional to the fraction of energy used for photosynthesis (Kalaji *et al.*, 2017 and references therein).
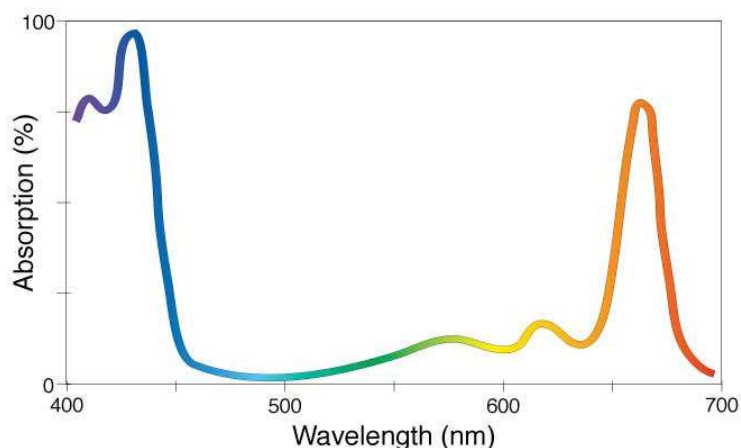


Figure 2-5 Absorption spectrum of chlorophyll-a (after (Schirber, 2013))

Compared to spectrophotometry or fluorometric methods, direct phytoplankton biomass calculation processes involve elaborating phytoplankton samples then subsequently calculate their biomass. These processes are labour-intensive, and because there is variability in the phytoplankton chlorophyll-to-carbon ratio (Felip and Catalan, 2000 and references therein), it requires investigators with taxonomic skills (Kasprzak *et al.*, 2008 and references therein).

In relation to eutrophication studies, a number of studies in the 1970s (Dillon & Rigler, 1974; Jones & Bachmann, 1976; Sakamoto, 1966) found strong correlations between chlorophyll and phosphorus in temperate lakes. Not long after those publications, Carlson (1977) proposed the Trophic State Index (TSI). The TSI represents the trophic index for a particular lake based on Secchi

disk transparency, chlorophyll-a, and total phosphorus. Both the chlorophyll - phosphorus relations and TSI depend on the assumption that phosphorus is the primary limiting factor for phytoplankton growth.

The publication of chlorophyll - phosphorus relationships and TSI are said to be the driving force for the subsequent use of chlorophyll-a as a surrogate for algal biomass in lake research, regulation and management (Canfield Jr et al., 2019; Yuan & Jones, 2020). The wide use of these findings is further enhanced by the fact that chlorophyll-a is more easily measured with smaller budgets than algal biomass, while also representing a readily visible indicator of trophic status (Dillon et al., 1988). In recent times, the availability of ocean colour satellite images, which are used to determine the chlorophyll-a concentration in the water, further encourage the use of chlorophyll-a as a proxy for algal biomass.

Both the strong chlorophyll - phosphorus relations and TSI were originally observed and established for temperate lakes, but another study (Brylinsky & Mann, 1973) has also found that the very strong correlation between chlorophyll-a and phytoplankton biomass (with correlation coefficients of up to r=0.98) is also preserved in lakes and reservoirs, not only in temperate regions, but tropical to arctic regions too.

More recently  (Kasprzak et al., 2008) found that there are differences in the precision of chlorophyll-a derived phytoplankton biomass across the trophic gradient of lakes. In oligotrophic lakes, phytoplankton biomass calculated from chlorophyll-a tends to be higher than the biomass derived from microscopic counts. Furthermore, for mesotrophic and eutrophic lakes, there is a respectively an increasing trend of underestimation.

For the purpose of calculating primary productivity in water bodies, chlorophyll-a as a proxy for phytoplankton biomass is still debatable. Brylinsky and Mann (1973) suggested that chlorophyll-a concentration is a good indicator of nutrient conditions, but for estimating gross phytoplankton production, not only the chlorophyll-a itself but a combination of chlorophyll and variables related to energy, such as solar radiation, is also required.

As for lake management applications involving the determination of total phosphorus from chlorophyll-a concentrations, this is a topic that remains under research. A very recent study used extensive (13000 pairs) data from lakes in Europe and North America to identify and recommend the use of chlorophyll-a as a phytoplankton biomass proxy in circumstances when resources are limited (Canfield Jr et al., 2019). Another recent study that used data from 3874 lakes distributed across 47 countries around the world (Quinlan et al., 2021) found that 44% of the variation of total phosphorus and chlorophyll-a values can be explained by a sigmoidal relationship. This

implies that there is a range of values within which total phosphorus and chlorophyll-a have a linear correlation, and below and above that range, there is no apparent relationship. The nonlinear segments of the relationship best-described lakes located in very cold (mean annual temperature =−10 C) and hot (> 25 C) climates. The very cold lakes are dominated by lakes with low total phosphorus concentrations, and the very hot lakes are mostly lakes with high total phosphorus concentration. The study also emphasised that there is a high degree of variability in chlorophyll-a between lakes at similar total phosphorus levels, that is controlled by the variability of the physical characteristics of the lakes such as mean depth, Secchi depth, and elevation. The study suggested that the variability highlighted the difficulty in simply decreasing nutrient inputs to manage eutrophication in lakes worldwide. But it also shows that although some existing knowledge can be used as guidelines, each lake needs to be studied, to be able to set its own standard or model for its water quality management.

# Chapter 3     Study Area: Tonle Sap Lake

## 3.1   Geographical Setting

The Mekong River is an international river that flows through 6 countries: China, Myanmar, Lao PDR, Thailand, Cambodia and Vietnam (Fig 3-1). The Mekong River Basin can be divided into two parts: the Lower Mekong Basin and the Upper Mekong Basin. The Upper Mekong Basin comprises 23% of the total catchment area (some 185,000 km$^2$) and is located mainly within China and Myanmar. The remaining 77% is known as the Lower Mekong Basin, which covers an area of 625,000 km$^2$ encompassing Lao PDR, Thailand, Cambodia and Vietnam (Kamoto & Juntopas, 2007). In Vietnam, the Mekong River flows through a complex delta system (MRC, 2005), before entering the South China Sea.



Figure 3-1 Mekong River basin by Kamoto & Juntopas (2007)

One of the key features of the Lower Mekong basin is the Tonle Sap Lake, also known as Cambodia's Great Lake, which is situated in the central plains of Cambodia (Fig 3-2). The Tonle Sap Lake is linked to the Mekong by the Tonle Sap River, the two rivers joining at the so-called 'Chaktomuk Junction' in Phnom Penh. The lake and its surrounding floodplains form the largest freshwater body in Southeast Asia (Kummu et al., 2014), with the drainage basins that feed the lake covering an area of approximately 85,786 km$^2$, which is roughly 43% of Cambodia's total land area (Sokhem & Sunada, 2006).
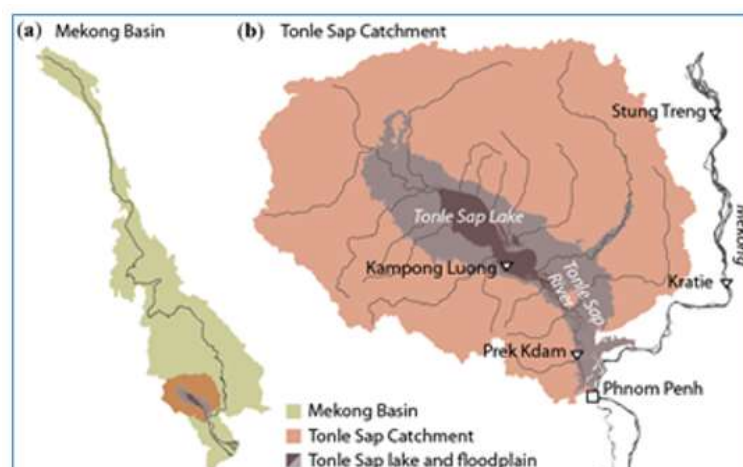


Figure 3-2 Mekong basin, Tonle Sap catchment and Tonle Sap Lake and floodplain (from Keskinen *et al.*, 2015).

## 3.2 Hydrology of Tonle Sap Lake

The Tonle Sap Lake is fed throughout the year by its tributaries and by direct rainfall on its surface, but during the rainy season it also receives water from the Mekong River (see below) (Fujii et al., 2003; Morishita, Garsdal and Manusthiparom, 2004 in Kummu et al., 2006). In fact, the majority (53.5%) of water entering the lake originates from the Mekong main stem, with the lake's tributaries playing a secondary (but important) role, contributing 34%, while 12.5% of the lake's water is derived from precipitation (Kummu et al., 2014). The average of water residence time of Tonle Sap Lake is estimated 71 days (see Appendix C for details).

The hydrological behaviour of the Tonle Sap Lake is largely influenced by the hydrological fluctuations of the Mekong River (Sithirith, 2015). In particular, differences between the water level in the lake and the water level in the main-stem of the Mekong cause an unusual flow reversal to occur in the Tonle Sap River. Specifically, during the flood season (June - October), the water in the Mekong rises to levels that are higher than those in the Tonle Sap Lake. The resulting adverse pressure gradient forces the Tonle Sap River to change its flow direction back towards the Tonle Sap Lake, in effect 'sucking in' water from the Mekong main-stem. During the dry season,

starting in late September when the water level in the Mekong main-stem falls, water flows back out of the lake down the Tonle Sap River and into the Mekong. Importantly, this means that during the driest part of the year, from December to February, water from the lake provides approximately 50% of the total water flow to the Mekong delta (Fujii et al., 2003; Morishita et al., 2004), thereby playing an important role in modulating dry-season water availability in this agriculturally productive region.

In the wet season, with the inflow of considerable volumes of water from the Mekong, the Tonle Sap Lake increases in area six-fold, and tenfold in depth as compared to the dry season values (Fig 3-3). Specifically, the areal extent increases from 2,500-3,000 km$^2$ to 10,000 - 16,000 km$^2$ (Fujii et al., 2003; MRC, 2005). The incoming water from the Mekong causes flooding that extends over a large floodplain, covering forests, shrubland and rice fields (Chadwick & Juntopas, 2008). As a result, the water volume stored within the Lake increases over 60-fold, from about 1.3 km$^3$ up to 60 - 80 km$^3$ depending on the flood intensity (Kummu et al., 2006). The size of the lake also expands from 160 km long and 35 km wide, to 250 km long and 100 km wide (Keskinen et al., 2011) as the Mekong maximum and the peak of the South-West monsoon's precipitation culminate in September and early October (MRC, 2005). During the wet season, the Tonle Sap Lake, therefore, acts as an important zone of flood storage that helps to significantly attenuate flood levels in the Mekong River downstream of Phnom Penh.
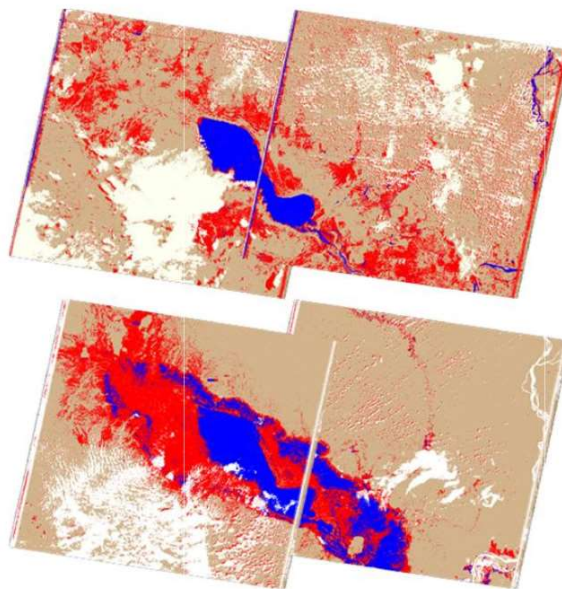


Figure 3-3 Tonle Sap Lake at the start (above) and peak (below) of the wet season, captured by Landsat 5 TM in October 2011 (Azman et al., 2016). Blue, red, brown and white colors are water body, flooded areas, land, and cloud.

## 3.3   Societal Significance of the Tonle Sap Lake

The Tonle Sap Lake plays an important role in the economic, ecological and socio-cultural life of Cambodia and, indeed the broader South East Asia region. To illustrate the significance of the lake, it has been estimated that more than 4.5 million people live within the Tonle Sap Basin, while about 1.2 million Cambodians, in approximately 160 communes, live on the lake's floodplains (Chadwick & Juntopas, 2008). Approximately 1.7 million people are directly dependent on its rich natural resources for their livelihoods (Keskinen et al., 2011).

Due to the large scale of the exchanges of water between the Mekong River and the Tonle Sap Lake, the Tonle Sap functions as a natural floodwater reservoir for the Mekong system as a whole and therefore is an essential source of water for the Mekong Delta during the dry season (Kummu et al., 2005). The reverse flow from Tonle Sap is vital to balance the Mekong Delta in Vietnam during the dry season, ensuring freshwater flow into the Mekong Delta and protecting against seawater intrusion. In the wet season, the Tonle Sap Lake functions as a floodwater storage reservoir: thus, the Mekong Delta would experience much higher water levels during the flood season without the reverse flow of a portion of the Mekong River water into the Tonle Sap Lake.

These inflows and outflows also enrich local fisheries (Kummu et al., 2006). The lake is reported to be a highly productive ecosystem (Rainboth, 1996; Sverdrup-Jensen, Bishop, Clayton, Barlow, & Commission, 2002). It has been estimated that the fishery, in particular, provides 68-75% of the animal protein in the average Cambodian's diet, a figure that is even higher for the communities surrounding the lake itself (Chadwick & Juntopas, 2008). The average fish consumption per capita is the highest in the Mekong region, and this relatively cheap source of protein is very significant for the mass poor who make up around a third of the population (MRC, 2010b).

Fisheries from the Tonle Sap provide supplies of fish not only to Cambodia but also to neighbouring Mekong countries. It also generates employment and income both inside and outside Cambodia via regional and international value chains from Tonle Sap's "farm gate" to markets in Thailand, Vietnam, other Asian countries, Europe and North America (Chadwick & Juntopas, 2008). In terms of its economic value, the overall fishing sector accounts for 10 to 12% of gross domestic product (GDP) and contributes more to income, jobs and food security than in any other country (MRC, 2011).

Cambodia is located in an ecologically rich tropical region classified as Indo-Burma Biosphere Hotspot (Birdlife International, 2007) by the International Union for Conservation of Nature (IUCN) (Baromey, 2008). Indeed, Tonle Sap lake itself is categorised as a Biosphere Reserve area by UNESCO for its ecological diversity (MRCS/UNDP, 1998). Tonle Sap lake is a habitat for

numerous species of algae, higher plants, aquatic invertebrates, fish, amphibians, reptiles, birds, and mammals (I. C. Campbell et al., 2006).

Tourism in Cambodia is of growing economic importance. The annual GDP growth of this sector is 7.2% on average for 2011 to 2015, and is estimated to remain the same for the next five years, with a total contribution to Cambodia's GDP at 32.4% of GDP in 2017 (OECD, 2019). As a tool to reduce the poverty rate, tourism is considered a significant mitigation mechanism to help rebuild the country's economy and enhance global political, cultural and economic integration by the government of Cambodia (Baromey, 2008). One of the tourism attractions in Cambodia is eco-tourism to Tonle Sap lake. Floating villages, lake cruises and floating restaurants are some activities enjoyed by the visitors in Tonle Sap lake.

## 3.4   Environmental Threats to the Tonle Sap Lake

The Mekong Basin is undergoing rapid development, including deforestation (FAO, 2006; Shi, 2008), the introduction of large irrigation schemes (Hori, 2000; Kummu, Varis, et al., 2008), intensification of agriculture, and the construction of hydropower dams with large reservoirs (Grumbine & Xu, 2011; Hori, 2000; King et al., 2007; Kummu et al., 2010; MRC, 2008). These alterations are predicted to change the hydrological regime of the Mekong River and the Mekong Basin as a whole. Findings in a recent study indicate that hydropower operations have already considerably modified river discharges since 2011, with the largest changes to date being observed in 2014. In Kratie, Cambodia there were 41–74% increases in March-May 2014 and 0–6% decreases in July-August 2014 discharges (Räsänen et al., 2017).

The Cambodian floodplains and the Mekong Delta receive over 90% of their available water resources and 95% of the total suspended sediment flux from the Mekong upstream (Kummu et al., 2014). Thus, changes in the Mekong Basin have the clear potential to impact on the hydrological regime (and hence associated livelihoods) affecting the Cambodian floodplains and the Mekong Delta. As the ecosystem in the Tonle Sap Lake is driven by the flood pulse that exchanges flow from and to the Mekong River, changes in the Mekong River will also alter the Tonle Sap River flow and therefore could potentially affect the Tonle Sap Lake ecosystem on which so many people depend (see Section 3.3).

Alteration to the Tonle Sap flow regime will likely result in a decrease in annual water level (Arias et al., 2014). A recent study (D. Li et al., 2017) shows evidence that the operation of dams reduces streamflow in wet seasons and increases the streamflow in dry seasons, observations that are consistent with the modelling predictions of Arias *et al.* (2012). A reduction of 23% and 11% in the water rising and falling rates, respectively, at Prek Kdam (a gauging station on the Tonle Sap River,

marked in Figure 3-2), provides evidence of a diminished Tonle Sap flood pulse post-1991 (Cochrane et al., 2014).

In addition, a simulation study on flooding in Tonle Sap lake (Arias et al., 2012) found an increase in the area of open water of 22% owing to the water-related development in a 20 year period, where the impact simulated conditions in 2030. This study also found that changes in ecological habitats has actually happened. For example, an area in the vicinity of Tonle Sap Lake which was previously defined as shrubland (flooded for 5-8 months in an average hydrological year) has been newly defined as gallery forest (flooded for 9 months in an average hydrological year). If the lake level rises as predicted, part of the seasonally flooded forest in the vicinity of the Tonle Sap Lake would remain inundated throughout the year, which could destroy it (Kummu et al., 2005).

Although the impact is less than that from water-related development in the Mekong River, global climate change is also predicted to be contributing to the alteration of the Tonle Sap ecosystem (Arias et al., 2012; Keskinen et al., 2015). The global climate change will lead to average and maximum water levels that are predicted to increase (up to 0.2 meter and 0.3 meter respectively) during the period 2010–2049 (Västilä et al., 2010).  The area of open water of the Tonle Sap Lake is projected to increase from 2%–21%, also owing to climate change (Arias et al., 2012). In another study the increase is predicted to be up to 31% (Keskinen et al., 2015). Projections (up to the year 2042) from the same study show that climate change is likely to lead to substantial change in the flooded area, where the future floodplain is estimated to be varying from 92% to 109% of the current average floodplain. More complicated, shifts in tropical cyclones as the result of climate change are also found to reduce suspended solid delivery to the Mekong delta (Darby et al., 2016).

Threats to the Tonle Sap ecosystem are not only coming from the two aspects (developments in the Mekong Basin and climate change) elaborated above, but also from within the country itself. For example, local development and the fast-growing population are increasing pressure on its natural resources (Chadwick & Juntopas, 2008; Salmivaara et al., 2016). For example, the area of the seasonally flooded forest in the vicinity of the Tonle Sap Lake is decreasing because of illegal logging and increasing demand for wood for fishing gear, boats and firewood. The forest is crucially important for the Tonle Sap ecosystem, forming a shelter for the floodplain and providing suitable conditions for fish to breed (Kummu et al., 2005). Deforestation impacts on hydrology and related processes, such as flooding, soil erosion and mass soil movement, society and the economy. The progressive disappearance of the flooded forest in the downstream Tonle Sap area, in turn, will be a serious threat to fish reproduction and refuges (FAO, 2011). With less

of the fish that used to eat mosquitoes, the Tonle Sap community is far more susceptible to mosquito-borne diseases like malaria and dengue fever.

As the nation's main livelihood is agriculture (Keskinen et al., 2015), demographic pressures also seem likely to require an intensification of agricultural activities. Agricultural activities need irrigation. Cambodia has far less land under irrigation than the other countries in the Lower Mekong Basin. Only 3.6% of the rice cultivation area is irrigated, which is only 2% of that in Thailand (Varis et al., 2006), one of the world's leading rice exporters. In the mainstream Mekong River, the increase of phosphorus (see the next section for the extent) is considered partly because of agricultural development (Liljeström et al., 2012). However, for the Tonle Sap lake, there has not yet been any evaluation of how agricultural intensification in Cambodia is impacting the lake. Moreover, as introduced in Section 2.2.1, Cambodia is one of the leading garment exporters in the world. Sadly, this industry is found as the biggest polluter (Muong, 2006) in the country. There are no published studies on the environmental impacts of this pollution, but effluent from garment industries may be a source of excessive nutrients, as elaborated in Section 2.2.1.

These considerations raise the issue of whether Cambodia's Great Lake may be at risk of trending to a eutrophic state. This risk is discussed further in the next section.

## 3.5 Eutrophication in Tonle Sap Lake

Despite its economic, ecological and historical-cultural importance, unfortunately little is known about the eutrophication status of Tonle Sap Lake and water quality monitoring efforts are woefully inadequate.

Indeed, there are only two studies that explicitly mention the eutrophication status of the Tonle Sap Lake. The first study was a study modelling the flow regime and water quality of the Tonle Sap, which included field measurements of physical-chemical and biological data, established only for a few months nearly two decades ago, in the summer of 2001 (Sarkkula et al., 2003). This study measured the water quality parameters at various points in the open lake around Chong Khneas River outlet and the south part of the lake. The study revealed that in the rainy months, inundated areas of Tonle Sap Lake are mostly anoxic, and during the dry season, the lake water is quite turbid, limiting the growth of phytoplankton, which is commonly estimated using chlorophyll-$a$ (see Section 2.3.3).

It also observed that both chlorophyll-a and the phytoplankton biomass peak in the low water period (which is in April). The results of the study by Sarkkula $et$ $al.$ (2003) also show that the high

phytoplankton biomass coincided with the highest TSS concentrations, which is during the low water period when wind-generated waves are able to re-suspend sediment deposited on the lake bed, making the water practically non-transparent. The writers argued that this phenomenon happened because the positive buoyancy of the *Anabaena*-filaments has kept them on the topmost centimetres of the surface water.

Overall, the Sarkulla et al study concludes that the traditional concept of eutrophication does not fit well into the Tonle Sap Lake. Massive algal blooms are not reported to be typical for the lake (at least at the time of their study), and the naturally high primary production is affected by the high-end production. The situation of the time shows the slightest increase in the nutrient loading would be offset by the fish production without negative side effects.

However, the second study (Burnett et al., 2017), published over a decade after the first one, clearly states that the Tonle Sap Lake can generally be considered eutrophic (and sometimes hypertrophic), based on observed chlorophyll-*a* concentrations within the lake (mean of 20 ± 15 μg/L in the high water season and 39 ± 25 μg/L in the low water season). The highest chlorophyll-*a* concentrations (64 μg/L) were found during the lowest water period. It may be inferred that a number of important changes may (recognising that the limited number of studies makes it difficult to have confidence in establishing trends) have occurred since the first study was published in 2003. Several big dams in the Upper Mekong River have become operational and are believed to be affecting both the hydrological regime and in turn, the nutrient fluxes, of the Mekong River. Due to the strong hydrological connection between the Mekong River and the Tonle Sap Lake, these changes have the potential to affect the Tonle Sap Lake.

Furthermore, an analysis based on data from 2000 to 2008 (MRC, 2010) shows evidence of increasing levels of phosphorus in the mainstream Mekong River. The maximum value increased from 0.2 mg/L to 0.5 mg/L in this period, albeit the median value adjusted only from 0.05 mg/L to 0.9 mg/L. Sharply growing levels of total phosphorus were observed since 2005, where the maximum value doubled from around 0.25 mg/L to 0.5 mg/L.

Moreover, Liljeström, Kummu and Varis (2012) found a steep increase (up to 3.41 ton/year) in nitrogen levels, again in the main Mekong River, over a 20-year time span (1985-2005), albeit with only a slight phosphorus increase (0.55 ton/year in Luang Prabang, Laos). Liljeström argued that the inconsistency of the results of the two studies regarding phosphorus comes from the difference in the time windows used in both observations, suggesting that in recent years the lake may have become more exposed to increasing levels of nutrients. This is consistent with a recent study that also found increasing nitrate concentration (up to 50%) in the Sesang, Sekong, Srepok

watersheds, three of the Lower Mekong's major tributaries, although there was also a projected decrease (up to around 30%) in the long term future (Oeurng et al., 2016).

However, nutrient monitoring on and around Tonle Sap Lake itself is scarce and often undertaken only as part of the broader study of Lower Mekong Basin. Chea, Grenouillet and Lek (2016) used Total Phosphorus (TP) and nitrate data measured by the Mekong River Commission to calculate the level of water quality in the Lower Mekong Basin, including Cambodia. They concluded that the Tonle Sap Lake is a pollution hotspot as several water quality indicators, including total phosphorus (TP) and dissolved oxygen (DO), were found to have levels higher and lower, respectively, than the main Mekong River. TP in the Tonle Sap Lake was found to be up to 0.230 mg/L, whereas TP in the main Mekong River (excluding the delta) is 0.075 mg/L at maximum. The DO at Tonle Sap Lake is in the range of 4.71 mg/L to 6 mg/L, compared to 6.10 mg/L to 8.10 mg/L in the mainstream of the Mekong River. These differences were evident within both the dry and rainy season and is possibly associated with agricultural development, urbanisation and industrial waste.

The Mekong River Commission (MRC) regularly monitors water quality on 48 stations in the Lower Mekong Basin, but there is only one gauging station located on Tonle Sap Lake, which is at Kampong Luong (see Figure 3-2 for the location), and the available data from this gauging station only from 1996 to 2017. Some of the very few studies about Tonle Sap lake water quality (Chea et al., 2016; Fukushima et al., 2017; Soum et al., 2021) use data from this gauging station, however whether it is representative of water quality conditions experienced elsewhere across the whole lake remains an open question.

Studies that focus on nutrient dynamics within the Tonle Sap Lake are very limited. Irvine *et al.* (2011) analysed trends in dissolved oxygen (DO) and turbidity of Tonle Sap Lake and found that there are seasonal and spatial trends in those water quality parameters as shown in Figure 3-4. DO levels declined by the end of October as the freshwater drained back down the Mekong and Bassac River. In August, when the water levels in the Tonle Sap lake rise, turbidity was increasing. Yet they argued that as the monitoring is conducted on a monthly basis, it is impossible to capture short-lived, extreme events such as night-time anoxia.
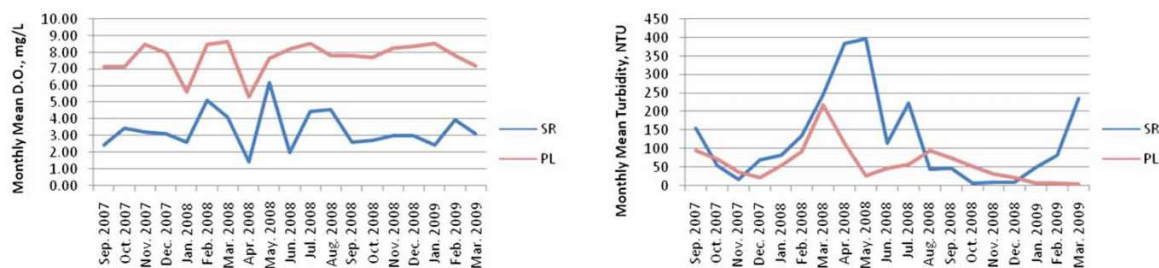
Figure 3-4 Monthly Mean Dissolved Oxygen (DO) (left) and turbidity (right), measured in Tonle Sap lake (SR) and the Mekong River (PL). From Irvine *et al.* (2011).

Burnett *et al.* (2013 and 2017) attempted to model the phosphorus budget of the lake. He found that the concentrations of dissolved inorganic phosphorus (DIP) in Tonle Sap River is almost twice that of Tonle Sap lake, i.e., 0.64µM and 0.38µM, respectively, but the groundwater has the highest concentration of 1.3µM. The groundwater contributes up to 35% of DIP to Tonle Sap lake, while the net flux from Tonle Sap River/Mekong River is as small as 4%. The tributaries account for almost half of the flux, but the calculation is based on the assumption that the DIP concentration in the tributaries is the same as that in Tonle Sap River. This is because there is no data about DIP concentration in the tributaries, which could be influenced greatly from human sources such as fertiliser and sewage.

Tonle Sap lake is the most studied area of the whole Mekong Basin. However, until now it has not been clear whether the Tonle Sap Lake is phosphorus limited or nitrogen limited. The pilot study elaborated previously (Sarkkula et al., 2003) stated that the lake most of the time is phosphorus limited and occasionally nitrogen limited, notably during the low water period. Burnett *et al.* (2017) agreed that the lake is phosphorus limited, at least for most of the time.

Being elusive, the nutrient fluxes on Tonle Sap Lake can be considered to be complex and variable because of its flood pulse characteristics. The nutrient dynamics of the main Mekong River is suggested to differ from tributary nutrient dynamics, as the nutrient fluxes of the mainstream are highest between July and September, whereas the peak months for the tributaries feeding the lake are June–October (Liljeström et al., 2012). The same study also found that water quantity movement does not correlate with the nutrient flux. Thus it can be hypothesised that even though more than half of the lake's water flows from the Mekong River, this may not be representative of the nutrients carried into the lake from that source. A study on nutrient fluxes, in particular regarding the eutrophication level of the lake, is clearly needed.

Furthermore, as significant urban development and population growth occur, the potential for the delivery of excessive nutrients from anthropogenic sources is increasing (e.g Irvine *et al.*, 2011; Liljeström, Kummu and Varis, 2012; Chea, Grenouillet and Lek, 2016; Oeurng *et al.*, 2016;

Burnett *et al.*, 2017). However, previous studies do not quantitatively assess those anthropogenic factors, in terms of sourcing excessive nutrients. Among the anthropogenic sources, fertilisation in the agricultural sector and from raw sewage needs the most attention in regards to the risk of eutrophication. Data shows a significant increase of imported NPK fertiliser products, from around 137,877 tonnes in 2002 to 433,120 tonnes in 2011, indicating a 210% rise in demand over a 10-year period (Theng et al., 2014). Nevertheless, this amount is not as much as in neighbouring countries, such as Myanmar or Thailand (Yu & Diao, 2011); the vast majority of Cambodian farmers use animal manure as natural fertilisers.

Raw sewage discharges also need to be considered in order to analyse the eutrophication level of the Tonle Sap Lake. Cambodia in particular discharges 84% of its sewage directly into inland water bodies (World Bank, 2008).

The most visible eutrophication sign i.e., phytoplankton blooms, have occurred in Tonle Sap lake near Siem Reap, a famous tourist destination, for example in February 2012 (Fukushima et al., 2017) and more recent blooms have been reported also by local people who assisted during the fieldwork of this study. Yet, despite these shreds of evidence, and the importance of Tonle Sap lake to the regional economy, to date there has not been a systematic appraisal of spatial and temporal trends in water quality that would provide the guidance necessary to assess the possible risk of eutrophication in the Tonle Sap lake. Even where the limited data do exist (see studies cited above), the vast spatial extent of the lake means that each of its feeder basins has different characteristics (I. C. Campbell et al., 2006), further compounding the challenge of analysing the lake's water quality. With the fact that Cambodia is extremely prone to two water-related natural disasters: drought and flood, which are predicted to become more extreme under climate change (Arias et al., 2012; Keskinen et al., 2015; Oeurng et al., 2019), long term data would be very helpful in establishing conceptual models of water quality parameters against water availability. It is for this reason that the potential of remote sensing to retrieve estimates of long-term (multi-decadal) trends in water quality over the large spatial extent of the lake is explored in Chapter 4.

# Chapter 4 Methodology: Using Satellite-Based Remote Sensing to Estimate Water Quality Trends in Tonle Sap Lake

In sections 4.1 and 4.2, the background literature on using remote sensing to estimate key water quality parameters is reviewed. In the subsequent sections of this chapter, the various stages of the methodological workflow, as applied to the specific case of the Tonle Sap Lake, are developed. Thus, in 0, the various field data sets used to build site-specific calibrations linking TSS and chl-a to surface reflectance properties (as derived from satellite images) are outlined, the development and testing of these calibrations being the subject of section 4.4. In section 4.5, details of the specific focus areas within Tonle Sap Lake are provided, along with an overview of the number of images within the study period (1990-2019) that are affected by cloud cover. Finally, in section 4.6, details of the statistical tests used in the analysis of Landsat-based estimates of TSS and chl-a during 1990-2019 are outlined.

## 4.1 Water Quality Monitoring from Space

Traditional methods of data collection for water quality monitoring typically require in situ sampling, then returning the samples to the laboratory to measure various water quality indicators (e.g., chl-a and TSS). The extensive efforts involved in water sampling (Hunter et al., 2009) are time-consuming and expensive, and the data collected is prone to measurement errors and often has gaps in either (or both) the temporal or spatial coverage (Guanter et al., 2010). In terms of cyanobacterial blooms, traditional approaches are very often not suitable as such blooms are both short-lived and widely dispersed in space (L. Li & Song, 2017 and references therein), making it challenging to sample them directly.

Cost is a common factor that hinders water quality monitoring, particularly in developing countries. Even in many developed countries, the standard traditional mapping and monitoring techniques used for water quality monitoring of lakes and other water bodies are considered too expensive, where sample collection would use up 70% of the total cost (Caughlan & Oakley, 2001).

The advent of satellite-based remote sensing technology has allowed measurements on a global scale, covering large and remote areas, and the archive of historical satellite images now also covers a relatively long period of time. Satellite-based remote sensing has proved useful in monitoring coastal waters, estuaries, lakes and reservoirs, and is relevant to water quality

managers (e.g., Haag et al., 2009). Remotely sensed earth images, which now are frequently accessible to the public at no cost, therefore provide an opportunity to build an achievable water quality monitoring system. UNESCO, through its International Initiative on Water Quality (IIWQ) provides supports to its member nations in responding to water quality challenges and has launched the first comprehensive worldwide water quality online portal for freshwater systems, lakes and rivers, retrieved from satellite-based earth observation data (worldwaterquality.org), to assist with global water quality assessment and capacity building.

Water quality parameters commonly estimated based on the use of remote sensing images include color, dissolved organic matters, total suspended solids, chlorophyll-a, algal blooms, and macrophyte abundance (D. R. Mishra et al., 2017). The use of remote sensing typically involves methodologies that are based on directly observing the optical properties of the water surface, i.e., the characteristics of the water surface in reflecting, absorbing or scattering the sunlight, and then inferring water quality properties (e.g., suspended organic and inorganic particles and dissolved substances) through their impacts on the optical characteristics.

Fortunately, it has been shown in extensive prior work that numerous water constituents show distinctive spectral features. For example, an absorption peak around 675 nm is related to the presence of chlorophyll-a (Bricaud et al., 1995; G. Campbell et al., 2011; Gilerson et al., 2010; Matthews & Bernard, 2013). Similarly, TSS in low concentrations interacts with light in the wavelengths of 440 nm or 550nm (Giardino et al., 2017), while TSS in high concentrations produce a signal in the water reflectance of 700 nm and beyond (Ruddick et al., 2006). Consequently, the content of some water quality parameters can be estimated by remote sensing.

The concept of the detection of spectral variations in the water-leaving radiance has provided the basis for various satellite missions focused on ocean monitoring (Table 4.1). These satellites have been specifically designed to carry sensors with suitable spectral and spatial resolutions capable of detecting marine pollutants and some other water quality parameters. Indeed, the success of satellite image utilisation for marine water quality monitoring has opened the possibility of expansion to the monitoring of inland water bodies (Table 4.1). Inland water bodies are more challenging as their optical properties are significantly influenced by other constituents, such as mineral particles and colored dissolved organic matter (CDOM), and their concentrations do not covary with phytoplankton (Mobley et al., 2004; Palmer et al., 2015). These characteristics are different from the ocean, whose optical properties are determined mainly by phytoplankton and other covarying compounds, such as CDOM (Ogashawara et al., 2017).

Table 4-1 Satellites Used for Water Quality Monitoring

| Satellite and Sensor | Spectral Band Range | Revisit Time | Spatial Resolution | Operational Lifetime | Intended Use |
|---|---|---|---|---|---|
| CZCS | 6 spectral bands (443 to 750 nm) | - | 800 meters | Oct 1978 - June 1986 | Ocean Color |
| SeaWiFS | 8 spectral bands (412 to 865 nm) | 1 day | 1 km and 4 km | August 1997 - Dec 2010 | Ocean Color |
| MODIS | 36 spectral bands (620 – 14385 nm) | 1 or 2 days | 250m or 500 m or 1000m | 1999 (Terra sensor)/ 2002 (Aqua Sensor) - present | Ocean color and atmospheric parameters |
| VIIRS | 22 spectral bands (402 to 1249 nm) | 14 hours | 375m or 750m (resampled to 500m and 1km) | Oct 2011 - present | Ocean color |
| MERIS | 15 spectral bands (390 to 1040nm) | 35 days | Ocean: 1040m x 1200m Land: 260m x 300m | 2002 - 2012 | Ocean color and terrestrial-monitoring |
| Sentinel 2 | 12 spectral bands (443 to 2190 nm) | 5 days | 10m or 20m or 60m | June 2015 - present | Terrestrial monitoring |
| Sentinel 3 OLCI | 21 spectral bands (400 to 1020nm) | 27 days | 300 m and 1.2 km | 2016 - present | Ocean color |
| Landsat 5 TM | 7 spectral bands (450 to 2350 nm) | 16 days | 30 m or 120 m | March 1984 - Jun 2013 | Terrestrial monitoring |
| Landsat 7 ETM+ | 8 spectral bands (441 to 896 nm) | 16 days | 15 m or 30 m 60 m | Apr 1999 - present | Terrestrial monitoring |
| Landsat 8 OLI | 11 spectral bands (430 to 1251 nm) | 16 days | 15 m or 30m or 100m | 2013 - present | Terrestrial monitoring |

Table 4-1 provides an overview of the satellites typically used for water quality monitoring. A number of satellites originally launched for other more general monitoring of the landscape (such as Landsat and Sentinel) are also often used for inland water quality monitoring, given their accessibility and finer spatial resolutions. CSCZ (Coastal Zone Color Scanner) was launched as a proof of concept for ocean color measurement utilising satellite technology. The CSCZ sensor was boarded on the Nimbus-7 satellite and needed to share its power source and data recorder with other instruments on the satellite. As a result, data collection was not uniform in time or space (NASA, n.d.-a). Although intermittent, satellite images from CSCZ provided insights into phytoplankton concentrations in some coastal areas during the 1980s (Luis & Kawamura, 2004).

Following the success of CSCZ, SeaWiFS (O'Reilly et al., 1998) was launched on the Orb View-2 satellite to monitor ocean biological activity. It has a very high temporal resolution (1 day) but a poor spatial resolution (4 km for the readily used images). Nevertheless, it was the first satellite sensor that enabled the estimation of global chlorophyll biomass values (e.g., Uitz *et al.*, 2006) or global ocean primary production (e.g., Arrigo, van Dijken and Bushinsky, 2008). After 13 years of operation, in 2010, SeaWIFS stopped sending communications to its earth-based station.

MODIS instruments are carried by two satellites: Terra that passes the earth from north to south across the equator in the morning, and Aqua that passes south to north over the equator in the afternoon (NASA, n.d.-b). Having morning and afternoon sensors allow observations of changes that occur over the course of the day, such as sea or land surface temperature. As with SeaWiFS, with its very high temporal resolution, MODIS is useful to track changes in the landscape over time, for example, the monitoring of vegetation health.

The Visible Infrared Imaging Radiometer Suite (VIIRS) is aboard the National Oceanic and Atmospheric Administration's polar-orbiting NOAA-20 satellite. VIIRS is designed to expand upon data taken by MODIS, with global coverage every 14 hours as the result of having a wider swath width. VIIRS has a higher spatial resolution, visible capabilities for night-time imaging using the day/night band, and is very light-sensitive in that it can catch not only light from cities but also areas of wildfires or gas flaring that occurs as a result of oil and gas extraction (Hillger et al., 2013; Schroeder et al., 2014).

Meris is one of the instruments in ESA's (European Space Agency) Envisat (environmental satellite) mission which is launched to improve environmental study. MERIS measures the reflectance of the earth. Although MERIS has a low spatial resolution (1 km) for ocean areas,

many algorithms for estimating chlorophyll-a concentrations from surface reflectance have been built based on MERIS wavelength (e.g., Dall'Olmo, Gitelson and Rundquist, 2003; Moses *et al.*, 2009; Mishra and Mishra, 2012). The lost communication between the Envisat satellite and its earth control station limits MERIS images to only ten years of data.

Sentinel missions replaced the Envisat program, providing continuity of land and ocean monitoring. Newly launched, they can only provide data a few years back; hence are not suitable for studies that require a long period. Sentinel-2, although designed for terrestrial monitoring, with its fine spatial resolution, is also used for water applications (e.g., Pahlevan *et al.*, 2020).

In this study, the Landsat family is used. Particularly for field data calibration, Landsat 8 OLI is used. The principal advantage afforded by Landsat is that the Landsat platforms together provide the longest continuous global data collection, which is now approaching 50 years (Wulder et al., 2019).  Depending on the parameters to be monitored, Landsat's revisit period of 16 days can hamper its ability to observe daily changes (compared, for example, to MODIS, which has 1 or 2 days of revisit day). Nevertheless, the 30 meters spatial resolution for all Landsat visible and NIR bands (compared to MODIS with 250 meters/500 meters/1 km resolution) can provide an opportunity to observe waterbodies in detail. The freely available nature of Landsat data also affords a significant advantage when undertaking water quality monitoring in countries of the Global South where other water quality monitoring programs are weakly established, for example, the UNESCO's International Initiative on Water Quality (IIWQ) program that has been explained previously.

Landsat has been used for estimating water quality in inland water bodies in a wide range of previous studies for rivers (e.g., eKuhn et al., 2019; Mertes et al., 1993; J. Wang et al., 2009), reservoirs (e.g., Bernardo et al., 2017; Ledesma et al., 2019), and lakes (examples in Subsections 4.2.1 and 4.2.2), for various water quality parameters (see section 4.2 below).  Overall, these studies demonstrate that the OLI sensor, although not specifically designed for coastal or ocean monitoring, can provide robust estimates of the water quality properties of freshwater bodies (Pahlevan et al., 2014).

## 4.2    Prediction of Freshwater Lake Water Quality Parameters using Landsat Imagery

The literature suggests that Landsat has spectral and spatial characteristics that are suited to monitor the water quality of small water bodies such as lakes, water reservoirs, rivers, or estuaries. For freshwater environments, the water quality parameters that have been estimated

in prior studies with Landsat images are various. The most common ones are chlorophyll-a concentrations, water clarity in the form of SDD (Secchi Disk Depth), turbidity, and Total Suspended Solid concentrations.

Chlorophyll-a studies have been conducted in the Norfolk Broads, UK with Landsat TM data (Baban, 1993), in lakes in South East Australia (D. J. Carpenter & Carpenter, 1983), Lake Beysehir, Turkey using Landsat TM (Nas et al., 2010), Reelfoot Lake, Tennesse with Landsat TM (Wang et al., 2006), lakes in The Ozark/Ouachita-Appalachian Forest ecoregion (OOAF), Oklahoma with Landsat TM and ETM+ (Barrett & Frazier, 2016), Minnesota Lake with Landsat TM (Brezonik et al., 2005), Río Tercero Reservoir in Argentina using Landsat TM and ETM+ images (Bonansea et al., 2015), Lower Peninsula of Michigan with Landsat TM imageries (Torbick et al., 2013), a geodatabase consists of around 8000 lake data in northern Poland, using Landsat OLI (Urbanski et al., 2016), Beaver Reservoir in Arkansas, USA with Landsat TM (Sudheer et al., 2006), Lake Columbia Water Supply Reservoir with Landsat TM (Kulkarni, 2011), Chagan lake in China Landsat TM (Song et al., 2011), hypereutrophic Qaraoun reservoir using Landsat ETM+ and Landsat OLI (Deutsch et al., 2018), Lakes Yenicaga and Abant, Turkey with Landsat ETM+ (Karakaya et al., 2011), reservoirs with contrasting trophic states in Zimbabwe, using Landsat OLI (Masocha et al., 2018), lake Tana Eithopia with Landsat ETM+ (Moges et al., 2017), Lake Kissimmee, Florida with Landsat TM (Chebud et al., 2012), and the hypertrophic Albufera de Valencia lake in Spain using Landsat TM and ETM+ (Dona et al., 2015).

Many of those chlorophyll-a studies also estimate water clarity (denoted as Secchi Disk Depth) from Landsat imageries, for example, the studies in the Norfolk Broads, UK (Baban, 1993), Lake Beysehir, Turkey (Nas et al., 2010), Reelfoot Lake, Tennesse (Wang et al., 2006), Río Tercero reservoir (Argentina) with TM and ETM+ (Bonansea et al., 2015), Lower Peninsula of Michigan (Torbick et al., 2013), 8000 lakes in northern Poland (Urbanski et al., 2016), Albufera de Valencia lake in Spain using Landsat TM and ETM+ (Dona et al., 2015), Qaraoun reservoir In Lebanon (Deutsch et al., 2018), Lakes Yenicaga and Abant in Turkey (Karakaya et al., 2011). Other studies on water clarity are in lakes of two river basins located in southern Finland Landsat ETM+ (Kallio et al., 2008), Lake Michigan with Landsat TM (Lathrop, 1992), Manzala Lagoon, Egypt with Landsat TM (Dewidar & Khedr, 2001), Gulf of Finland (Yuanzhi Zhang et al., 2003), Himalayan lake with Landsat OLI (Mushtaq & Nee Lala, 2017), 10000 of Minnesota lakes (Olmanson et al., 2002), Songhua River basin's with Landsat TM, ETM+ and OLI (Tao et al., 2021) and Lake Chicot in Arkansas using Landsat MSS (Harrington Jr et al., 1992).

Many of those studies also attempted to predict turbidity from Landsat data. For example the studies in Lake Beysehir, Turkey (Nas et al., 2010), Reelfoot Lake, Tennesse (Wang et al., 2006),

The Ozark/Ouachita-Appalachian Forest ecoregion (OOAF), Oklahoma (Barrett & Frazier, 2016), Lakes Yenicaga and Abant in Turkey (Karakaya et al., 2011), reservoirs in Zimbabwe (Masocha et al., 2018), Lake Columbia Water Supply Reservoir (Kulkarni, 2011),  lake Tana Eithopia (Moges et al., 2017), Lake Kissimmee, Florida (Chebud et al., 2012), Lake Chicot in Arkansas (Harrington Jr et al., 1992). There are also other studies on turbidity prediction in lakes in South East Australia with Landsat MSS (D. J. Carpenter & Carpenter, 1983), in Nebraska Sand Hills lakes suing Landsat TM (Fraser, 1998), El Guájaro reservoir, Colombia suing Landsat OLI (González-Márquez et al., 2018), in lakes of two river basins located in southern Finland using Landsat ETM+  (Kallio et al., 2008), Gulf of Finland (Yuanzhi Zhang et al., 2003), Chagan lake in China using  Landsat TM (Song et al., 2011) and in Saint John River, Canada using Landsat-8 (Sharaf El Din, 2020). Along with SDD, turbidity was also estimated in Lake Chicot, Arkansas using Landsat MSS (Harrington Jr et al., 1992).

Jointly estimated from Landsat images in many of those studies cited above is the suspended solids concentration. For example, in the studies in Norfolk Broads (Baban, 1993), Lake Beysehir, Turkey (Nas et al., 2010),  Reelfoot Lake, Tennesse (Wang et al., 2006), Lower Peninsula of Michigan (Torbick et al., 2013), Beaver Reservoir in Arkansas, USA (Sudheer et al., 2006), Lake Columbia Water Supply Reservoir (Kulkarni, 2011), Gulf of Finland (Yuanzhi Zhang et al., 2003), Himalayan lake (Mushtaq & Nee Lala, 2017), ) Saint John River, Canada (Sharaf El Din, 2020), Qaraoun reservoir  (Deutsch et al., 2018), reservoirs in Zimbabwe (Masocha et al., 2018), Lady Bird Lake, Texas (Tu et al., 2018) and Lake Chicot, Arkansas (Harrington Jr et al., 1992). A study of the Danube River, Slovakia used Landsat TM, ETM+, and OLI (Onderka & Pekárová, 2008).

Other water quality parameters in the freshwater environment that are predicted with Landsat satellite imagery include the total phosphorus (TP), total nitrogen (TN), and dissolved oxygen (DO).

Total phosphorus estimation was attempted in the studies in the Norfolk Broads, UK (Baban, 1993), Lower Peninsula of Michigan (Torbick et al., 2013), Manzala Lagoon, Egypt (Dewidar & Khedr, 2001), Chagan lake in China (Song et al., 2011) and Lake Kissimmee, Florida (Chebud et al., 2012). The estimation of total nitrogen can be found in the studies of Lower Peninsula of Michigan (Torbick et al., 2013),  Manzala Lagoon, Egypt (Dewidar & Khedr, 2001), and Lady Bird Lake, Texas (Tu et al., 2018). Dissolved oxygen was predicted from Landsat OLI images for El Guájaro reservoir, Colombia (González-Márquez et al., 2018), Landsat-5 TM at Manzala Lagoon, Egypt (Dewidar & Khedr, 2001), and Landsat ETM+ images of Lakes Yenicaga and Abant, Turkey (Karakaya et al., 2011).

Many of the studies mentioned above have also tried to estimate other water quality parameters from Landsat images, such as electrical conductivity (González-Márquez et al., 2018; Mushtaq & Nee Lala, 2017), pH (Dewidar & Khedr, 2001; González-Márquez et al., 2018; Mushtaq & Nee Lala, 2017), water depth (Dewidar & Khedr, 2001; González-Márquez et al., 2018), CDOM (Brezonik et al., 2005; Kallio et al., 2008; Song et al., 2011; Urbanski et al., 2016), salinity (Baban, 1993), temperature (Baban, 1993; Karakaya et al., 2011), dissolved organic carbon (DOC)(Urbanski et al., 2016), the biomass of (submerged, floating, and emergent) aquatic plants (Dewidar & Khedr, 2001), Chloride (Mushtaq & Nee Lala, 2017), and alkalinity (Mushtaq & Nee Lala, 2017).

Most of these studies employ an empirical approach where atmospherically-corrected satellite-received radiance, in terms of Landsat bandwidth values, are correlated with ground-referenced data (collected at the time of the satellite overpass) for the parameters of interest through simple or multivariate regression analysis. To increase the strength of the correlations between Landsat bandwidth and the estimated parameters, some studies have employed machine learning techniques, instead of regression analysis, such as artificial neural networks (Chebud et al., 2012; Sudheer et al., 2006). For a similar reason, a number of studies have embedded ancillary environmental factors as additions to the Landsat bandwidth values in the regression analysis. The environmental factors taken into account include water surface temperature and rainfall (Bonansea et al., 2015), synthetic aperture radar data (Yuanzhi Zhang et al., 2003), NDVI images (Mushtaq & Nee Lala, 2017), Aqua MODIS bandwidth data  (Dona et al., 2015), seasonality (Deutsch et al., 2018), wind speed (Tu et al., 2018), and the difference in the trophic state (Karakaya et al., 2011).

This study will estimate two parameters from Landsat images, namely chlorophyll-a concentrations and TSS concentrations. Chlorophyll-a has been used as a proxy for phytoplankton biomass, which could show the direct effect of nutrient enrichment in water bodies, as explained previously in Section 2.3.

Suspended solids may limit light penetration, and high levels of total suspended solids will increase water temperatures and decrease dissolved oxygen (DO) because suspended particles absorb more heat from solar radiation than the water molecules. More importantly, in terms of nutrient enrichment in water bodies, the resuspension of sediment is a potential source of phosphorus release, which may account for up to 80% of the dissolved phosphorus in water bodies (see Section 2.2.3).

**4.2.1        Estimating Total Suspended Solids (TSS) Concentration in Lakes**

TSS concentrations are one of the most commonly used water quality parameters that can be estimated by remote sensing due to the strong effect of suspended solids on backscattering and water leaving radiance (Giardino et al., 2017). Table 4-2 lists a number of studies that have estimated TSS concentrations using Landsat imagery in freshwater lakes.

As with the other the water quality parameters elaborated before, most of these studies employ statistical models to link the surface reflectance directly observed from the image with the field measured values of TSS concentration. Regression equations between the bandwidth and the TSS concentrations are then used to estimate TSS concentration from any available images of the study area.

Although variable depending on the specific water constituents, it has commonly been found that surface reflectance and TSS concentration have a high correlation in the green, red, and near-infrared (NIR) spectral bands. A number of studies have also found that the blue band is needed to be considered in the TSS concentration calculation in lakes (Kulkarni, 2011; Torbick et al., 2013). With the use of Landsat 8 OLI, the first band of OLI, which is the coastal blue band, also needs to be incorporated into the equation, such as studies by Tu, Smith and Filippi (2018) and Mohsen, Elshemy and Zeidan (2021). The SWIR band (Östlund et al., 2001) or NDVI (Mushtaq & Nee Lala, 2017) acts as the best predictor in some studies.

It has been found, that algorithms based on the green or red spectral bands have proven most suitable for estimating TSS with lower concentrations (up to 50 mg/L), and at higher concentrations, above 100 mg/L, NIR bands can often provide better estimates (Maciel et al., 2019). However, although TSS concentration variations can be predicted with coefficient of determinations up to 0.9 as seen in Table 4-2, in some cases the best-fit regression line can only explain 24% of the variability in the relations (Kulkarni, 2011).

Table 4-2 Studies on TSS concentrations in Lakes using Landsat Sensors

| Landsat Sensor | Band used | $R^2$ | Location and Reference |
|---|---|---|---|
| Landsat 4 MSS | red | 0.71 | Lake Chicot, Arkansas (Harrington Jr et al., 1992) |
| Landsat 4 MSS<br>Landsat 5 TM | NIR1 or NIR2<br>NIR | 0.7<br>0.7 | Moon Lake, Missisipi (Ritchie et al., 1990) |
| Landsat 5 TM | green and red | 0.9 | Frisian Lakes, the Netherlands (Dekker et al., 2002) |
|  | red | 0.67 | Beysehir Lake, Turkey (Nas et al., 2010). |
|  | SWIR | 0.79 | Lake Erken, Sweden (Östlund et al., 2001) |
|  | blue, green, red, NIR | 0.35 | Lower peninsula of Michigan (Torbick et al., 2013) |
|  | blue, green, red | 0.24 | Lake Columbia, Michigan (Kulkarni, 2011) |
| Landsat 7 ETM+ | NIR | 0.9 | Lake Taihu, China (Ma & Dai, 2005) |
| Landsat 7 ETM+ and 8 OLI | NIR<br>Or<br>NIR and red | 0.8 (OLI only)<br>0.4 (ETM+ only)<br>0.7 (OLI and ETM+ | Sahelian Lakes, Mali (Robert et al., 2017) |
| Landsat 5 TM, 7 ETM+ and 8 OLI | Red (TM and ETM+) and visible blue (OLI) | 0.7 | Lady Bird Lake, Texas (Tu et al., 2018) |
| Landsat 8 OLI | NDVI<br>( (nir-red)/(nir+red) | 0.6 | Himalayan Lake (Mushtaq & Nee Lala, 2017) |
|  | Coastal blue, green, NIR | 0.67 | Lake Burullus, Egypt (Mohsen et al., 2021) |

**4.2.2        Estimating Chlorophyll-a Concentration in Lakes**

Table 4-3 provides an overview of previous studies that have estimated chlorophyll-a concentrations in lakes utilising Landsat sensors. As for the estimation of TSS concentrations using Landsat (section 4.2.1), all of these prior studies are empirical studies. The prior work has shown that the remotely-sensed surface reflectance in three visible bands, i.e., blue, green, red, and the Near Infrared (NIR), can be used successfully to infer chlorophyll-a concentrations in lakes.

In these studies, correlations between surface reflectance recorded by Landsat sensor and the ground-reference water quality parameters were mostly achieved from linear regression, with the coefficient of determination in some cases as low as 0.1 (Barrett & Frazier, 2016) or as high as 0.8 (e.g., Brivio, Giardino and Zilioli, 2001; Tebbs, Remedios and Harper, 2013).  Studies that preferred a black box method such as neural network (Chebud et al., 2012; Dona et al., 2015) have accounted for  90% of the variations in the surface reflectance and ground reference data.

One study (Ma & Dai, 2005) also analysed the effect of the pixel window size on the precision of water quality parameter estimation. They found that an area of 7x7 or 5x5 pixels is mostly suitable to estimate chlorophyll-a concentration, whereas 3x3 pixels or less is more suitable for estimating TSS concentrations.

Table 4-3 Studies of chlorophyll-a concentrations in lakes using Landsat Sensors

| Landsat Sensor | Band Used | R² | Location and Reference |
|---|---|---|---|
| Landsat 5 TM | green and red | 0.7 | Reelfoot Lake, Tennesse (F. Wang et al., 2006) |
| | blue | 0.48 | Moon Lake, Mississippi (Ritchie et al., 1990) |
| | blue, green, red | 0.8 | Lake Garda, Italy (Brivio et al., 2001) |
| | | 0.8 | Chagan Lake, China (Song et al., 2011) |
| | blue, green, NIR | 0.6 | Beysehir Lake, Turkey (Nas et al., 2010). |
| | Band 1 -7 (neural network) | 0.95 | Lake Kissimmee, Florida (Chebud et al., 2012) |
| | green | 0.5 | Lake Tenmile, Oregon (Waxter, 2014) |
| | Blue, red, NIR, SWIR | 0.7 | Lower peninsula of Michigan (Torbick et al., 2013) |
| | green or blue or green and blue, or green and red, or green and NIR | 0.7 | Minnesota lakes (Brezonik et al., 2005) |
| | green and red | 0.7 – 0.8 | Lake Columbia, Michigan (Kulkarni, 2011) |
| Landsat 5 TM and Landsat 7 ETM+ | SWIR and NIR | 0.1 | Lakes in The Ozark/Ouachita-Appalachian Forest ecoregion (OOAF), Oklahoma (Barrett & Frazier, 2016) |
| Landsat 5 TM and Landsat 7 ETM+ (and MODIS) | Band 1 – 5 and 7 (neural network) | 0.94 | Albufera de Valencia Lake (Dona et al., 2015) |
| Landsat 7 ETM+ | NIR and red | 0.8 | Lake Bogoria, Kenya (Tebbs et al., 2013) |
| | red | 0.6 | Lake Taihu, China (Ma & Dai, 2005) |
| | NIR and red | 0.84 | Lakes Yenicaga and Abant, Turkey (Karakaya et al., 2011) |
| Landsat 8 OLI | Blue and red | 0.52 – 0.76 | A database of 8000 lakes in northern Poland (Urbanski et al., 2016) |
| | NIR and red Red (more polluted) | 0.84 0.69 | Lake Chivero, Zimbabwe (Masocha et al., 2018) |
| | Coastal blue and green | 0.86 | Lake Burullus, Egypt (Mohsen et al., 2021) |

As shown by Figure 2-5, absorption of chlorophyll-a is maximal on the spectrum of blue and orange-red light. Chlorophyll-a estimation algorithms that use blue and green wavelengths often provide a relatively accurate estimate of chlorophyll-a in clear water such as the open ocean where phytoplankton dominates the total non-water absorption (S. Mishra & Mishra, 2012). However, in turbid productive waters, optically active constituents that do not co-vary with chlorophyll-a such as suspended solids hold absorption features that overlap with chlorophyll-a (Dall'Olmo & Gitelson, 2005; Gitelson et al., 2008), different concentrations of suspended solids give different spectral signature for cholorphyll-a (Hunter et al., 2008). For these turbid waters, the absorption maxima on the orange-red spectrum can often be seen as its spectral signatures (Svab et al., 2005), although several algorithms built with blue-green ratio, that originally intended for ocean waters can are found able to provide the best cholorphyl-a estimation in inland waters with high suspended matter, as studied by Neil et al. (2019a), few of which are used to compare the algorithm used in this study (see section 4.4.5). Nevertheless, the combinations of all visible bandwidth and NIR wavelength are needed to achieve high accuracy on the estimation, especially when using black-box methods such as neural network as shown in Table 4-3 .

## 4.3     Data Collection Methods Employed on the Tonle Sap Lake

The field campaign for this research was undertaken during 2$^{nd}$ to 18$^{th}$ of February 2019. Specifically, it was selected to give the maximum chances of clear skies during the dry season, and was also timed to coincide with the overpass of the satellite in order to have coincident Landsat imagery and ground-referenced water quality parameters. Three types of in-situ data were measured during the campaign: Total Suspended Solids concentrations, chlorophyll-a concentrations (both from within the lake), and the reflectance properties of various surface land covers (both within and around the lake); the former data were used to build correlations between the surface reflectance from Landsat images and the data (see Sections 4.4.3 and 4.4.4) while the latter data were used to analyse Landsat's surface reflectance products used in this study (see Section 4.4.1) and to evaluate the random forest algorithm used to estimate chlorophyll-a concentrations from the Landsat images (see Section 4.4.5). Locations of the water samples taken for use when calculating the Total Suspended Solids and chlorophyll-a concentrations are shown in Figure 4-1, which highlights how these samples were collected from the northern part of Tonle Sap Lake. Figure 4-1 also shows the sampling locations for remote sensing reflectances which were collected within the lake and surrounding land areas.
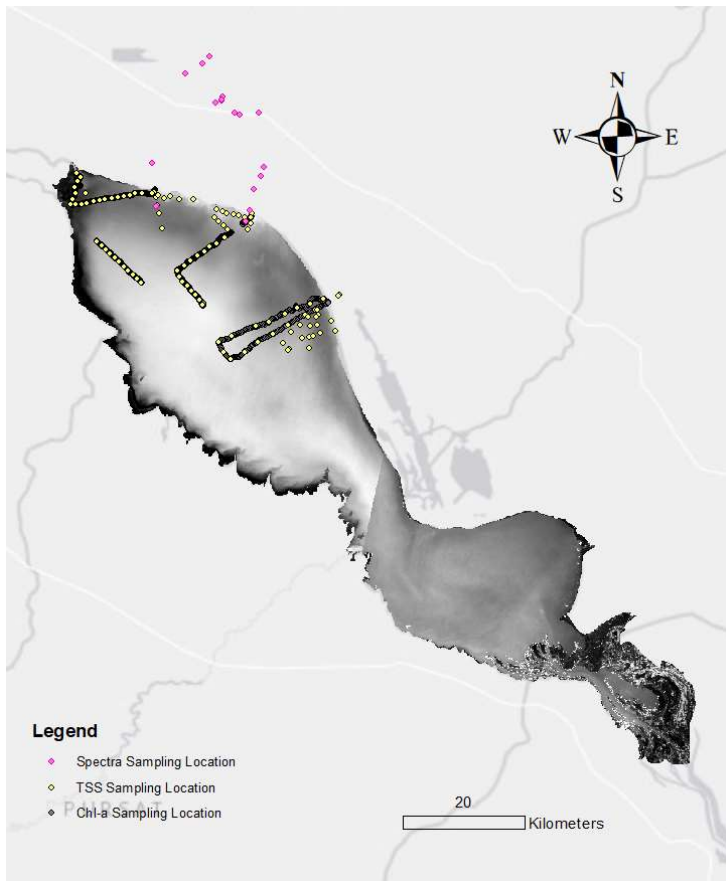
Figure 4-1 Water sampling locations. The shading on the lake's background represents variations in the surface reflectance of the water.

### 4.3.1    Chlorophyll-a measurements

Chlorophyll-a was measured using an EXO2 water quality sonde (YSI Incorporated) deployed from a moving boat, with a GPS device with ±3 meter of positional accuracy used to georeference the sonde measurements. During the deployment, the boat speed was controlled to maintain speeds sufficiently low to maintain the sonde under the surface of the water (around a half-meter below the surface) and to avoid cavitation around the sensor head.  The sampling strategy was to deploy the sonde (at a sampling frequency of 1Hz) along transects (Figure 4.1) covering a range of lake environments (e.g., locations near river outlets, close to the shore, within the centre of the lake, etc, see also Section 4.5), following different water colours shown on typical historical Landsat imagery, with the aim being to capture as much variability in chlorophyll-a as possible. In total, the sonde measurements were captured along 125 km of transect (Figure 4-1), providing a database of some 46514 individual measurements with chlorophyll-a values ranging from 0.85 to 60.84 µg/L (mean value = 7.1 µg/L ) and covering 4160 unique pixels of Landsat imagery (3071 usable pixels), providing a robust basis for the calibrations developed in Section 4.4.4.

In terms of the individual measurements, the EXO sonde measures chlorophyll-a fluorescence. Chlorophyll-a fluorescence can be defined as light re-emitted after being absorbed by photosynthetic tissues or organisms. The emitted color is red to far-red light, which occurs when the organisms are illuminated by the light of approximately 400–700 nm (photosynthetically active radiation or PAR) (Kalaji et al., 2017). The EXO sonde generates a blue excitation beam that directly excites the chlorophyll-a molecule, after which the fluorescence sensor generates an estimate of the pigment concentration in μg/L. The EXO chlorophyll readings show very low interference from turbidity and dissolved organics, increasing data accuracy. The EXO2 sonde measurement range is 0 to 400 μg/L chl-a, with a resolution of 0.01 μg/L chl-a. The EXO2 sonde has $R^2 > 0.999$ of linearity with 0-400 μg/L Chl equivalents of Rhodamin WT solution, a common dye for environmental studies which is used to pre-calibrate the sensor.

### 4.3.2    Total Suspended Solids (TSS)

Water samples for the measurement of TSS concentrations were taken every few kilometers along the transects employed for the EXO2 water quality sonde. As the route was determined to cross areas of the lake with different optically visible colours (as shown in Figure 3-1), the intention was that taking water samples along those lines would maximise the range of TSS concentrations acquired.

Water samples were collected using a Van Dorn sampler from a depth of a half-meter below the surface. The TSS were measured by filtering the water samples using a glass microfiber filter (0.7 μm pore size). The filters were pre-weighed after being dried at 105° for 24 hours and were dried again and weighed after water filtration. TSS concentrations were calculated by taking the difference between the dry weights after and before filtering and dividing by the volume of filtered water. The precision of the measurement scale is 0.0001 grams.

A total of 102 locations were sampled for TSS. However, a number of measurements subsequently needed to be removed because they are outlying of the correspondent surface reflectance values of the pixel. After removing such measurements, 87 TSS concentration measurements were used to develop a regression analysis between TSS concentration and surface reflectance values (see Section 4.4.3). The TSS concentrations values acquired during the fieldwork ranged from 2.9 to 314.3 mg/L (mean value = 80.9 mg/L ), similar to the range measured by a sediment study (Siev et al., 2018) of Tonle Sap lake in 2017 which is 3 - 652 mg/L (mean 192.4 ± 111.2 for March observations) , or 2 - 1000 mg/L (annual mean value 77 mg/L) measured in 2001 (Sarkkula et al., 2003).

### 4.3.3        Field Spectra

The surface reflectances of several varying land cover types were measured to analyse the surface reflectance products for Landsat satellite, i.e., to compare the surface reflectances measured by the Landsat satellite versus those measured on the ground. Surface reflectance measurements were conducted on three days, i.e., the 2nd, 14th, and 18th February 2019, these dates being timed to coincide with the overpass of the Landsat OLI for the study area. Landsat 8 OLI overpassed the study area on the 2nd and 18th of February. The 14th of February was chosen for convenience but remained within the 7-day window of the satellite overpassing.

Remote sensing reflectances of various land covers were measured using an ASD Fieldspec HH2 spectroradiometer. For all measurements, the white reference method was applied. The white reference method uses a white spectralon panel to quantify the incoming solar radiance, assuming that the panel reflects 99.99% of the incoming solar radiance. The white spectralon panel was first measured, followed by the land or water surface. For water surfaces, a guide introduced by (Mobley, 1999; Mueller et al., 2000) which is to stand in the position of 135° from the sun azimuth and a zenith angle of 40° to avoid sun glitch, was followed. For the land surfaces, measurement was conducted by taking shots from perpendicular directions while avoiding creating self-shadows.
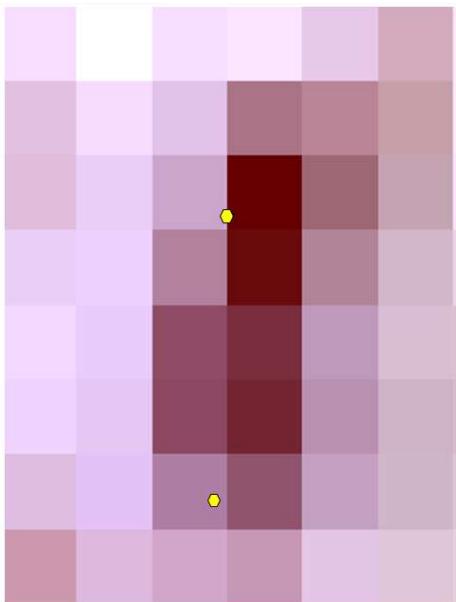


Figure 4-2 Example of mixed pixel locations of the reflectance measurement. The top yellow dot was a measurement taken on the border of two pixels. The bottom yellow dot was a measurement taken close to the border of two pixels.

Table 4-4 describes the measured surface reflectances acquired here, with the mixed pixel value indicating the extent to which the measurement was acquired in a location within (or otherwise) a

single Landsat pixel. Thus mixed pixel values of 1, 0, and 0.5 indicate that the field surface reflectance measurement was taken on the borderline of two pixels, in the middle of a pixel, and close to the borderline of two pixels, respectively. In the subsequent data analysis, measurements taken on the borderline of two pixels (code 1) were regarded as invalid measurements. Figure 4-2 illustrates an example of a mixed pixel value of 1 (top green dot) and a mixed pixel value of 0.5 (bottom green dot).

Table 4-4 Land cover reflectance measurement

| Date | Land Cover type | Mixed Pixel | Picture and Note |
|------|-----------------|-------------|------------------|
| 2 Feb 2019 | Lake water | 0 | Not available |
| 2 Feb 2019 | Pond water | 0 |  |
| 14 Feb 2019 | Surrounding water of Angkor Wat | 0.5 | Not available<br>Note: Covered by cloud on 18 Feb the Landsat image |
| 18 Feb 2019 | Lake water | 0 | Not available |
| 18 Feb 2019 | Green bean | 0 |  |

| Date | Land Cover type | Mixed Pixel | Picture and Note |
|------|-----------------|-------------|------------------|
| 18 Feb 2019 | Kampong Phluk vegetation | 0 |  |
| 18 Feb 2019 | Green paddy field | 0 |  |
| 18 Feb 2019 | Newly harvested paddy field | 0.5 |  |
| 18 Feb 2019 | Dry paddy field | 0.5 |  |
| 18 Feb 2019 | Dry paddy field with burning straw | 1 |  |

| Date | Land Cover type | Mixed Pixel | Picture and Note |
|---|---|---|---|
| 18 Feb 2019 | Dry grass land | 0.5 |  |
| 18 Feb 2019 | Bare soil | 0 |  |
| 18 Feb 2019 | Bare soil | 1 |  |
| 18 Feb 2019 | Bare soil (different soil type) | 0 |  |
| 18 Feb 2019 | Bare soil (different soil type) | 0 |  |

| Date | Land Cover type | Mixed Pixel | Picture and Note |
|---|---|---|---|
| 18 Feb 2019 | Green pond water | 0 |  |
| 18 Feb 2019 | Green water pond | 1 |  |

Figure 4-3 shows the remote sensing surface reflectance spectra of several land cover types from the in-situ measurements. These reflectance values were obtained by dividing the ASCII value of surface reflectance of the land cover with the ASCII value of the white spectralon reflectance. The conversion of measured DN (digital number) to ASCII value was performed with ViewSpecPro software (one feature of ASD RS3 Spectral Acquisition Software).
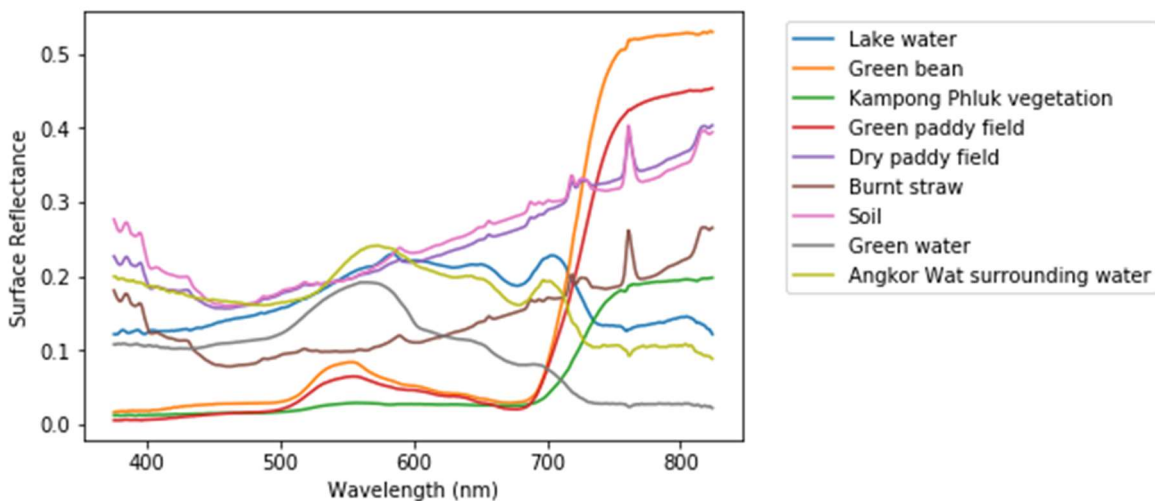


Figure 4-3 Remote sensing spectra measured with ASD for various land covers in the study area

Tonle Sap lake water and the water surrounding Angkor Wat temple are showing footages of chlorophyll-a pigment material dominated water with local peaks at the wavelengths of 560, 650, and 710 nm (Mahama, 2016). Meanwhile, for healthy vegetation such as the green bean,

Kampong Phluk vegetation, and green paddy field, the visible region (400–700 nm) is dominated by light absorption of the leaf pigments, but with less absorption over the "green" wavelengths (500–600 nm) (Artiola et al., 2004). Soil reflectances are seen to increase with increasing wavelength from 400 nm to 1000 nm (Artiola et al., 2004). Dry paddy fields have similar characteristics to bare soil. Overall the measured spectra follow the spectral signature of surface reflectance of water surface and land covers. The extent of the closeness of these field measured surface reflectance and the surface reflectance measured by the Landsat satellite are analysed in the following Section 4.4.1.

## 4.4 Development and Validation of Chlorophyll-a and TSS Concentration Prediction Algorithms for the Tonle Sap Lake
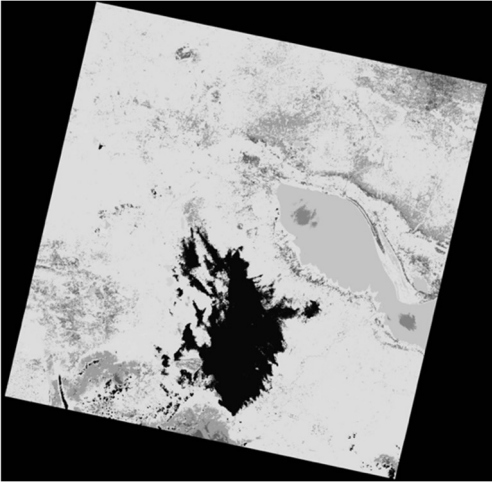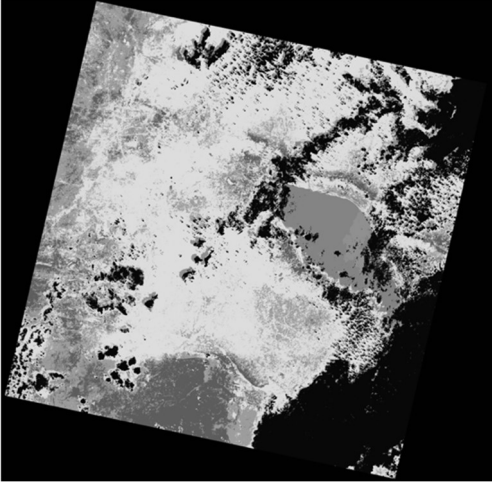
### 4.4.1 Analysis of Landsat Surface Reflectance for the Tonle Sap Lake Area

The model used to estimate the water quality parameters (TSS and chlorophyll-a) in Tonle Sap lake was built empirically by building correlations between the surface reflectance properties of Landsat imagery and the in-situ field data (discussed in Section 4.3). Here the relevant Landsat images are those acquired by the Landsat 8 OLI sensor on the day closest to the field data acquisition timing. In this study, these OLI images were acquired on the 2nd and 18th of February 2019 (Table 4-5).

The Landsat OLI Images used are surface reflectance products provided by NASA. The images were collected from the USGS (United States Geological Survey) Earth Explorer data gateway. The surface reflectance products are images that have already been atmospherically corrected using the Landsat 8 Surface Reflectance (L8SR) algorithm (Vermote et al., 2016). These surface reflectance products are reported as having good performance for inland water studies (Bernardo et al., 2017; Wei et al., 2018; Yepez et al., 2017).

Chapter 4

Table 4-5 Corresponding Landsat OLI images for fieldwork data with their aerosol band. The black
shadow is cloud cover.

| Date of image | Cloud Cover | Landsat 8 Level 2 Collection (Aerosol Band) |
|---|---|---|
| 2 Feb 2019 | 7% |  |
| 18 Feb 2019 | 22% |  |

Surface reflectance products are part of the Landsat Science Product, with the available images
being provided in three tiers, i.e., Real-Time (RT), Tier 1 (T1), and Tier 2 (T2) (Table 4-6) and three
processing levels, i.e., TP, GT, and GS (Table 4-7). Both the Tier and level designation is visible at
the end of the Landsat Product Identifier.

Table 4-6 Landsat Product Tiers

| Real-Time (RT) | Tier 1(T1) | Tier 2 (T2) |
|---|---|---|
| Newly-acquired data. Available for download in | Highest available data quality. Tier 1 includes Level-1 Precision and Terrain (L1TP) corrected data (see Table 4-7). The georegistration of | Adhere to the same radiometric standard as Tier 1 scenes but do not meet the Tier 1 geometry specification due to less accurate orbital information (specific to |

| less than 12 hours. | Tier 1 scenes is consistent and within prescribed image-to-image tolerances of $\leqq$ 12-meter RMSE. | older Landsat sensors), significant cloud cover, insufficient ground control, or other factors. Includes Systematic Terrain (L1GT) and Systematic (L1GS) processed data. |
|---|---|---|

In this study, to ensure the quality of the time series generated, only images corresponding to the Tier 1 and TP level were used. Further, in order to evaluate the surface reflectance products of Landsat OLI for the Tonle Sap lake area, the in-situ surface reflectances (Section 4.3) were first used to produce simulated OLI reflectances (for each land cover type) for comparison with the USGS product.

Table 4-7 Landsat Level-1 processing levels

| TP (Terrain Precision Correction) | GT (Systematic Terrain Correction) | GS (Geometric Systematic Correction) |
|---|---|---|
| Radiometrically calibrated. Orthorectified using ground control points (GCPs) and digital elevation model (DEM) data to correct relief displacement. Suitable for pixel-level time series analysis. | Radiometrically calibrated. Systematic geometric corrections were applied using the spacecraft ephemeris data and DEM data to correct for relief displacement. | Radiometrically calibrated. Systematic geometric corrections were applied using only the spacecraft ephemeris data. |

The generation of simulated OLI reflectances employed here uses the spectral response functions (SRF) of Landsat OLI's bands. Here, the SRF deployed are those of the four bands (blue, green, red, and near-infrared) used in the TSS and chlorophyll-a concentrations estimation. For each band, the simulated OLI reflectances were generated by convoluting the spectra within the range of OLI's band with the Spectral Response Function (SRF) of the OLI's band (Pahlevan et al., 2017) as shown by the Equation 1:

$$Sim\,R_{rs}(\lambda_i) = \frac{\sum_{i=1}^{n} R_{rs}(\lambda_i) x RSR(\lambda_i)}{\sum_{i=1}^{n} R_{rs}(\lambda_i)} \qquad (1)$$

In this equation, $n$ is the total number of wavelengths in the band's range, $R_{rs}(\lambda_i)$ is the wavelength for wavelength $i$, and $RSR(\lambda_i)$ is the spectral response function for the wavelength $i$.

Figure 4-4 shows the comparison between the simulated reflectances and OLI's reflectances for each of the different land covers investigated (see Section 4.3). For two land covers, i.e., green bean and dry paddy fields, the comparison of simulated versus OLI surface reflectances yield a root mean square error (RMSE) of 0.1, while for the other six land covers investigated here, all the yielded RMSE's are below 0.1. The lake water surface, in particular, has an RMSE of just 0.06. This shows that the Landsat OLI surface reflectances very closely replicate the surface reflectances of the investigated land cover categories around Tonle Sap lake, especially on the lake surface itself, giving confidence in the use of the Landsat OLI product for this study.
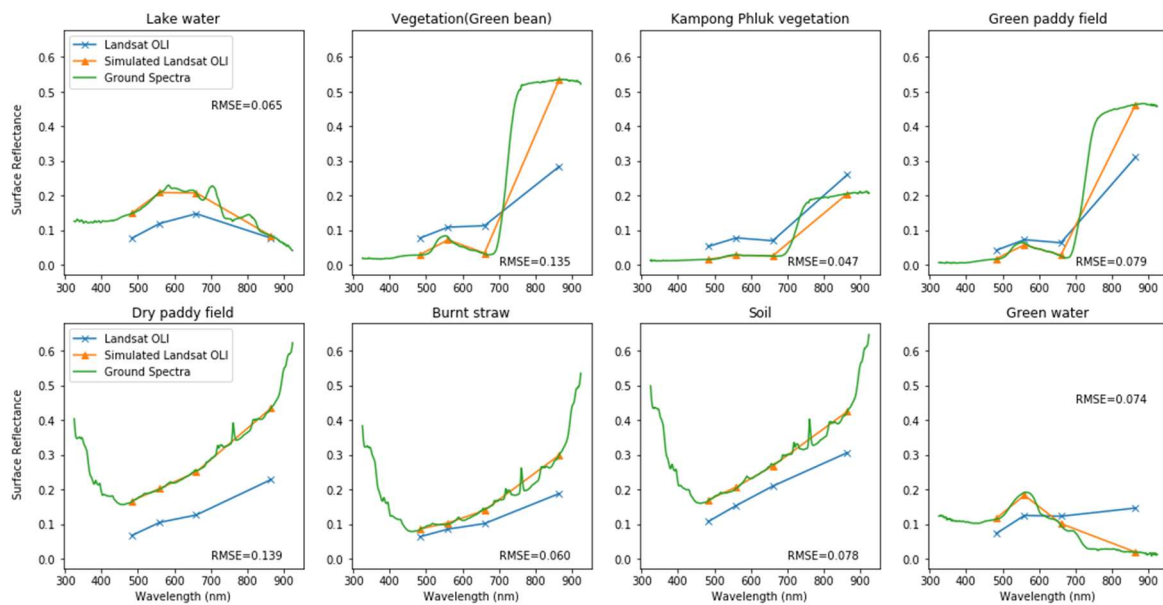


Figure 4-4 Comparison of surface reflectance values between the Landsat 8 OLI product, and simulated Landsat 8 OLI values as derived from the field measured spectra for 8 varying land cover categories in the Tonle Sap lake study area

## 4.4.2    Inter-sensor Calibration of Landsat Satellites for the Tonle Sap Lake Area

In the next step of the analysis, empirical relationships between surface reflectance values (as derived from the Landsat 8 OLI imagery) and the field measurements of the water quality parameters (TSS and chlorophyll-a) were developed as the basis for estimating TSS or chlorophyll-a from the Landsat 8 OLI images. Further, in order to apply these calibration functions over the longer term (i.e., to the period before the advent of the Landsat OLI), calibrations between the various different Landsat sensors were also developed.

Table 4-8 Calibration equations between Landsat 8 OLI and Landsat 7 ETM+ established by Roy et al. (2016)

| Band | Transformation Functions | $R^2$ |
|------|--------------------------|-------|
| Blue | ETM+ = 0.0183 + 0.8850 OLI | 0.750 |
| Green | ETM+ = 0.0123 + 0.9317 OLI | 0.790 |
| Red | ETM+ = 0.0123 + 0.9372 OLI | 0.848 |
| NIR | ETM+ = 0.0448 + 0.8339 OLI | 0.706 |

In this study, calibrations between the Landsat 8 OLI and Landsat 7 ETM+ (and Landsat 5 TM) imagery were established by applying the equations (Table 4-8) developed by Roy et al. (2016). In this study, it was assumed that the calibrations between Landsat 8 OLI and Landsat 5 TM can employ the same relationships as those developed for the Landsat 7ETM+; this is reasonable because the TM and ETM+ sensors have very similar bandwidths (Table 4-9). The bandwidths for these two sensors are not exactly identical, with the use of indices such as NDVI giving smaller errors than single band use (Vogelmann et al., 2001), and hence they have been considered for calibration in several studies (Banskota et al., 2014; Homer et al., 2004), but in many other studies, it is generally accepted that no calibrations are needed between Landsat 5 TM and Landsat 7 ETM+ (e.g. Dona *et al.*, 2015; Barrett and Frazier, 2016; Tu, Smith and Filippi, 2018; Setiawan *et al.*, 2019).

Table 4-9 Spectral range of Landsat 7 ETM+ and Landsat 5 TM

| Band | Landsat TM (µm) | Landsat ETM+ (µm) |
|------|-----------------|-------------------|
| blue | 0.45 ~ 0.52 | 0.450 ~ 0.515 |
| green | 0.52 ~ 0.60 | 0.525 ~ 0.605 |
| red | 0.63 ~ 0.69 | 0.630 ~ 0.690 |
| NIR | 0.76 ~ 0.90 | 0.775 ~ 0.900 |

Chapter 4

An evaluation of the inter-sensor calibrations used here was performed by comparing the surface reflectance obtained between the various different sensors. Pixels were selected from the same pseudo-invariant objects (i.e., objects that reflect relatively the same amount of solar radiance over time) in two images acquired by two different Landsat satellites with the closest date (8 days apart). Here, these pixels were chosen from the airport at Siem Reap, a site within Angkor Wat, and a green forest area around Angkor Wat.

Table 4-5 shows the comparison results of the surface reflectance of the chosen pixels for bands blue, green, red, and NIR. The top graph compares surface reflectance values of the Landsat 5 TM with Landsat 7 ETM+. The middle chart compares surface reflectance values of the OLI simulated Landsat 7 ETM+ (i.e., Landsat 7 ETM+ that have been transformed to OLI comparable values using the functions in Table 4-8) and the Landsat 8 OLI. The bottom graph compares Landsat 7 ETM+ with Landsat 8 OLI.
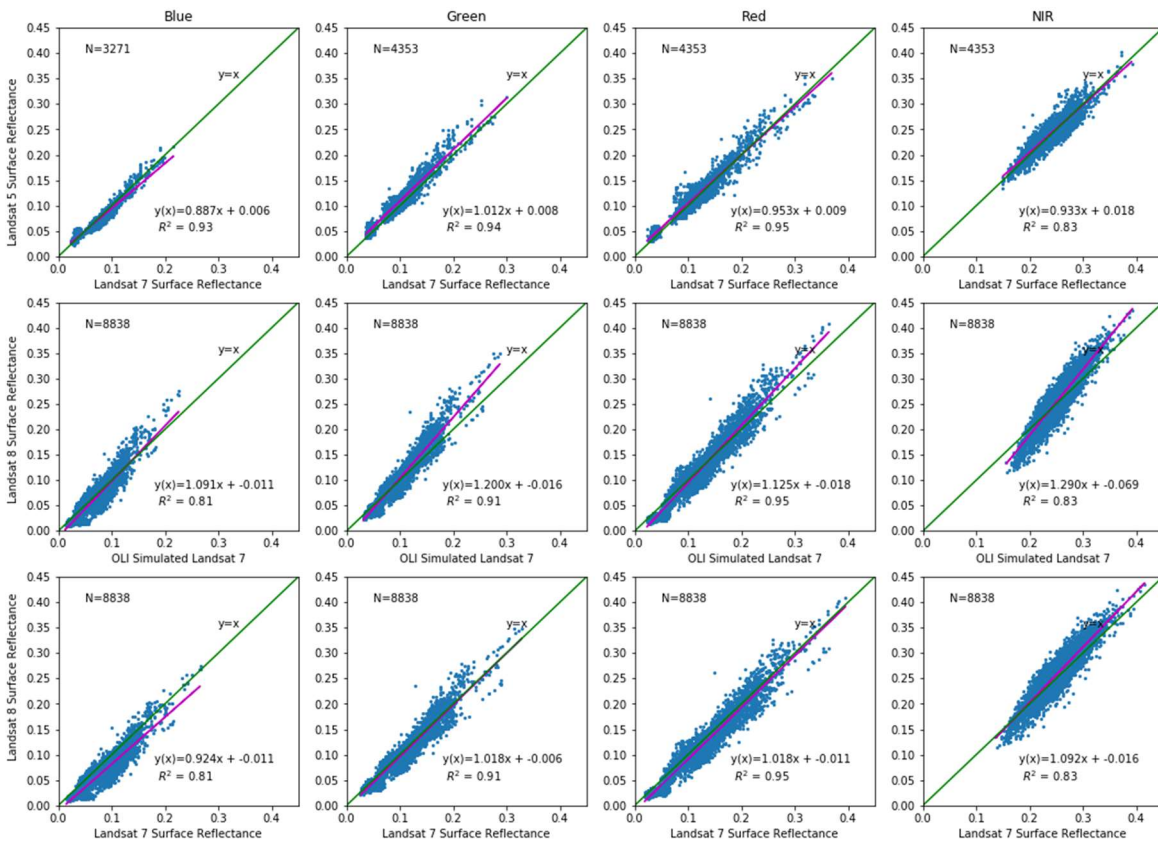


Figure 4-5 Comparison of remote sensing surface reflectance values between Landsat 5 ETM and Landsat 7 ETM+ (top), OLI simulated Landsat 7 ETM+ and Landsat 8 OLI(bottom) and Landsat 7 ETM+ and Landsat 8 OLI(bottom)

For all bands, the coefficients of determination show a very strong relationship between each Landsat sensor. For the comparison of Landsat 5 TM and Landsat 7 ETM+ surface reflentances, across 3 bands (the exception is the NIR band) around 95% of the surface reflectance from one of

Landsat sensors can predict the other. For the NIR band it is 83%. Meanwhile, for the comparison of the surface reflectances of Landsat 8 OLI with Landsat 7 ETM+, with Landsat 8 OLI and OLI simulated Landsat 7 ETM+, the coefficient of determination for the blue band is also around 0.8.

There is no change in the coefficient determination for each band, when comparing the surface reflectances of Landsat 8 OLI with Landsat 7 ETM+, with Landsat 8 OLI and OLI simulated Landsat 7 ETM+. However, in the further analysis, Landsat ETM+ surface reflectances were converted to OLI comparable values from the original study (Roy et al., 2016) where the equations came because that study used far more pixels (nearly 30 million) compared to this study ( 4,000 ~ 8,000).

### 4.4.3 Total Suspended Solids Estimation for Tonle Sap Lake

Here, stepwise regression was used to develop relationships between Landsat OLI's band values (blue, green, red, and NIR) and the field-measured TSS concentrations, using the statistical analysis software R version 3.4.3. The regressions for all four bands were significant ($p < 0.05$), with the coefficient of determination $R^2 = 0.64$, RMSE = 35.93 and normalized RMSE = 0.11 . The complete statistics table for the multiple regression is shown in Table 4-10. Figure 4-6 gives examples of pairs of TSS concentrations and surface reflectance values of band 2 to band 5 of Landsat 8 OLI, and the coefficients for each band in the multiple linear regression equations found between the Landsat OLI bands and the TSS concentrations. Complete data of pairs of TSS concentrations value and surface reflectance values of band 2 to band 5 of Landsat 8 OLI can be seen in Appendix D.

TSSC = -10.1375 - 0.8505 *B2* + 0.3620 *B3* + 0.1809 *B4* + 0.1124 *B5*

| TSSC | B2 | B3 | B4 | B5 |
|---|---|---|---|---|
| 33.58209 | 0.0665 | 0.1053 | 0.1072 | 0.0374 |
| 51.02041 | 0.0736 | 0.1152 | 0.1281 | 0.0498 |
| 57.16667 | 0.0771 | 0.1196 | 0.1359 | 0.0544 |
| 58.10345 | 0.0815 | 0.1236 | 0.1404 | 0.0553 |
| 43.58209 | 0.0847 | 0.1246 | 0.1373 | 0.0567 |
| 42.34375 | 0.0829 | 0.1222 | 0.1283 | 0.0472 |
| … | … | … | … | … |
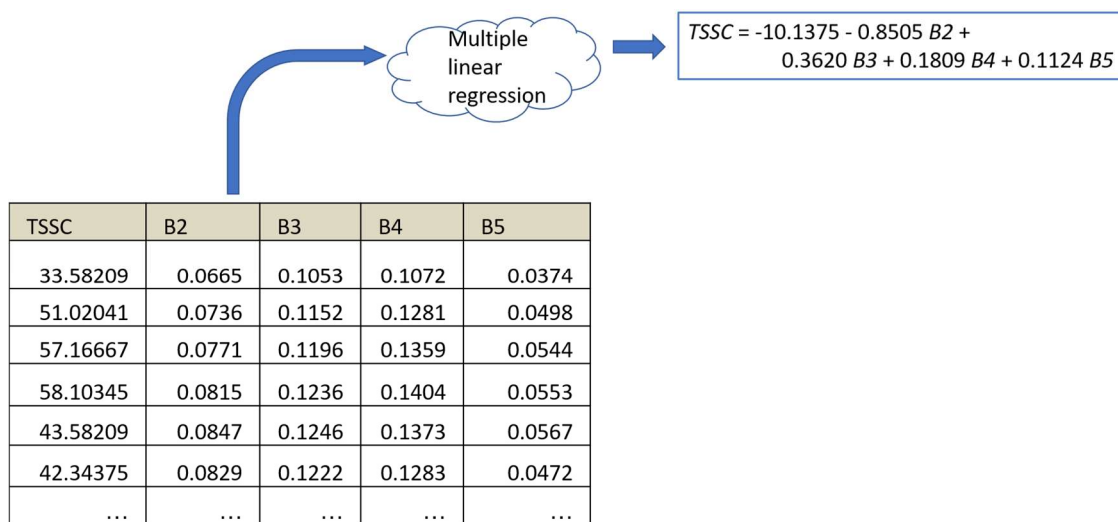
Figure 4-6 Examples of pairs of TSS concentrations and surface reflectance values of band 1 to band 5 of Landsat OLI,  and the coefficients of each band in the multiple linear regression equation between Landsat OLI bands and the TSS concentrations.

Table 4-10 Statistics table of multiple regression linear between Landsat OLI bands and the TSS concentrations.

| Variable | Coefficient | Std. Error | t-ratio | P-value |
|---|---|---|---|---|
| Intercept | -10.1375 | 41.467 | -0.244 | 0.807 |
| B2 | -8505.3887 | 1004.327 | -8.469 | ≤ 0.0001 |
| B3 | 3620.0391 | 651.520 | 5.556 | ≤ 0.0001 |
| B4 | 1808.6029 | 448.231 | 4.035 | ≤ 0.0001 |
| B5 | 1123.5743 | 241.015 | 4.662 | ≤ 0.0001 |

R-squared = 63.7 %          R-squared (adjusted) = 61.9%

s =  85 with 80 − 4 = degrees of freedom

### 4.4.4      Chlorophyll-a Estimation for Tonle Sap Lake

Initial analyses (following those undertaken in Section 4.4.3) that attempted to find correlations between all possible combinations of the Landsat optical bands and the field-measured chlorophyll-a concentrations data did not show any significant linearity between them. Therefore, alternative methods (Support Vector Regression and Random Forest) were employed to establish

the necessary empirical functions between the Landsat-derived surface reflectance and chlorophyll-a (as shown in Figure 4-7).



| Chl-a | B1 DN | B2 DN | B3 DN | B4 DN |
|-------|-------|-------|-------|-------|
| 8.79 | 872 | 1408 | 1786 | 1449 |
| 7.20 | 879 | 1402 | 1780 | 1513 |
| 10.87 | 872 | 1397 | 1764 | 1508 |
| 11.36 | 885 | 1407 | 1764 | 1459 |
| 10.91 | 895 | 1421 | 1790 | 1441 |
| 10.37 | 886 | 1402 | 1751 | 1288 |
| ... | ... | ... | ... | ... |

Random Forest → $R^2 = 0.6$

Support Vector Regression → $R^2 = 0.07$

Multiple linear regression → $R^2 = 0.2$
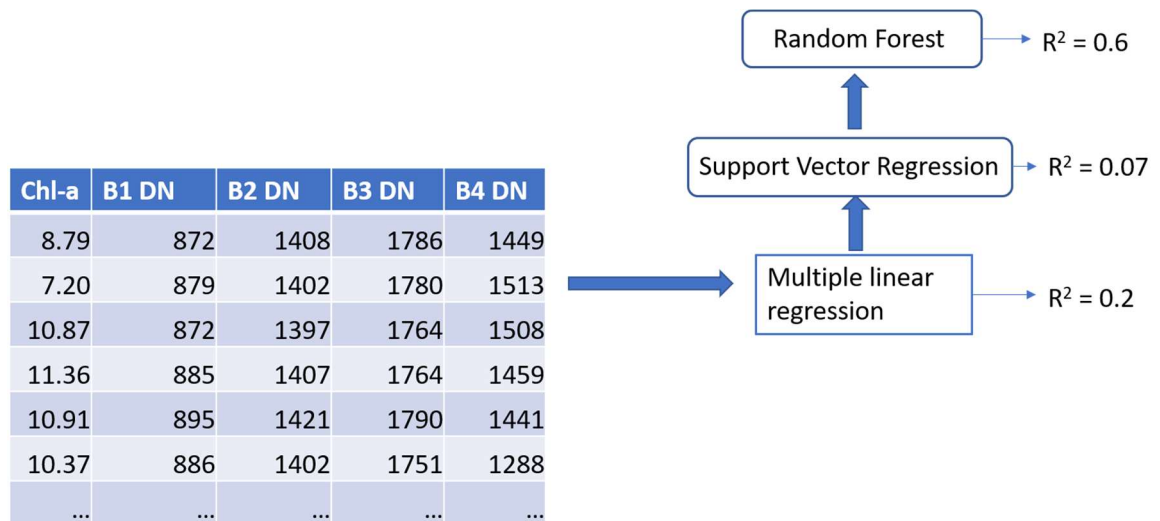
Figure 4-7 The process of the correlation analysis between surface reflectance of Landsat OLI bands and chlorophyll-a concentrations.

Support Vector Regression (SVR) performs non-linear regression by employing Support Vector Machines in which the kernel function of transformation maps the original input space into a high dimensional feature space where the non-linear relationship can be modeled in a linear way (Üstün et al., 2007). The best fit model is referred to as a hyperplane in the feature space. The position and the orientation of the hyperplane are determined through the help of the data points on either side of the hyperplane, that are closest to the hyperplane (which are called Support Vectors). The SVR does not try to minimize the error between the real and predicted value; instead, it tries to fit the best line within a threshold value (maximum error) which is determined by the dataset, hence giving flexibility in the acceptable error for a particular problem. SVR has been used in studies to predict storm surges, reservoir porosity, and tourism demand (Al-Anazi & Gates, 2010; K. Y. Chen & Wang, 2007; Rajasekaran et al., 2008). In the remote sensing field, a study (Camps-Valls et al., 2006) attempted to use it to predict chlorophyll-a concentrations from MERIS bandwidth value.

Random Forest is one of ensemble methods (Dietterich, 2000) in predictive modelling that merges multiple decision trees to gain more accurate predictions. It has been shown that the generalization error converges, enabling this technique to avoid overfitting (Breiman, 2001). Random Forest can be used in classification and regression problems (Liaw & Wiener, 2002) and has been applied widely to various study areas (e.g., Petralia *et al.*, 2015; Wang *et al.*, 2015; Nicolas *et al.*, 2016; Thompson *et al.*, 2017). In studies using remote sensing, Random Forest has

been used, for example, for predicting nitrogen concentrations in sugarcane from hyperspectral images (Abdel-Rahman et al., 2013), and to estimate wheat biomass (L. Wang et al., 2016).

Recalling from Section 4.3 that the EXO sonde measured values of chlorophyll-a concentration every second. Therefore, in the first step of the analysis, the individual concentration values obtained from the sonde were averaged across the area of each unique Landsat pixel. In total, this provided 3071 pixel-averaged samples. For the random forest methods, 70% of these pixels were used for training and 30% for testing (see Section 4.4.5).

Deploying the GridSearchCV function from scikit-learn (version 0.20.3) with 5-fold cross-validation, a random forest was established with a maximum depth for each tree of 32, and 250 estimators (number of trees in the forest). This random forest gives a correlation between Landsat bandwidths' value and chlorophyll-a concentrations with a coefficient of determination $R^2 = 0.56$, a mean absolute error of 1.43 and a mean squared error 7.19.

### 4.4.5 Evaluation of the Random Forest Chlorophyll-a Prediction Algorithm for Tonle Sap Lake

A number of previous studies (Table 4-11) have developed bio-optical models that have been used to retrieve chlorophyll-a concentrations from satellite remote sensing. Here it is shown that the Random Forest algorithm developed for the Tonle Sap lake in 4.4.4 provides significantly improved predictions relative to these previous approaches. Note that in Table 4-11, $Chl_a$ is the chlorophyll-a concentration, while $R$ shows the remote sensing reflectance at specific wavelengths. The analytical models (2BDA and 3BDA) are built to match the MERIS sensor band configuration, naturally so for the NDCI algorithm that was derived from both 2BDA and 3BDA algorithms. The algorithms 2BDA and 3BDA are developed for turbid water, use the red-orange spectrum range to avoid the interference of spectral signal of chlorophyll-a from other optically active constituents such as suspended solids (Dall'Olmo & Gitelson, 2005; Gitelson et al., 2008; S. Mishra & Mishra, 2012).

ACLUS dan JCLUS are algorithms for a specific inland water type, tuned from the 2BDA and NDCI algorithm, respectively, in a rigorous study by Claire Neil et al. (2019). Their research found 13 different optical water types (OWT) for inland water (Figure 4-8 Left). ACLUS and JCLUS are empirical modesl found most suitable for Optical Water Type 11 and 12 (OWT11 and OWT12, respectively), the categories whose surface reflectances are similar with the surface reflectance of Tonle Sap lake (Figure 4-8 Right), that have relatively high suspended matter. Derived from the

2BDA and NDCI algorithms, ACLUS and JCLUS also use the MERIS bandwidth. Table 4-11 Existing major chlorophyll-a concentration prediction algorithms

| Algorithm | Reference | Model | Original Use (Satellite) |
|---|---|---|---|
| 2BDA | (Dall'Olmo & Gitelson, 2005) | $Chl_a \approx \dfrac{R(708)}{R(665)}$ | Turbid water (Non-satellite/Analytical) |
| 3BDA | (Gitelson et al., 2003) | $Chl_a \approx \dfrac{R(753)}{R(665) - R(708)}$ | Turbid water (Non-satellite/Analytical) |
| NDCI | (S. Mishra & Mishra, 2012) | $Chl_a \approx \dfrac{R(708) - R(665)}{R(708) + R(665)}$ | Estuarine and coastal water (MERIS) |
| ACLUS | (Neil et al., 2019) | $Chl_a = 53.18 +\ 80.7x\ \dfrac{R(708)}{R(665)}$ | Inland water (MERIS) |
| JCLUS | (Neil et al., 2019) | $Chl_a$ $\approx 19.31 + 153.5$ $* \dfrac{R(708) - R(665)}{R(708) + R(665)} + 105.4$ $* (\dfrac{R(708) - R(665)}{R(708) + R(665)})^2$ | Coastal turbid water |

Figure 4-9 depicts the Spectral Response Functions (SRFs) of Landsat OLI and MERIS. The blue and red vertical lines point to the MERIS wavelengths used in the primer chlorophyll-a algorithms for waterbodies. The blue line is the centre of MERIS' red bandwidth, and the red line is the centre of the NIR bandwidth of MERIS.
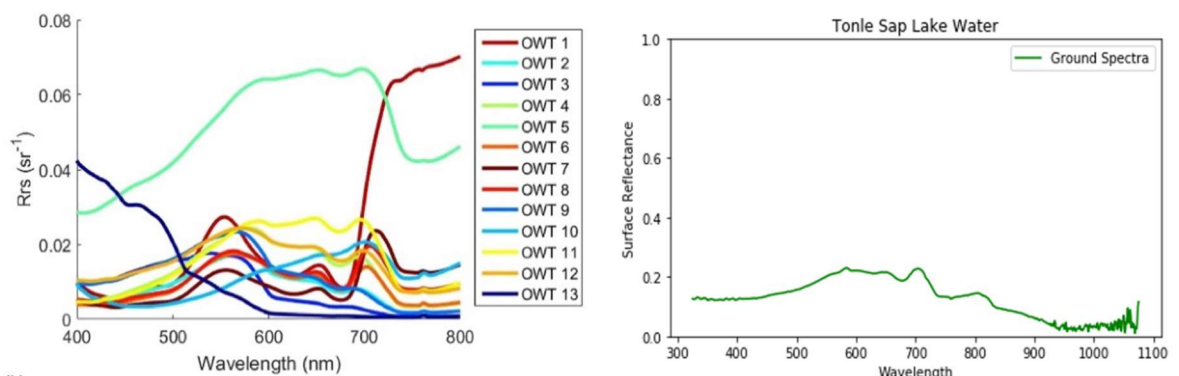


Figure 4-8 Left: Average surface reflectance of different water types according to (Claire Neil et al., 2019). Right: field-measured surface reflectance of Tonle Sap lake's water (right)
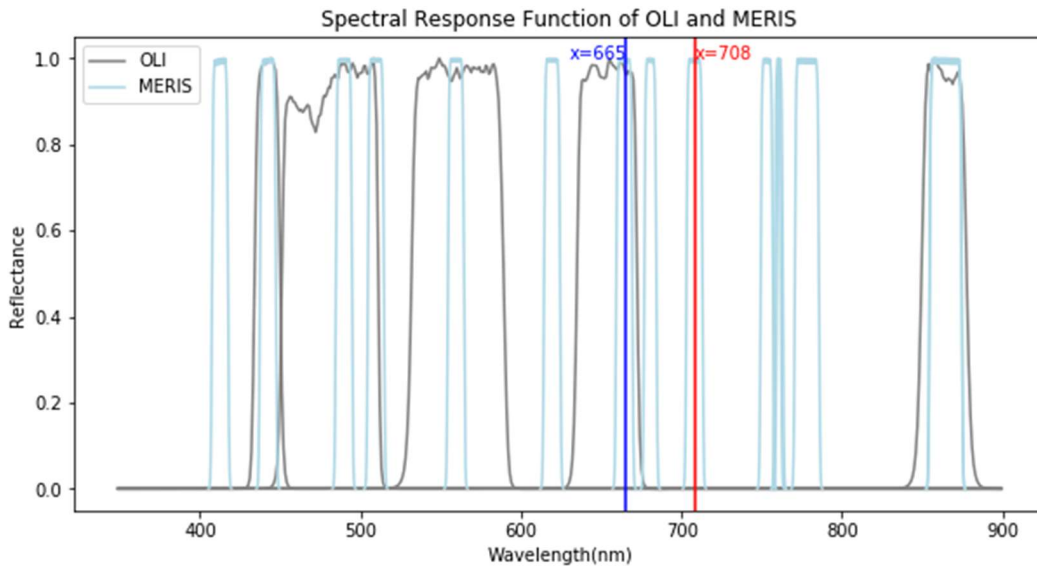
Figure 4-9 Spectral Response Functions (SRFs) of Landsat OLI and MERIS

Figure 4-10 shows the simulated MERIS reflectance for ground spectra of different objects. To gain a comparative view, the simulated OLI reflectance and Landsat OLI surface reflectance (Figure 4-4) are also plotted in the figure.
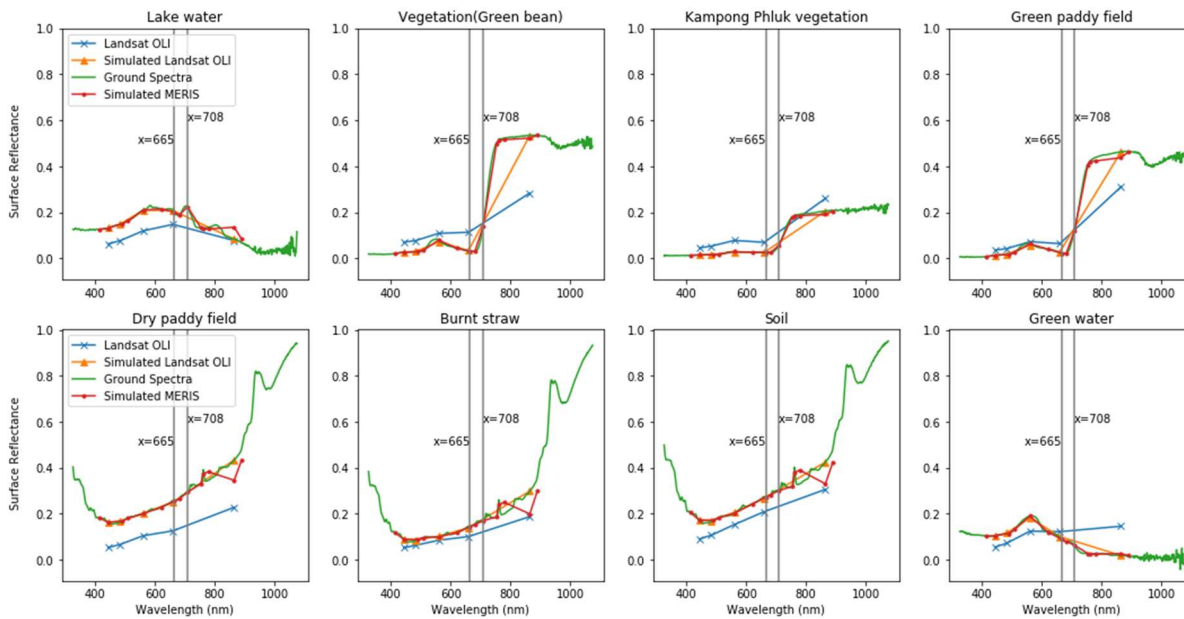


Figure 4-10 Simulated MERIS surface reflectance for ground spectra of various land covers

The main chlorophyll-a retrieval algorithms (Table 4-11) then were tested for their ability to estimate chlorophyll-a concentration in Tonle Sap lake. To apply Landsat OLI's surface reflectances into the algorithms, the surface reflectances were interpolated to get the surface

reflectances in MERIS wavelengths, i.e., 665 nm and 708 nm, which are used in the main chlorophyll-a retrieval algorithms evaluated (Table 4-11).

Figure 4-11 shows the interpolation of Landsat OLI bandwidth value undertaken to obtain the MERIS-equal bandwidth value at the wavelengths of 665 nm and 798 nm. The MERIS-equal reflectance value of the two wavelengths are generated from the closest Landsat OLI's band, which has a wavelength range of 0.64 to 0.67 nm.
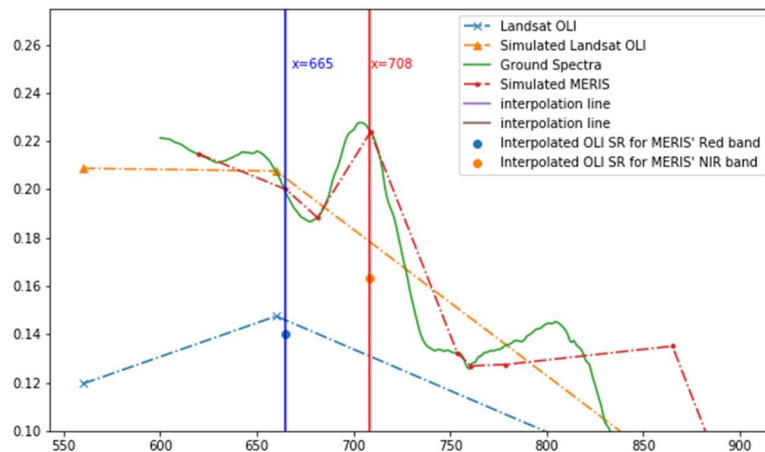


Figure 4-11 Interpolation of OLI' spectra to obtain MERIS-equal surface reflectance

The chlorophyll-a estimation results from 4 existing algorithms, as well as the random forest algorithm, were verified with in-situ chlorophyll-a data. Table 4-12 tabulates the constant and multiplication factors for each algorithm.

Table 4-12 Verification results of existing major chlorophyll-a prediction algorithms with field measured chlorophyll-a concentration

| Algorithm | Model | $R^2$ |
|---|---|---|
| 2BDA | $Chl_a = -20.7 + 23.3 * 2BDA$ | 0.10 |
| 3BDA | $Chl_a = 3BDA$ | 0.10 |
| NDCI | $Chl_a = -27 - 60.7 * NDCI$ | 0.10 |
| ACLUS | $Chl_a = 53.18 + 80.7 * ACLUS$ | 0.07 |
| JCLUS | $Chl_a = 19.31 + 153.5 * NDCI + 105.4 * NDCI^2$ | 0.07 |
| Random Forest (RF) | $Chl_a \approx RF\big(R(483), R(560), R(660), R(865)\big)$ | 0.56 |

Figure 4-12 describes the comparison between the field-measured chlorophyll-a and the estimated chlorophyll-a obtained from each algorithm, showing that while the well-known chlorophyll-a algorithms are unable to estimate the chlorophyll-a concentrations in Tonle Sap lake; the new Random Forest method developed here delivers much improved results.
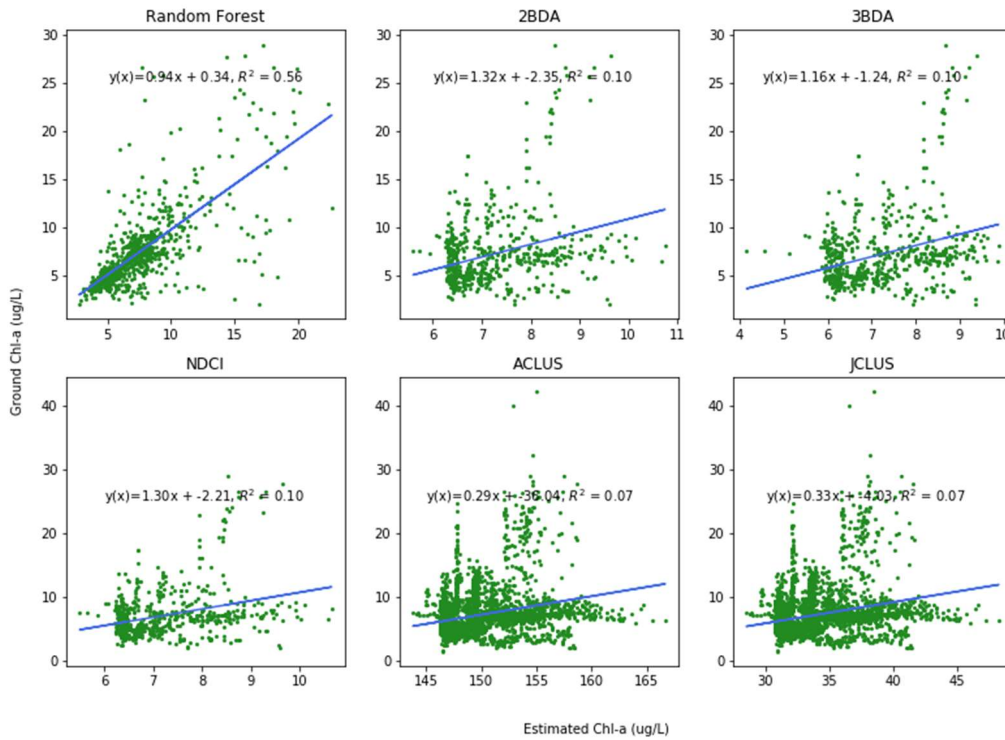


Figure 4-12 Comparison between field-measured chlorophyll-a and estimated chlorophyll-a from the existing algorithms and random forest

Random Forest is known to poorly estimate extrapolation of values outside the training set (Hengl et al., 2018). In the random forest built for this study, the train and test data set split was done randomly by scikit-learn. The split process was repeated until the train set contains the maximum and the minimum values of the whole chlorophyll-a data, which is 42.19 µg/L and 1.56 µg/L, respectively. Having these maximum and minimum values in the train set can guarantee that the predicted values of chlorophyll-a were not generated from poor extrapolation in the estimation by the random forest regressor.

## 4.5    Study Site Locations and Data Availability
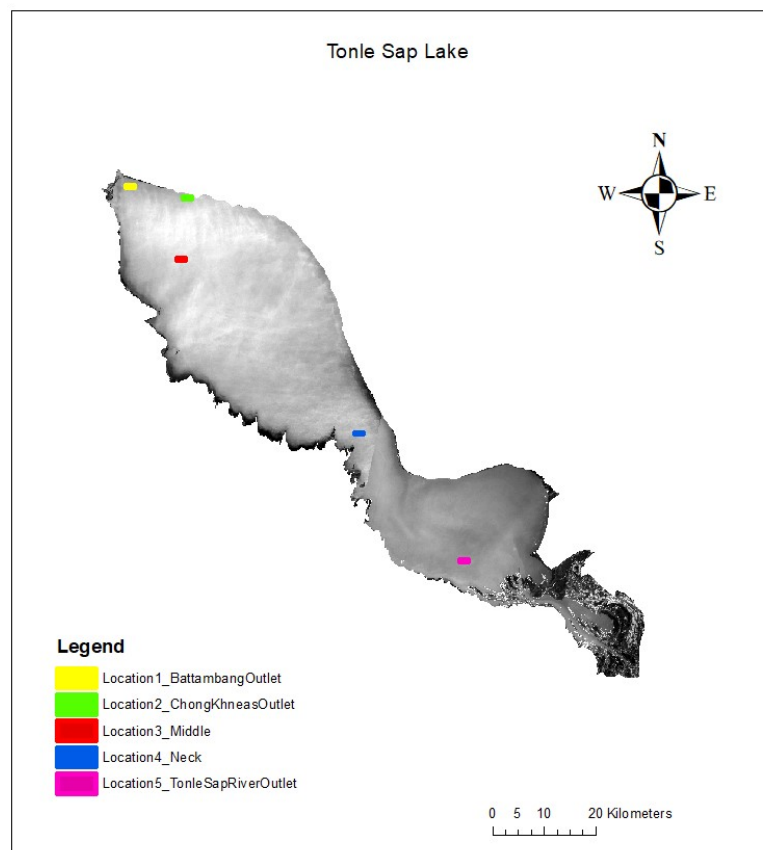


Figure 4-13 The five study site locations chosen for detailed analysis of water quality parameters within the Tonle Sap Lake. The shading represents variations in the surface reflectance of the water.

### 4.5.1    Study Site Locations within Tonle Sap Lake

A total of five locations (Figure 4-13) from within Tonle Sap Lake were chosen to undertake focused analysis of water quality parameters. The five locations were selected to represent discrete zones of the lake that may be affected by drivers of change in different ways. The specific locations were selected as follows:

1. *Battambang River outlet*

    The outlet of the Battambang River is located at the northwest tip of the Tonle Sap lake. The river drains much of Battambang province, one of Cambodia's important agricultural regions (Mund, 2011). These areas have intensive agricultural systems, with fertiliser often applied above the recommended application limits (Srean et al., 2018). The region of the lake close to the outlet of the Battambang River may therefore be affected by

excessive nutrients (N, P), potentially triggering comparatively higher phytoplankton growth.

2. *Chong Khneas River outlet*

    The outlet of the Chong Khneas River is one of a few locations where floating villages, whose populations live on boats, are predominant. This river outlet also constitutes a tourism port with a number of floating restaurants. Here, household wastewater both from the floating dwellings and restaurants is discharged directly to the lake. Phytoplankton blooms observed by the local people in recent years are most likely to result from the excessive nutrients from the growing tourism activities.

3. *The middle part of the lake*

    The middle part of the lake was selected to represent areas of the lake that are located furthest from the potential sources of excessive nutrients discharging from the lake's tributaries.

4. *The neck of the lake*

    The area of the 'neck of the lake' refers to the zone that forms a distinctive 'neck' shape that connects the wide area of the northern part of the lake, to the narrower southern part of the lake. This area was selected for analysis due to the potential key role that it plays in connecting the two major portions of the lake.

5. *Tonle Sap River outlet*

    The point at which the lake connects to form the Tonle Sap River, which in turn is the conduit that connects the lake to the Mekong River system, was also selected. This site represents a critical location as it is either the point of input (for Mekong-sourced water during the wet season) or the point of output (for lake waters draining to the Mekong during the dry season) for the significant volumes of water exchanged between the lake and the broader Mekong system.

### 4.5.2 Landsat Data Availability for Tonle Sap Lake

Two Landsat scenes covering the Tonle Sap lake area, i.e., path 127 row 51 (south basin) and path 126 row 51 (north basin) (Table 4-5 Corresponding Landsat OLI images for fieldwork data with their aerosol band. The black shadow is cloud cover.) from January 1990 to April 2020, were acquired. There were 1624 images in total, 803 images for the south basin, and 824 images for the north basin

Figure 4-14 shows the distributions of images from the acquisition of three Landsat satellites in the study period 1990 to 2020. Landsat 5 TM covers the year 1990 to 2011. From 1999 to 2011, Landsat 5 TM alternates with Landsat 7 ETM+. Then, from 2013 to 2020, Landsat 7 ETM+

alternates with Landsat 8 OLI. For those alternating periods, Landsat images are available every eight days.
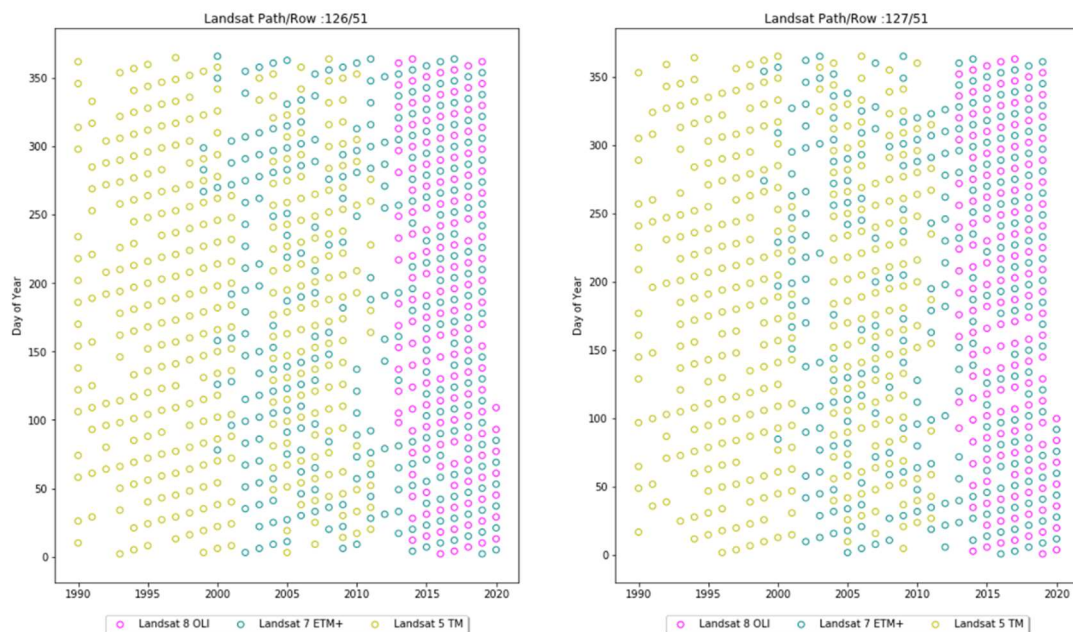


Figure 4-14 Landsat image availability for path/row 126/51 and 127/51

For the TSS and chl-a estimation undertaken herein, all Tier-1 and Tier-2 images were used. For a year when two Landsat satellites are operating, only images from one were used in order to avoid any inadvertent bias when averaging the water quality parameters for a particular season (e.g., dry season). When there is a data gap (e.g., because of cloud cover), images from other Landsat platforms were used (where available).

Each of the five study locations encompasses an area of 25 x 15 Landsat pixels, i.e., an area of 0.3 km$^2$. Cloud-covered pixels were determined with the qa band of Landsat and were assigned a null value. If the 0.3 km$^2$ point location contained more than 50% of null pixels, the final estimated value (of TSS or chlorophyll-a) was also regarded as null.

Each estimated value of TSS concentration used in subsequent analyses was determined from the mean TSS concentration of the (up to, depending on cloud cover) 375 pixels contained in each of the 5 study locations. The associated standard deviations were found to be below 50mg/L (excluding the outliers) in all areas except for location (a): Battambang River Outlet (see Figure 4-15). The Battambang River outlet had a standard deviation of up to 65 mg/L with more outliers than four other locations. Standard deviations computed for each data point are presented in Figure 5-2.
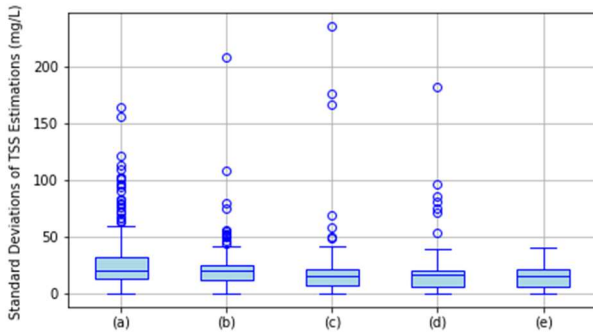
Figure 4-15 Distributions of the standard deviations in the estimation of the Total Suspended Solids concentrations at the 5 study locations: (a) Battambang River outlet, (b) Chong Khneas River outlet, (c) the middle of the lake, (d) the neck of the lake, and (e) Tonle Sap River outlet

As for the chl-a concentrations, each estimated value was again computed using the mean of the value recorded in the (up to) 375 pixels representing each study areas. The standard deviations were found to be below 3 µg/L (excluding the outliers, which are up to 3 µg/L) in all areas except for location (a): Battambang River Outlet (see Figure 4-16). The Battambang River Outlet had a standard deviation of up to 6 µg/L with outliers of up to 9 µg/L. The standard deviation for each data point is presented in Figure 5-4.
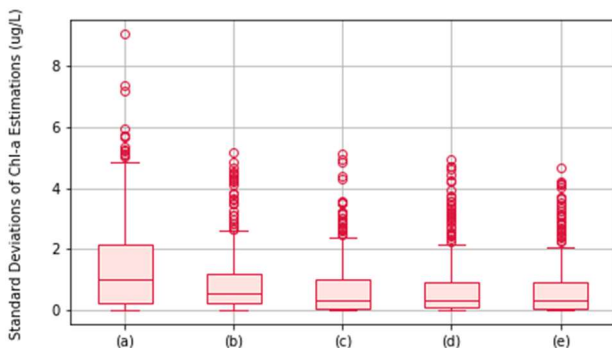


Figure 4-16 Distributions of the standard deviations in the estimation of the chlorophyll-a concentration at the 5 study locations: (a) Battambang river outlet, (b) Chong Khneas river outlet, (c) the middle of the lake, (d) the neck of the lake, and (e) Tonle Sap River outlet

Figure 4-17 and Figure 4-18 show the percentage of null and valid data for each season across every year of the analysis, for the TSS and chlorophyll-a estimation, respectively. The dry season is here defined as January to June, and the wet season July to December. These periods were defined as such to reconcile the time period used in the results elaborated in the next Chapter 5

and Chapter 6. These figures do not incorporate the year 2020, as 2020 will not be included for some analyses, such as the annual maximum TSS concentrations.
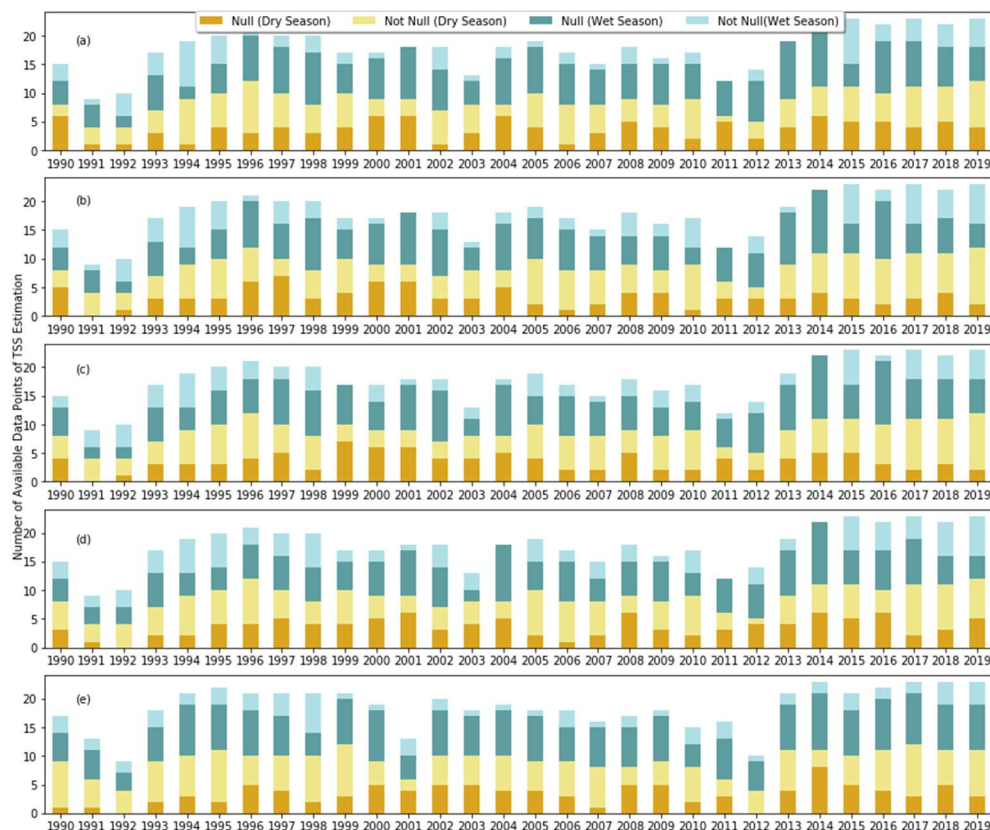


Figure 4-17 Percentage of null data for estimation of Total Suspended Solids concentrations in each season in the 5 locations of interest: (a) Battambang River Outlet, (b) Chong Khneas River Outlet, (c) The Middle of the Lake, (d) The Neck of the Lake and (e) Tonle Sap River Outlet.

For both TSS and chl-a estimation, high null values were found in the wet season, as the study area is frequently covered by heavy clouds at this time of the year. There are more null values than valid values for some years. For the year 2014, there is no valid value at all in the rainy season in 4 of the 5 locations, the exception being the Tonle Sap River outlet.

For some years (for example, 2013 and 2014 at location 5: Tonle Sap River Outlet), TSS has more null values than chl-a. This may be explained by the fact that the multiple linear regression used to estimate TSS in some cases gave spurious negative TSS concentration values, while the Random Forest algorithm always gives positive values of chlorophyll-a.
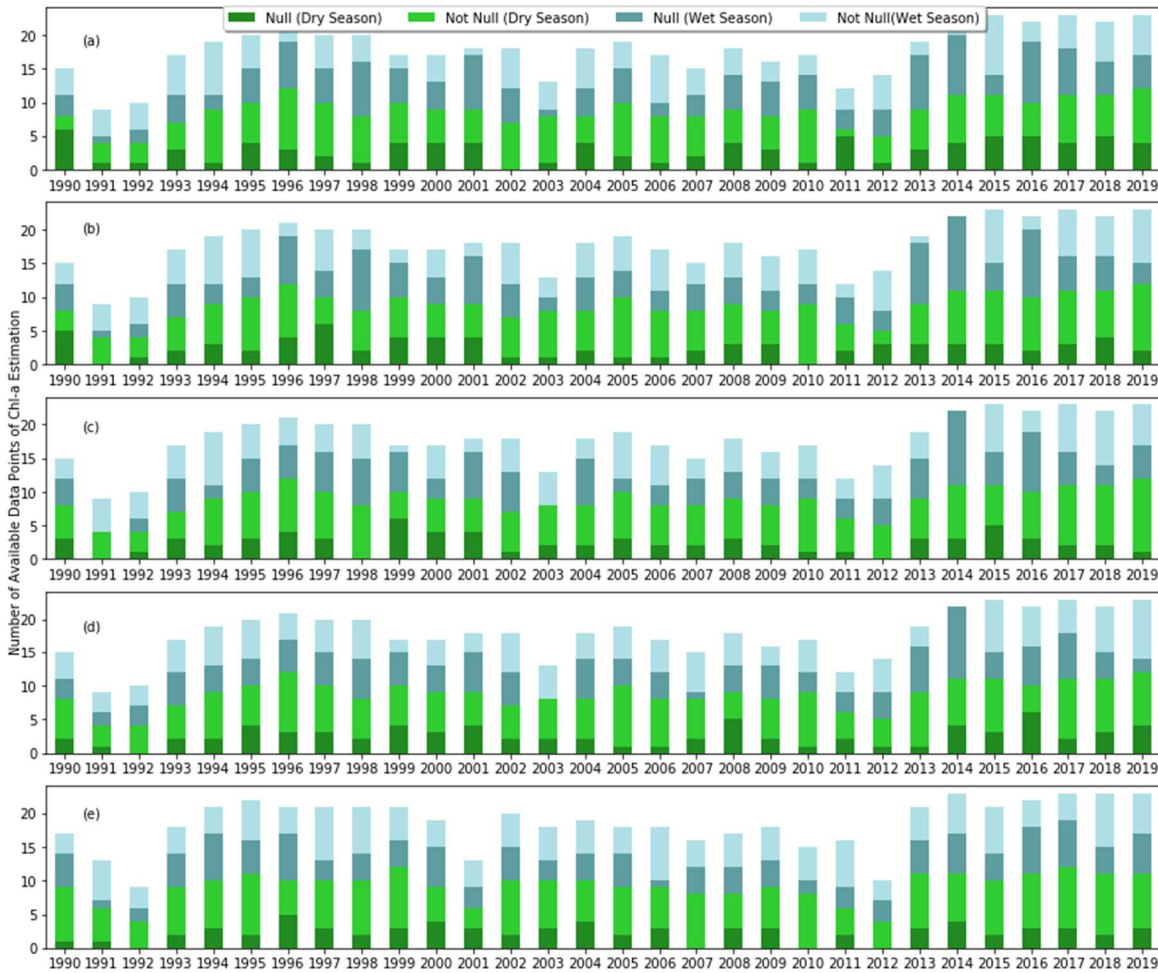
Figure 4-18 Percentage of null data for estimation of chlorophyll-a concentration in each season in 5 locations of interest: (a) Battambang River Outlet, (b) Chong Khneas River Outlet, (c) The Middle of the Lake, (d) The Neck of the Lake and (e) Tonle Sap River Outlet.

## 4.6    Mann-Kendall Trend Test

The non-parametric Mann-Kendall test was used to examine whether there are statistically significant long term trends present in the satellite-derived TSS and chl-a concentration records. This test is not particularly sensitive to missing data or outliers and requires no assumption of data distributions; hence it is suitable for use in this study (Helsel & Hirsch, 1992; Räike et al., 2003). Sen's slope estimator is also used to quantify the rate of change of any trend, assuming that any detected trend is linear (Gilbert, 1987; Sen, 1968).

In the Mann-Kendall test, the null hypothesis ($H_0$) is that there is no trend in the observed time series. The alternative hypothesis ($H_1$) is that there is a trend in the observed time series. The statistic $S$ for the time series is first calculated using:

$$S = \sum_{i=1}^{n-1} \sum_{j=i+1}^{n} sign(X_j - X_i) \tag{2}$$

where $n$ is the length of the time series and $sign(X_j - X_i)$ shows the relation between a data point and the successive data point in the time series. $sign(X_j - X_i)$ is computed with equation ( 3 ), while the variance $S_t$ of the statistics $S$ is derived using equation ( 4 ).

$$sign(X_j - X_i) = \begin{cases} +1, & (X_j - X_i) < 0 \\ 0, & (X_j - X_i) = 0 \\ -1, & (X_j - X_i) < 0 \end{cases} \tag{3}$$

$$S_t = \frac{1}{18}[n(n-1)(2n+5) - \sum_{p=1}^{q} t_p(t_p-1)(2t_p+5)] \tag{4}$$

In equation ( 4 ), $t_p$ is the number of ties for the $p$th value, and $q$ is the number of tied values. The Mann-Kendall test statistic $Z$ is then computed using:

$$Z = \begin{cases} (S-1)/\sqrt{S_t}, & S_t < 0 \\ 0, & S_t = 0 \\ (S+1)/\sqrt{S_t}, & S_t < 0 \end{cases} \tag{5}$$

The trend is statistically significant at the 95% significance level when the test statistic $Z$ falls beyond the confidence interval of ±1.96. A positive value of Z indicates that there is an increasing trend, while a negative value represents a decreasing trend.

# Chapter 5    Results – Multidecadal Trends of Water Quality Parameters for the Tonle Sap Lake

Two water quality parameters -Total Suspended Solids and chlorophyll-a concentration - were estimated for the Tonle Sap lake using Landsat images, following the methodology described in Chapter 4. Specifically, Landsat scenes from 1990 to the beginning of 2020 were used to obtain a comprehensive understanding of the seasonal variations and long-term trends in these two water quality parameters.  A total of five locations (Figure 4-13) across different areas of Tonle Sap lake were chosen to represent discrete zones of the lake that may be affected by drivers of change in different ways. The results, detailed in the following sub-sections, show any potential trend in the water quality parameters over the 30 year study period. It should be noted that these following sub-sections present and describe the results, whereas explanations for them will be discussed in the subsequent chapters.

## 5.1    Total Suspended Solids

Total Suspended Solids (TSS) concentrations at each location of interest were estimated using the linear regression function established in 4.4.3. The spatial and temporal variations of the estimated TSS concentrations over the 30 year study period for these five investigated locations are depicted in Figure 5-1.



Figure 5-1 Seasonal variations in estimated Total Suspended Solid concentrations during 1990-2020 at: (a) Battambang River outlet, (b) Chong Khneas River outlet, (c) The middle of the lake, (d) The neck of the lake, and (e)Tonle Sap River outlet. The box describes the interquartile ranges (IQR) of the TSS concentrations (with the median depicted by the line and the mean by triangles) recorded during the study period at each specific location. The whiskers depict the top and bottom 25% data which are within the one

and a half of the IQR. The mean values represented by the triangles in the box plots are the mean value for each seasonal interval over the 30 year period.

In Figure 5-1, the seasonal periods are defined following Hoshikawa et al. (2019), i.e., the late outflow period (January to March), low water (April and May), inflow (June to September), and early outflow (October to December) periods, with a slight modification. Specifically, in this study the inflow period is split into the months of both June and July to allow temporal resolution during these periods that brings sediment from the Mekong to the Tonle Sap lake. The inflow from the Mekong River typically begins in June, but in drought years, June can experience low water conditions. July is shown in detail to observe the dilution effect (if any) that the very early inflow water brings.

Figure 5-1 indicates that across all study sites, the TSS concentrations exhibit significant seasonal fluctuations. The lowest values typically occur in the early outflow period (October to December), with mean sediment concentrations varying from 13 mg/L to 36 mg/L across the 5 study sites. Mean TSS concentrations then rise during the periods of late outflow (January to March) and low water (April to May) before reaching their highest values in June, which is the end of the low water season or the beginning of the inflow water from the Mekong River, depending on the precise timing of the onset of the rainy season. The highest mean TSS concentrations vary between 187 mg/L to 285 mg/L, depending on the specific study site, with TSS concentrations then receding during the subsequent inflow periods (July to September). The interpretation of these temporal variations is discussed later in section 7.2.

In terms of the spatial variations of TSS between the study sites, the Chong Khneas River outlet (b) and the middle of the lake (c) consistently record the highest TSS concentrations throughout the year. The mean annual TSS concentrations at these locations are 133 mg/L and 136 mg/L, respectively, with the mean annual TSS values ranging from 98 to 107 mg/L at the other three study locations. Of the 5 study locations, the site located near the outlet of the Tonle Sap River (e) has the lowest TSS concentration, except during the late inflow season (August and September), when the region at the neck of the lake exhibits the lowest TSS concentrations. Section 7.3 provides discussions of these spatial variations.

The variations of the estimated TSS concentration for the five investigated locations over the full 1990-2020 study period are shown in Figure 5-2. Recalling that each study region is represented by a total of 375 Landsat pixels, data for each location is plotted as a mean value of the TSS concentrations across these pixels, while error bars reflect the associated standard deviation (see Section 4.5.2).
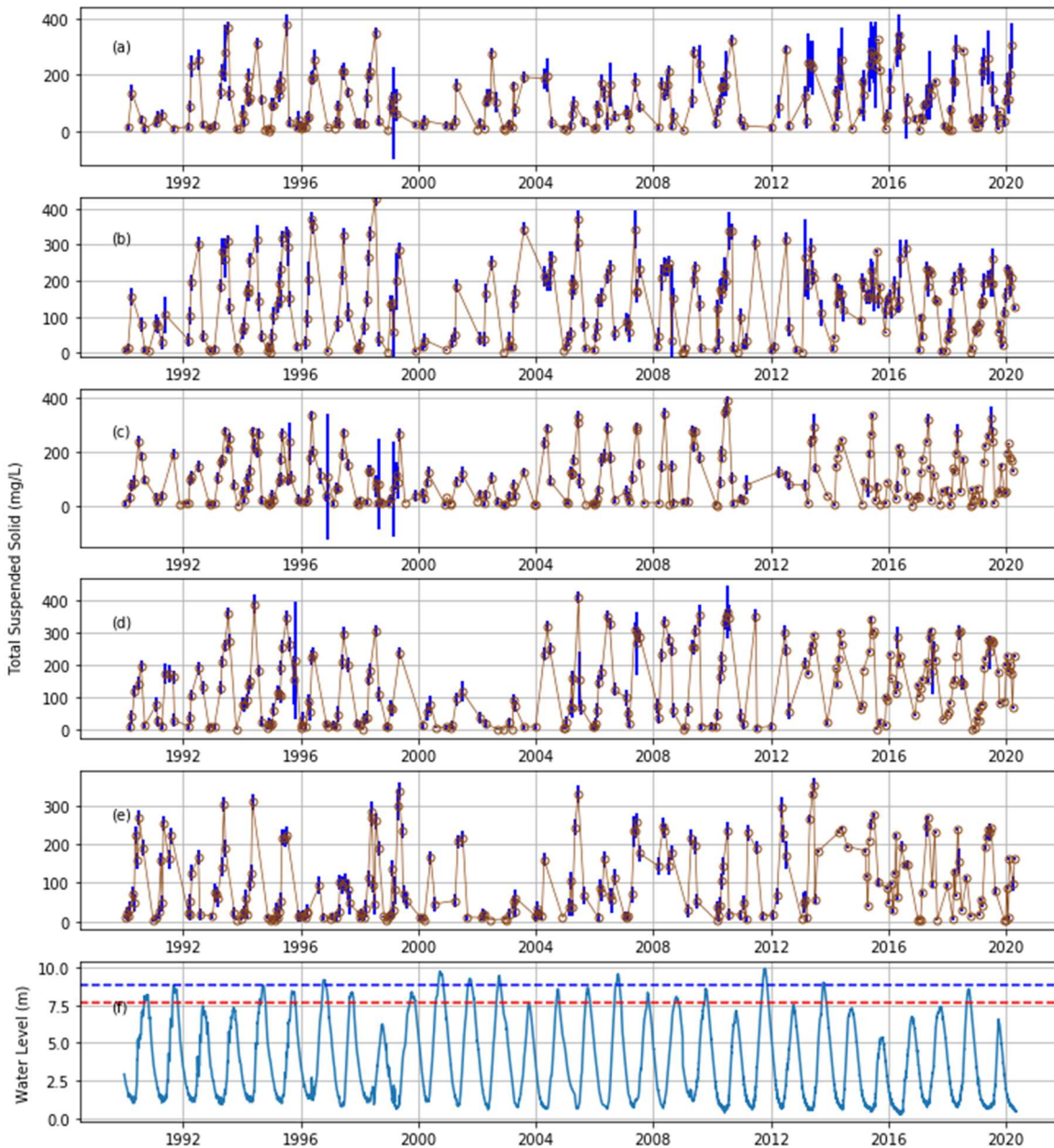
Figure 5-2 Total Suspended Solids concentrations from 1990 to 2020, as estimated from Landsat

images, for five different locations of the Tonle Sap lake: (a) Battambang River outlet,

(b) Chong Khneas River outlet, (c) The middle of the lake, (d) the neck of the lake, and

(e) Tonle Sap River outlet, along with the variation of water levels (f). In panel (f), the

blue and red horizontal lines indicate the thresholds for classifying 'flood' and

'drought' years (see Chapter 6 for definition of 'flood' and 'drought'). Error bars (in

blue) depict the standard deviation of the estimated TSS concentrations within the

375 Landsat pixels that represent each study area.

The variations in lake water level during this same period of analysis was estimated using data

from the Kampong Luong gauging station. This water level data has some periods of missing data

(January 1990 to June 1996, August to December 1997, January to July 1998, December 1998, and

January to April 2009). These missing data were estimated via interpolation of water level data from the gauging station at Phnom Penh Port, which is located at the downstream limit of the Tonle Sap River, some 160 km downstream of the lake (see Appendix A for details).

The time series shows the clear seasonality of TSS concentration discussed above, which is in opposite phase with the seasonal fluctuations of water level in the lake that is shown in the lowermost panel of Figure 5-2. A notable feature of all the time series is that, during the three consecutive 'flood' years of 2000 to 2002, the TSS concentration at all sites is much lower than the annual mean concentration level. This dilution effect by the flood is also reflected and explained in Figure 6-5 and discussed further there.

Table 5-1 Results of Mann-Kendall tests on the Landsat derived TSS concentrations at 5 study locations during the period from 1990 to 2020. The values of z in the brackets indicate the Sen slope, showing the annual rate of change of TSS concentrations. * shows a 5% significance level, ** shows a 10% significance level.

| Period | Battambang River outlet | Chong Khneas River outlet | The middle of the lake | The neck of the lake | Tonle Sap River outlet |
|---|---|---|---|---|---|
| Late Outflow (Jan-March) | increasing** (z=1.72) | increasing** (z=2.08) | increasing* (z=2.73) | no trend | increasing* (z=1.23) |
| Low Water (Apr &May) | increasing* (z=3.9) | no trend | increasing* (z=5.07) | increasing* (z=3.87) | no trend |
| Inflow (Jun-Sept) | no trend | no trend | no trend | no trend | no trend |
| Early Outflow (Oct-Dec) | increasing** (z=1.33) | no trend | no trend | increasing* (z=1.4) | no trend |
| June | no trend | decreasing* (z=-4.62) | no trend | no trend | no trend |
| July | no trend | no trend | no trend | no trend | no trend |
| Annual | increasing* (z=0.19) | increasing* (z=0.13) | increasing* z=0.34) | no trend | increasing* (z=0.17) |

Chapter 5

To investigate the long-term trend of the Landsat derived-TSS concentrations, Mann-Kendall tests (see section 4.6) were performed (using Python library pymannkendall version 1.2) on various derivative statistics.

Table 5-1 summarises the test results.

Table 5-1 shows that for 4 of 5 investigated locations (the exception is at the neck of the lake), at the annual scale there have been statistically significant (at the 5% significance level) increases in TSS concentrations during 1990-2020, albeit the increases are very small, i.e., at rates of change of less than 1 mg/L per year. One particular decreasing trend in June at Chong Khneas river outlet is a result of decreasing TSS concentrations in the drought years, while the other locations show increasing TSS concentrations over time.

At the Battambang River outlet, TSS concentrations have increased during the 1990-2020 study period during each seasonal interval, with the exception of the inflow period. At Chong Khneas River outlet, TSS concentrations during the late outflow period are also increasing (at a rate of 2.08 mg/L/yr). This is also true for the Tonle Sap River outlet (at a rate of 1.23 Y mg/L/yr). It is only at the neck of the lake that there are no significant trends in TSS over 1990-2020 during the late outflow period. However, the neck of the lake also sees an increasing trend during the low water and early outflow periods (at rates of 3.87 and 1.4 mg/L/yr, respectively). The increase during the low water period is steeper than the increase during the early outflow. In fact, the increases during the low water period have the highest rates of increase: 5.07 mg/L/yr at the middle of the lake, 3.9 mg/L/yr at the Battambang River outlet and 3.87 mg/L/yr at the neck of the lake, although the 2 other locations investigated here do not experience any trend of TSS during the low water period during 1990-2020.

The increasing trends are happening in the late outflow (January to March) and the low water periods (April and May). In contrast, there is no trend of TSS detected for the period when water is inflowing from the Mekong river (June to September). For the early outflow period, the Battambang River outlet and the neck of the lake encounter an increasing trend (at rates of 1.33 and 1.4 mg/L/yr, respectively), albeit the trend detected in the Battambang River outlet has a lower significance level. The potential causes and consequences of this

phenomenon are discussed in Section 7.5.

## 5.2    Chlorophyll-a Dynamics of Tonle Sap Lake

Chlorophyll-a (chl-a) concentrations at each location of interest were estimated using the Random Forest methods established in Section 4.4.4. The spatial and seasonal variations of the estimated chl-a concentrations over the 30 year study period at each of the five investigated locations are illustrated in Figure 5-3.

In  Figure 5-3, the seasonal periods of the water level are again defined following Hoshikawa et al. (2019), using the approach taken for TSS concentrations in Section 5.1. With the new supply of suspended sediment from the Mekong River, if there is any effect of the suspended sediment (such as phosphorus release) on the chlorophyll-a concentration, these periods potentially show it.
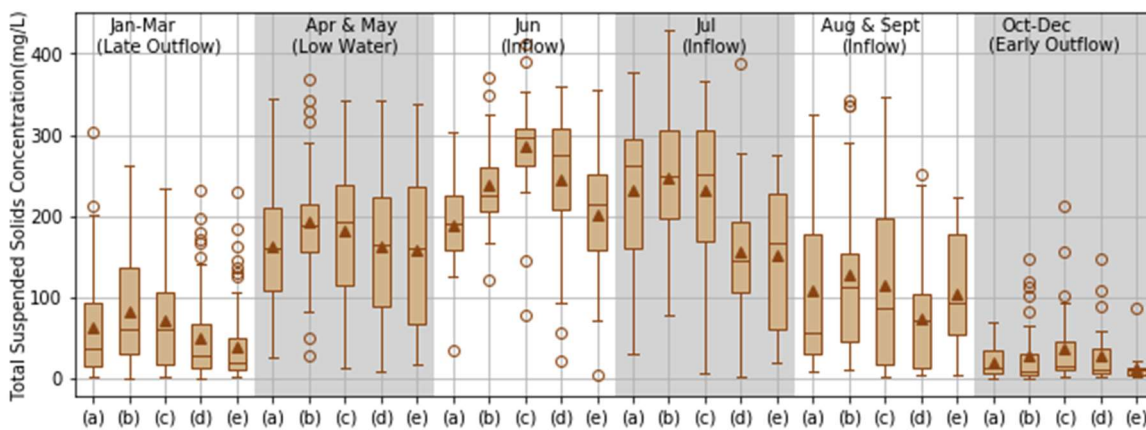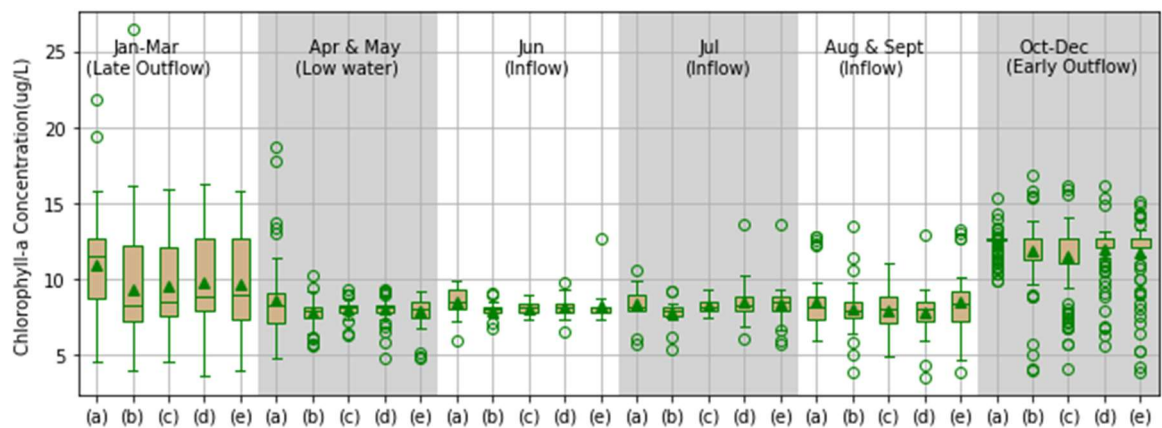


Figure 5-3 Seasonal variations in estimated chlorophyll-a concentrations during 1990-2020 at: (a) Battambang River outlet, (b) Chong Khneas River outlet, (c) The middle of the lake, (d) The neck of the lake, and (e) the Tonle Sap River outlet. The box describes the interquartile ranges (IQR) of the cholorophyll-a concentrations (with the median depicted by the line and the mean by triangles) recorded during the study period at each specific location. The whiskers depict the top and bottom 25% concentration values which are within the one and a half of the IQR. The mean value represented by the triangle in the box plots is the mean value over the 30 years.

Figure 5-3 shows, although not as significant as the TSS concentrations, across all study sites, the mean chl-a concentrations also fluctuate over the changing annual cycle of the water level, but with rather different timings compared to those of the TSS concentrations reported in section 5.1. The lowest chl-a values typically occur in the low water period (April to May) and extend to the early inflow period (June and July). The mean chl-a concentration values for these periods are

almost homogenous across all five sites (varying between7.8 µg/L to 8.6 µg/L). Mean chl-a concentrations then rise to reach their highest values in the early outflow period (October to December). The mean chl-a concentration values in this early outflow period vary in a narrow range between 11.6 µg/L to 12.4 µg/L, depending on the specific study site. Mean chl-a concentrations then recede following the subsequent late outflow period (January to March). The interpretation of these temporal variations is discussed later in section 7.2.

In terms of spatial variations, the Battambang River outlet (location a) has the highest mean value in all water periods (mean values ranging from 8.4 µg/L to 12.4 µg/L). However, Chong Khneas River outlet (location b) records a point overpowering all others (26.5 µg/L), which occurred during the late outflow season (January to March) in the year 2011. During the peak chl-a concentration in the early outflow period (October to December), the neck of the lake tends to have the second highest concentration of the 5 study locations (12 µg/L). Section 7.3 provides discussions of these spatial variations.

A remarkable characteristic in the chl-a concentration data is the almost homogenous values obtained when the water level is low (April to May). This condition continues through to the period when the inflow arrives from the Mekong River (June to September), although the values begin to range at the end of this inflow period (August and September). The maximum mean chl-a concentrations, which occur in the early outflow (October to December) period, show very variable values. In particular, the Battambang River outlet (location a) has very different chl-a concentrations from year to year during this early outflow period. Chl-a concentration values also range widely during the late outflow (January to March) period. These phenomena are also discussed in more detail Section 7.3.

Time series of the estimated chl-a concentrations for the five investigated locations within the Tonle Sap lake are shown in Figure 5-4. Recalling again that each study region is represented by a total of 375 Landsat pixels, data for each location is plotted as a mean value of the chl-a concentrations across these pixels, while error bars reflect the associated standard deviation (see Section 4.5.2).

Similar to the TSS concentrations, the graphs depict a strong seasonality of the chl-a concentrations. In contrast to the TSS response curves, the estimated chl-a fluctuations are almost in phase with the seasonal fluctuations of water level in the lake (as shown in the lowermost panel of Figure 5-4), albeit with a small lag. While being seasonal, the chl-a concentration range value is remarkably similar from year to year, as mentioned before. A notable feature of the time series is two outlying (high values) chl-a concentrations, which both occured in 2011, at the Battambang River outlet (21.3 µg/L) and the Chong Khneas river outlet (26.5 µg/L),

respectively. There is no major change in chl-a concentration during the three consecutive 'flood' years of 2000 to 2002.
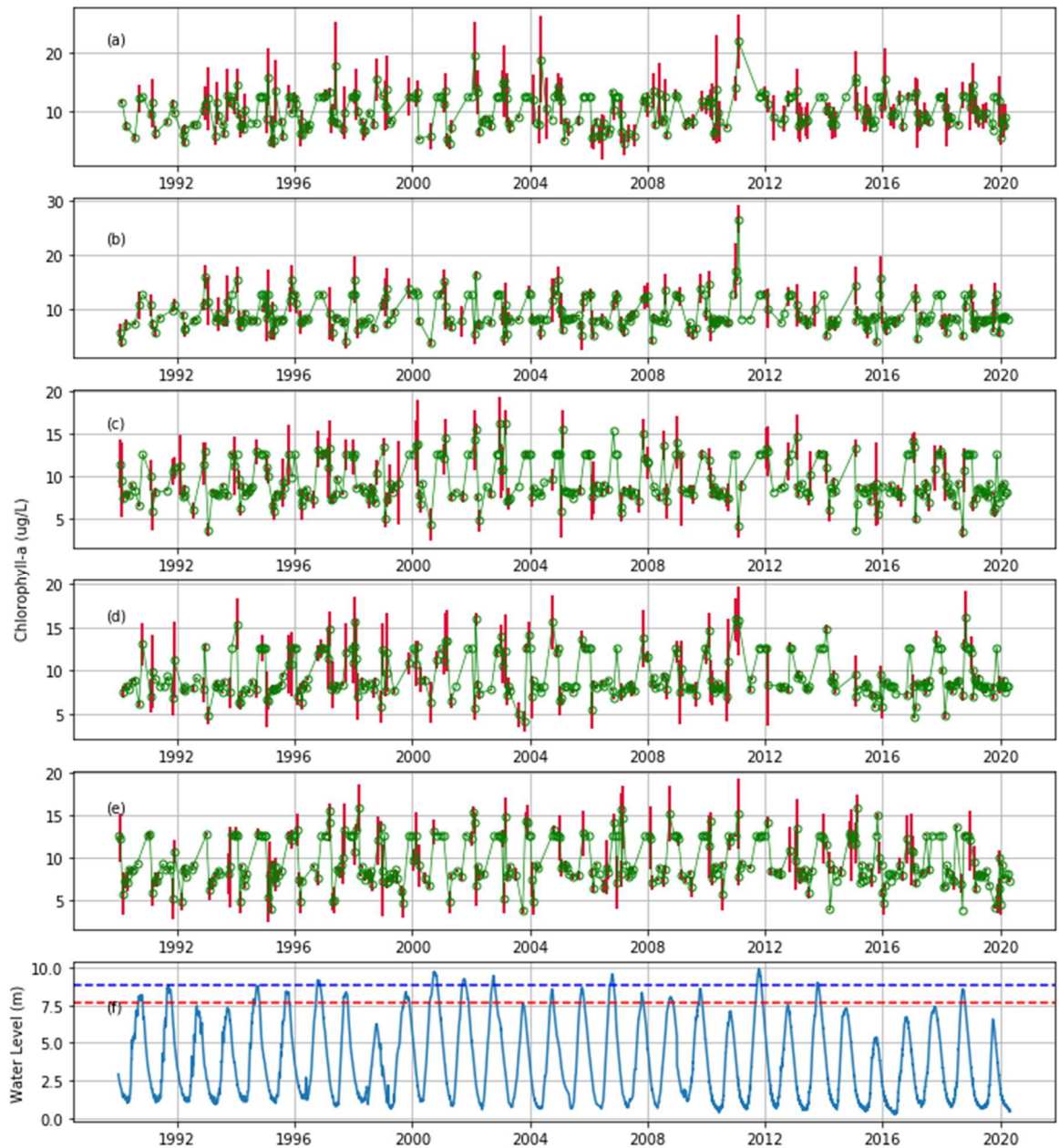


Figure 5-4 Chlorophyll-a concentrations from 1990 to 2020, as estimated from Landsat images, for five different locations of the Tonle Sap lake: (a) Battambang River outlet, (b) Chong Khneas River outlet, (c) the middle of the lake, (d) the neck of the lake, and (e) the Tonle Sap River outlet, along with the variation of water levels (f). In panel (f), the blue and red horizontal lines indicate the thresholds for classifying 'flood' and 'drought' years (see Chapter 6 for definitions of 'flood' and 'drought'). Error bars (in red) depict the standard deviation of the estimated Chlorophyll-a concentrations within the 375 Landsat pixels that represent each study area.

Further, to investigate the long-term trend of the Landsat derived-chl-a concentrations, Mann-Kendall tests (see section 4.6) were performed (using Python library pymannkendall version 1.2) on various derivative statistics. Table 5-2 summarises the test results.

Table 5-2 Results of Mann-Kendall tests on the Landsat derived chl-a concentrations at 5 study locations during the period from 1990 to 2020. The values of z in the brackets indicate the Sen slope, showing the annual rate of change of chl-a concentrations. * shows a 5% significance level, ** shows a 10% significance level. Z in the brackets are the Sen slope.

| Period | Battambang River Outlet | Chong Khneas River Outlet | The Middle of the Lake | The Neck of the Lake | Tonle Sap River Outlet |
|---|---|---|---|---|---|
| Late Outflow (Jan-March) | no trend | no trend | no trend | no trend | no trend |
| Low Water (Apr &May) | increasing** (z=0.057) | no trend | no trend | increasing* (z=0.017) | no trend |
| Inflow (Jun - Sept) | no trend | no trend | no trend | no trend | no trend |
| Early Outflow (Oct-Nov) | no trend | no trend | no trend | no trend | no trend |
| June | no trend | decreasing** (z=-0.032) | no trend | no trend | decreasing** (z=-0.025) |
| July | no trend | no trend | no trend | no trend | no trend |
| Annual | no trend | no trend | no trend | no trend | no trend |

Overall, the results indicate that essentially there is little evidence of any statistically significant long-term increase (or decrease) in chl-a concentrations within the Tonle Sap lake. Any such increases seem to be restricted only to the low water period, in the Battambang river outlet (rate

of increase 0.057 μg/L/yr), and the neck of the lake (rate of increase 0.017 μg/L/yr). These increases are probably caused by the increase of TSS concentrations during the same period in which phosphorus release is observed (Burnett et al., 2017). There are three locations that see an increase of TSS concentrations during the low water period: the Battambang River outlet, the neck of the lake, and the middle of the lake. The author could not find any explanation as to why the increase of TSS concentrations in the middle of the lake, which has the biggest increase among the three locations, does not also bring an increase in the chl-a concentrations at this location.

A decreasing trend in Chl-a is evident during the end of the low water season (June) in 2 locations, at the Chong Khneas River outlet (rate of decrease of 0.032 μg/L/yr) and the Tonle Sap River outlet (rate of decrease of 0.025 μg/L/yr). The small decrease of chlorophyll-a concentrations at Chong Khneas river outlet is possibly related to the decrease of TSS concentrations during the same period at the same location, as the decrease of TSS concentrations means less phosphorus release for the phytoplankton to grow. See Chapter 7 for the full discussions of these results.

# Chapter 6 Water Quality Variations in Relation to Tonle Sap Lake Hydrology

This chapter explores whether there is a link between year-to-year variations in the Tonle Sap lake water quality parameters (as estimated in Chapter 5) and variations in hydrological conditions, with the latter presumed to be a key driving factor governing the lake's water quality.

Table 6-1 lists the results of Mann Kendall trend analyses of the water level data of Tonle Sap Lake at Kampong Luong for the 30 years period. It shows that water levels have exhibited a small but statistically significant declining trend during 1990-2020, over the whole 30-year time span, and at all the seasonal intervals considered (annual, low water period, inflow period, early outflow period, and the late outflow period). Annually, the water level in Tonle Sap lake is decreasing by 0.7 mm every year. Results presented in Chapter 5 reveal a strong seasonal variation in total suspended solids (TSS) and (to a lesser extent) chlorophyll-a (chl-a) concentrations. Yet, the Mann-Kendall trend analyses conducted in Chapter 5 do not show any significant long-term trends in TSS or chl-a (with the exception of TSS concentrations at some locations/times of the year).

Table 6-1  Results of Mann-Kendall analysis of the Tonle Sap Lake water level (at Kampong Luong) during the period from 1990 to 2020. The values in the brackets are the significance level. * shows a 5% significance level, ** shows a 10% significance level. The Z values in the brackets represent the Sen slope.

| Late Outflow (Jan-March) | Low Water (Apr &May) | Inflow (Jun-Sept) | Early Outflow (Oct-Dec) | Annual |
|---|---|---|---|---|
| decreasing* (z=-0.002) | decreasing* (z=-0.003) | decreasing* (z=-0.009) | decreasing* (z=-0.005) | decreasing* (z=-0.0007) |

Hoshikawa *et al.* (2019) found that in Tonle Sap Lake, the annual maximum water levels have a strong negative correlation with TSS concentrations, particularly during the late outflow period (January to March). However, the annual maximum TSS concentrations do not necessarily correlate to the (minimum) water level.  Hoshikawa *et al.* also found that flooding results in higher TSS concentrations during the inflow period (June to September).

In terms of chlorophyll-a concentrations in Tonle Sap lake, there have been very few prior studies. However, Irvine *et al.* (2011) found that the monthly mean dissolved oxygen (a proxy for primary productivity) in Tonle Sap lake is generally around 8.5 mg/L, declining to a minimum (approximately 5.5 mg/L) twice a year, in January and April.

Davies, Bunn and Hamilton (2008) suggested that hydrological characteristics such as precipitation patterns play a vital role in tropical systems, where the precipitation patterns can control the timing and magnitude of aquatic primary production.

The analysis above indicates that hydrological variability may need to be invoked to explain the variations in water quality identified in Chapter 5. In particular, the focus in this chapter is on exploring the potential influence of hydrological variability, in terms of episodes of floods and droughts at inter-annual timescales, as well as the large-scale seasonal variations that affect the lake each year, on TSS and chl-a dynamics, ultimately leading to the derivation of data-led conceptual models of TSS and chl-a concentration-response for Tonle Sap lake.

## 6.1    Floods and Droughts in Tonle Sap Lake

Episodes of flood and drought are common natural disasters in Cambodia (Chhinh & Millington, 2015; G. I. Davies et al., 2015; UNDP, 2019), and affect the dynamics of the Total Suspended Solid concentration in Tonle Sap lake (Hoshikawa et al., 2019). Two potentially interrelated factors may drive floods in this region. First, high water levels on the mainstem Mekong River reflect hydro-climatological responses covering the entire Mekong basin. Second, high water levels on the Tonle Sap lake's tributaries are more reflective of local or regional hydro-climatological responses.

Meanwhile, episodes of drought occur as a result of a number of different factors (National Committee for Disaster Management, 2008), including the delay of rainfall onset, the amount and duration of wet season rainfall, the early ending of rain during the wet season, and the common occurrence of mini-droughts of three weeks or more during the wet season (which can damage or destroy rice crops without irrigation). As a result, any given year can experience episodes of drought during the dry season (because of a late rainy season) and/or flood in the rainy season (because of the high volume of water coming from Mekong and precipitation). If the rain ends earlier, a sequence of drought, flood, and drought may happen in one year. Table 6-2 lists episodes of floods and drought that have occurred in the last 30 years in Cambodia.

Over the course of a hydrological year, and as discussed in Chapter 5, the Tonle Sap lake water level fluctuates through four distinct periods: the period of lowest water at the height of the dry season (April and May), the inflow period when the Tonle Sap River undergoes its seasonal

reversal and waters from the Mekong begin to infill the lake (June to September), the early

outflow period when water levels in the Mekong drop back below the Tonle Sap lake, the Tonle

Sap River starts to drain the infilled lake back towards the Mekong (October to December), and

the period of late outflow (January to March) when water is draining from Tonle Sap lake towards

the Mekong River at Phnom Penh (National Committee for Disaster Management, 2003). These

water level periods are illustrated in different colors in Figure 6-1, with additional partitioning of

the months of June and July within the infilling period in order to resolve the timing of water

inflow from the Mekong river in each year.

Table 6-2 Episodes of drought and flood occurrence in Cambodia, collated from National

        Committee for Disaster Management (2003), (G. I. Davies et al., 2015), and ODC

        (2016).

| Year | Type of Disaster | Year | Type of Disaster |
|---|---|---|---|
| 1990 | - | 2005 | Drought (Jan to April) |
| 1991 | Flood (August) | 2006 | Flood |
| 1992 | - | 2007 | Flood |
| 1993 | - | 2008 | Flood and drought (end of the year) |
| 1994 | Drought (June) and Flood (July) | 2009 | Drought then flood, then drought |
| 1995 | drought | 2010 | Flood (rainy season), drought |
| 1996 | Flood (September) | 2011 | Flood |
| 1997 | - | 2012 | Drought then Flood |
| 1998 | Drought (Early 1998) | 2013 | Flood |
| 1999 | Flood (rainy season) | 2014 | - |
| 2000 | Flood (rainy season) | 2015 | Drought |
| 2001 | Drought and Flood | 2016 | Drought |
| 2002 | Drought and Flood | 2017 | - |
| 2003 | Drought | 2018 | - |

| 2004 | Drought (October onwards) | 2019 | - |
|------|---------------------------|------|---|

Floods and droughts in Tonle Sap lake can also be inferred from the water levels and the timing of their occurrence. For example, a flood year may result in water still flowing into the lake in October, a time of year when it would normally begin to flow out to the Mekong River. Examples of such October inflow periods include the years 1997, 2006, 2007, 2009, 2010, 2011, 2012, and 2017.
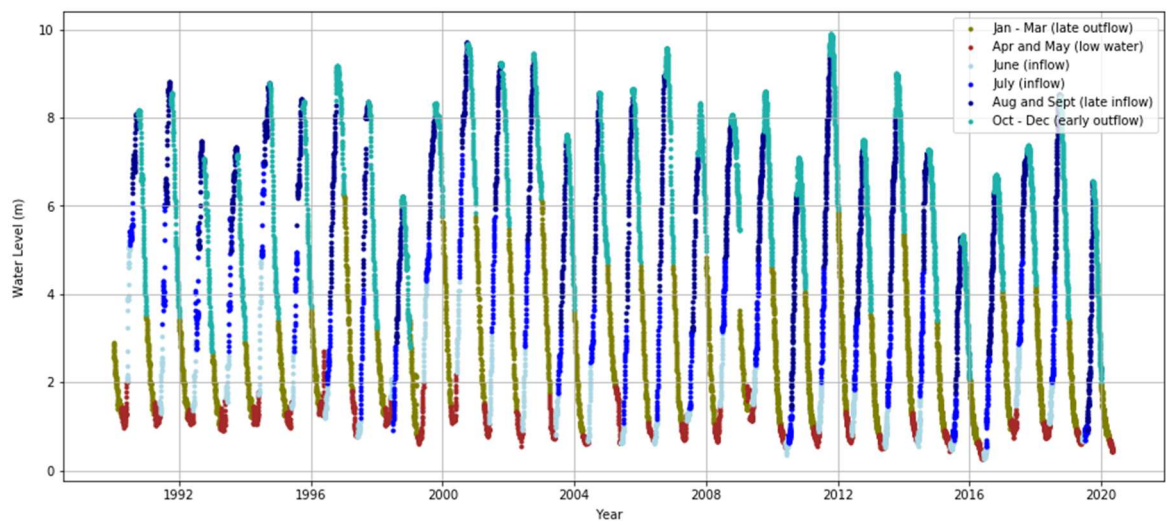


Figure 6-1 Water level of Tonle Sap Lake at Kampong Luong, from 1990 to April 2020

In contrast, droughts associated with the delayed onset of the rainy season may mean that the inflow season is delayed from its normal occurrence in June or even July, extending further the low water period of April and May. Such droughts were observed in 1997, 2005, 2006, 2010, 2015, 2016, and 2019, when the June or even July water level is only about 1 meter.

However, there are discrepancies in flood and drought data when inferred from water level data versus reported instances as extracted from the published literature. Such discrepancies arise in part because the published literature may also include partial drought that happened in the basin of the tributaries and not in Tonle Sap lake itself. For example, such partial droughts episodes may occur due to a few weeks of a dry spell during the rainy season.

To simplify the analysis, a flood is defined here as an abnormally high water-level, which is higher than 8.5 meters. At the same time, drought is here defined when the maximum water level is less than 7.2 meters (both thresholds refer to water levels at the Kampong Luong gauging station). These numbers are determined from the information of flood and drought occurrence in Table 6-2 while considering also the actual water level for that year. The flood threshold of 8.5 meters is the lowest water level of all years where a flood is reported to have occurred, and the water level data indeed show a higher level than the average. Similarly, the drought threshold of 7.2 meters is

the highest water level of all years where drought is reported to have occurred, and the water level data indeed show a lower level than the average. The mean maximum water level during 1990-2019 is 8.14 meters. The determined flood and drought points are 0.36 meters higher and 0.94 meters lower than this mean maximum level.

## 6.2    Total Suspended Solids Dynamics

Figure 6-2 shows the relationships between annual mean TSS concentrations in each water level period and the mean water level in the same period at the five study locations. The columns list the studied locations, from left to right: Battambang River outlet, Chong Khneas River outlet, the middle of the lake, the neck of the lake, and the Tonle Sap River outlet. The first to sixth rows denote late outflow (January to March), low water (April and May), end of low water (June), early inflow (July), inflow (August to September), and early outflow (October to December) periods, respectively.

During the late outflow period, when water is draining from Tonle Sap lake towards the Mekong River at Phnom Penh, water levels strongly negatively correlate to the TSS concentrations at the Battambang River outlet (r = -0.63) and Chong Khneas River outlet (r = -0.62). There is also a moderate negative correlation in the middle of the lake (r = -0.47), but the correlation between water level and TSS is much weaker at the other two study locations.

When the water level is at its lowest, correlations with TSS concentrations at the Battambang River outlet and the middle of the lake are moderately negative (r= -0.52 and r = -0.54, respectively). In June, which is the beginning of the inflow from the Mekong River, or still in low water conditions when the inflow is late, the water level also moderately negatively correlates with the TSS concentrations in the middle of the lake (r = -0.43) and the Tonle Sap river (r = -0.41) locations.

However, there is no strong correlation between TSS and water level during the late inflow period when the water in its highest level, except for a moderate negative correlation at the Chong Khneas river outlet (r =  -0.44). When the water begins to flow out to the Mekong river, only the locations at Chong Khneas and the Tonle Sap river outlet show moderately negatively TSS – water level correlations (r =- 0.56 and r = -0.43, respectively).

Figure 6-3 shows the same relationships between the water level and TSS concentrations during each hydrological period (late outflow, low water, inflow, and early outflow) as shown in Figure 6-2, but in this diagram the data are further separated into the flood, drought, and normal years defined in Section 6.1.

Figure 6-2 Relationship between annual mean TSS concentration and mean water level in each hydrological period at the five study locations. The first to the fifth columns are the Battambang River outlet, Chong Khneas River outlet, the middle of the lake, the neck of the lake, and Tonle Sap River outlet. The first to the sixth rows are the late outflow (January to March), low water (April and May), end of low water (June), early inflow

(July), inflow (August to September), and early outflow (October to December) periods, respectively.

In the late outflow (January to March) period, TSS concentrations are higher in the drought years than during the flood and normal years. This is seen at all study locations (a) to (e). At the Battambang River outlet (a), the mean TSS in the drought years is 81.9 mg/L, compared to 52.2 mg/L and 52.9 mg/L in the flood and normal years, respectively.  At the Chong Khneas River outlet (b), the mean TSS in the drought years is 103.8 mg/L compared to 77.4 mg/L and 64.5 mg/L in the flood and normal years, respectively. At the middle of the lake (c) it is 93.5 mg/L compared to 56.1 mg/L and 77.3 mg/L. At the neck of the lake the comparison is 71.0 mg/L versus 34.9 mg/L and 58.1 mg/L. Finally, at the Tonle Sap River outlet, the mean TSS concentrations during the late outflow period are 45.0 mg/L, 34.4 mg/L and 33.1 mg/L during drought, flood and drought years, respectively. In the low water period, the lowest TSS concentrations occur during the flood years.



Figure 6-3 Variations in Landsat-derived TSS concentrations and water level as measured at Kampong Luong for each of the 5 study locations over the period 1990-2020. The coloured lines separate the data into flood (blue lines), drought (orange lines), and normal (green lines) years. The first to the fourth rows are the different stages of the lake's hydrological fluctuations: late outflow (January to March), low water (April and May), inflow (June to September), and early outflow (October to December).

In contrast, during the inflow period it is the flood years that exhibit higher TSS concentrations as compared to the TSS concentrations observed during the drought years. This difference is particularly marked at the neck of the lake (n), with a mean TSS of 160.9 mg/L during the flood year inflow periods, compared to 145.7 mg/L during the drought years. However, the flood years seems to have a dilution effect on the TSS concentrations, as the TSS concentrations during the normal year inflow periods are higher than those observed in the flood years. This difference is particularly marked in the middle of the lake (where the mean TSS during the inflow of a normal year 27 mg/L higher than during flood years; see subplot (m)), and the Tonle Sap river outlet where the difference is 13 mg/L (subplot o).

The trends observed during the early outflow (October to December) period are similar to those of the inflow period, with the TSS concentrations lower during the high flood years as compared to the drought and normal flood years. This is seen in all study locations, as illustrated in the subplots (p) to (s). At three locations: Battambang River outlet (subplot p), the middle of the lake (subplot r), and the neck of the lake (subplot s), the TSS concentrations during drought years are lower than during normal flood years. At the Battambang River outlet (subplot p), TSS concentrations during the normal flood and drought years are higher by 52 mg/L and 16 mg/L, respectively, compared to the high flood years. Indeed, this location sees the biggest differences in TSS concentrations between the high flood and normal flood years. At Chong Khneas River outlet (subplot q), the comparison between the mean TSS concentrations observed during the high flood years to the normal and drought years is 28 mg/L and 37 mg/L lower, respectively. Chong Khneas River outlet (subplot q) experiences the biggest differences in TSS concentrations between the flood and the drought years. At the middle of the lake (subplot r), the mean TSS concentrations during the early outflow period for normal flood and drought years are higher by 37 mg/L and 27 mg/L, compared to the high flood years, respectively. At the neck of the lake (s), the TSS concentrations are higher 14 mg/L and 8 mg/L during the normal flood and the drought years. The Tonle Sap River outlet (t) experiences the lowest differences, with mean TSS concentrations during the early outflow period for the normal flood and drought years higher by 3 mg/L and 8 mg/L, compared to the high flood years, respectively.

Figure 6-4 reillustrates the Landsat-estimated TSS concentrations, in a full annual cycle in each study location, for each different type of hydrological year (normal, flood, and drought). On this diagram, the different periods of the year are again highlighted using different colours, such that the annual cycle of the lake's flood pulse can be tracked by following a clockwise trajectory around each diagram in a squashed oval shape.

It is evident that the annual fluctuations in TSS concentrations follow similar trajectories at each study location, with the highest TSS concentrations in the very early water period, a subsequent dilution of TSS concentration during the rest of inflow period, and the lowest TSS concentrations evident during the outflow period.

However, subtle differences are evident in the TSS concentrations associated with each type of year. Drought years present higher TSS concentrations during the early and late outflow periods. This pattern exhibits a 'drifting' oval shape, which is noticeable in subplots (f) and (g). Similarly, normal flood years, when compared to high flood years, show higher TSS concentrations in the inflow period. This creates a rather fat oval shape, which is apparent in subplots (l) and (m).



Figure 6-4 Variations in Landsat-derived TSS concentrations and water level as measured at Kampong Luong for each of the 5 study locations over the period 1990-2020. The coloured lines denote the different stages of the lake's hydrological fluctuations: late outflow (dark blue lines), low water (red lines), inflow (green lines), and early outflow (light blue lines).

Figure 6-5 presents a simplified data-driven conceptual model of the annual cycle of TSS concentration fluctuations resulting from the water flow variations, as based on the data presented in Figure 6-3 and Figure 6-4. This conceptual model depicts the temporal variations in the TSS concentrations in Tonle Sap lake over the course of its annual cycle.

During the low water season, the shallow depth and large fetch over the lake mean that wind-driven waves can re-suspend significant volumes of the fine-grained lake bed sediments, causing TSS concentrations to reach their maximum levels during the low water season (Hoshikawa et al.,

2019). During the early inflow period, the sediment-charged waters of the Mekong can further elevate TSS concentrations (this increase being highest in normal flood years and lowest in drought years) prior to the water discharge from the Mekong causing a subsequent dilution effect and attendant decline in TSS concentrations during the later phases of the inflow. Similarly, for the outflow period, as water levels fall, wind again becomes effective in driving sediment resuspension in the lake, though with a smaller effect than during the low water season.
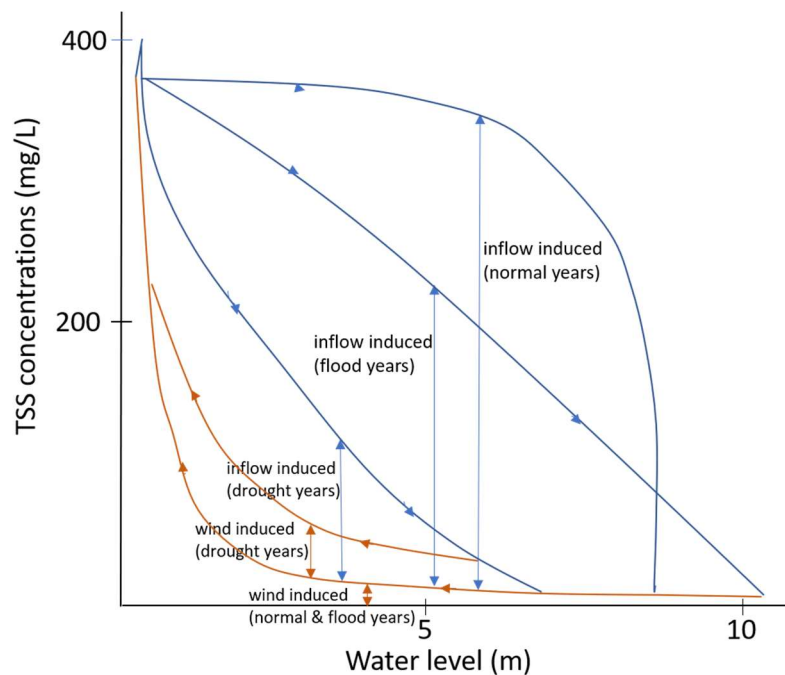


Figure 6-5 Simplified model of the annual cycle of TSS concentration fluctuations in Tonle Sap Lake.

All five study locations generally follow the trajectory of the model shown in Figure 6-5, with subtle variations in the precise dynamics between each study location. For example, the Chong Khneas river outlet has higher TSS concentrations resulting from the wind during the early and late outflow periods, especially in the drought and flood years. Another variation is for the Tonle Sap River outlet in the drought years, where the inflow begins from relatively low TSS concentrations.

## 6.3 Chlorophyll-a Dynamics

Figure 6-6 shows the relationships between the annual mean chl-a concentrations in each phase of the annual hydrological cycle and the mean water level in the same period at each of the five

study locations. The columns list the studied locations, from left to right: Battambang River outlet, Chong Khneas River outlet, the middle of the lake, the neck of the lake, and the Tonle Sap River outlet. The first to sixth rows represent the late outflow (January to March), low water (April and May), end of low water (June), early inflow (July), inflow (August to September), and early outflow (October to December) periods, respectively.
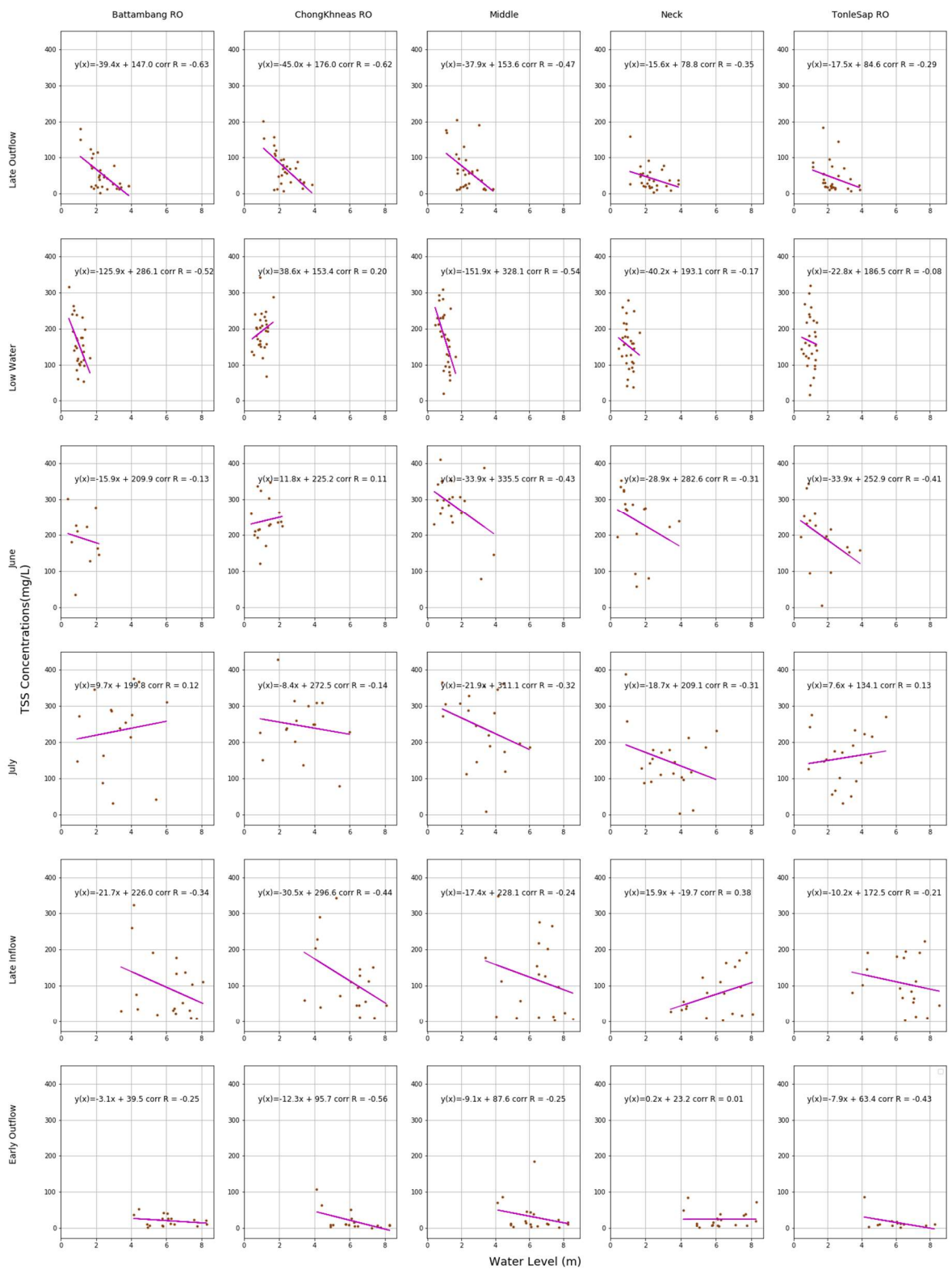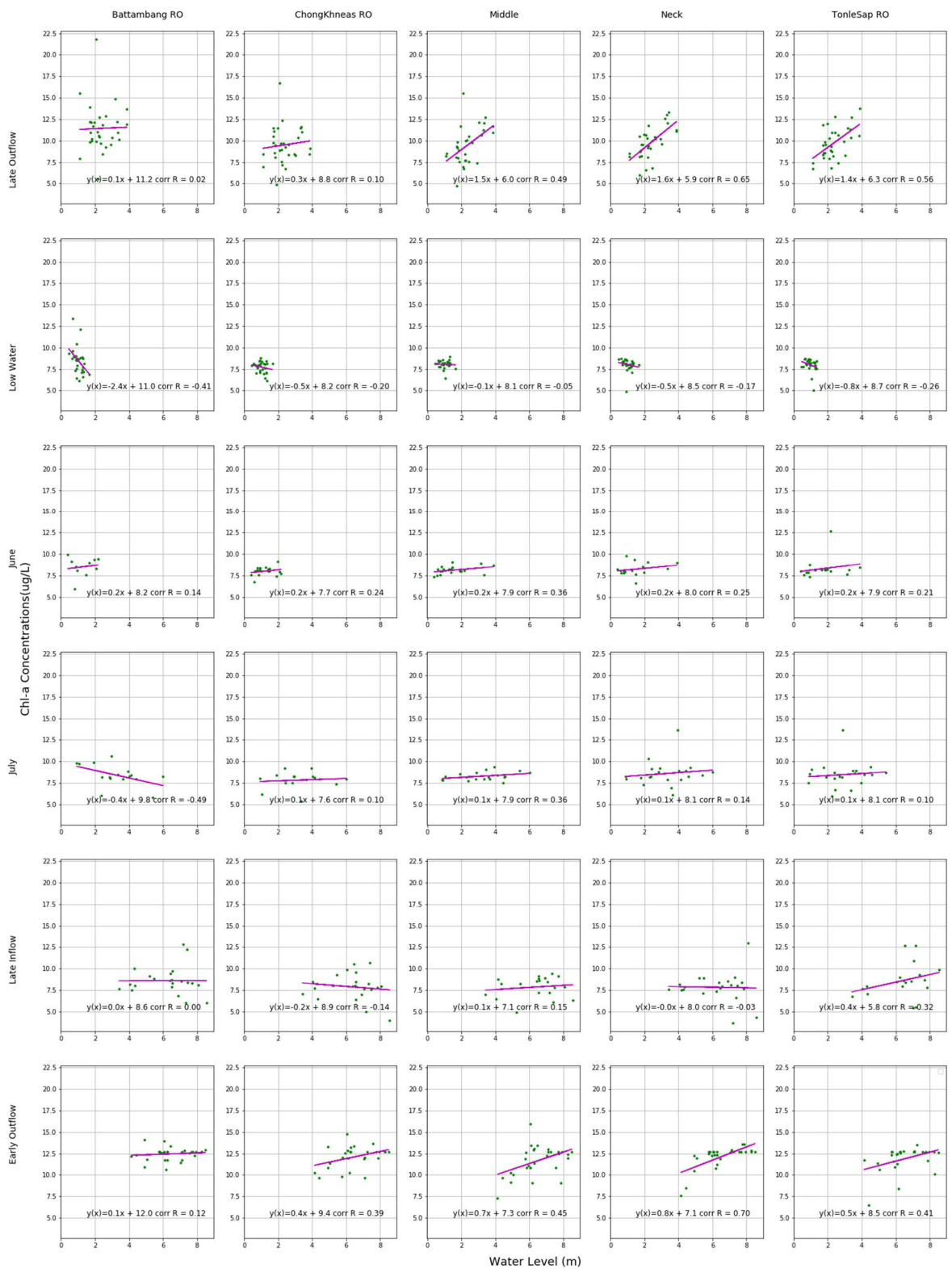
Figure 6-6 Relationship between annual mean chl-a concentrations and mean water level in each

hydrological period at the five study locations. The first to the fifth columns

represent the Battambang River outlet, Chong Khneas River outlet, the middle of the

lake, the neck of the lake, and Tonle Sap River outlet. The first to the sixth rows are

late outflow (January to March), low water (April and May), end of low water (June),

early inflow (July), inflow (August to September), and early outflow (October to December) periods.

During the late outflow period, which is at the end of wet season when water is draining from Tonle Sap lake towards the Mekong River in January to March, the water levels are moderately to strongly correlated with the chl-a concentrations in the south part of Tonle Sap lake, from the middle (r = 0.49), through the neck of the lake (r = 0.64), up to the Tonle Sap River outlet (r = 0.56). However, in the low water period and the early inflow period of July, only the Battambang River outlet shows any significant correlation, negative in direction and moderate in strength (r = -0.41).
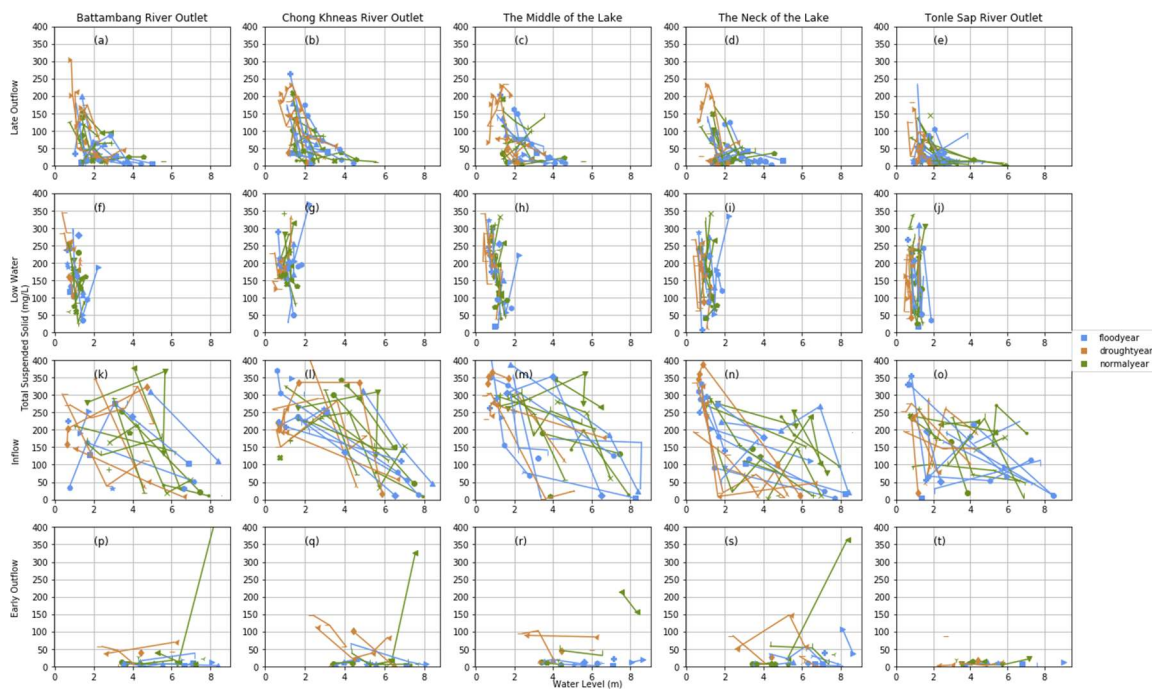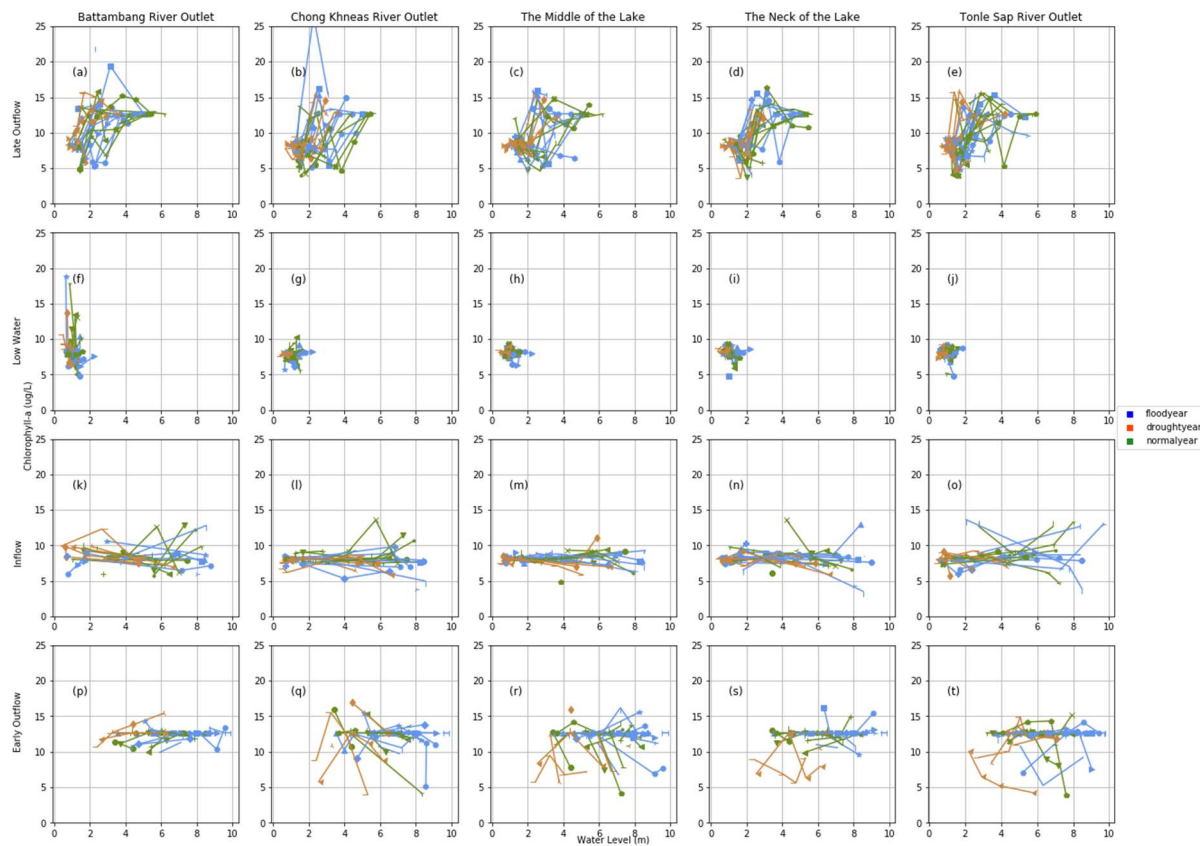


Figure 6-7 Variations in Landsat-derived chl-a concentrations and water level as measured at Kampong Luong for each of the five study locations over the period 1990-2020. The coloured lines denote the water level conditions: high flood years (blue lines), drought years (orange lines), and normal flood years (green lines). The first to the fourth rows represent the different phases of the lake's annual cycle: the late outflow (January to March), low water (April and May), inflow (June to September), and early outflow (October to December) periods.

Figure 6-7 shows the same relationships between the chl-a concentrations and the water level during each hydrological period (late outflow, low water, inflow, and early outflow) as shown in

Figure 6-6, but in this diagram the data are separated into the high flood, drought, and normal flood years as defined in Section 6.1.

During the late outflow period when the Tonle Sap Lake is draining to the Mekong River (January to March), high flood years tend to exhibit higher mean chl-a concentrations at four locations, as illustrated in subplots (b) to (e). The biggest difference with the normal flood years is found at the Chong Khneas River outlet (subplot b; a difference of 2 µg/L), while the lowest difference (between high and normal flood years) is located at the neck of the lake (subplot d; a difference of 0.2 µg/L). The Battambang River outlet location (subplot a) experienced very high chl-a concentrations during the flood seasons in two years (2002 and 2011) but this location has relatively low chl-a concentrations in many other years, hence the lower chl-a concentrations. The Tonle Sap River outlet (e) see almost no difference in the chl-a concentrations observed during the late outflow period, across for all the varying types (high flood, normal flood, drought) of year.

During the low water (April and May) period, compared to all the other 4 locations, the Battambang River outlet (subplot f) has distinctly higher chl-a concentrations during the drought and normal flood years as compared to the high flood years. The differences in the mean chl-a concentrations compared to all other 4 locations, during the drought and normal flood years are between 0.3 to 0.7 µg/L and between 1.6 µg/L to 2 µg/Ls, respectively.

During the inflow period, although there are only modest variations between the 5 study locations (see subplots k to o), during this period the drought years tend to have lower (but very small; in the range 0.1 to 0.4 µg/L) chl-a concentrations compared to those seen in the normal flood years in four locations (see subplots l to o).

However, during the early outflow period, the drought years are associated with relatively lower chl-a concentrations compared to the normal flood years. This trend is noted at four locations (see subplots q to t), with differences (between ethe normal flood and drought years) of Chl-a concentration ranging between 0.4 to 2 µg/L. The exception is located at the Battambang River outlet (subplot p) which experiences very similar chl-a concentrations in both the drought and normal flood years.
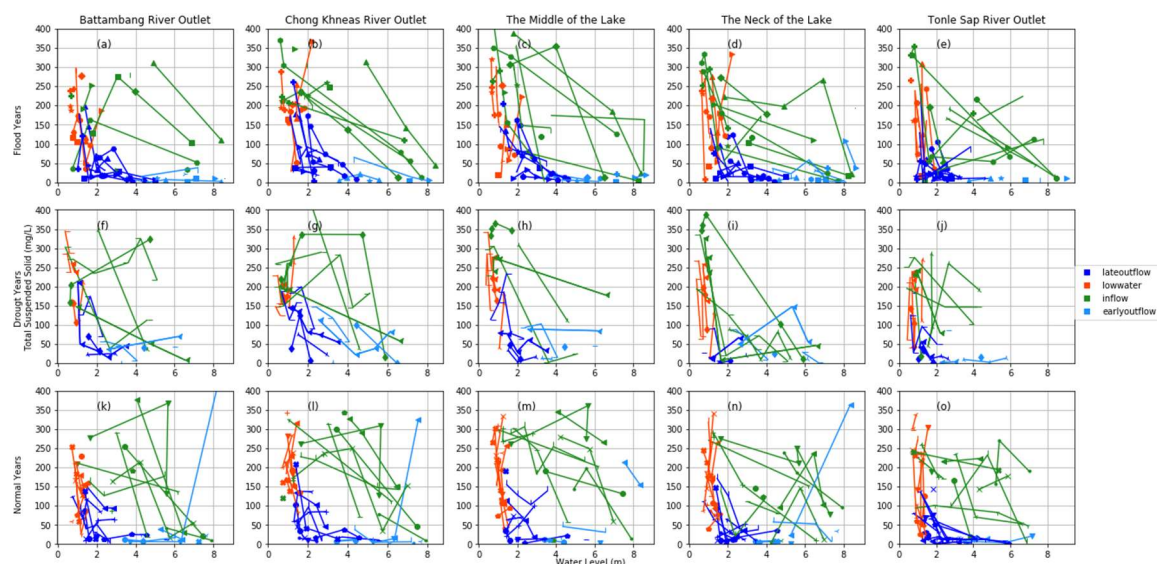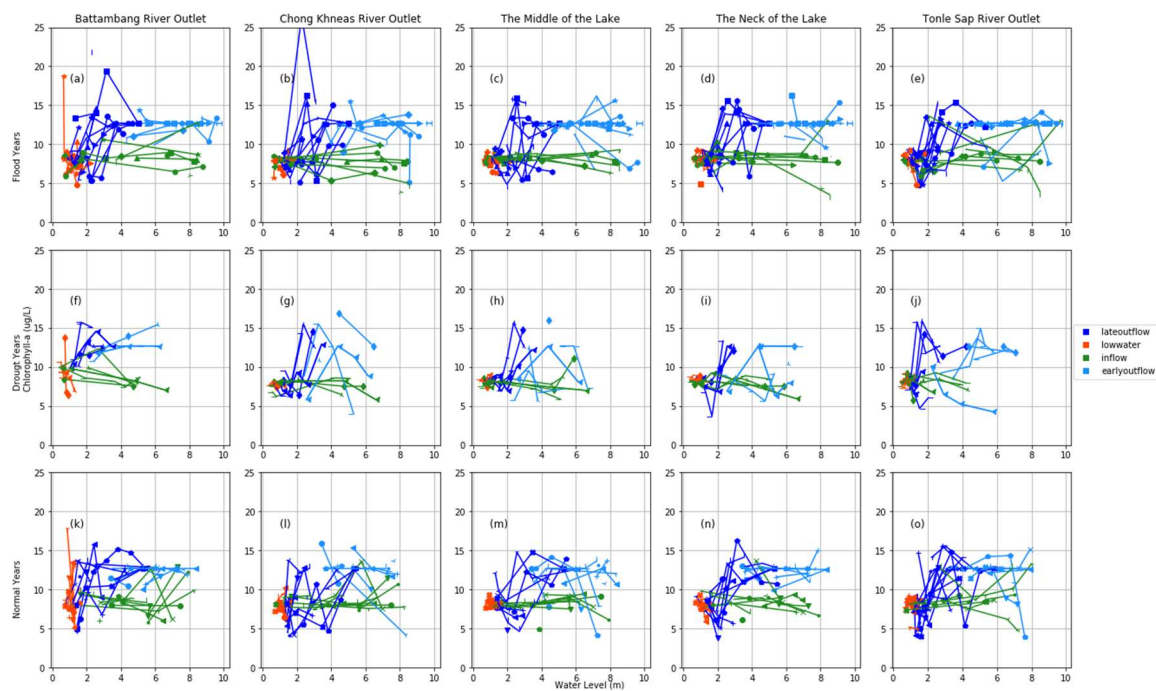
Figure 6-8 Variations in Landsat-derived chl-a concentrations and water level as measured at Kampong Luong for each of the five study locations over the period 1990-2020. The coloured lines denote the late outflow (dark blue lines), low water (red lines), inflow (light blue lines) and early outflow (green lines) periods, with the first to third rows representing the high flood, drought and normal flood years, respectively.

Figure 6-8 reillustrates the Landsat-estimated chl-a concentrations, across the full annual cycle for each study location, split into the hydrological year categories (normal flood years, high flood years, and drought years). On this diagram, the different periods of the year are highlighted using different colours, such that the annual cycle of the lake's flood pulse can be tracked by following a counter-clockwise trajectory around each diagram, in a squashed rectangle shape.

It is evident that the annual fluctuations in chl-a concentrations follow similar trajectories at each study location, with the highest chl-a concentrations observed in the outflow period, which then decrease to the lowest point experienced in the entire annual cycle at the end of the outflow period, before slightly rising again during the low water period. In the subsequent inflow period, chl-a concentrations then decrease again until the outflow period begins.

However, subtle differences are evident in the chl-a concentrations associated with each type of year. For example, normal flood years typically have higher chl-a concentrations during the late outflow period, especially in the north part of the lake. This transforms the rectangular shape of the response curve to more of a 'sock' shape, as is apparent in panels (a) and (b). The lower maximum water levels during the drought years consequently shrink the width of the rectangle, as is noticeable in panels (f) to (j).

Figure 6-9 presents a simplified data-driven conceptual model of the annual cycle of chl-a concentration fluctuations resulting from the water level variations, as based on the data presented in Figure 6-7 and Figure 6-8. This conceptual model depicts the temporal variations in the chl-a concentrations in Tonle Sap lake over the course of its annual cycle. Two-way arrows show the chl-a concentrations during the outflow and low water period (when Tonle Sap lake receives nutrients from its tributaries and the nutrient recycling within the lake), and the inflow period (when Tonle Sap lake lake receives nutrients from the Mekong River). The directional arrows show the 'cycle' of the variations of chl-a concentrations.
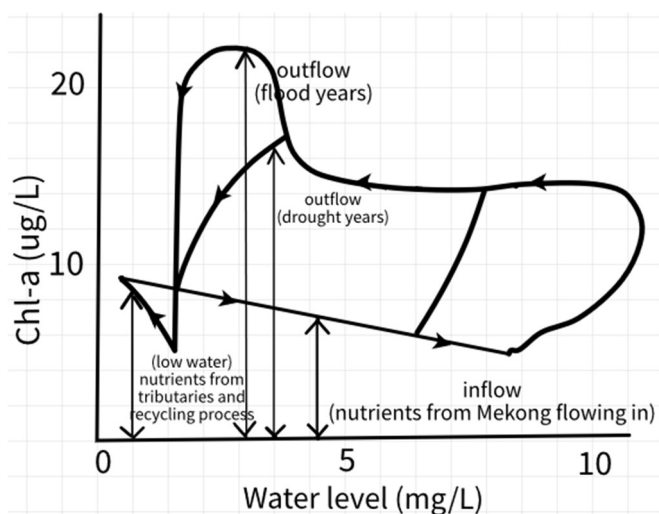


Figure 6-9 Simplified model of the annual cycle of chl-a concentration fluctuations resulting from the water flow and the nutrients it may bring into the lake. Two-way arrows show the chl-a concentrations during the outflow and low water period (when Tonle Sap lake receives nutrients from its tributaries and the nutrient recycling within the lake), and the inflow period (when Tonle Sap lake lake receives nutrients from the Mekong River). The directional arrows show the 'cycle' of the variations of chl-a concentrations.

It is seen that the chl-a concentrations are low when the water is inflowing from the Mekong River. The chl-a concentrations subsequently rapidly increase after the outflow phase begins, probably after the phytoplankton utilise the nutrients brought in by the inflow and proliferate. The increase in chl-a concentration continues until it reaches a maximum value during the flow recession period. After this point, the chl-a concentrations decrease along with the water level, reaching a minimum at the very end of the outflow period. Then, notably during the very end of the low water period, there is a slight increase of chl-a concentration typically decreases again as

the inflowing water begins to infill the lake. Exceptionally high chl-a concentrations during the outflow period in high flood years are evident at two locations: the Battambang River Outlet and the Chong Khneas River outlet.

This model shows clear differences on the temporal variations of chl-a and TSS (Figure 6-5) over the course of the lake's water level cycle.  The maximum TSS concentrations occur in the very early inflow period (right after the low water period) and the maximum chl-a concentrations occur in the outflow period.
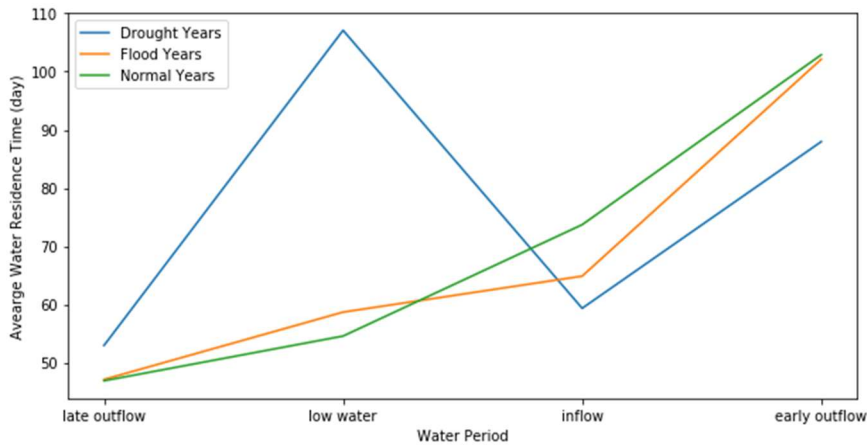


Figure 6-10 The average water residence time of Tonle Sap Lake during the late outflow, low water, inflow, early outflow period, in the drought, flood, and normal years.

Figure 6-10 shows the average residence time of Tonle Sap Lake during the late outflow, low water, inflow, early outflow period, in drought, flood, and normal years, estimated from the water level of Tonle Sap Lake (please see Appendix C for the details). The water residence time is increasing along the day of the year. The shortest water residence time occurs during the late outflow (January to March) which is 46 days in the normal years, and the highest is during the early outflow (October – December) which is 103 days in the normal years). An exception is for the drought years, whose longest water residence time occurs during the low water period (April and May).

The residence time may also influence the proliferation of phytoplankton in Tonle Sap Lake. The chl-a concentration in Tonle Sap Lake is at its lowest during (the end of) late outflow, then rises during the low water, inflow period and reaches the highest in the early outflow, when the water residence time of the lake is in its longest. Nevertheless, the markedly long residence time during the low water period in the drought years does not yield differences in the chl-a concentrations during the flood and normal years.

# Chapter 7  Discussion and Conclusions

## 7.1  Long Term Eutrophication Status of Tonle Sap Lake

Based on the results presented in Chapter 5, during the past 30-years the range of chlorophyll-a concentration in Tonle Sap Lake is estimated to be 3.6 – 26.5 µg/L, with an average value of 9.6 µg/L.  The maximum chlorophyll-a concentration (26.5 µg/L) was recorded during a low-water period, on February 4th 2011, at the outlet of Chong Khneas River. For context, other studies have measured chlorophyll-a concentrations in the range 4 - 14 µg/L in 2001 (Sarkkula et al., 2003), and an average of 20 µg/L during a 2012–2014 field study located at the neck and southern part of the lake (Fukushima et al., 2017). The chl-a concentrations measured in this study are, therefore, broadly consistent with those undertaken by these prior investigations. In comparison, the hypereutrophic Taihu lake in China sites reaches chlorophyll-a concentrations of up to 80 µg/L (F. Zhang et al., 2019), while Lake Erie in the USA experiences concentrations in the range 14 -74 µg/L (Rowland et al., 2019), depending on the precise location.

As indicated by the data in Figure 7-1, during the 1990-2020 study period, the Tonle Sap lake may be classified as a mesotrophic lake for most of the time, albeit the Chong Khneas River outlet attained a eutrophic state once during the low-water period in 2011. The duration of this eutrophic state is not clear, as it is estimated based on a single Landsat OLI scene, recalling that Landsat OLI has a 16 days revisit duration.

With a mean chlorophyll-a concentration of 9.6 µg/L, the mesotrophic status of the Tonle Sap lake as determined in this study is distinct from the eutrophic classification proposed by William C Burnett et al. (2017), who, from their four field campaigns  (January, June, July, November), recorded that November has the  lowest maximum concentration of 35 µg/L (Supplementary Data of Burnett et al., 2017) ,  and at some other limited points in the year (June, around the end of low water season) the Tonle Sap lake even moves to hypereutrophic conditions.

Chapter 5 also revealed that, over the last three decades, the Tonle Sap lake has not exhibited any statistically significant change in chlorophyll-a concentration (which is used here as a proxy for phytoplankton biomass). The hypothesis made by Sarkkula and colleagues (2003), that the traditional concept of eutrophication, i.e., of high productivity and algal blooming, does not fit to Tonle Sap lake, remains unchanged after almost twenty years, and for at least ten years before it. Indeed, diatoms found in Tonle Sap sediments (Penny, 2006), dominated by *Aulocoseira* (see Section 7.2 for details on diatoms and *Aulocoseira* in Tonle Sap lake), are likely an indication that

the (non) eutrophic status of Tonle Sap lake has remained broadly the same since the early
Holocene.
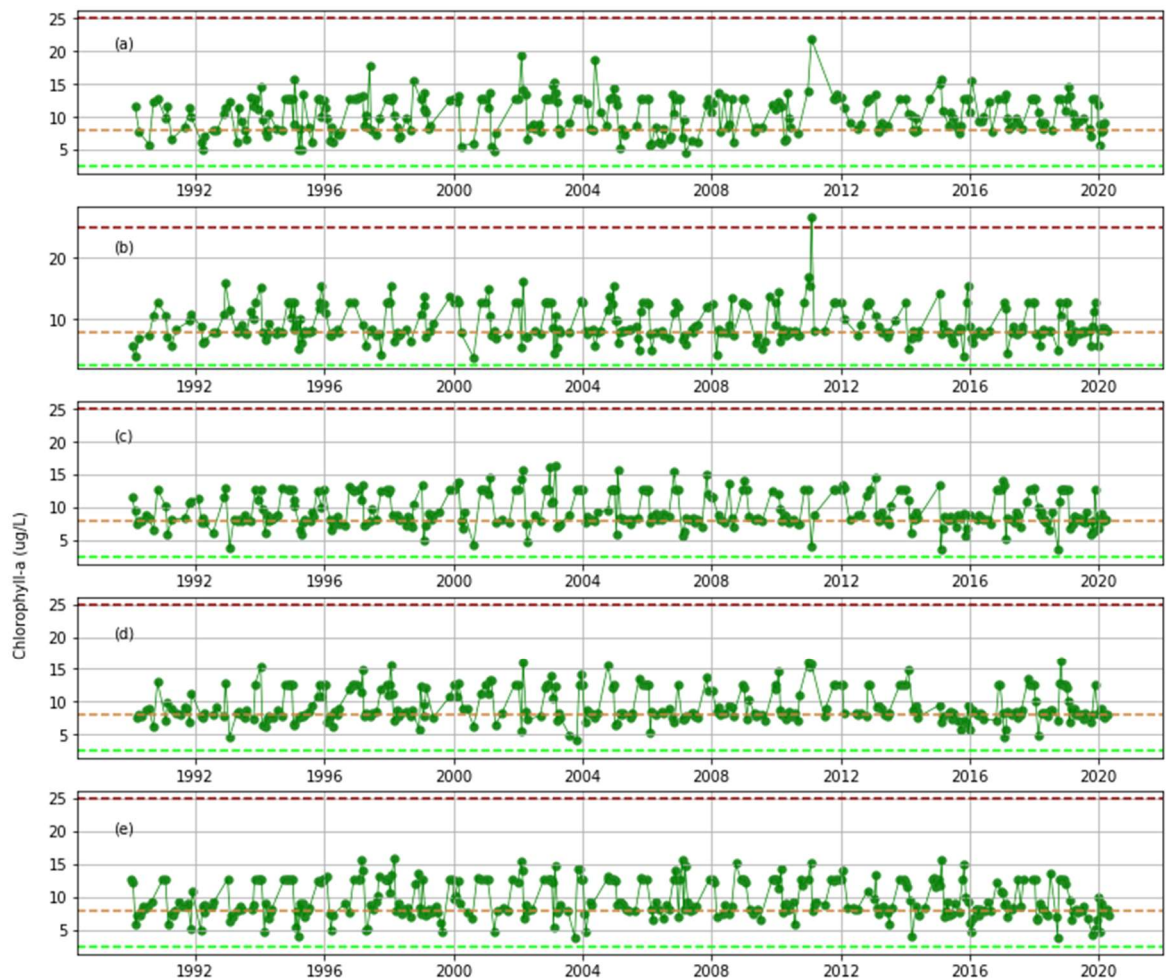


Figure 7-1 Chlorophyll-a concentrations from 1990 to the beginning of 2020, as estimated from
Landsat images, in 5 different locations of the lake: (a) Battambang river outlet, (b)
Chong Khneas river outlet, (c) the middle of the lake, (d) the neck of the lake, and (e)
the Tonle Sap River outlet. The horizontal dashed lines show the lower boundary of
the OECD defined eutrophic levels (EPA, 2008) based on maximum chl-a
concentration values. Green is oligotrophic; gold is mesotrophic, and brown is
eutrophic.

Phosphorus released from accumulated sediment within the lake may delay the results of the
efforts to manage eutrophication by reducing external loading (Søndergaard et al., 2003 and
references therein). However, in this study, TSS concentrations over the 30 year time period do
not show any statistically significant increasing trend. Sedimentation in Tonle Sap lake occurs
mostly in the flooded forest region (Sarkkula et al., 2003), which becomes inaccessible during the

dry season when other chemical and physical factors favour cyanobacterial blooms. Even though Tonle Sap lake receives a significant amount of sediments from the Mekong River (X. Lu et al., 2014), the main focus of sedimentation on the forested floodplain, along with its slow rate accumulation of 0.2 – 0.4 mm/year in the open water (Kummu, Penny, et al., 2008), may limit the extent to which sediment-related phosphorus internal loading could exacerbate eutrophication.

## 7.2    Temporal Variations of Phytoplankton Biomass in Tonle Sap Lake

The results of this thesis (Section 5.2) show that chlorophyll-a concentrations in the Tonle Sap lake typically peak each year after the water level reaches a maximum in the rainy season. Slightly earlier than this timing, Blache (1950 in Campbell et al., 2006 and Ohtaka et al., 2010) recorded the highest concentrations chlorophyll-a in September, which is the end of the inflow period. However, some other studies (Burnett et al., 2017; Sarkkula et al., 2003) observed the highest chlorophyll-a concentrations during the period of low water (April – June). In part, the differences in these prior studies and the present study may be explained by the observation that the analysis in Chapter 6 shows an increase in chlorophyll-a concentration at the end of the low water period, following a decrease during the end of the late outflow.

Nutrient availability for the optimal growth of the phytoplankton could be a cause of the maximum chlorophyll-a, and there are several explanations for the possibility of nutrient availability also maximising during the rainy season. First it can be postulated that the Mekong River water, which accounts for more than half of the water feeding the Tonle Sap during the rainy season, might be relatively nutrient-rich. Nutrients in the Mekong River (as measured at the Chiang Saeng and Pakse gauging stations), particularly phosphorus and nitrogen, have a positive correlation with both the river water discharge (S. Li & Bush, 2015), and sediment load (X. Lu et al., 2014). A more recent finding is that nitrate concentration in the Mekong River is at its highest during the rainy season, whereas phosphorus although it is diluted by the monsoon flows, also experiences its largest flux during the wet season (Whitehead et al., 2019). Similarly, a phosphorus budget model (Burnett et al., 2017) for Tonle Sap lake shows that the biggest phosphorus inflow to the lake is from the Tonle Sap River during the rainy season.

The sediment resuspensions in Tonle Sap lake will also highly-likely release phosphate (Burnett et al., 2017). Even though the highest TSS *concentrations* occur during the very early inflow period right after the end of the low water season (Chapter 5), the total suspended sediment (by mass) within the lake is higher in the early outflow period (when the lake volume is at its maximum) than in the very early inflow water season. The average TSS concentration is 36 mg/L (in the middle of the lake) during the early outflow period and 285 mg/L during the the very early

inflowseason, while the average lake volumes during the low and high flow seasons are roughly 1.6 km$^3$ and 60 km$^3$, respectively. It follows that the total suspended sediment mass within the lake during the early outflow period (assuming the maximum lake volume occurs during this period), is likely approximately a factor of 4 higher than the total suspended sediment mass within the lake during the low water period. Intriguingly, the analysis in Chapter 5 shows that the TSS concentrations are higher in the low water season than at the end of the late outflow. However, the analysis of chl-a trends in Chapter 6 also shows that the chl-a concentration also typically temporarily increases during the low water season, after decreasing during the late outflow, before reaching its lowest concentrations at the end of the late outflow period. These trends in chl-a concentrations would be consistent with a high rate of phosphorus release from the resuspended sediment during the lowest water condition (around 1 meter flow depth).

However, even if nutrients are abundant, short water residence time may effect the proliferation of the phytoplankton (Elliott, 2010; Elliott & Defew, 2011; Kawara et al., 1998). The long water residence time during the early outflow (Appendix C) may also affect the maximum growth of phytoplankton in Tonle Sap Lake.

A second possibility is that nutrient cycling by fish and other animals is more efficient in the high water season, as the result of fish migration into the Tonle Sap lake from the Mekong River. Although it has never been studied for Tonle Sap lake, other studies have found that animals in the freshwater ecosystem can supply nitrogen and phosphorus at rates comparable to major nutrient sources, and nutrient cycling by animals can support a substantial proportion of the nutrient demands of primary producers (Vanni, 2002). Fish migration takes place from the Mekong River to the Tonle Sap lake through the Tonle Sap River at the beginning of the rainy season, and in the reverse direction at the start of the dry season. The majority of these migratory species reproduce at the start of the rainy season in the flooded forests and the lake floodplains (Lim et al., 1999). Species richness and abundance peak at approximately 2–2.5 and 4 months, respectively, after the peak flow (Ngor et al., 2018).

A third possibility is that the wetlands that fringe the lake enable the mobilisation of nutrients during the high water season. Hiroki et al. (2020) have suggested that the primary productivity of Tonle Sap lake cannot be explained by the lake's water quality parameters alone and concluded that sediment stored in the fringing wetlands contributes to the high productivity of the lake. Wetlands are, in general, known to play important roles in the phosphorus, nitrogen, and silica cycles (see Section 2.2).

Finally, there is one other aspect that has never been elaborated in prior discussions of seasonal dynamics of nutrients or chlorophyll-a in Tonle Sap lake: the phytoplankton community

succession in Tonle Sap lake. A number of studies on the phytoplankton assemblages in Tonle Sap lake have been conducted (Ohtaka et al., 2010; Tudesque et al., 2019). Those studies and other observations (e.g., Sarkkula et al., 2003) reveal that there is a seasonal change in the distribution of phytoplankton species (see Appendix B for details). Specifically, most reports have observed diatom domination in the high-water season, while cyanobacteria dominate in the low water season. One study (I. C. Campbell et al., 2006) has reported green algae dominating in the high water season. The overall illustration of the phytoplankton community succession in Tonle Sap lake is shown in Figure 7-2, and the potential role of seasonal phytoplankton community succession in driving nutrients, and hence chlorophyll-a, dynamics is discussed in greater detail in the sub-sections below.
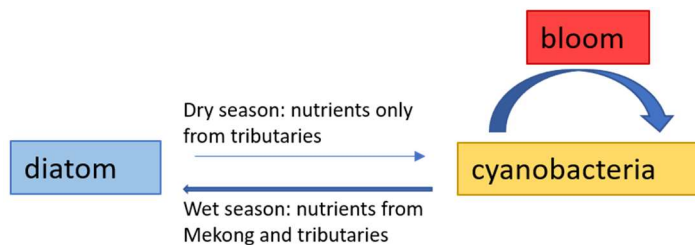


Figure 7-2 Phytoplankton community shift in Tonle Sap lake

**Diatom Dominance in the High Water Season**

In Tonle Sap lake, the diatom species that is most abundant during the high water season is *Aulacoseira* and the cyanobacteria species that are most abundant during the low water season are *Microcystis* and *Dolichospermum spp* (formerly *Anabaena*). The presence of *Aulacoseira granulata* indicates a higher trophic state than that of *Microcystis* (Padisák et al., 2009; Colin S Reynolds et al., 2002). The change of phytoplankton community structure from the cyanobacteria dominant in the low water season to the *Aulacoseira* dominant in the high water season can, therefore, be considered an indication of the higher eutrophic level of Tonle Sap Lake during the high water season, though as noted in Chapter 6 it is emphasised that the results of this thesis indicate that the lake is generally mesotrophic, even during the rainy season.

*Aulacoseira*, or indeed diatoms in general, is known to increase with an increase of dissolved nitrogen and/or phosphorus (Nakano et al., 1996; Queimaliños et al., 1998). As discussed above, this may be consistent with the long assumed hypothesis that the inflow from the Mekong River brings nutrients to the lake. Diatoms are r-strategists (Zhao et al., 2008) in the three phytoplankton functional groups (Colin S Reynolds et al., 2002). This means that *Aulacoseira* has a

competitive advantage through a higher growth rate than other phytoplankton species when nutrient levels are high (Papanikolopoulou et al., 2018; Zhao et al., 2008). Specifically, their higher growth rates afford a competitive advantage compared to *Microcystis* (Huisman et al., 2004), a species of cyanobacteria that dominates the Tonle Sap Lake during the low water period.

Diatoms tend to be limited by the availability of silica (Gibson et al., 2000), not nitrogen or phosphorus. The growth of diatoms depends on the presence of dissolved silica, while the growth of non-diatom phytoplankton does not (Conley et al., 1993). This likewise would potentially indicate a high level of silica in Tonle Sap lake during the high water season. Indeed, from data taken roughly every 3 months by William C Burnett et al. ( 2017) (see Table 3 within the paper), silica was found to be highest, by a factor of 3, in July (229 ± 68 µM) which is the beginning of the high water season, before declining in November (78.8 ± 46.5 µM), and reaching its lowest levels in the subsequent June (data for January were not available in this study).

One source of this high silica during the wet season could well be the inflowing water from the Mekong River. Data from 1985 to 2011 for the lower basin of the Mekong River revealed that the dissolved silica flux during the rainy season contributes around 75% (monthly average 7933 µM at Pakse) of the total annual flux (S. Li & Bush, 2015). Two Tonle Sap tributaries, the Sangkhae River and Pursat River, also contain relatively high levels of silica during the rainy season (Yoshikawa et al., 2020), which is around 7000 µg/L to 14000 µg/L (Figure 8 within the paper). Another source is possibly dissolved silica that could be released back by plants (e.g Struyf & Conley, 2009; Vandevenne et al., 2012). Some parts of the Tonle Sap lake floodplain comprise grassland (McMeans et al., 2019), and grass is known as one of plant species that contains high silica (Melzer et al., 2012 and references therein).

Phytoplankton community succession from or to diatoms as a result of silica depletion or repletion has been recorded in the literature. Depletion of reactive silica in summer results in a replacement of diatoms by cyanobacteria (Teubner & Dokulil, 2002 and the references therein). In the upper Mekong, a reservoir that retains dissolved silica has high diatom abundance, and in the subsequent reservoir downstream with relatively low dissolved silica, diatoms were completely replaced by green algae (Q. Chen et al., 2020).

Very few studies have directly measured nutrients in the Tonle Sap Lake, and silica is almost entirely neglected from those Tonle Sap Lake studies, or even studies on the Mekong River more generally. The fact that silica hungry diatoms remain available even after the succession to cyanobacteria in the dry season possibly indicates that sediment resuspension in Tonle Sap lake may release not only phosphorus (Burnett et al., 2017), but silica as well (Arai et al., 2012; Arai & Fukushima, 2014; Goto et al., 2013; Tallberg, 2000).

**Green Algae Dominance in the High Water Season**

Campbell et al. (2006) reported green algae dominance during the rainy season of 2003. He postulated that in that year, diatoms were not dominating because diatom is a river phytoplankton and 2003 is a drought year with minimal inflowing water from the Mekong River to bring diatom species into the lake. However, in fact, diatoms are very common in most freshwater lakes, indeed diatom algae are often the dominant primary producers, at times comprising most of the phytoplankton biovolume (Rühland et al., 2015). Hence it is very likely that because of the minimal water inflow from the Mekong River, the amount of silica needed to trigger diatom growth was insufficient.  In other studies, the occurrence of a long-term increase of nitrogen and phosphorus at low levels of silica has generated dramatic shifts in the phytoplankton structure from diatoms to cyanobacteria (Teubner & Dokulil, 2002 and the references therein).

Other factors that are known to promote chlorophyte dominance include extreme nitrogen pollution to phosphorus-rich waters (Barica et al., 1980; Hyenstrand et al., 2000; Vis et al., 2008), high ammonium($NH_4$) concentrations (Andersen et al., 2020), or simply a very high nitrogen loading (Bogard et al., 2020), as well as high levels of $CO_2$ concentration (Low-Decarie et al., 2011). However, due to limited information about those parameters in Tonle Sap lake, further inferences can not readily be drawn.

**Cyanobacteria Dominance in the Low Water Season**

During the low water period, the algae community in Tonle Sap lake shifts from being dominated by diatoms or green algae (as in the high water period) to cyanobacteria (Figure 7-2). This shift possibly indicates that fewer nutrients are available in the lake at this time, as compared to the high water season. Smaller types of phytoplankton like cyanobacteria need fewer nutrients and a community shift can occur when nutrient levels are depleted (Lindsey & Scott, 2010). Diatoms which are larger than cyanobacteria tend to dominate phytoplankton communities when growth conditions are optimal (e.g., under high nutrient concentrations), but when nutrients run out, they would congregate then quickly sink (Bopp et al., 2005).

Temperature may play a role as well. It is commonly observed that warm temperatures favour cyanobacteria (Dokulil & Teubner, 2000 and references therein), with blooms tending to occur during the spring or summer months in temperate lakes (Paerl & Huisman, 2008). The Tonle Sap lake temperature is higher during the dry season than the rainy season, with the highest

temperatures recorded in April and the lowest in November (Daly et al., 2020; Okumura, 2005; Oyagi et al., 2018). However, the overall temperature range is only around 6°C (Figure 6 in Daly et al., 2020).

Cyanobacteria during the low water period in Tonle Sap lake are dominated by *Microcystis* and *Dolichospermum* spp (formerly *Anabaena*). *Microcystis* is a nitrogen non-fixer (J. Lu et al., 2019), which means the water in which *Microcystis* found is not nitrogen limited. Although, parts of the lake where *Anabaena* are found may experience nitrogen limitation. Laboratory studies have found a correlation between increasing nitrogen and *Microcystis* growth; furthermore, *Microcystis* (and *Dolichospermum* as well) can efficiently utilize both organic and inorganic species of nitrogen (O'Neil et al., 2012). Among other nitrogen species, organic species are known to compose major fractions in the lake's sediment (see Section 2.2.2). With the highest sediment concentration during the low water period, the *Microcystis* community may utilize the organic nitrogen available in the sediment. However, a study in Mekong lakes and reservoirs, including Tonle Sap lake, cannot confirm this nitrogen-algae relation (Fukushima et al., 2017).

Water transparency, which relates to the light penetration, has been found to have a strong negative connection to cyanobacteria (Dokulil & Teubner, 2000). Under low-light levels (25 µmol $m^{-2} s^{-1}$), the growth rates of *Microcystis* and *Anabaena* are high, however, under high-light level (200 µmol $m^{-2} s^{-1}$ or over), these growth rates become smaller (Islam & Beardall, 2017; Muhetaer et al., 2020; Venugopal et al., 2006). There has been no direct measurement on the magnitude of the radiance within Tonle Sap lake, but water transparency in Tonle Sap lake is extremely low during the dry season, due to the very high suspended sediment concentrations. The dominance of cyanobacteria during the low water season probably arises because the cyanobacteria species in Tonle Sap lake are those that are sufficiently buoyant to keep them on the surface, as mentioned by Sarkkula et al. (2003). A recent study found that temperature regulates buoyancy, where *Microcystis* become buoyant in the higher temperature (You et al., 2018).

Generally, cynobacteria are known to favour low nitrogen to phosphorus ratio conditions (Smith, 1983). Increased nitrogen loading in many phosphorus-rich lakes with low nitrogen to phosphorus ratios can stimulate the growth and abundance of potentially toxic cyanobacteria including *Microcystis* (Bogard et al., 2020 and references therein). Over one year, with measurements taken every 3 months, William C Burnett et al. ( 2017) observed that the lowest nitrogen to phosphorus ratio (with a lowest value of 11 and a mean of 21.6) in the Tonle Sap Lake was recorded in July. This finding is in agreement with a study by (Ung et al., 2019) that found the cyanobacteria abundance peaked in the dry season to wet season transition month.

Sarkkula et al., (2003) mentioned *Anabaena* was dominating during their fieldwork. An alternating dominance between *Microcystis* and *Anabaena* has been recorded in many other lakes (Harke et al., 2016; Havens et al., 2003; Nalewajko & Murphy, 2001). In these other lake environments, the general trend has been the replacement of *Anabaena* by *Microcystis* under low phosphorus and high nitrogen conditions, with replacement of *Microcystis* by *Anabaena* under low nitrogen and high phosphorus conditions (Chia et al., 2018). It can be inferred that in Tonle Sap lake, dissolved inorganic phosphorus released from the sediment resuspension during the 4 months (May-August) of the low water period (Burnett et al., 2017) is low in locations where *Microcystis* is dominating.

In several other tropical regions, as the temperature is always within the optimal growth range, cyanobacteria show persistent annual dominance with relatively small changes during the year (e.g., Figueredo & Giani, 2009; Soares et al., 2009). Tonle Sap lake, however, presents a distinctive example amongst tropical lakes in that the annual reversing flow creates turbulence which is not an optimum environment for the cyanobacteria.

## 7.3  Spatial Variations of Phytoplankton Biomass in Tonle Sap Lake

The outlet of the Battambang River (location 1; see Figure 4-13) and Chong Khneas River (location 2) show relatively higher chlorophyll-a concentrations than the other three study locations. The fact that Battambang and Siem Reap are among the areas of the lake that consistently host high fish biomass (Chan et al., 2020) is likely related to this finding. It also can be postulated that the outlets of the Battambang and Chong Khneas Rivers may be more polluted (Chea et al., 2016) by nutrients, possibly as the result of agricultural intensification in Battambang province or tourism-related development in Siem Reap, the major city in the basin of the Chong Khneas River.

The phytoplankton biomass (as inferred from chl-a concentrations) in the Chong Khneas River outlet does not show any correlations with the water level, except for a weak correlation (r = 0.39) in the early outflow period (Figure 6-6). This finding indicates that the consistently high chl-a concentrations observed at the Chong Khneas River outlet (compared to other sites) is not caused by the nutrients that may be brought by the water, although exceptionally high chl-a concentrations in the Chong Khneas river outlet are observed only in the flood years.

Meanwhile, the phytoplankton biomass (proxied by the chl-a concentrations) at the Battambang River Outlet negatively correlate (to some extent) with the water level during the low water period and at the beginning of the inflow period (July). During the same period, TSS concentrations correlate with the water level. Thus it is safe to infer that for the low water and the early inflow periods, phosphorus released from the suspended sediment may play a role in

controlling the high chl-a values at the Battambang River outlet, and for all other periods, the nutrient contributions from the Battambang River basin likely play a more important role in controlling the high chl-a concentrations observed there.

Ohtaka et al. (2010) reported that during the dry season, they observed cyanobacteria domination at all their survey stations (north and south basin, open water, and coastal area) except for the open water of the north basin, which is where the diatoms are dominating. This information also suggests that the trophic level of the north-basin is higher in the low water season (albeit not reaching a fully eutrophic state, as per the findings of Chapter 5).

A recent study concludes that Tonle Sap lake is phosphorus limiting, at least most of the time (Burnett et al., 2017). However, clear water with submerged macrophytes was observed in the north basin of Tonle Sap lake during the fieldwork undertaken for this thesis. This location is possibly nitrogen-limited, has high phosphorus concentrations, but with nitrogen concentrations below 1.2 mg N/L (Søndergaard, 2007).

## 7.4    Harmful Algal Blooms in Tonle Sap Lake

However, algal scum, which is the most notable sign of eutrophication, does exist at some locations and at some points in time in Tonle Sap lake. Instances of algal scum have been recorded since at least 40 years ago (Mizuno & MORI, 1970 in Ohtaka et al., 2010), Ohtaka and colleagues (2010) observed it often occurs in the dry season, and it was also reported to happen near Siem Reap in February 2012 (Fukushima et al., 2017). Local people who assisted the fieldwork of this study suggested that algal blooms frequently happen during the lowest water season (March and April), notably near the Chong Khneas River outlet.

Although Ohtaka et al. (2010) noticed algal scum on several occasions during their field studies from 2003 to 2005, they mentioned that it was hardly found in the high-water seasons. *Aulocoseira*, which is the dominating genera in Tonle Sap lake during the high-water season, is known as a bloom former, but it seems that the necessary conditions for it to bloom in Tonle Sap lake may never be met, at least over the extensive spatial scales that would be necessary for them to be detected using the satellite-based methods employed in this study.

Temperature is one of several meteorological variables that could trigger algal blooms (Paerl & Huisman, 2008). Furthermore, in terms of nutrient availability, nitrate depletion under high phosphorus concentrations is reported to likewise generate algal blooms (Smith & Bennett, 1999; Vis et al., 2008). In particular for *Microcystis* dominated blooms (a genus found dominating in the

Tonle Sap lake's cyanobacteria community), such blooms appear highly responsive to ammonium rather than other nitrogen species (Chaffin & Bridgeman, 2014; Harke et al., 2016).

However, so far there have been no direct nutrient measurements within Tonle Sap lake particularly during algal blooms, neither are there details of the genera that bloomed. Published literature records that Lake Erie experienced a bloom in which *Microcystis* and *Dolichospermum* (two genera found dominating the cyanobacteria community in Tonle Sap lake) alternated in relation to changing nitrogen availability. It was the $N_2$ non-fixer *Microcystis* bloom which then changed to the $N_2$ fixer *Dolichospermum* bloom when nitrogen depleted, the nitrogen possibly having been consumed by the bloomed *Microcystis* beforehand. This situation could be repeated for algal blooms in Tonle Sap lake.

Another important feature of algal blooms in Tonle Sap lake is that they do not linger. During the fieldwork for this research (lasting 20 days in February 2019) blooms were seen on two different days, each in a different location, but each had disappeared on the following day. Compared to this, Lake Winnipeg in North America for example, recorded up to 145 days of bloom (Binding et al., 2018).

Physical parameters, along with the nutrients, are known to regulate the dynamics of algal blooms. These physical conditions include adaptations to low light conditions (Scheffer et al., 1997) by regulating their buoyancy, high temperature and water column stability (Paerl & Huisman, 2009), resistance to herbivory (Wilson et al., 2006), flushing (Elliott, 2010; Romo et al., 2013) and suspended clay particles (Allende et al., 2009; Cuker et al., 1990). In tropical regions, the ability of rainfall to trigger a physical disturbance in the water column is sometimes considered to be more important than temperature and solar radiation (Figueredo & Giani, 2009).

Again, so far algal blooms in the Tonle Sap lake have never been studied. Information about the related physical conditions simply does not exist. The estimated values of chlorophyll-a in Tonle Sap Lake obtained in this study from the Landsat satellites during the last 30 years are not consistent with the extreme chlorophyll-a levels normally associated with major episodes of blooming. The blooms that have developed in the last 30 years may well have not lingered, or were rather small in extent, and hence were not captured by the Landsat satellites employed herein, whose earth-cycling period is 16 days.

## 7.5    Potential Eutrophication of Tonle Sap Lake in the Future

As the water of Tonle Sap Lake mainly comes from two different places, i.e., the lake tributaries and the Mekong River, changes in the basins of both the tributaries and Mekong River may impact

Tonle Sap Lake. Climate change, land use, and dam development are suggested to shape the future of the Mekong River (Pokhrel et al., 2018). Although there is no systematic review of the changes in these factors from within the country of Cambodia, pieces of evidence such as growing tourism in Chong Khneas, for example, or agricultural intensification in Battambang are consistent with a potentially growing adverse impact on the quality of river water flowing into the Tonle Sap Lake. It depends on what effects those changes will bring to the water properties, but they do have the potential to impact the cyanobacteria community that is dominating during the dry season, as the characteristics of Tonle Sap Lake's water during the dry season is influenced by the tributaries (Yoshikawa et al., 2020).

Climate change may also impact Tonle Sap Lake as well. One of the consequences of climate change is a rising temperature, which indeed has been observed in Tonle Sap lake. Specifically, the lake's dry season monthly average temperature increased by 0.03°C/year between 1988 and 2018 (Daly et al., 2020). Warming would increase herbivores' consumption more strongly than primary production consumption, which leads to rising grazing rates. This will affect phytoplankton production and algal species composition  (Winder & Sommer, 2012).  Warming will also increase the duration of the thermal stratification, which in turn influences the availability of nutrients, but this does not generally apply to Tonle Sap lake as it is a well-mixed lake. However, stratification may occur in Tonle Sap lake during the high water season (at least at night) and would present conditions unfavourable to large-celled diatoms such as *Aulocoseira* that favour a strongly mixed water column (Rühland et al., 2015).

Many studies have suggested that higher temperatures are predicted to increase the occurrence, duration, and intensity of cyanobacterial blooms (Adrian et al., 2009; Domis et al., 2007; Huber et al., 2012; Paerl & Huisman, 2009). More cyanobacteria eventually will impact fish production in terms of the amount and fish type (Moustaka-Gouni & Sommer, 2020) because cyanobacteria are less edible than diatoms or green algae. Cyanobacteria are found as inadequate quality food for higher organisms in the food chain. They are aggregating, making them too large to be ingested by zooplankton, and they contain lower amounts of many important biomolecules (Vuorio et al., 2019 and references therein). This condition can further stress the Tonle Sap Lake fishery, that is currently said to be overfished.

As for the algal bloom, there does not exist a study about the intensity of microcystin or other toxins from *Dolichospermum* (formerly *Anabaena*) and *Microcystis*, which are reported to dominate the cyanobacteria community in Tonle Sap Lake, and are among the most toxic cyanobacteria genera (Chia et al., 2018). But more cyanobacteria will mean more cyanotoxins in Tonle Sap lake water. Local people have reported (by personal communication) skin problems

that are happening in recent years in the Tonle Sap floating village community, which may be caused by the cyanotoxins from the cyanobacteria (Pilotto et al., 2004).

Dam developments along the Mekong River are predicted to create higher water levels in the wet season and lower water levels during the dry season. The conceptual model presented here (Section 6.3) shows that floods and droughts have only modest impacts in terms of chlorophyll-a concentration. However, if the hypothesis is that during the rainy season in the drought years the phytoplankton community will be dominated by chlorophyte instead of diatoms, there may still be ecological consequences to the food web, if there will be a change from a diatom based food web to a chlorophyte based food web as the phytoplankton composition is known to cascade throughout aquatic food webs (Adrian et al., 2006; Winder & Schindler, 2004).

In this study, the conceptual model of total suspended sediment (Section 6.2) for some locations is in agreement with the study of Hoshikawa et al. (2019), with further findings that high flood years cause lower TSS concentrations compared to the normal flood years, although drought will result in even lower TSS concentrations in Tonle Sap Lake. Regardless of these extreme hydrological conditions, sediment delivery in the Mekong River is reported to be declining (Darby et al., 2016), which will mean reduced particulate phosphorus and inorganic nitrogen as the biggest fraction of phosphorus and nitrogen and sediments. This future decline of nitrogen and phosphorus flux has also been projected by Whitehead *et al.*(2019), although, under higher temperature increase and high population, the simulation results show that the phosphorus flux increases, reflecting the increased effluent discharge.

The increasing trends of TSS concentrations which is happening in the late outflow (January to March) and the low water periods (April and May) (Table 5-1) are probably related to the decreasing water, as in these periods, TSS concentrations show strong negative correlations with water level (Figure 6-2). This increasing TSS concentration could translate to an increase of phosphorus release that could become a growth trigger for phytoplankton.

Dam developments also suggest that in the future fewer nutrients may be transported to the Tonle Sap Lake. However, very recent findings (Q. Chen et al., 2020) show that from 1985 to 2015, there has been no decline in bioavailable nitrogen and phosphorus downstream of six dams in the upper Mekong River (China area), although there was a slight increase in both dissolved and bioavailable phosphorus. Furthermore, a significant finding from the study is that silica was retained behind the dams, which impacted the subsequent dam to have a phytoplankton community shift from diatom to chlorophyte. This is particularly important for Tonle Sap Lake, where diatoms dominating during the wet season need silica for their growth. These changes are happening in the upper Mekong River, thus there is a possibility that the water will regain its silica

content when flowing through the karst area in Central Lao PDR (I. C. Campbell et al., 2006). However, dam developments within and downstream of Lao PDR will also potentially change the silica content of the Mekong River, in turn potentially leading to community shifts in Tonle Sap lake.

## 7.6 Conclusions

This study has identified temporal variations in TSS concentrations in Tonle Sap lake. Specifically, TSS concentrations fluctuate significantly over the seasonal water cycle. The lowest values (13 mg/L to 36 mg/L) typically occur in the early outflow period (October to December), but then rise through the periods of late outflow (January to March) and low water (April to May). TSS concentrations reach their highest values in June (187 mg/L to 285 mg/L), which is the end of the low water season or the beginning of the inflow water from the Mekong River, depending on when the rainy season onset begins, before receding following the subsequent inflow periods (July to September).

This study also identified a clear spatial variation in TSS concentrations in Tonle Sap lake. The Chong Khneas River outlet and the middle of the lake record the highest TSS concentrations for all water periods (mean annual of 133 mg/L and 136 mg/L, respectively). Of the 5 study locations, the site located near the outlet of the Tonle Sap River has the lowest TSS concentration (mean annual of 98 mg/L), except during the late inflow season (August and September), when the TSS concentrations are lowest in the neck part of the lake.

However, unlike the variations over seasonal timescales, the evidence for longer term (over three decades) changes in TSS concentration is rather less well developed. A very small increase over time (0.13 – 0.34 mg/L/yr) in all study locations, with the neck of the lake being the only location investigated at which there is no statistically significant increasing trend.

This study has also identified temporal variations of the phytoplankton biomass (proxied as chlorophyll-a concentration) in Tonle Sap Lake. The mean chl-a concentrations also fluctuate over the cycle of the water level but with different timings from that of the TSS concentrations. The lowest values (7.8 µg/L to 8.6 µg/L) typically occur in the low water period (April to May) and extend to the early inflow (June and July), before rising to reach their highest values (11.6 µg/L to 12.4 µg/L) in the early outflow (October to December) period. Chl-a concentrations then recede following the subsequent late outflow period (January to March).

There are also clear spatial variations in chl-a concentrations in Tonle Sap lake. The Battambang River outlet has the highest mean value in all water periods (8.4 µg/L to 12.4 µg/L). The maximum concentration of chl-a recorded in this study was at the Chong Khneas River outlet (26.5 µg/L) occurred during the late outflow season (January to March) of the extreme flood year 2011.

A notable finding of this research is the remarkable characteristic in the chl-a concentrations that they have almost homogenous values when the water level is low (April to May). This condition continues to the period of inflow coming from the Mekong River (June to September), although spatial variability in chl-a begins to increase at the end of this inflow period (August and September). The maximum mean chl-a concentrations, which occur in the early outflow (October to December) period, show very variable values. In particular, the Battambang River outlet has very different chl-a concentrations from year to year.

Long term trend analysis trend shows that there is little evidence of any statistically significant long-term increase (or decrease) in chl-a concentrations within the Tonle Sap lake during 1990-2020. The only such increase was restricted to the low water period, at the Battambang river outlet (rate of 0.057 µg/L/yr), and the neck of the lake (rate of 0.017 µg/L/yr) study sites.

A data-driven conceptual model (Figure 6-5) for the annual cycle of TSS concentration fluctuations resulting from the water flow variations was developed. The model shows the temporal variations of TSS concentrations in Tonle Sap lake, which has been explained above. The model also shows that flood and drought affect the TSS concentration in Tonle Sap lake remarkably during the inflow and outflow periods. TSS concentrations during the inflow period are lower in the high flood years compared to the normal flood years, but the TSS concentrations during the drought years are the lowest of all. For the outflow period, wind generated waves are especially important in generating higher TSS concentrations during the drought years.

A data-driven conceptual model (Figure 6-9) for the annual cycle of chl-a concentration fluctuations resulting from the water flow variations was also constructed. The model shows the temporal variations of chl-a concentrations in Tonle Sap lake, as explained above. The model also shows that flood and drought affect chl-a concentration in Tonle Sap lake, notably in the inflow period, where drought years exhibit lower chl-a concentrations compared to those observed in the flood years. Overall, this study shows that in the 30 year time period (1990-2019), or probably even from the early Holocene, Tonle Sap Lake is in a mesotrophic condition. However, algal blooms as  a bioindicator of eutrophication are evident. The coarse temporal resolution (16 days) of Landsat probably could not capture the incidence of the algal bloom in this study. However, excessive nutrients source activities such as agricultural intensification, garment industries, tourism in Tonle Sap lake are still growing within Cambodia. The Mekong River and its basin,

which is inseparable from the Tonle Sap lake, are seeing numerous changes. Simulation studies have projected increasing phosphorus and nitrogen delivery to the Mekong River, as a result of dam development and the climate change. The Tonle Sap lake is already experiencing rising water surface temperature, possibly the result of climate change. The future of the Tonle Sap lake is problematic, complicated, and uncertain, meaning that further research is needed to help sustain the ecological integrity of this globally important lake.

# List of References

Abdel-Rahman, E. M., Ahmed, F. B., & Ismail, R. (2013). Random forest regression and spectral band selection for estimating sugarcane leaf nitrogen concentration using EO-1 Hyperion hyperspectral data. *International Journal of Remote Sensing*, *34*(2), 712–728.

Adrian, R., O'Reilly, C. M., Zagarese, H., Baines, S. B., Hessen, D. O., Keller, W., Livingstone, D. M., Sommaruga, R., Straile, D., & Van Donk, E. (2009). Lakes as sentinels of climate change. *Limnology and Oceanography*, *54*(6part2), 2283–2297.

Adrian, R., Wilhelm, S., & Gerten, D. (2006). Life-history traits of lake plankton species may govern their phenological response to climate warming. *Global Change Biology*, *12*(4), 652–661.

Al-Anazi, A. F., & Gates, I. D. (2010). Support vector regression for porosity prediction in a heterogeneous reservoir: A comparative study. *Computers & Geosciences*, *36*(12), 1494–1503.

Allende, L., Tell, G., Zagarese, H., Torremorell, A., Pérez, G., Bustingorry, J., Escaray, R., & Izaguirre, I. (2009). Phytoplankton and primary production in clear-vegetated, inorganic-turbid, and algal-turbid shallow lakes from the pampa plain (Argentina). *Hydrobiologia*, *624*(1), 45–60.

Andersen, I. M., Williamson, T. J., González, M. J., & Vanni, M. J. (2020). Nitrate, ammonium, and phosphorus drive seasonal nutrient limitation of chlorophytes, cyanobacteria, and diatoms in a hyper-eutrophic reservoir. *Limnology and Oceanography*, *65*(5), 962–978.

Anderson, D. M., Glibert, P. M., & Burkholder, J. M. (2002). Harmful algal blooms and eutrophication: nutrient sources, composition, and consequences. *Estuaries*, *25*(4), 704–726.

Andres, L., Boateng, K., Borja-Vega, C., & Thomas, E. (2018). A review of in-situ and remote sensing technologies to monitor water and sanitation interventions. *Water*, *10*(6), 756.

Anguelov, N. (2015). *The dirty side of the garment industry: Fast fashion and its negative impact on environment and Society*. CRC Press.

ANZECC. (2000). *Australian and New Zealand guidelines for fresh and marine water quality*. https://www.waterquality.gov.au/anz-guidelines/resources/previous-guidelines/anzecc-armcanz-2000

Arai, H., & Fukushima, T. (2014). Impacts of long-term increase in silicon concentration on diatom blooms in Lake Kasumigaura, Japan. *Annales de Limnologie-International Journal of Limnology*, *50*(4), 335–346.

Arai, H., Fukushima, T., & Komatsu, K. (2012). Increase in silicon concentrations and release from suspended solids and bottom sediments in Lake Kasumigaura, Japan. *Limnology*, *13*(1), 81–95.

Arias, M. E., Cochrane, T. A., Piman, T., Kummu, M., Caruso, B. S., & Killeen, T. J. (2012). Quantifying changes in flooding and habitats in the Tonle Sap Lake (Cambodia) caused by water infrastructure development and climate change in the Mekong Basin. *Journal of Environmental Management*, *112*, 53–66.

Arias, M. E., Piman, T., Lauri, H., Cochrane, T. A., & Kummu, M. (2014). Dams on Mekong tributaries as significant contributors of hydrological alterations to the Tonle Sap Floodplain in Cambodia. *Hydrology and Earth System Sciences*, *18*(12), 5303.

Arrigo, K. R., van Dijken, G. L., & Bushinsky, S. (2008). Primary production in the Southern Ocean, 1997–2006. *Journal of Geophysical Research: Oceans*, *113*(C8).

Artiola, J. F., Brusseau, M. L., & Pepper, I. L. (2004). *Environmental monitoring and characterization*. Academic Press.

Auer, M. T., Auer, N. A., Barkdoll, B. D., Bornhorst, T. J., Brooks, C. N., Dempsey, D., Doskey, P. V, Green, S. A., Hyslop, M., & Kerfoot, W. C. (2014). The Great Lakes: Nutrients, sediments, persistent pollutants, and policy perspectives for a sustainable future. *Comprehensive Water Quality and Purification*.

Azman, E., Eu, G. Y. Y., Lim, Y. Y. G., Seah, Y., Wu, B. S., & Irvine, K. N. (2016). *An exploratory application of remote sensing technologies and statistical analysis to provide rapid and cost effective inundation predictions for the Tonle Sap Lake floodplain system*.

Baban, S. M. J. (1993). Detecting water quality parameters in the Norfolk Broads, UK, using Landsat imagery. *International Journal of Remote Sensing*, *14*(7), 1247–1267.

Back, A. J. (1997). *Ammonification, nitrification and denitrification in the forested ecotone of a small, Oligotrophic Lake in Algonquin Park, Ontario*.

Banskota, A., Kayastha, N., Falkowski, M. J., Wulder, M. A., Froese, R. E., & White, J. C. (2014). Forest monitoring using Landsat time series data: A review. *Canadian Journal of Remote*

*Sensing*, *40*(5), 362–384.

Barica, J., Kling, H., & Gibson, J. (1980). Experimental manipulation of algal bloom composition by nitrogen addition. *Canadian Journal of Fisheries and Aquatic Sciences*, *37*(7), 1175–1183.

Baromey, N. (2008). *Ecotourism as a tool for sustainable rural community development and natural resources management in the Tonle Sap Biosphere Reserve*. kassel university press GmbH.

Barrett, D. C., & Frazier, A. E. (2016). Automated method for monitoring water quality using Landsat imagery. *Water*, *8*(6), 257.

Bellinger, E. G., & Sigee, D. C. (2015). *Freshwater algae: identification and use as bioindicators*. John Wiley & Sons.

Bengtsson, L., & Hellström, T. (1992). Wild-induced resuspension in a small shallow lake. *Hydrobiologia*, *241*(3), 163–172.

Bennett, E. M., Carpenter, S. R., & Caraco, N. F. (2001). Human Impact on Erodable Phosphorus and Eutrophication: A Global Perspective: Increasing accumulation of phosphorus in soil threatens rivers, lakes, and coastal oceans with eutrophication. *AIBS Bulletin*, *51*(3), 227–234.

Berg, G. M., Balode, M., Purina, I., Bekere, S., Béchemin, C., & Maestrini, S. Y. (2003). Plankton community composition in relation to availability and uptake of oxidized and reduced nitrogen. *Aquatic Microbial Ecology*, *30*(3), 263–274.

Bernardo, N., Watanabe, F., Rodrigues, T., & Alcântara, E. (2017). Atmospheric correction issues for retrieving total suspended matter concentrations in inland waters using OLI/Landsat-8 image. *Advances in Space Research*, *59*(9), 2335–2348.

Bernhard, A. (2010). The Nitrogen Cycle: Processes, Players, and Human Impact. *Nature Education Knowledge*, *3*(10), 25.

Bernhardt, J., Elliott, A. J., & Jones, I. D. (2008). Modelling the effects on phytoplankton communities of changing mixed depth and background extinction coefficient on three contrasting lakes in the English Lake District. *Freshwater Biology*, *53*(12), 2573–2586.

Beversdorf, L. J., Miller, T. R., & McMahon, K. D. (2013). The role of nitrogen fixation in cyanobacterial bloom toxicity in a temperate, eutrophic lake. *PloS One*, *8*(2), e56103.

Binding, C. E., Greenberg, T. A., McCullough, G., Watson, S. B., & Page, E. (2018). An analysis of satellite-derived chlorophyll and algal bloom indices on Lake Winnipeg. *Journal of Great Lakes Research*. https://doi.org/10.1016/j.jglr.2018.04.001

Björn, L. O., Papageorgiou, G. C., Blankenship, R. E., & Govindjee. (2009). A viewpoint: why chlorophyll a? *Photosynthesis Research*, *99*(2), 85–98.

Blache, J. (1951). Apercu sur le plancton des eaux douces du Cambodge. *Cybium*, *6*, 62–94.

Blache, Jacques. (1950). *Considérations sur le plancton de surface des eaux douces du Cambodge*.

Bloesch, J. (1982). Inshore–offshore sedimentation differences resulting from resuspension in the eastern basin of Lake Erie. *Canadian Journal of Fisheries and Aquatic Sciences*, *39*(5), 748–759.

Bogard, M. J., Vogt, R. J., Hayes, N. M., & Leavitt, P. R. (2020). Unabated Nitrogen Pollution Favors Growth of Toxic Cyanobacteria over Chlorophytes in Most Hypereutrophic Lakes. *Environmental Science & Technology*, *54*(6), 3219–3227.

Bonansea, M., Rodriguez, M. C., Pinotti, L., & Ferrero, S. (2015). Using multi-temporal Landsat imagery and linear mixed models for assessing water quality parameters in Río Tercero reservoir (Argentina). *Remote Sensing of Environment*, *158*, 28–41.

Bopp, L., Aumont, O., Cadule, P., Alvain, S., & Gehlen, M. (2005). Response of diatoms distribution to global warming and potential implications: A global model study. *Geophysical Research Letters*, *32*(19).

Boström, B., Persson, G., & Broberg, B. (1988). Bioavailability of different phosphorus forms in freshwater systems. In *Phosphorus in Freshwater Ecosystems* (pp. 133–155). Springer.

Brasil, J., Attayde, J. L., Vasconcelos, F. R., Dantas, D. D. F., & Huszar, V. L. M. (2016). Drought-induced water-level reduction favors cyanobacteria blooms in tropical shallow lakes. *Hydrobiologia*, *770*(1), 145–164.

Breiman, L. (2001). Random forests. *Machine Learning*, *45*(1), 5–32.

Brezonik, P., Menken, K. D., & Bauer, M. (2005). Landsat-based remote sensing of lake water quality characteristics, including chlorophyll and colored dissolved organic matter (CDOM). *Lake and Reservoir Management*, *21*(4), 373–382.

Bricaud, A., Babin, M., Morel, A., & Claustre, H. (1995). Variability in the chlorophyll-specific

List of References

absorption coefficients of natural phytoplankton: Analysis and parameterization. *Journal of Geophysical Research: Oceans*, *100*(C7), 13321–13332.

Britannica, E. (n.d.). *Nitrogen Fixation*. Retrieved October 13, 2020, from https://www.britannica.com/science/nitrogen-fixation

Brivio, P. A., Giardino, C., & Zilioli, E. (2001). Determination of chlorophyll concentration changes in Lake Garda using an image-based radiative transfer code for Landsat TM images. *International Journal of Remote Sensing*, *22*(2–3), 487–502.

Broberg, O., & Persson, G. (1988). Particulate and dissolved phosphorus forms in freshwater: composition and analysis. *Hydrobiologia*, *170*(1), 61–90.

Brown, J. S. (1969). Absorption and fluorescence of chlorophyll a in particle fractions from different plants. *Biophysical Journal*, *9*(12), 1542–1552.

Brylinsky, M., & Mann, K. (1973). An analysis of factors governing productivity in lakes and reservoirs. *Limnology and Oceanography*, *18*(1), 1–14.

Burnett, W. C., Peterson, R. N., Chanyotha, S., Wattayakorn, G., & Ryan, B. (2013). Using high-resolution in situ radon measurements to determine groundwater discharge at a remote location: Tonle Sap Lake, Cambodia. *Journal of Radioanalytical and Nuclear Chemistry*, *296*(1), 97–103.

Burnett, W. C., Wattayakorn, G., Supcharoen, R., Sioudom, K., Kum, V., Chanyotha, S., & Kritsananuwat, R. (2017). Groundwater discharge and phosphorus dynamics in a flood-pulse system: Tonle Sap Lake, Cambodia. *Journal of Hydrology*, *549*, 79–91.

Burson, A., Stomp, M., Greenwell, E., Grosse, J., & Huisman, J. (2018). Competition for nutrients and light: testing advances in resource competition with a natural phytoplankton community. *Ecology*, *99*(5), 1108–1118.

Campbell, G., Phinn, S. R., & Daniel, P. (2011). The specific inherent optical properties of three sub-tropical and tropical water reservoirs in Queensland, Australia. *Hydrobiologia*, *658*(1), 233–252.

Campbell, I. C., Poole, C., Giesen, W., & Valbo-Jorgensen, J. (2006). Species diversity and ecology of Tonle Sap Great Lake, Cambodia. *Aquatic Sciences*, *68*(3), 355–373.

Camps-Valls, G., Bruzzone, L., Rojo-Álvarez, J. L., & Melgani, F. (2006). Robust support vector

regression for biophysical variable estimation from remotely sensed images. *IEEE Geoscience and Remote Sensing Letters*, *3*(3), 339–343.

Canfield Jr, D. E., Bachmann, R. W., Hoyer, M. V, Johansson, L. S., Søndergaard, M., & Jeppesen, E. (2019). To measure chlorophyll or phytoplankton biovolume: an aquatic conundrum with implications for the management of lakes. *Lake and Reservoir Management*, *35*(2), 181–192.

Carlson, R. E. (1977). A trophic state index for lakes. *Limnology and Oceanography*, *22*(2), 361–369.

Carpenter, D. J., & Carpenter, S. M. (1983). Modeling inland water quality using Landsat data. *Remote Sensing of Environment*, *13*(4), 345–352.

Carpenter, S. R., Caraco, N. F., Correll, D. L., Howarth, R. W., Sharpley, A. N., & Smith, V. H. (1998). Nonpoint pollution of surface waters with phosphorus and nitrogen. *Ecological Applications*, *8*(3), 559–568.

Carvalho, L., Miller, C., Scott, E., Codd, G., Davies, P., & Tyler, N. (2011). Cyanobacterial blooms: statistical models describing risk factors for national-scale lake assessment and lake management. *Science of the Total Environment*, *409*(24), 5353–5358.

Carvalho, L., Miller, C., Spears, B. M., Gunn, I. D. M., Bennion, H., Kirika, A., & May, L. (2011). Water quality of Loch Leven: responses to enrichment, restoration and climate change. In *Loch Leven: 40 years of scientific research* (pp. 35–47). Springer.

Caughlan, L., & Oakley, K. L. (2001). Cost considerations for long-term ecological monitoring. *Ecological Indicators*, *1*(2), 123–134.

Chadwick, M., & Juntopas, M. (2008). *Sustaining Tonle Sap: An assessment of development challenges facing the Great Lake*. Sustainable Mekong Research Network (Sumernet).

Chaffin, J. D., & Bridgeman, T. B. (2014). Organic and inorganic nitrogen utilization by nitrogen-stressed cyanobacteria during bloom conditions. *Journal of Applied Phycology*, *26*(1), 299–309.

Chan, B., Brosse, S., Hogan, Z. S., Ngor, P. B., & Lek, S. (2020). Influence of Local Habitat and Climatic Factors on the Distribution of Fish Species in the Tonle Sap Lake. *Water*, *12*(3), 786.

Chea, R., Grenouillet, G., & Lek, S. (2016). Evidence of water quality degradation in lower Mekong basin revealed by self-organizing map. *PloS One*, *11*(1), e0145527.

List of References

Chebud, Y., Naja, G. M., Rivero, R. G., & Melesse, A. M. (2012). Water quality monitoring using remote sensing and an artificial neural network. *Water, Air, & Soil Pollution*, *223*(8), 4875–4887.

Chen, F., He, W., Tian, Z., & Wang, L. (2020). Impacts of Silk Garment Production on Water Resources and Environment. *International Conference on Sustainable Development of Water and Environment*, 311–319.

Chen, K. Y., & Wang, C. H. (2007). Support vector regression with genetic algorithms in forecasting tourism demand. *Tourism Management*, *28*(1), 215–226.

Chen, Q., Shi, W., Huisman, J., Maberly, S. C., Zhang, J., Yu, J., Chen, Y., Tonina, D., & Yi, Q. (2020). Hydropower reservoirs on the upper Mekong River modify nutrient bioavailability downstream. *National Science Review*.

Chhinh, N., & Millington, A. (2015). Drought monitoring for rice production in Cambodia. *Climate*, *3*(4), 792–811.

Chia, M. A., Jankowiak, J. G., Kramer, B. J., Goleski, J. A., Huang, I.-S., Zimba, P. V, do Carmo Bittencourt-Oliveira, M., & Gobler, C. J. (2018). Succession and toxicity of Microcystis and Anabaena (Dolichospermum) blooms are controlled by nutrient-dependent allelopathic interactions. *Harmful Algae*, *74*, 67–77.

Chorus, I., & Welker, M. (2021). *Toxic cyanobacteria in water: a guide to their public health consequences, monitoring and management*. Taylor & Francis.

Chrispim, M. C., Scholz, M., & Nolasco, M. A. (2019). Phosphorus recovery from municipal wastewater treatment: Critical review of challenges and opportunities for developing countries. *Journal of Environmental Management*, *248*, 109268.

Clevinger, C. C. (2013). *Nitrifiers and their contribution to oxygen consumption in Lake Erie*. Kent State University.

Clevinger, C. C., Heath, R. T., & Bade, D. L. (2014). Oxygen use by nitrification in the hypolimnion and sediments of Lake Erie. *Journal of Great Lakes Research*, *40*(1), 202–207.

Cochrane, T. A., Arias, M. E., & Piman, T. (2014). Historical impact of water infrastructure on water levels of the Mekong River and the Tonle Sap system. *Hydrology and Earth System Sciences*, *18*(11), 4529–4541.

Codd, G. A., Bell, S., Kaya, K., Ward, C., Beattie, K., & Metcalf, J. (1999). Cyanobacterial toxins, exposure routes and human health. *European Journal of Phycology*, *34*(4), 405–415.

Codd, G. A., Lindsay, J., Young, F. M., Morrison, L. F., & Metcalf, J. S. (2005). Harmful cyanobacteria. In *Harmful cyanobacteria* (pp. 1–23). Springer.

Conley, D. J., Schelske, C. L., & Stoermer, E. F. (1993). Modification of the biogeochemical cycle of silica with eutrophication. *Marine Ecology Progress Series*, 179–192.

Crowe, S. A., Treusch, A. H., Forth, M., Li, J., Magen, C., Canfield, D. E., Thamdrup, B., & Katsev, S. (2017). Novel anammox bacteria and nitrogen loss from Lake Superior. *Scientific Reports*, *7*(1), 1–7.

Cuker, B. E., Gama, P. T., & Burkholder, J. M. (1990). Type of suspended clay influences lake productivity and phytoplankton community response to phosphorus loading. *Limnology and Oceanography*, *35*(4), 830–839.

Dai, M., Guo, X., Zhai, W., Yuan, L., Wang, B., Wang, L., Cai, P., Tang, T., & Cai, W.-J. (2006). Oxygen depletion in the upper reach of the Pearl River estuary during a winter drought. *Marine Chemistry*, *102*(1–2), 159–169.

Dall'Olmo, G., & Gitelson, A. A. (2005). Effect of bio-optical parameter variability on the remote estimation of chlorophyll-a concentration in turbid productive waters: experimental results. *Applied Optics*, *44*(3), 412–422.

Dall'Olmo, G., Gitelson, A. A., & Rundquist, D. C. (2003). Towards a unified approach for remote estimation of chlorophyll-a in both terrestrial vegetation and turbid productive waters. *Geophysical Research Letters*, *30*(18).

Daly, K., Ahmad, S. K., Bonnema, M., Beveridge, C., Hossain, F., Nijssen, B., & Holtgrieve, G. (2020). Recent warming of Tonle Sap Lake, Cambodia: Implications for one of the world's most productive inland fisheries. *Lakes & Reservoirs: Research & Management*, *25*(2), 133–142.

Daniel, T. C., Sharpley, A. N., Edwards, D. R., Wedepohl, R., & Lemunyon, J. L. (1994). *Minimizing surface water eutrophication from agriculture by phosphorus management*.

Darby, S. E., Hackney, C. R., Leyland, J., Kummu, M., Lauri, H., Parsons, D. R., Best, J. L., Nicholas, A. P., & Aalto, R. (2016). Fluvial sediment supply to a mega-delta reduced by shifting tropical-cyclone activity. *Nature*, *539*(7628), 276–279.

List of References

Davies, G. I., McIver, L., Kim, Y., Hashizume, M., Iddings, S., & Chan, V. (2015). Water-borne diseases and extreme weather events in Cambodia: Review of impacts and implications of climate change. *International Journal of Environmental Research and Public Health*, *12*(1), 191–213.

Davies, P. M., Bunn, S. E., & Hamilton, S. K. (2008). Primary production in tropical streams and rivers. In D. Dudgeon (Ed.), *Tropical Stream Ecology.*

Dekker, A. G., Vos, R. J., & Peters, S. W. M. (2002). Analytical algorithms for lake water TSM estimation for retrospective analyses of TM and SPOT sensor data. *International Journal of Remote Sensing*, *23*(1), 15–35.

Deutsch, E. S., Alameddine, I., & El-Fadel, M. (2018). Monitoring water quality in a hypereutrophic reservoir using Landsat ETM+ and OLI sensors: how transferable are the water quality algorithms? *Environmental Monitoring and Assessment*, *190*(3), 1–19.

Dewidar, K., & Khedr, A. (2001). Water quality assessment with simultaneous Landsat-5 TM at Manzala Lagoon, Egypt. *Hydrobiologia*, *457*(1–3), 49–58.

Diaz, M. M., & Pedrozo, F. L. (1996). Nutrient limitation in Andean-Patagonian lakes at latitude 40-41 S. *Archiv Für Hydrobiologie*, *138*(1), 123–143.

Dietterich, T. G. (2000). Ensemble methods in machine learning. *International Workshop on Multiple Classifier Systems*, 1–15.

Dillon, P. J., Nicholls, K. H., Locke, B. A., De Grosbois, E., & Yan, N. D. (1988). Phosphorus—phytoplankton relationships in nutrient-poor soft-water lakes in Canada: With 4 tables in the text. *Internationale Vereinigung Für Theoretische Und Angewandte Limnologie: Verhandlungen*, *23*(1), 258–264.

Dillon, P. J., & Rigler, F. H. (1974). The phosphorus-chlorophyll relationship in lakes. *Limnology and Oceanography*, *19*(5), 767–773.

Dodds, W. K. (2006). Eutrophication and trophic state in rivers and streams. *Limnology and Oceanography*, *51*(1part2), 671–680.

Dodds, W. K., & Whiles, M. (2002). Nitrogen, sulfur, phosphorus, and other nutrients. In *Freshwater Ecology*. Elsevier Inc. https://www.sciencedirect.com/science/article/pii/B9780122191350500143

Dodds, W. K., & Whiles, M. R. (2010). Nitrogen, Sulfur, Phosphorus, and Other Nutrients. In *Freshwater Ecology: Concepts and Environmental Applications of Limnology*. Academic Press London.

Dodds, W. K., & Whiles, M. R. (2020). Nitrogen, sulfur, phosphorus, and other nutrients. In *Freshwater Ecology (Third Edition)*. Elsevier Inc. https://www.sciencedirect.com/science/article/pii/B9780128132555000144#ab0010

Dokulil, M. T., & Teubner, K. (2000). Cyanobacterial dominance in lakes. *Hydrobiologia*, *438*(1–3), 1–12.

Domingues, R. B., Barbosa, A. B., Sommer, U., & Galvão, H. M. (2011). Ammonium, nitrate and phytoplankton interactions in a freshwater tidal estuarine zone: potential effects of cultural eutrophication. *Aquatic Sciences*, *73*(3), 331–343.

Domis, L. N. D. S., Mooij, W. M., & Huisman, J. (2007). Climate-induced shifts in an experimental phytoplankton community: a mechanistic approach. In *Shallow Lakes in a Changing World* (pp. 403–413). Springer.

Dona, C., Chang, N.-B., Caselles, V., Sánchez, J. M., Camacho, A., Delegido, J., & Vannah, B. W. (2015). Integrated satellite data fusion and mining for monitoring lake water quality status of the Albufera de Valencia in Spain. *Journal of Environmental Management*, *151*, 416–426.

Donald, D. B., Bogard, M. J., Finlay, K., Bunting, L., & Leavitt, P. R. (2013). Phytoplankton-specific response to enrichment of phosphorus-rich surface waters with ammonium, nitrate, and urea. *PloS One*, *8*(1), e53277.

Donald, D. B., Bogard, M. J., Finlay, K., & Leavitt, P. R. (2011). Comparative effects of urea, ammonium, and nitrate on phytoplankton abundance, community composition, and toxicity in hypereutrophic freshwaters. *Limnology and Oceanography*, *56*(6), 2161–2175.

Dubois, N., Saulnier-Talbot, É., Mills, K., Gell, P., Battarbee, R., Bennion, H., Chawchai, S., Dong, X., Francus, P., & Flower, R. (2018). First human impacts and responses of aquatic systems: A review of palaeolimnological records from around the world. *The Anthropocene Review*, *5*(1), 28–68.

Edmondson, W. T. (1969). *Eutrophication in North America*.

EEA. (2021). *Nutrients in Freswater in Europe*. European Environment Agency. https://www.eea.europa.eu/data-and-maps/indicators/nutrients-in-freshwater/nutrients-

List of References

in-freshwater-assessment-published-10

Elliott, A. J. (2010). The seasonal sensitivity of cyanobacteria and other phytoplankton to changes in flushing rate and water temperature. *Global Change Biology*, *16*(2), 864–876.

Elliott, A. J., & Defew, L. (2011). Modelling the response of phytoplankton in a shallow lake (Loch Leven, UK) to changes in lake retention time and water temperature. In *Loch Leven: 40 years of scientific research* (pp. 105–116). Springer.

Elser, J. J., Marzolf, E. R., & Goldman, C. R. (1990). Phosphorus and nitrogen limitation of phytoplankton growth in the freshwaters of North America: a review and critique of experimental enrichments. *Canadian Journal of Fisheries and Aquatic Sciences*, *47*(7), 1468–1477.

EPA. (2008). *Water Quality in Ireland 2004-2006*. https://www.epa.ie/pubs/reports/water/waterqua/waterrep/

European Commission. (1991). Council Directive of 21. May 1991 concerning urban waste water treatment (91/271/EEC). In *Council Directive 91/271/EEC of 21 May 1991 concerning urban waste water treatment. O.J. L135, 30.5.*

Evans, A. E. V, Mateo-Sagasta, J., Qadir, M., Boelee, E., & Ippolito, A. (2019). Agricultural water pollution: key knowledge gaps and research needs. *Current Opinion in Environmental Sustainability*, *36*, 20–27.

FAO. (2006). Global Forest Resources Assessment 2005: Progress towards sustainable forest management. In *FAO Forestry Paper*.

FAO. (2011). *Mekong Basin, Water Report* (No. 37).

FAO. (2020). *World Food and Agriculture - Statistical Yearbook 2020*. https://doi.org/10.4060/cb1329en

Farmer, A. . (2018). Phosphate pollution: A global overview of the problem. In *Phosphorus: Polluter and Resource of the Future: Motivations, Technologies and Assessment of the Elimination and Recovery of Phosphorus from Wastewater* (Phosphorus). London IWA Publishing.

Felip, M., & Catalan, J. (2000). The relationship between phytoplankton biovolume and chlorophyll in a deep oligotrophic lake: decoupling in their spatial and temporal maxima.

*Journal of Plankton Research*, *22*(1), 91–106.

Ferreira, J. G., Andersen, J. H., Borja, A., Bricker, S. B., Camp, J., Da Silva, M. C., Garcés, E., Heiskanen, A.-S., Humborg, C., & Ignatiades, L. (2011). Overview of eutrophication indicators to assess environmental status within the European Marine Strategy Framework Directive. *Estuarine, Coastal and Shelf Science*, *93*(2), 117–131.

Ferris, J. A., & Lehman, J. T. (2007). Interannual variation in diatom bloom dynamics: roles of hydrology, nutrient limitation, sinking, and whole lake manipulation. *Water Research*, *41*(12), 2551–2562.

Figueredo, C. C., & Giani, A. (2009). Phytoplankton community in the tropical lake of Lagoa Santa (Brazil): conditions favoring a persistent bloom of Cylindrospermopsis raciborskii. *Limnologica*, *39*(4), 264–272.

Forsberg, C. (1989). Importance of sediments in understanding nutrient cyclings in lakes. *Hydrobiologia*, *176*(1), 263–277.

Foy, R. H., Gibson, C. E., & Smith, R. V. (1976). The influence of daylength, light intensity and temperature on the growth rates of planktonic blue-green algae. *British Phycological Journal*, *11*(2), 151–163.

Fragoso Jr, C. R., Marques, D. M. L. M., Collischonn, W., Tucci, C. E. M., & van Nes, E. H. (2008). Modelling spatial heterogeneity of phytoplankton in Lake Mangueira, a large shallow subtropical lake in South Brazil. *Ecological Modelling*, *219*(1–2), 125–137.

Fraser, R. N. (1998). Multispectral remote sensing of turbidity among Nebraska Sand Hills lakes. *International Journal of Remote Sensing*, *19*(15), 3011–3016.

Fukushima, M., Tomioka, N., Jutagate, T., Hiroki, M., Murata, T., Preecha, C., Avakul, P., Phomikong, P., & Imai, A. (2017). The dynamics of pico-sized and bloom-forming cyanobacteria in large water bodies in the Mekong River Basin. *PloS One*, *12*(12), e0189609.

Galloway, J. N., Townsend, A. R., Erisman, J. W., Bekunda, M., Cai, Z., Freney, J. R., Martinelli, L. A., Seitzinger, S. P., & Sutton, M. A. (2008). Transformation of the nitrogen cycle: recent trends, questions, and potential solutions. *Science*, *320*(5878), 889–892.

Gardner, W. S., Newell, S. E., McCarthy, M. J., Hoffman, D. K., Lu, K., Lavrentyev, P. J., Hellweger, F. L., Wilhelm, S. W., Liu, Z., & Bruesewitz, D. A. (2017). Community biological ammonium demand: a conceptual model for Cyanobacteria blooms in eutrophic lakes. *Environmental*

*Science & Technology*, *51*(14), 7785–7793.

Gerten, D., & Adrian, R. (2002). Effects of climate warming, North Atlantic Oscillation, and El Nino-Southern Oscillation on thermal conditions and plankton dynamics in northern hemispheric lakes. *TheScientificWorldJOURNAL*, *2*, 586–606.

Giardino, C., Bresciani, M., Braga, F., Cazzaniga, I., De Keukelaere, L., Knaeps, E., & Brando, V. E. (2017). Bio-optical Modeling of Total Suspended Solids. In *Bio-optical Modeling and Remote Sensing of Inland Waters* (pp. 129–156). Elsevier Inc. https://doi.org/10.1016/B978-0-12-804644-9.00005-7

Gibson, C. E., Wang, G., & Foy, R. H. (2000). Silica and diatom growth in Lough Neagh: the importance of internal recycling. *Freshwater Biology*, *45*(3), 285–293.

Gilbert, R. O. (1987). *Statistical methods for environmental pollution monitoring*. John Wiley & Sons.

Gilerson, A. A., Gitelson, A. A., Zhou, J., Gurlin, D., Moses, W., Ioannou, I., & Ahmed, S. A. (2010). Algorithms for remote estimation of chlorophyll-a in coastal and inland waters using red and near infrared bands. *Optics Express*, *18*(23), 24109–24125.

Gitelson, A. A., Dall'Olmo, G., Moses, W., Rundquist, D. C., Barrow, T., Fisher, T. R., Gurlin, D., & Holz, J. (2008). A simple semi-analytical model for remote estimation of chlorophyll-a in turbid waters: Validation. *Remote Sensing of Environment*, *112*(9), 3582–3593.

Gitelson, A. A., Gritz, Y., & Merzlyak, M. N. (2003). Relationships between leaf chlorophyll content and spectral reflectance and algorithms for non-destructive chlorophyll assessment in higher plant leaves. *Journal of Plant Physiology*, *160*(3), 271–282.

Glibert, P. M., Wilkerson, F. P., Dugdale, R. C., Raven, J. A., Dupont, C. L., Leavitt, P. R., Parker, A. E., Burkholder, J. M., & Kana, T. M. (2016). Pluses and minuses of ammonium and nitrate uptake and assimilation by phytoplankton and implications for productivity and community composition, with emphasis on nitrogen-enriched conditions. *Limnology and Oceanography*, *61*(1), 165–197.

González-Márquez, L. C., Torres-Bejarano, F. M., Torregroza-Espinosa, A. C., Hansen-Rodríguez, I. R., & Rodríguez-Gallegos, H. B. (2018). Use of LANDSAT 8 images for depth and water quality assessment of El Guájaro reservoir, Colombia. *Journal of South American Earth Sciences*, *82*, 231–238.

Goto, N., Azumi, H., Akatsuka, T., Kihira, M., Ishikawa, M., Anbutsu, K., & Mitamura, O. (2013). Highly efficient silica sink in monomictic Lake Biwa in Japan. *Annales de Limnologie-International Journal of Limnology*, *49*(2), 139–147.

Goto, N., Iwata, T., Akatsuka, T., Ishikawa, M., Kihira, M., Azumi, H., Anbutsu, K., & Mitamura, O. (2007). Environmental factors which influence the sink of silica in the limnetic system of the large monomictic Lake Biwa and its watershed in Japan. *Biogeochemistry*, *84*(3), 285–295.

Grami, B., Rasconi, S., Niquil, N., Jobard, M., Saint-Béat, B., & Sime-Ngando, T. (2011). Functional effects of parasites on food web properties during the spring diatom bloom in Lake Pavin: a linear inverse modeling analysis. *PLoS One*, *6*(8), e23273.

Grizzetti, B., Passy, P., Billen, G., Bouraoui, F., Garnier, J., & Lassaletta, L. (2015). The role of water nitrogen retention in integrated nutrient management: assessment in a large basin using different modelling approaches. *Environmental Research Letters*, *10*(6), 65008.

Grumbine, R. E., & Xu, J. (2011). Mekong hydropower development. *Science*, *332*(6026), 178–179.

Guan, Q., Feng, L., Hou, X., Schurgers, G., Zheng, Y., & Tang, J. (2020). Eutrophication changes in fifty large lakes on the Yangtze Plain of China derived from MERIS and OLCI observations. *Remote Sensing of Environment*, *246*, 111890.

Guanter, L., Ruiz-Verdú, A., Odermatt, D., Giardino, C., Simis, S., Estellés, V., Heege, T., Domínguez-Gómez, J. A., & Moreno, J. (2010). Atmospheric correction of ENVISAT/MERIS data over inland waters: Validation for European lakes. *Remote Sensing of Environment*, *114*(3), 467–480.

Haag, A. S., Walker, N. D., Pilley, C. T., Comeaux, J. C., Calvasina, J. J., & Firth, R. (2009). Satellite surveillance of the Gulf and beyond: An overview of the LSU Earth Scan Laboratory's ocean observing capabilities. *OCEANS 2009*, 1–8.

Hamilton, H. A., Ivanova, D., Stadler, K., Merciai, S., Schmidt, J., Van Zelm, R., Moran, D., & Wood, R. (2018). Trade and the role of non-food commodities for global eutrophication. *Nature Sustainability*, *1*(6), 314–321.

Harke, M. J., Steffen, M. M., Gobler, C. J., Otten, T. G., Wilhelm, S. W., Wood, S. A., & Paerl, H. W. (2016). A review of the global ecology, genomics, and biogeography of the toxic cyanobacterium, Microcystis spp. *Harmful Algae*, *54*, 4–20.

Harper, D. M. (1992). *Eutrophication of freshwaters*. Springer.

List of References

Harrington Jr, J. A., Schiebe, F. R., & Nix, J. F. (1992). Remote sensing of Lake Chicot, Arkansas: Monitoring suspended sediments, turbidity, and Secchi depth with Landsat MSS data. *Remote Sensing of Environment*, *39*(1), 15–27.

Havens, K. E., James, R. T., East, T. L., & Smith, V. H. (2003). N: P ratios, light limitation, and cyanobacterial dominance in a subtropical lake impacted by non-point source nutrient pollution. *Environmental Pollution*, *122*(3), 379–390.

Helsel, D. R., & Hirsch, R. M. (1992). *Statistical methods in water resources* (Vol. 49). Elsevier.

Hendriks, A. T. W. M., & Langeveld, J. G. (2017). *Rethinking wastewater treatment plant effluent standards: nutrient reduction or nutrient control?* ACS Publications.

Hengl, T., Nussbaum, M., Wright, M. N., Heuvelink, G. B. M., & Gräler, B. (2018). Random forest as a generic framework for predictive modeling of spatial and spatio-temporal variables. *PeerJ*, *6*, e5518.

Hillger, D., Kopp, T., Lee, T., Lindsey, D., Seaman, C., Miller, S., Solbrig, J., Kidder, S., Bachmeier, S., & Jasmin, T. (2013). First-light imagery from Suomi NPP VIIRS. *Bulletin of the American Meteorological Society*, *94*(7), 1019–1029.

Hiroki, M., Tomioka, N., Murata, T., Imai, A., Jutagate, T., Preecha, C., Avakul, P., Phomikong, P., & Fukushima, M. (2020). Primary production estimated for large lakes and reservoirs in the Mekong River Basin. *Science of The Total Environment*, 141133.

Homer, C., Huang, C., Yang, L., Wylie, B., & Coan, M. (2004). Development of a 2001 national land-cover database for the United States. *Photogrammetric Engineering & Remote Sensing*, *70*(7), 829–840.

Hori, H. (2000). *The Mekong: environment and development.* United Nations University Press.

Hoshikawa, K., Fujihara, Y., Siev, S., Arai, S., Nakamura, T., Fujii, H., Sok, T., & Yoshimura, C. (2019). Characterization of total suspended solid dynamics in a large shallow lake using long-term daily satellite images. *Hydrological Processes*, *0*(ja). https://doi.org/10.1002/hyp.13525

Hossain, L., Sarker, S. K., & Khan, M. (2018). Evaluation of present and future wastewater impacts of textile dyeing industries in Bangladesh. *Environmental Development*, *26*, 23–33.

Hoverman, J. T., & Johnson, P. T. (2012). *Ponds and Lakes: A Journey Through the Life Aquatic*. Nature Education Knowledge 3(6):17.

Huang, Y., Ciais, P., Goll, D. S., Sardans, J., Peñuelas, J., Cresto-Aleina, F., & Zhang, H. (2020). The shift of phosphorus transfers in global fisheries and aquaculture. *Nature Communications*, *11*(1), 1–10.

Huber, V., Wagner, C., Gerten, D., & Adrian, R. (2012). To bloom or not to bloom: contrasting responses of cyanobacteria to recent heat waves explained by critical thresholds of abiotic drivers. *Oecologia*, *169*(1), 245–256.

Huisman, J., Sharples, J., Stroom, J. M., Visser, P. M., Kardinaal, W. E. A., Verspagen, J. M. H., & Sommeijer, B. (2004). Changes in turbulent mixing shift competition for light between phytoplankton species. *Ecology*, *85*(11), 2960–2970.

Hunter, P. D., Tyler, A. N., Gilvear, D. J., & Willby, N. J. (2009). Using remote sensing to aid the assessment of human health risks from blooms of potentially toxic cyanobacteria. *Environmental Science & Technology*, *43*(7), 2627–2633.

Hunter, P. D., Tyler, A. N., Présing, M., Kovács, A. W., & Preston, T. (2008). Spectral discrimination of phytoplankton colour groups: The effect of suspended particulate matter and sensor spectral resolution. *Remote Sensing of Environment*, *112*(4), 1527–1544.

Huszar, V. L. M., Caraco, N., Roland, F., & Cole, J. (2006). Nutrient-chlorophyll relationships in tropical-subtropical lakes: do temperate models fit? In *Nitrogen Cycling in the Americas: Natural and Anthropogenic Influences and Controls* (pp. 239–250). Springer.

Huszar, V. L. M., & Reynolds, C. S. (1997). Phytoplankton periodicity and sequences of dominance in an Amazonian flood-plain lake (Lago Batata, Pará, Brasil): responses to gradual environmental change. *Hydrobiologia*, *346*(1–3), 169–181.

Huszar, V. L. M., Silva, L., Domingos, P., Marinho, M., & Melo. (1998). Phytoplankton species composition is more sensitive than OECD criteria to the trophic status of three Brazilian tropical lakes. In *Phytoplankton and Trophic Gradients* (pp. 59–71). Springer.

Hyenstrand, P., Burkert, U., Pettersson, A., & Blomqvist, P. (2000). Competition between the green alga Scenedesmus and the cyanobacterium Synechococcus under different modes of inorganic nitrogen supply. *Hydrobiologia*, *435*(1–3), 91–98.

Irvine, K. N., Richey, J. E., Holtgrieve, G. W., Sarkkula, J., & Sampson, M. (2011). Spatial and temporal variability of turbidity, dissolved oxygen, conductivity, temperature, and fluorescence in the lower Mekong River–Tonle Sap system identified using continuous monitoring. *International Journal of River Basin Management*, *9*(2), 151–168.

List of References

Islam, M. A., & Beardall, J. (2017). Growth and photosynthetic characteristics of toxic and non-toxic strains of the cyanobacteria Microcystis aeruginosa and Anabaena circinalis in relation to light. *Microorganisms*, *5*(3), 45.

Istvánovics, V. (2009). Eutrophication of Lakes and Reservoirs. In *Encyclopedia of Inland Waters* (pp. 157–165). Elsevier Inc. https://doi.org/10.1016/B978-012370626-3.00141-1

James, R. T., Gardner, W. S., McCarthy, M. J., & Carini, S. A. (2011). Nitrogen dynamics in Lake Okeechobee: forms, functions, and changes. *Hydrobiologia*, *669*(1), 199–212.

Jansson, M., Olsson, H., & Pettersson, K. (1988). Phosphatases; origin, characteristics and function in lakes. In *Phosphorus in Freshwater Ecosystems* (pp. 157–175). Springer.

Jenny, J.-P., Normandeau, A., Francus, P., Taranu, Z. E., Gregory-Eaves, I., Lapointe, F., Jautzy, J., Ojala, A. E. K., Dorioz, J.-M., & Schimmelmann, A. (2016). Urban point sources of nutrients were the leading cause for the historical spread of hypoxia across European lakes. *Proceedings of the National Academy of Sciences*, *113*(45), 12655–12660.

Jones, J. R., & Bachmann, R. W. (1976). Prediction of phosphorus and chlorophyll levels in lakes. *Journal (Water Pollution Control Federation)*, 2176–2182.

Joosse, P. J., & Baker, D. B. (2011). Context for re-evaluating agricultural source phosphorus loadings to the Great Lakes. *Canadian Journal of Soil Science*, *91*(3), 317–327.

Joyce, S. (2000). The dead zones: oxygen-starved coastal waters. *Environmental Health Perspectives*, *108*(3), A120–A125.

Kalaji, H. M., Schansker, G., Brestic, M., Bussotti, F., Calatayud, A., Ferroni, L., Goltsev, V., Guidi, L., Jajoo, A., & Li, P. (2017). Frequently asked questions about chlorophyll fluorescence, the sequel. *Photosynthesis Research*, *132*(1), 13–66.

Kallio, K., Attila, J., Härmä, P., Koponen, S., Pulliainen, J., Hyytiäinen, U.-M., & Pyhälahti, T. (2008). Landsat ETM+ images in the estimation of seasonal lake water quality in boreal river basins. *Environmental Management*, *42*(3), 511–522.

Kamoto, M., & Juntopas, M. (2007). Lower Mekong Basin: Existing environment and development needs. *Geographical Review of Japan*, *80*(12), 704–715.

Karakaya, N., Evrendilek, F., Aslan, G., Gungor, K., & Karakas, D. (2011). *Monitoring of lake water quality along with trophic gradient using landsat data*.

Kasprzak, P., Padisak, J., Koschel, R., Krienitz, L., & Gervais, F. (2008). Chlorophyll a concentration across a trophic gradient of lakes: An estimator of phytoplankton biomass? *Limnologica*, *38*(3–4), 327–338.

Kawara, O., Yura, E., Fujii, S., & Matsumoto, T. (1998). A study on the role of hydraulic retention time in eutrophication of the Asahi River Dam reservoir. *Water Science and Technology*, *37*(2), 245–252.

Kearney, J. (2010). Food consumption trends and drivers. *Philosophical Transactions of the Royal Society B: Biological Sciences*, *365*(1554), 2793–2807.

Keiser, D. A., Kling, C. L., & Shapiro, J. S. (2019). The low but uncertain measured benefits of US water quality policy. *Proceedings of the National Academy of Sciences*, *116*(12), 5262–5269.

Kemp, A. L. W., & Mudrochova, A. (1972). Distribution and forms of nitrogen in a Lake Ontario sediment core. *Limnology and Oceanography*, *17*(6), 855–867.

Keskinen, M., Someth, P., Salmivaara, A., & Kummu, M. (2015). Water-energy-food nexus in a transboundary river basin: The case of Tonle Sap Lake, Mekong River Basin. *Water*, *7*(10), 5416–5436.

Khan, F., & Ansari, A. A. (2005). Eutrophication: an ecological vision. *The Botanical Review*, *71*(4), 449–482.

Khan, S., & Malik, A. (2014). Environmental and health effects of textile industry wastewater. In *Environmental deterioration and human health* (pp. 55–71). Springer.

King, P., Compliance, O. A. E., Network, E., Bird, J., & Haas, L. J. M. (2007). *The current status of environmental criteria for hydropower development in the Mekong region: a literature compilation*. Citeseer.

Köhler, J. (2006). Detergent phosphates: an EU policy assessment. *Journal of Business Chemistry*, *3*(2).

Kosten, S., Huszar, V. L. M., Bécares, E., Costa, L. S., van Donk, E., Hansson, L., Jeppesen, E., Kruk, C., Lacerot, G., & Mazzeo, N. (2012). Warmer climates boost cyanobacterial dominance in shallow lakes. *Global Change Biology*, *18*(1), 118–126.

Kristensen, P., Søndergaard, M., & Jeppesen, E. (1992). Resuspension in a shallow eutrophic lake. *Hydrobiologia*, *228*(1), 101–109.

List of References

Kroeze, C., Hofstra, N., Ivens, W., Löhr, A., Strokal, M., & van Wijnen, J. (2013). The links between global carbon, water and nutrient cycles in an urbanizing world—the case of coastal eutrophication. *Current Opinion in Environmental Sustainability*, *5*(6), 566–572.

Kuhn, C., de Matos Valerio, A., Ward, N., Loken, L., Sawakuchi, H. O., Kampel, M., Richey, J., Stadler, P., Crawford, J., Striegl, R., Vermote, E., Pahlevan, N., & Butman, D. (2019). Performance of Landsat-8 and Sentinel-2 surface reflectance products for river remote sensing retrievals of chlorophyll-a and turbidity. *Remote Sensing of Environment*, *224*, 104–118. https://doi.org/10.1016/j.rse.2019.01.023

Kulkarni, A. (2011). Water quality retrieval from Landsat TM imagery. *Procedia Computer Science*, *6*, 475–480.

Kummu, M., Koponen, J., & Sarkkula, J. (2005). Modelling sediment transportation in Tonle Sap Lake for impact assessment. *Proceedings of the 2005 International Conference on Simulation & Modeling, SimMod*, *5*, 369–377.

Kummu, M., Lu, X. X., Wang, J. J., & Varis, O. (2010). Basin-wide sediment trapping efficiency of emerging reservoirs along the Mekong. *Geomorphology*, *119*(3–4), 181–197.

Kummu, M., Penny, D., Sarkkula, J., & Koponen, J. (2008). Sediment: curse or blessing for Tonle Sap Lake? *AMBIO: A Journal of the Human Environment*, *37*(3), 158–163.

Kummu, M., Sarkkula, J., Koponen, J., & Nikula, J. (2006). Ecosystem management of the Tonle Sap Lake: an integrated modelling approach. *International Journal of Water Resources Development*, *22*(3), 497–519.

Kummu, M., Tes, S., Yin, S., Adamson, P., Józsa, J., Koponen, J., Richey, J., & Sarkkula, J. (2014). Water balance analysis for the Tonle Sap Lake–floodplain system. *Hydrological Processes*, *28*(4), 1722–1733.

Kummu, M., Varis, O., & Sarkkula, J. (2008). Impacts of land surface changes on regional hydrology—mainland Southeast Asia. In *A Common Need for Action: Global Environmental Change and Development in Monsoon Southeast Asia*. Gerakbudaya, Kuala Lampur, Malesia.

Kuypers, M. M. M., Lavik, G., Woebken, D., Schmid, M., Fuchs, B. M., Amann, R., Jørgensen, B. B., & Jetten, M. S. M. (2005). Massive nitrogen loss from the Benguela upwelling system through anaerobic ammonium oxidation. *Proceedings of the National Academy of Sciences*, *102*(18), 6478–6483.

Kuypers, M. M. M., Marchant, H. K., & Kartal, B. (2018). The microbial nitrogen-cycling network. *Nature Reviews Microbiology*, *16*(5), 263.

Larsen, T. A., Hoffmann, S., Lüthi, C., Truffer, B., & Maurer, M. (2016). Emerging solutions to the water challenges of an urbanizing world. *Science*, *352*(6288), 928–933.

Lathrop, R. G. (1992). Landsat Thematic Mapper monitoring of turbid inland water quality. *Photogrammetric Engineering & Remote Sensing*, *58*(4), 465–470.

Le, C., Zha, Y., Li, Y., Sun, D., Lu, H., & Yin, B. (2010). Eutrophication of lake waters in China: cost, causes, and control. *Environmental Management*, *45*(4), 662–668.

Ledesma, M. M., Bonansea, M., Ledesma, C. R., Rodríguez, C., Carreño, J., & Pinotti, L. (2019). Estimation of chlorophyll-a concentration using Landsat 8 in the Cassaffousth reservoir. *Water Supply*, *19*(7), 2021–2027.

Lewis Jr, W. M. (1996). Tropical lakes: how latitude makes a difference. *Perspectives in Tropical Limnology*, *4364*.

Lewis Jr, W. M. (2002). Causes for the high frequency of nitrogen limitation in tropical lakes. *Internationale Vereinigung Für Theoretische Und Angewandte Limnologie: Verhandlungen*, *28*(1), 210–213.

Li, A., Kroeze, C., Kahil, T., Ma, L., & Strokal, M. (2019). Water pollution from food production: lessons for optimistic and optimal solutions. *Current Opinion in Environmental Sustainability*, *40*, 88–94.

Li, D., Long, D., Zhao, J., Lu, H., & Hong, Y. (2017). Observed changes in flow regimes in the Mekong River basin. *Journal of Hydrology*, *551*, 217–232.

Li, L., & Song, K. (2017). *Chapter 8 - Bio-optical Modeling of Phycocyanin* (D. R. Mishra, I. Ogashawara, & A. A. B. T.-B. M. and R. S. of I. W. Gitelson (eds.); pp. 233–262). Elsevier. https://doi.org/https://doi.org/10.1016/B978-0-12-804644-9.00008-2

Li, S., & Bush, R. T. (2015). Rising flux of nutrients (C, N, P and Si) in the lower Mekong River. *Journal of Hydrology*, *530*, 447–461.

Li, Y., Cao, W., Su, C., & Hong, H. (2011). Nutrient sources and composition of recent algal blooms and eutrophication in the northern Jiulong River, Southeast China. *Marine Pollution Bulletin*, *63*(5–12), 249–254.

List of References

Liaw, A., & Wiener, M. (2002). Classification and regression by randomForest. *R News*, *2*(3), 18–22.

LibreTexts. (2020). *spectrophotometry*. https://chem.libretexts.org/@go/page/1431

Liddle, M. J., & Scorgie, H. R. A. (1980). The effects of recreation on freshwater plants and animals: a review. *Biological Conservation*, *17*(3), 183–206.

Liljeström, I., Kummu, M., & Varis, O. (2012). Nutrient Balance Assessment in the Mekong Basin: nitrogen and phosphorus dynamics in a catchment scale. *International Journal of Water Resources Development*, *28*(2), 373–391.

Lim, P., Lek, S., Touch, S. T., Mao, S.-O., & Chhouk, B. (1999). Diversity and spatial distribution of freshwater fish in Great Lake and Tonle Sap river (Cambodia, Southeast Asia). *Aquatic Living Resources*, *12*(6), 379–386.

Lindsey, R., & Scott, M. (2010). What are Phytoplankton? *NASA Earth Observatory*.

Lovett, G. M., Burns, D. A., Driscoll, C. T., Jenkins, J. C., Mitchell, M. J., Rustad, L., Shanley, J. B., Likens, G. E., & Haeuber, R. (2007). Who needs environmental monitoring? *Frontiers in Ecology and the Environment*, *5*(5), 253–260.

Low-Decarie, E., Fussmann, G. F., & Bell, G. (2011). The effect of elevated CO2 on growth and competition in experimental phytoplankton communities. *Global Change Biology*, *17*(8), 2525–2535.

Lu, J., Zhu, B., Struewing, I., Xu, N., & Duan, S. (2019). Nitrogen–phosphorus-associated metabolic activities during the development of a cyanobacterial bloom revealed by metatranscriptomics. *Scientific Reports*, *9*(1), 1–11.

Lu, X., Kummu, M., & Oeurng, C. (2014). Reappraisal of sediment dynamics in the Lower Mekong River, Cambodia. *Earth Surface Processes and Landforms*, *39*(14), 1855–1865.

Luis, A. J., & Kawamura, H. (2004). Air-sea interaction, coastal circulation and primary production in the eastern Arabian Sea: a review. *Journal of Oceanography*, *60*(2), 205–218.

Lukman, L., Subehi, L., Dina, R., Mayasari, N., Melati, I., Sudriani, Y., & Ardianto, D. (2019). Pollution loads and its impact on Lake Toba. *IOP Conference Series: Earth and Environmental Science*, *299*(1), 12051.

Lv, J., Wu, H., & Chen, M. (2011). Effects of nitrogen and phosphorus on phytoplankton

composition and biomass in 15 subtropical, urban shallow lakes in Wuhan, China. *Limnologica*, *41*(1), 48–56.

Ma, R., & Dai, J. (2005). Investigation of chlorophyll-a and total suspended matter concentrations using Landsat ETM and field spectral measurement in Taihu Lake, China. *International Journal of Remote Sensing*, *26*(13), 2779–2795.

Maberly, S. C., King, L., Dent, M. M., Jones, R. I., & Gibson, C. E. (2002). Nutrient limitation of phytoplankton and periphyton growth in upland lakes. *Freshwater Biology*, *47*(11), 2136–2152.

Maberly, S. C., Pitt, J.-A., Davies, P. S., & Carvalho, L. (2020). Nitrogen and phosphorus limitation and the management of small productive lakes. *Inland Waters*, *10*(2), 159–172.

Macedonio, F., Drioli, E., Gusev, A. A., Bardow, A., Semiat, R., & Kurihara, M. (2012). Efficient technologies for worldwide clean water supply. *Chemical Engineering and Processing: Process Intensification*, *51*, 2–17.

Maciel, D., Novo, E., Sander de Carvalho, L., Barbosa, C., Flores Júnior, R., & de Lucia Lobo, F. (2019). Retrieving Total and Inorganic Suspended Sediments in Amazon Floodplain Lakes: A Multisensor Approach. *Remote Sensing*, *11*(15), 1744.

Mahama, P. N. (2016). *Assessment of the utility of smartphones for water quality monitoring*. University of Twente.

Masocha, M., Dube, T., Nhiwatiwa, T., & Choruma, D. (2018). Testing utility of Landsat 8 for remote assessment of water quality in two subtropical African reservoirs with contrasting trophic states. *Geocarto International*, *33*(7), 667–680.

Mason, C. F. (2002). *Biology of freshwater pollution*. Pearson Education.

Matthews, M. W., & Bernard, S. (2013). Characterizing the absorption properties for remote sensing of three small optically-diverse South African reservoirs. *Remote Sensing*, *5*(9), 4370–4404.

May, L., Aura, C. M., Becker, V., Briddon, C. L., Carvalho, L. R., Dobel, A. J., Jamwal, P., Kamphuis, B., Marinho, M. M., & McGowan, S. (2021). Getting into hot water: Water quality in tropical lakes in relation to their utilisation. *IOP Conference Series: Earth and Environmental Science*, *789*(1), 12021.

List of References

McMeans, B. C., Kadoya, T., Pool, T. K., Holtgrieve, G. W., Lek, S., Kong, H., Winemiller, K., Elliott, V., Rooney, N., & Laffaille, P. (2019). Consumer trophic positions respond variably to seasonally fluctuating environments. *Ecology*, *100*(2), e02570.

Mekonnen, M. M., & Hoekstra, A. Y. (2018). Global anthropogenic phosphorus loads to freshwater and associated grey water footprints and water pollution levels: A high-resolution global study. *Water Resources Research*, *54*(1), 345–358.

Melzer, S. E., Chadwick, O. A., Hartshorn, A. S., Khomo, L. M., Knapp, A. K., & Kelly, E. F. (2012). Lithologic controls on biogenic silica cycling in South African savanna ecosystems. *Biogeochemistry*, *108*(1–3), 317–334.

Mertes, L. A. K., Smith, M. O., & Adams, J. B. (1993). Estimating suspended sediment concentrations in surface waters of the Amazon River wetlands from Landsat images. *Remote Sensing of Environment*, *43*(3), 281–301.

Milford, A. B., Le Mouël, C., Bodirsky, B. L., & Rolinski, S. (2019). Drivers of meat consumption. *Appetite*, *141*, 104313.

Milne, B. F., Toker, Y., Rubio, A., & Nielsen, S. B. (2015). Unraveling the intrinsic color of chlorophyll. *Angewandte Chemie International Edition*, *54*(7), 2170–2173.

Mischke, U. (2003). Cyanobacteria associations in shallow polytrophic lakes: influence of environmental factors. *Acta Oecologica*, *24*, S11–S23.

Mishra, D. R., Ogashawara, I., & Gitelson, A. A. (2017). Bio-optical Modeling and Remote Sensing of Inland Waters. In *Bio-optical Modeling and Remote Sensing of Inland Waters*.

Mishra, S., & Mishra, D. R. (2012). Normalized difference chlorophyll index: A novel model for remote estimation of chlorophyll-a concentration in turbid productive waters. *Remote Sensing of Environment*. https://doi.org/10.1016/j.rse.2011.10.016

Mizuno, T., & MORI, S. (1970). Preliminary hydrobiological survey of some Southeast Asian inland waters. *Biological Journal of the Linnean Society*, *2*(2), 77–118.

Mobley, C. D. (1999). Estimation of the remote-sensing reflectance from above-surface measurements. *Applied Optics*, *38*(36), 7442–7455.

Mobley, C. D., Stramski, D., Paul Bissett, W., & Boss, E. (2004). Optical modeling of ocean waters: Is the case 1-case 2 classification still useful? *Oceanography*, *17*(SPL. ISS. 2), 60.

Moges, M. A., Schmitter, P., Tilahun, S. A., Ayana, E. K., Ketema, A. A., Nigussie, T. E., & Steenhuis, T. S. (2017). Water quality assessment by measuring and using landsat 7 ETM+ images for the current and previous trend perspective: Lake Tana Ethiopia. *Journal of Water Resource and Protection*, *9*(12), 1564.

Mohsen, A., Elshemy, M., & Zeidan, B. (2021). Water quality monitoring of Lake Burullus (Egypt) using Landsat satellite imageries. *Environmental Science and Pollution Research*, *28*(13), 15687–15700.

Morgan, N. C. (1970). Changes in the fauna and flora of a nutrient enriched lake. *Hydrobiologia*, *35*(3), 545–553.

Mortimer, C. H. (1971). CHEMICAL EXCHANGES BETWEEN SEDIMENTS AND WATER IN THE GREAT LAKES-SPECULATIONS ON PROBABLE REGULATORY MECHANISMS 1. *Limnology and Oceanography*, *16*(2), 387–404.

Moses, W. J., Gitelson, A. A., Berdnikov, S., & Povazhnyy, V. (2009). Satellite estimation of chlorophyll-a concentration using the red and NIR bands of MERIS—The Azov sea case study. *IEEE Geoscience and Remote Sensing Letters*, *6*(4), 845–849.

Moustaka-Gouni, M., & Sommer, U. (2020). Effects of Harmful Blooms of Large-Sized and Colonial Cyanobacteria on Aquatic Food Webs. *Water*, *12*(6), 1587.

Mowe, M. A. D., Mitrovic, S. M., Lim, R. P., Furey, A., & Yeo, D. C. J. (2015). Tropical cyanobacterial blooms: a review of prevalence, problem taxa, toxins and influencing environmental factors. *Journal of Limnology*.

MRC. (2005). Overview of the Hydrology of the Mekong Basin. *Mekong River Commission, Vientiane*, *82*.

MRC. (2008). Map of the Existing, Under Construction and Planned/Proposed Hydropower Projects in the Lower Mekong Basin, September 2008. *Map Produced by the Mekong River Commission (MRC). Available Online at: Http://Www. Mrcmekong. Org/Programmes/Hydropower. Htm*.

MRC. (2010). Assessment of basin-wide development scenarios–main report. *Mekong River Commission (MRC), Vientiane, Lao PDR*.

MRC. (2011). Assessment of Basin-wide Development Scenarios. *Basin Development Plan Programme Phase 2*, *2011*(April), 1–254.

List of References

http://gradschool.ucs.louisiana.edu/sites/research.ucs.louisiana.edu/files/Mekong dams.pdf%5Cnpapers3://publication/uuid/55184911-37F6-43E4-968D-FD5DD593D5B8

MRCS/UNDP. (1998). *Natural Resources-based Development Strategy for the Tonle Sap Area*.

Mueller, J. L., Davis, C., Arnone, R., Frouin, R., Carder, K., Lee, Z. P., Steward, R. G., Hooker, S., Mobley, C. D., & McLean, S. (2000). Above-water radiance and remote sensing reflectance measurements and analysis protocols. *Ocean Optics Protocols for Satellite Ocean Color Sensor Validation Revision*, *2*, 98–107.

Muhetaer, G., Asaeda, T., Jayasanka, S. M. D. H., Baniya, M. B., Abeynayaka, H. D. L., Rashid, M. H., & Yan, H. (2020). Effects of Light Intensity and Exposure Period on the Growth and Stress Responses of Two Cyanobacteria Species: Pseudanabaena galeata and Microcystis aeruginosa. *Water*, *12*(2), 407.

Mund, J.-P. (2011). The agricultural sector in Cambodia: Trends, processes and disparities. *Pacific News*, *35*, 10–14.

Muong, S. (2006). *Implementation of effluent taxes for Cambodian industry: an assessment of pollutant levies*.

Mushtaq, F., & Nee Lala, M. G. (2017). Remote estimation of water quality parameters of Himalayan lake (Kashmir) using Landsat 8 OLI imagery. *Geocarto International*, *32*(3), 274–285.

Nakano, S., Seike, Y., Sekino, T., OKUMURA, M., KAWABATA, K., FUJINAGA, K., NAKANISHI, M., MITAMURA, O., KUMAGAI, M., & HASHITANI, H. (1996). A rapid growth of Aulacoseira granulata (Bacillariophyceae) during the typhoon season in the south basin of Lake Biwa. *Japanese Journal of Limnology (Rikusuigaku Zasshi)*, *57*(4–2), 493–500.

Nalewajko, C., & Murphy, T. P. (2001). Effects of temperature, and availability of nitrogen and phosphorus on the abundance of Anabaena and Microcystis in Lake Biwa, Japan: an experimental approach. *Limnology*, *2*(1), 45–48.

Nas, B., Ekercin, S., Karabörk, H., Berktay, A., & Mulla, D. J. (2010). An application of Landsat-5TM image data for water quality mapping in Lake Beysehir, Turkey. *Water, Air, & Soil Pollution*, *212*(1), 183–197.

NASA. (n.d.-a). *CSCZ*. Retrieved January 1, 2021, from https://oceancolor.gsfc.nasa.gov/data/czcs/

NASA. (n.d.-b). *MODIS*. Retrieved January 1, 2021, from
https://oceancolor.gsfc.nasa.gov/data/terra/

National Committee for Disaster Management. (2003). *Mapping Vulnerability To Natural Disasters in Cambodia* (Issue March).

National Committee for Disaster Management. (2008). *Strategic National Action Plan For Disaster Risk Reduction 2008 ~ 2013*.

Ndebele-Murisa, M. R., Musil, C. F., & Raitt, L. (2010). A review of phytoplankton dynamics in tropical African lakes. *South African Journal of Science*, *106*(1–2), 13–18.

Neil, C., Spyrakos, E., Hunter, P. D., & Tyler, A. N. (2019). A global approach for chlorophyll-a retrieval across optically complex inland waters based on optical water types. *Remote Sensing of Environment*, *229*, 159–178. https://doi.org/10.1016/j.rse.2019.04.027

Ngor, P. B., Grenouillet, G., Phem, S., So, N., & Lek, S. (2018). Spatial and temporal variation in fish community structure and diversity in the largest tropical flood-pulse system of South-East Asia. *Ecology of Freshwater Fish*, *27*(4), 1087–1100.

Nicolas, G., Robinson, T. P., Wint, G. R. W., Conchedda, G., Cinardi, G., & Gilbert, M. (2016). Using random forest to improve the downscaling of global livestock census data. *PLoS One*, *11*(3), e0150424.

Niinimäki, K., Peters, G., Dahlbo, H., Perry, P., Rissanen, T., & Gwilt, A. (2020). The environmental price of fast fashion. *Nature Reviews Earth & Environment*, *1*(4), 189–200.

Nizzoli, D., Welsh, D. T., & Viaroli, P. (2020). Denitrification and benthic metabolism in lowland pit lakes: The role of trophic conditions. *Science of the Total Environment*, *703*, 134804.

Novotny, V., & Olem, H. (1994). Water Quality: Prevention. *Identification, and Management Of*.

Noyola, A., Padilla-Rivera, A., Morgan-Sagastume, J. M., Güereca, L. P., & Hernández-Padilla, F. (2012). Typology of municipal wastewater treatment technologies in Latin America. *Clean–Soil, Air, Water*, *40*(9), 926–932.

O'Neil, J. M., Davis, T. W., Burford, M. A., & Gobler, C. J. (2012). The rise of harmful cyanobacteria blooms: the potential roles of eutrophication and climate change. *Harmful Algae*, *14*, 313–334.

O'Reilly, J. E., Maritorena, S., Mitchell, B. G., Siegel, D. A., Carder, K. L., Garver, S. A., Kahru, M., &

List of References

    McClain, C. (1998). Ocean color chlorophyll algorithms for SeaWiFS. *Journal of Geophysical Research: Oceans*, *103*(C11), 24937–24953.

ODC. (2016). *Drought*. Open Development Cambodia. https://opendevelopmentcambodia.net/topics/drought/

OECD. (2019). *Economic Outlook for Southeast Asia, China and India 2019: Towards Smart Urban Transportation*. https://www.oecd.org/dev/asia-pacific/saeo-2019-Cambodia.pdf

Oeurng, C., Cochrane, T. A., Arias, M. E., Shrestha, B., & Piman, T. (2016). Assessment of changes in riverine nitrate in the Sesan, Srepok and Sekong tributaries of the Lower Mekong River Basin. *Journal of Hydrology: Regional Studies*, *8*, 95–111.

Oeurng, C., Cochrane, T. A., Chung, S., Kondolf, M. G., Piman, T., & Arias, M. E. (2019). Assessing climate change impacts on river flows in the Tonle Sap Lake Basin, Cambodia. *Water (Switzerland)*, *11*(3). https://doi.org/10.3390/w11030618

Ogashawara, I., Mishra, D. R., & Gitelson, A. A. (2017). *Chapter 1 - Remote Sensing of Inland Waters: Background and Current State-of-the-Art* (D. R. Mishra, I. Ogashawara, & A. A. B. T.-B. M. and R. S. of I. W. Gitelson (eds.); pp. 1–24). Elsevier. https://doi.org/https://doi.org/10.1016/B978-0-12-804644-9.00001-X

Ohtaka, A., Watanabe, R., Im, S., Chhay, R., & Tsukawaki, S. (2010). Spatial and seasonal changes of net plankton and zoobenthos in Lake Tonle Sap, Cambodia. *Limnology*, *11*(1), 85–94.

Okumura, Y. (2005). Meteorological Characteristics of Siem Reap City, Cambodia. *Proc. First Int. Symp. on Evaluation of Mechanisms Sustaining the Biodiversity in Lake Tonle Sap, Cambodia, Phnom Penh, Cambodia, 2005*.

Olmanson, L. G., Bauer, M. E., & Brezonik, P. L. (2002). Use of Landsat imagery to develop a water quality atlas of Minnesota's 10,000 lakes. *Proceedings of FIEOS 2002, Conference/Land Satellite Information IV/ISPRS Commission I*.

Omer, N. H. (2019). Water Quality Parameters. In *Water Quality-Science, Assessments and Policy*. IntechOpen.

Onderka, M., & Pekárová, P. (2008). Retrieval of suspended particulate matter concentrations in the Danube River from Landsat ETM data. *Science of the Total Environment*, *397*(1–3), 238–243.

Orihel, D. M., Bird, D. F., Brylinsky, M., Chen, H., Donald, D. B., Huang, D. Y., Giani, A., Kinniburgh, D., Kling, H., & Kotak, B. G. (2012). High microcystin concentrations occur only at low nitrogen-to-phosphorus ratios in nutrient-rich Canadian lakes. *Canadian Journal of Fisheries and Aquatic Sciences*, *69*(9), 1457–1462.

Östlund, C., Flink, P., Strömbeck, N., Pierson, D., & Lindell, T. (2001). Mapping of the water quality of Lake Erken, Sweden, from imaging spectrometry and Landsat Thematic Mapper. *Science of the Total Environment*, *268*(1–3), 139–154.

Oyagi, H., ENDOH, S., ISHIKAWA, T., OKUMURA, Y., & TSUKAWAKI, S. (2018). Seasonal changes in water quality as affected by water level fluctuations in lake tonle sap, Cambodia. *Geographical Review of Japan Series B*, *90*(2), 53–65.

Padisák, J., Crossetti, L. O., & Naselli-Flores, L. (2009). Use and misuse in the application of the phytoplankton functional classification: a critical review with updates. *Hydrobiologia*, *621*(1), 1–19.

Paerl, H. W., Fulton, R. S., Moisander, P. H., & Dyble, J. (2001). Harmful freshwater algal blooms, with an emphasis on cyanobacteria. *TheScientificWorldJournal*, *1*.

Paerl, H. W., & Huisman, J. (2008). Blooms like it hot. *Science*, *320*(5872), 57–58.

Paerl, H. W., & Huisman, J. (2009). Climate change: a catalyst for global expansion of harmful cyanobacterial blooms. *Environmental Microbiology Reports*, *1*(1), 27–37.

Paerl, H. W., Xu, H., McCarthy, M. J., Zhu, G., Qin, B., Li, Y., & Gardner, W. S. (2011). Controlling harmful cyanobacterial blooms in a hyper-eutrophic lake (Lake Taihu, China): the need for a dual nutrient (N & P) management strategy. *Water Research*, *45*(5), 1973–1983.

Pahlevan, N., Lee, Z., Wei, J., Schaaf, C. B., Schott, J. R., & Berk, A. (2014). On-orbit radiometric characterization of OLI (Landsat-8) for applications in aquatic remote sensing. *Remote Sensing of Environment*, *154*, 272–284.

Pahlevan, N., Smith, B., Binding, C., & O'Donnell, D. M. (2017). Spectral band adjustments for remote sensing reflectance spectra in coastal/inland waters. *Optics Express*, *25*(23), 28650–28667.

Pahlevan, N., Smith, B., Schalles, J., Binding, C., Cao, Z., Ma, R., Alikas, K., Kangro, K., Gurlin, D., & Hà, N. (2020). Seamless retrievals of chlorophyll-a from Sentinel-2 (MSI) and Sentinel-3 (OLCI) in inland and coastal waters: A machine-learning approach. *Remote Sensing of*

List of References

  *Environment*, *240*, 111604.

Palacin-Lizarbe, C., Camarero, L., Hallin, S., Jones, C. M., & Catalan, J. (2020). Denitrification rates
  in lake sediments of mountains affected by high atmospheric nitrogen deposition. *Scientific*
  *Reports*, *10*(1), 1–9.

Palmer, S. C. J., Kutser, T., & Hunter, P. D. (2015). *Remote sensing of inland waters: Challenges,*
  *progress and future directions*. Elsevier.

Pannard, A., Bormans, M., & Lagadeuc, Y. (2007). Short-term variability in physical forcing in
  temperate reservoirs: effects on phytoplankton dynamics and sedimentary fluxes.
  *Freshwater Biology*, *52*(1), 12–27.

Papanikolopoulou, L. A., Smeti, E., Roelke, D. L., Dimitrakopoulos, P. G., Kokkoris, G. D., Danielidis,
  D. B., & Spatharis, S. (2018). Interplay between r-and K-strategists leads to phytoplankton
  underyielding under pulsed resource supply. *Oecologia*, *186*(3), 755–764.

Pauer, J. J., & Auer, M. T. (2000). Nitrification in the water column and sediment of a
  hypereutrophic lake and adjoining river system. *Water Research*, *34*(4), 1247–1254.

Penn, M. R., Auer, M. T., Doerr, S. M., Driscoll, C. T., Brooks, C. M., & Effler, S. W. (2000).
  Seasonality in phosphorus release rates from the sediments of a hypereutrophic lake under
  a matrix of pH and redox conditions. *Canadian Journal of Fisheries and Aquatic Sciences*,
  *57*(5), 1033–1041.

Penny, D. (2006). The Holocene history and development of the Tonle Sap, Cambodia. *Quaternary*
  *Science Reviews*, *25*(3–4), 310–322.

Penuelas, J., Poulter, B., Sardans, J., Ciais, P., Van Der Velde, M., Bopp, L., Boucher, O., Godderis,
  Y., Hinsinger, P., & Llusia, J. (2013). Human-induced nitrogen–phosphorus imbalances alter
  natural and managed ecosystems across the globe. *Nature Communications*, *4*(1), 1–10.

Petralia, F., Wang, P., Yang, J., & Tu, Z. (2015). Integrative random forest for gene regulatory
  network inference. *Bioinformatics*, *31*(12), i197–i205.

Pilotto, L., Hobson, P., Burch, M. D., Ranmuthugala, G., Attewell, R., & Weightman, W. (2004).
  Acute skin irritant effects of cyanobacteria (blue-green algae) in healthy volunteers.
  *Australian and New Zealand Journal of Public Health*, *28*(3), 220–224.

Poikāne, S., Alves, M. H., Argillier, C., Van den Berg, M., Buzzi, F., Hoehn, E., De Hoyos, C., Karottki,

I., Laplace-Treyture, C., & Solheim, A. L. (2010). Defining chlorophyll-a reference conditions in European lakes. *Environmental Management*, *45*(6), 1286–1298.

Pokhrel, Y., Burbano, M., Roush, J., Kang, H., Sridhar, V., & Hyndman, D. W. (2018). A review of the integrated effects of changing climate, land use, and dams on Mekong river hydrology. In *Water (Switzerland)* (Vol. 10, Issue 3). https://doi.org/10.3390/w10030266

Potter, J. D., McDowell, W. H., Merriam, J. L., Peterson, B. J., & Thomas, S. M. (2010). Denitrification and total nitrate uptake in streams of a tropical landscape. *Ecological Applications*, *20*(8), 2104–2115.

Qin, H., Han, C., Jin, Z., Wu, L., Deng, H., Zhu, G., & Zhong, W. (2018). Vertical distribution and community composition of anammox bacteria in sediments of a eutrophic shallow lake. *Journal of Applied Microbiology*, *125*(1), 121–132.

Queimaliños, C. P., Modenutti, B. E., & Balseiro, E. G. (1998). Phytoplankton responses to experimental enhancement of grazing pressure and nutrient recycling in a small Andean lake. *Freshwater Biology*, *40*(1), 41–49.

Quinlan, R., Filazzola, A., Mahdiyan, O., Shuvo, A., Blagrave, K., Ewins, C., Moslenko, L., Gray, D. K., O'Reilly, C. M., & Sharma, S. (2021). Relationships of total phosphorus and chlorophyll in lakes worldwide. *Limnology and Oceanography*, *66*(2), 392–404.

Räike, A., Pietiläinen, O.-P., Rekolainen, S., Kauppila, P., Pitkänen, H., Niemi, J., Raateland, A., & Vuorenmaa, J. (2003). Trends of phosphorus, nitrogen and chlorophyll a concentrations in Finnish rivers and lakes in 1975–2000. *Science of the Total Environment*, *310*(1–3), 47–59.

Rajasekaran, S., Gayathri, S., & Lee, T.-L. (2008). Support vector regression methodology for storm surge predictions. *Ocean Engineering*, *35*(16), 1578–1587.

Räsänen, T. A., Someth, P., Lauri, H., Koponen, J., Sarkkula, J., & Kummu, M. (2017). Observed river discharge changes due to hydropower operations in the Upper Mekong Basin. *Journal of Hydrology*, *545*, 28–41.

Regan, H. (2020). Asian rivers are turning black. And our colorful closets are to blame. *CNN*. https://edition.cnn.com/style/article/dyeing-pollution-fashion-intl-hnk-dst-sept/index.html

Reinhard, C. T., Planavsky, N. J., Gill, B. C., Ozaki, K., Robbins, L. J., Lyons, T. W., Fischer, W. W., Wang, C., Cole, D. B., & Konhauser, K. O. (2017). Evolution of the global phosphorus cycle. *Nature*, *541*(7637), 386–389.

List of References

Reynolds, Colin S. (1984). *The ecology of freshwater phytoplankton*. Cambridge university press.

Reynolds, Colin S. (2006). Phytoplankton. In C S Reynolds (Ed.), *The Ecology of Phytoplankton* (pp. 1–37). Cambridge University Press. https://doi.org/DOI: 10.1017/CBO9780511542145.002

Reynolds, Colin S, Huszar, V. L. M., Kruk, C., Naselli-Flores, L., & Melo, S. (2002). Towards a functional classification of the freshwater phytoplankton. *Journal of Plankton Research*, *24*(5), 417–428. https://academic.oup.com/plankt/article/24/5/417/1507791

Rijsberman, F. R. (2006). Water scarcity: fact or fiction? *Agricultural Water Management*, *80*(1–3), 5–22.

Ritchie, J. C., Cooper, C. M., & Schiebe, F. R. (1990). The relationship of MSS and TM digital data with suspended sediments, chlorophyll, and temperature in Moon Lake, Mississippi. *Remote Sensing of Environment*, *33*(2), 137–148.

Robert, E., Kergoat, L., Soumaguel, N., Merlet, S., Martinez, J.-M., Diawara, M., & Grippa, M. (2017). Analysis of suspended particulate matter and its drivers in Sahelian ponds and lakes by remote sensing (Landsat and MODIS): Gourma region, Mali. *Remote Sensing*, *9*(12), 1272.

Rockström, J., Steffen, W., Noone, K., Persson, Å., Chapin, F. S., Lambin, E. F., Lenton, T. M., Scheffer, M., Folke, C., & Schellnhuber, H. J. (2009). A safe operating space for humanity. *Nature*, *461*(7263), 472–475.

Romo, S., Soria, J., Fernandez, F., Ouahid, Y., & BARÓN-SOLÁ, Á. (2013). Water residence time and the dynamics of toxic cyanobacteria. *Freshwater Biology*, *58*(3), 513–522.

Rowland, F. E., Stow, C. A., Johengen, T. H., Burtner, A. M., Palladino, D., Gossiaux, D. C., Davis, T. W., Johnson, L. T., & Ruberg, S. (2019). Recent Patterns in Lake Erie Phosphorus and Chlorophyll a Concentrations in Response to Changing Loads. *Environmental Science & Technology*, *54*(2), 835–841.

Roy, D. P., Kovalskyy, V., Zhang, H., Vermote, E. F., Yan, L., Kumar, S. S., & Egorov, A. (2016). Characterization of Landsat-7 to Landsat-8 reflective wavelength and normalized difference vegetation index continuity. *Remote Sensing of Environment*. https://doi.org/10.1016/j.rse.2015.12.024

Ruddick, K. G., De Cauwer, V., Park, Y.-J., & Moore, G. (2006). Seaborne measurements of near infrared water-leaving reflectance: The similarity spectrum for turbid waters. *Limnology and Oceanography*, *51*(2), 1167–1179.

Rühland, K. M., Paterson, A. M., & Smol, J. P. (2015). Lake diatom responses to warming: reviewing the evidence. *Journal of Paleolimnology*, *54*(1), 1–35.

Sakamoto, M. (1966). Primary production by phytoplankton community in some Japanese lakes and its dependence on lake depth. *Arch Hydrobiol*, *62*, 1–28.

Salmivaara, A., Kummu, M., Varis, O., & Keskinen, M. (2016). Socio-economic changes in Cambodia's unique Tonle Sap lake area: A spatial approach. *Applied Spatial Analysis and Policy*, *9*(3), 413–432.

Sarkkula, J., Kiirikki, M., Koponen, J., & Kummu, M. (2003). Ecosystem processes of the Tonle Sap Lake. *Ecotone II-1 Workshop*.

Scheffer, M., Rinaldi, S., Gragnani, A., Mur, L. R., & van Nes, E. H. (1997). On the dominance of filamentous cyanobacteria in shallow, turbid lakes. *Ecology*, *78*(1), 272–282.

Schindler, D. W. (1974). Eutrophication and recovery in experimental lakes: implications for lake management. *Science*, *184*(4139), 897–899.

Schindler, D. W., Hecky, R. E., Findlay, D. L., Stainton, M. P., Parker, B. R., Paterson, M. J., Beaty, K. G., Lyng, M., & Kasian, S. E. M. (2008). Eutrophication of lakes cannot be controlled by reducing nitrogen input: results of a 37-year whole-ecosystem experiment. *Proceedings of the National Academy of Sciences*, *105*(32), 11254–11258.

Schirber, M. (2013). *The Full Palette of Photosynthesis*. NASA Goddard Institute for Space Studies. https://www.giss.nasa.gov/research/features/201311_kiang/

Schlesinger, W. H. (2005). *Biogeochemistry* (Vol. 8). Elsevier.

Schroeder, W., Oliva, P., Giglio, L., & Csiszar, I. A. (2014). The New VIIRS 375 m active fire detection data product: Algorithm description and initial assessment. *Remote Sensing of Environment*, *143*, 85–96.

Seitzinger, S., Harrison, J. A., Böhlke, J. K., Bouwman, A. F., Lowrance, R., Peterson, B., Tobias, C., & Drecht, G. Van. (2006). Denitrification across landscapes and waterscapes: a synthesis. *Ecological Applications*, *16*(6), 2064–2090.

Sellner, K. G., Lacouture, by R. V, & Parrish, C. R. (1988). Effects of increasing salinity on a cyanobacteria bloom in the Potomac River estuary. *Journal of Plankton Research*, *10*(1), 49–61.

List of References

Sen, P. K. (1968). Estimates of the regression coefficient based on Kendall's tau. *Journal of the American Statistical Association*, *63*(324), 1379–1389.

Seroja, R., Effendi, H., & Hariyadi, S. (2018). Tofu wastewater treatment using vetiver grass (Vetiveria zizanioides) and zeliac. *Applied Water Science*, *8*(1), 1–6.

Setiawan, F., Matsushita, B., Hamzah, R., Jiang, D., & Fukushima, T. (2019). Long-Term Change of the Secchi Disk Depth in Lake Maninjau, Indonesia Shown by Landsat TM and ETM+ Data. *Remote Sensing*, *11*(23), 2875.

Shapiro, J. (1984). Blue-green dominance in lakes: The role and management significance of pH and CO2. *Internationale Revue Der Gesamten Hydrobiologie Und Hydrographie*, *69*(6), 765–780.

Sharaf El Din, E. (2020). A novel approach for surface water quality modelling based on Landsat-8 tasselled cap transformation. *International Journal of Remote Sensing*, *41*(18), 7186–7201.

Sharip, Z., & Jusoh, J. (2010). Integrated lake basin management and its importance for Lake Chini and other lakes in Malaysia. *Lakes & Reservoirs: Research & Management*, *15*(1), 41–51.

Sharip, Z., Zaki, A. T. A., Shapai, M. A. H. M., Suratman, S., & Shaaban, A. J. (2014). Lakes of Malaysia: Water quality, eutrophication and management. *Lakes & Reservoirs: Research & Management*, *19*(2), 130–141.

Sharpley, A. N. (1999). Agricultural phosphorus, water quality, and poultry production: Are they compatible? *Poultry Science*, *78*(5), 660–673.

Sharpley, A. N., Chapra, S. C., Wedepohl, R., Sims, J. T., Daniel, T. C., & Reddy, K. R. (1994). Managing agricultural phosphorus for protection of surface waters: Issues and options. *Journal of Environmental Quality*, *23*(3), 437–451.

Sherman, B. S., Webster, I. T., Jones, G. J., & Oliver, R. L. (1998). Transitions between Auhcoseira and Anabaena dominance in a turbid river weir pool. *Limnology and Oceanography*, *43*(8), 1902–1915.

Shi, W. (2008). Rubber Boom in Luang Namtha. *A Transnational Perspective. GTZ RDMA*.

Siev, S., Yang, H., Sok, T., Uk, S., Song, L., Kodikara, D., Oeurng, C., Hul, S., & Yoshimura, C. (2018). Sediment dynamics in a large shallow lake characterized by seasonal flood pulse in Southeast Asia. *Science of the Total Environment*.

https://doi.org/10.1016/j.scitotenv.2018.03.066

Smith, V. H. (1983). Low nitrogen to phosphorus ratios favor dominance by blue-green algae in lake phytoplankton. *Science*, *221*(4611), 669–671.

Smith, V. H., & Bennett, S. J. (1999). Nitrogen: phosphorus supply ratios and phytoplankton community structure in lakes. *Archiv Für Hydrobiologie*, 37–53.

Smith, V. H., Joye, S. B., & Howarth, R. W. (2006). Eutrophication of freshwater and marine ecosystems. *Limnology and Oceanography*, *51*(1part2), 351–355.

Smith, V. H., Sieber-Denlinger, J., deNoyelles Jr, F., Campbell, S., Pan, S., Randtke, S. J., Blain, G. T., & Strasser, V. A. (2002). Managing taste and odor problems in a eutrophic drinking water reservoir. *Lake and Reservoir Management*, *18*(4), 319–323.

Soares, M. C. S., Rocha, M. I. de A., Marinho, M. M., Azevedo, S. M. F. O., Branco, C. W. C., & Huszar, V. L. M. (2009). Changes in species composition during annual cyanobacterial dominance in a tropical reservoir: physical factors, nutrients and grazing effects. *Aquatic Microbial Ecology*, *57*(2), 137–149.

Sokhem, P., & Sunada, K. (2006). The governance of the Tonle Sap Lake, Cambodia: integration of local, national and international levels. *International Journal of Water Resources Development*, *22*(3), 399–416.

Solomon, C. T., Hotchkiss, E. R., Moslemi, J. M., Ulseth, A. J., Stanley, E. H., Hall Jr, R. O., & Flecker, A. S. (2009). Sediment size and nutrients regulate denitrification in a tropical stream. *Journal of the North American Benthological Society*, *28*(2), 480–490.

Søndergaard, M. (2007). *Nutrient Dynamics in Lakes:-with Emphasis on Phosphorus Sediment and Lake Restoration*. NERI.

Søndergaard, M., Jensen, J. P., & Jeppesen, E. (2003). Role of sediment and internal loading of phosphorus in shallow lakes. *Hydrobiologia*, *506*(1–3), 135–145.

Søndergaard, M., Jensen, P. J., & Jeppesen, E. (2001). Retention and internal loading of phosphorus in shallow, eutrophic lakes. *TheScientificWorldJOURNAL*, *1*, 427–442.

Søndergaard, M., Jeppesen, E., Lauridsen, T. L., Skov, C., Van Nes, E. H., Roijackers, R., Lammens, E., & Portielje, R. O. B. (2007). Lake restoration: successes, failures and long-term effects. *Journal of Applied Ecology*, *44*(6), 1095–1105.

List of References

Song, K., Wang, Z., Blackwell, J., Zhang, B., Li, F., Zhang, Y., & Jiang, G. (2011). Water quality monitoring using Landsat Themate Mapper data with empirical algorithms in Chagan Lake, China. *Journal of Applied Remote Sensing*, *5*(1), 53506.

Soum, S., Ngor, P. B., Dilts, T. E., Lohani, S., Kelson, S., Null, S. E., Tromboni, F., Hogan, Z. S., Chan, B., & Chandra, S. (2021). Spatial and Long-Term Temporal Changes in Water Quality Dynamics of the Tonle Sap Ecosystem. *Water*, *13*(15), 2059.

Srean, P., Eang, B., Rien, R., & Martin, R. J. (2018). Paddy rice farming practices and profitability in northwest Cambodia. *Asian Journal of Agricultural and Environmental Safety*, *1*, 1–5.

Steffen, W., Richardson, K., Rockström, J., Cornell, S. E., Fetzer, I., Bennett, E. M., Biggs, R., Carpenter, S. R., De Vries, W., & De Wit, C. A. (2015). Planetary boundaries: Guiding human development on a changing planet. *Science*, *347*(6223).

Struyf, E., & Conley, D. J. (2009). Silica: an essential nutrient in wetland biogeochemistry. *Frontiers in Ecology and the Environment*, *7*(2), 88–94.

Sudheer, K. P., Chaubey, I., & Garg, V. (2006). Lake water quality assessment from landsat thematic mapper data using neural network: an approach to optimal band combination selection1. *JAWRA Journal of the American Water Resources Association*, *42*(6), 1683–1695.

Svab, E., Tyler, A. N., Preston, T., Presing, M., & Balogh, K. V. (2005). Characterizing the spectral reflectance of algae in lake waters with high suspended sediment concentrations. *International Journal of Remote Sensing*, *26*(5), 919–928.

Syandri, H., Azrita, A., & Mardiah, A. (2020). Water quality status and pollution waste load from floating net cages at Maninjau Lake, West Sumatera Indonesia. *IOP Conference Series: Earth and Environmental Science*, *430*(1), 12031.

Tallberg, P. (2000). *Silicon and its impacts on phosphorus in eutrophic freshwater lakes*.

Tao, H., Song, K., Liu, G., Wen, Z., Wang, Q., Du, Y., Lyu, L., Du, J., & Shang, Y. (2021). Songhua River basin's improving water quality since 2005 based on Landsat observation of water clarity. *Environmental Research*, *199*, 111299.

Tebbs, E. J., Remedios, J. J., & Harper, D. M. (2013). Remote sensing of chlorophyll-a as a measure of cyanobacterial biomass in Lake Bogoria, a hypertrophic, saline–alkaline, flamingo lake, using Landsat ETM+. *Remote Sensing of Environment*, *135*, 92–106.

Teubner, K., & Dokulil, M. T. (2002). Ecological stoichiometry of TN: TP: SRSi in freshwaters: nutrient ratios and seasonal shifts in phytoplankton assemblages. *Archiv Fur Hydrobiologie*, *154*(4), 625–646.

Teubner, K., Kabas, W., & Teubner, I. E. (2018). Phytoplankton in Alte Donau: response to trophic change from hypertrophic to mesotrophic over 22 years. In *The Alte Donau: Successful Restoration and Sustainable Management* (pp. 107–147). Springer.

Thamdrup, B., & Dalsgaard, T. (2002). Production of N2 through anaerobic ammonium oxidation coupled to nitrate reduction in marine sediments. *Applied and Environmental Microbiology*, *68*(3), 1312–1318.

Theng, V., Khiev, P., & Phon, D. (2014). *Development of the fertiliser industry in Cambodia: Structure of the market, challenges in the demand and supply sides, and the way forward*. Cambodia Development Research Institute.

Thompson, L. R., Sanders, J. G., McDonald, D., Amir, A., Ladau, J., Locey, K. J., Prill, R. J., Tripathi, A., Gibbons, S. M., & Ackermann, G. (2017). A communal catalogue reveals Earth's multiscale microbial diversity. *Nature*, *551*(7681), 457.

Torbick, N., Hession, S., Hagen, S., Wiangwang, N., Becker, B., & Qi, J. (2013). Mapping inland lake water quality across the Lower Peninsula of Michigan using Landsat TM imagery. *International Journal of Remote Sensing*, *34*(21), 7607–7624.

Toth, J. D., Dou, Z., Ferguson, J. D., Galligan, D. T., & Ramberg Jr, C. F. (2006). Nitrogen-vs. phosphorus-based dairy manure applications to field crops: Nitrate and phosphorus leaching and soil phosphorus accumulation. *Journal of Environmental Quality*, *35*(6), 2302–2312.

Tromas, N., Fortin, N., Bedrani, L., Terrat, Y., Cardoso, P., Bird, D., Greer, C. W., & Shapiro, B. J. (2017). Characterising and predicting cyanobacterial blooms in an 8-year amplicon sequencing time course. *The ISME Journal*, *11*(8), 1746–1763.

Tsiola, A., Pitta, P., Fodelianakis, S., Pete, R., Magiopoulos, I., Mara, P., Psarra, S., Tanaka, T., & Mostajir, B. (2016). Nutrient limitation in surface waters of the oligotrophic Eastern Mediterranean Sea: an Enrichment Microcosm Experiment. *Microbial Ecology*, *71*(3), 575–588.

Tu, M.-C., Smith, P., & Filippi, A. M. (2018). Hybrid forward-selection method-based water-quality estimation via combining Landsat TM, ETM+, and OLI/TIRS images and ancillary environmental data. *Plos One*, *13*(7), e0201255.

List of References

Tudesque, L., Pool, T. K., & Chevalier, M. (2019). Planktonic diatom community dynamics in a
    tropical flood-pulse lake: the Tonle Sap (Cambodia). *Diatom Research*, *34*(1), 1–22.

Uitz, J., Claustre, H., Morel, A., & Hooker, S. B. (2006). Vertical distribution of phytoplankton
    communities in open ocean: An assessment based on surface chlorophyll. *Journal of
    Geophysical Research: Oceans*, *111*(C8).

UN Water. (2017). *The United Nations World Water Development Report 2017: Wastewater The
    Untapped Resource*. UNESCO publishing.

UN Water. (2018). *The United Nations World Water Development Report 2018: Nature-Based
    Solutions for Water*. UNESCO publishing.

UN Water. (2020a). *The United Nations World Water Development Report 2020: Water and
    Climate Change*. UNESCO publishing.

UN Water. (2020b). *UN-Water input on Freshwater-Biodiversity Linkages: Response to the Zero-
    Draft Document from the Open-Ended Working Group on the Post-2020 Global Biodiversity
    Framework*.

UNDP. (2019). *Cambodia , Looking to the Horizon , Prepares for Drought*.
    https://www.adaptation-undp.org/cambodia-looking-horizon-prepares-drought

Ung, P., Peng, C., Yuk, S., Tan, R., Ann, V., Miyanaga, K., & Tanji, Y. (2019). Dynamics of bacterial
    community in Tonle Sap Lake, a large tropical flood-pulse system in Southeast Asia. *Science
    of the Total Environment*, *664*. https://doi.org/10.1016/j.scitotenv.2019.01.351

Urbanski, J. A., Wochna, A., Bubak, I., Grzybowski, W., Lukawska-Matuszewska, K., Łącka, M.,
    Śliwińska, S., Wojtasiewicz, B., & Zajączkowski, M. (2016). Application of Landsat 8 imagery
    to regional-scale assessment of lake water quality. *International Journal of Applied Earth
    Observation and Geoinformation*, *51*, 28–36.

USEPA. (2016). *National Lakes Assessment 2012: A Collaborative Survey of Lakes in the United
    States. EPA 841-R-16-113.* https://www.epa.gov/sites/production/files/2016-
    12/documents/nla_report_dec_2016.pdf

USEPA, U. S. E. P. A. (USEPA). (2001). *Nutrient Criteria Technical Guidance Manual Estuarine
    Coastal and Marine Waters, EPA-822-B-01-003*.

Üstün, B., Melssen, W. J., & Buydens, L. M. C. (2007). Visualisation and interpretation of support

vector regression models. *Analytica Chimica Acta*, *595*(1–2), 299–309.

Uwizeye, A., de Boer, I. J. M., Opio, C. I., Schulte, R. P. O., Falcucci, A., Tempio, G., Teillard, F., Casu, F., Rulli, M., & Galloway, J. N. (2020). Nitrogen emissions along global livestock supply chains. *Nature Food*, *1*(7), 437–446.

Vaccari, D. A. (2009). Phosphorus: a looming crisis. *Scientific American*, *300*(6), 54–59.

Van der Molen, D. T., Portielje, R., De Nobel, W. T., & Boers, P. C. M. (1998). Nitrogen in Dutch freshwater lakes: trends and targets. *Environmental Pollution*, *102*(1), 553–557.

Van Faassen, H. G., & Van Dijk, H. (1987). Manure as a source of nitrogen and phosphorus in soils. In *Animal Manure on Grassland and Fodder Crops. Fertilizer or Waste?* (pp. 27–45). Springer.

Vandevenne, F., Struyf, E., Clymans, W., & Meire, P. (2012). Agricultural silica harvest: have humans created a new loop in the global silica cycle? *Frontiers in Ecology and the Environment*, *10*(5), 243–248.

Vanni, M. J. (2002). Nutrient cycling by animals in freshwater ecosystems. *Annual Review of Ecology and Systematics*, *33*(1), 341–370.

Varis, O., Kummu, M., Keskinen, M., Sarkkula, J., Koponen, J., Heinonen, U., & Makkonen, K. (2006). Tonle Sap Lake, Cambodia: Nature's affluence meets human poverty. *Case Study For*, 1–8.

Västilä, K., Kummu, M., Sangmanee, C., & Chinvanno, S. (2010). Modelling climate change impacts on the flood pulse in the Lower Mekong floodplains. *Journal of Water and Climate Change*, *1*(1), 67–86.

Venugopal, V., Prasanna, R., Sood, A., Jaiswal, P., & Kaushik, B. D. (2006). Stimulation of pigment accumulation inAnabaena azollae strains: Effect of light intensity and sugars. *Folia Microbiologica*, *51*(1), 50–56.

Vermote, E., Justice, C., Claverie, M., & Franch, B. (2016). Preliminary analysis of the performance of the Landsat 8/OLI land surface reflectance product. *Remote Sensing of Environment*, *185*, 46–56. https://doi.org/10.1016/j.rse.2016.04.008

Vis, C., Cattaneo, A., & Hudon, C. (2008). Shift from chlorophytes to cyanobacteria in benthic macroalgae along a gradient of nitrate depletion 1. *Journal of Phycology*, *44*(1), 38–44.

Vitousek, P. M., Aber, J. D., Howarth, R. W., Likens, G. E., Matson, P. A., Schindler, D. W.,

List of References

Schlesinger, W. H., & Tilman, D. G. (1997). Human alteration of the global nitrogen cycle: sources and consequences. *Ecological Applications*, *7*(3), 737–750.

Vogelmann, J. E., Helder, D., Morfitt, R., Choate, M. J., Merchant, J. W., & Bulley, H. (2001). Effects of Landsat 5 Thematic Mapper and Landsat 7 Enhanced Thematic Mapper Plus radiometric and geometric calibrations and corrections on landscape characterization. *Remote Sensing of Environment*, *78*(1–2), 55–70.

Vollenweider, R. A., & Kerekes, J. (1982). *Eutrophication of waters: monitoring, assessment and control*. Organisation for Economic Co-operation and Development;[Washington, DC: Sold ….

von Sperling, M., & de Lemos Chernicharo, C. A. (2002). Urban wastewater treatment technologies and the implementation of discharge standards in developing countries. *Urban Water*, *4*(1), 105–114.

Vuorio, K., Järvinen, M., & Kotamäki, N. (2019). Phosphorus thresholds for bloom-forming cyanobacterial taxa in boreal lakes. *Hydrobiologia*, 1–12.

Wagner, S. C. (2011). *Biological Nitrogen Fixation*. Nature Education Knowledge. https://www.nature.com/scitable/knowledge/library/biological-nitrogen-fixation-23570419/

Wang, B., Xin, M., Wei, Q., & Xie, L. (2018). A historical overview of coastal eutrophication in the China Seas. *Marine Pollution Bulletin*, *136*, 394–400.

Wang, F., Han, L., Kung, H., & Van Arsdale, R. B. (2006). Applications of Landsat-5 TM imagery in assessing and mapping water quality in Reelfoot Lake, Tennessee. *International Journal of Remote Sensing*, *27*(23), 5269–5283.

Wang, H., Zhao, D., Chen, L., Giesy, J. P., Zhang, W., Yuan, C., Ni, L., Shen, H., & Xie, P. (2020). Light, but not nutrients, drives seasonal congruence of taxonomic and functional diversity of phytoplankton in a eutrophic highland lake in China. *Frontiers in Plant Science*, *11*, 179.

Wang, J., Lu, X. X., Liew, S. C., & Zhou, Y. (2009). Retrieval of suspended sediment concentrations in large turbid rivers using Landsat ETM+: an example from the Yangtze River, China. *Earth Surface Processes and Landforms*, *34*(8), 1082–1092.

Wang, L., Zhou, X., Zhu, X., Dong, Z., & Guo, W. (2016). Estimation of biomass in wheat using random forest regression algorithm and remote sensing data. *The Crop Journal*, *4*(3), 212–219. https://doi.org/10.1016/j.cj.2016.01.008

Wang, Q., & Yang, Z. (2016). Industrial water pollution, water environment treatment, and health risks in China. *Environmental Pollution*, *218*, 358–365.

Wang, R., Dearing, J. A., Langdon, P. G., Zhang, E., Yang, X., Dakos, V., & Scheffer, M. (2012). Flickering gives early warning signals of a critical transition to a eutrophic lake state. *Nature*, *492*(7429), 419–422.

Wang, X., Daigger, G., de Vries, W., Kroeze, C., Yang, M., Ren, N.-Q., Liu, J., & Butler, D. (2019). Impact hotspots of reduced nutrient discharge shift across the globe with population and dietary changes. *Nature Communications*, *10*(1), 1–12.

Wang, Y., Liu, D., Xiao, W., Zhou, P., Tian, C., Zhang, C., Du, J., Guo, H., & Wang, B. (2021). Coastal eutrophication in China: Trend, sources, and ecological effects. *Harmful Algae*, 102058.

Wang, Z., Lai, C., Chen, X., Yang, B., Zhao, S., & Bai, X. (2015). Flood hazard risk assessment model based on random forest. *Journal of Hydrology*. https://doi.org/10.1016/j.jhydrol.2015.06.008

Ward, B. B., Devol, A. H., Rich, J. J., Chang, B. X., Bulow, S. E., Naik, H., Pratihary, A., & Jayakumar, A. (2009). Denitrification as the dominant nitrogen loss process in the Arabian Sea. *Nature*, *461*(7260), 78–81.

Water, U. N. (2016). *Towards a Worldwide Assessmentof Freshwater Quality A UN-Water Analytical Brief*.

Waxter, M. T. (2014). *Analysis of Landsat satellite data to monitor water quality parameters in Tenmile Lake, Oregon*.

Wei, J., Lee, Z., Garcia, R., Zoffoli, L., Armstrong, R. A., Shang, Z., Sheldon, P., & Chen, R. F. (2018). An assessment of Landsat-8 atmospheric correction schemes and remote sensing reflectance products in coral reefs and coastal turbid waters. *Remote Sensing of Environment*, *215*. https://doi.org/10.1016/j.rse.2018.05.033

Welch, E. B., & Cooke, G. D. (2005). Internal phosphorus loading in shallow lakes: importance and control. *Lake and Reservoir Management*, *21*(2), 209–217.

Wetzel, R. G. (2001). *Limnology: lake and river ecosystems*. gulf professional publishing.

Whitehead, P. G., Jin, L., Bussi, G., Voepel, H. E., Darby, S. E., Vasilopoulos, G., Manley, R., Rodda, H., Hutton, C., & Hackney, C. (2019). Water quality modelling of the Mekong River basin:

List of References

Climate change and socioeconomics drive flow and nutrient flux changes to the Mekong Delta. *Science of the Total Environment*, *673*, 218–229.

Whitnall, T., & Pitts, N. (2019). Global trends in meat consumption. *Agricultural Commodities*, *9*(1), 96.

WHO. (2003). *Guidelines for safe recreational water environments: Coastal and fresh waters* (Vol. 1). World Health Organization.

WHO. (2004). *Guideline for Drinking-water Quality*.

Wijaya, I. M. W., & Soedjono, E. S. (2018). Domestic wastewater in Indonesia: Challenge in the future related to nitrogen content. *International Journal*, *15*(47), 32–41.

Willett, V. B., Reynolds, B. A., Stevens, P. A., Ormerod, S. J., & Jones, D. L. (2004). Dissolved organic nitrogen regulation in freshwaters. *Journal of Environmental Quality*, *33*(1), 201–209.

Wilson, A. E., Sarnelle, O., & Tillmanns, A. R. (2006). Effects of cyanobacterial toxicity and morphology on the population growth of freshwater zooplankton: Meta-analyses of laboratory experiments. *Limnology and Oceanography*, *51*(4), 1915–1924.

Winder, M., & Schindler, D. E. (2004). Climatic effects on the phenology of lake processes. *Global Change Biology*, *10*(11), 1844–1856.

Winder, M., & Sommer, U. (2012). Phytoplankton response to a changing climate. *Hydrobiologia*, *698*(1), 5–16.

Woese, C. R., Kandler, O., & Wheelis, M. L. (1990). Towards a natural system of organisms: proposal for the domains Archaea, Bacteria, and Eucarya. *Proceedings of the National Academy of Sciences*, *87*(12), 4576–4579.

World Bank. (2008). Economic Impacts of Sanitation in Southeast Asia: A four-country study conducted in Cambodia, Indonesia, the Philippines and Vietnam under the Economics of Sanitation Initiative (ESI). In *Water and Sanitation Program research report*.

Worsfold, P. J., Monbet, P., Tappin, A. D., Fitzsimons, M. F., Stiles, D. A., & McKelvie, I. D. (2008). Characterisation and quantification of organic phosphorus and organic nitrogen components in aquatic systems: a review. *Analytica Chimica Acta*, *624*(1), 37–58.

Wulder, M. A., Loveland, T. R., Roy, D. P., Crawford, C. J., Masek, J. G., Woodcock, C. E., Allen, R. G., Anderson, M. C., Belward, A. S., & Cohen, W. B. (2019). Current status of Landsat

program, science, and applications. *Remote Sensing of Environment*, *225*, 127–147.

Xia, X., Yang, Z., & Zhang, X. (2009). Effect of suspended-sediment concentration on nitrification in river water: importance of suspended sediment– water interface. *Environmental Science & Technology*, *43*(10), 3681–3687.

Yepez, S., Laraque, A., Martinez, J. M., De Sa, J., Carrera, J. M., Castellanos, B., Gallay, M., & Lopez, J. L. (2017). Retrieval of suspended sediment concentrations using Landsat-8 OLI satellite images in the Orinoco River (Venezuela). *Comptes Rendus - Geoscience*. https://doi.org/10.1016/j.crte.2017.08.004

Yoshikawa, T., Takagi, A. P., Ishikawa, S., Hori, M., Nakano, T., Shin, K.-C., Sitha, H., Cheasan, E., & Limsong, S. (2020). Major and trace elements in the surface water of Tonle Sap Lake, Mekong River, and other tributary rivers in Cambodia. *Environmental Monitoring and Assessment*, *192*(7), 1–17.

Yoshinaga, I., Amano, T., Yamagishi, T., Okada, K., Ueda, S., Sako, Y., & Suwa, Y. (2009). Distribution and diversity of anaerobic ammonium oxidation (anammox) bacteria in the sediment of a eutrophic freshwater lake, Lake Kitaura, Japan. *Microbes and Environments*, 1105060298.

You, J., Mallery, K., Hong, J., & Hondzo, M. (2018). Temperature effects on growth and buoyancy of Microcystis aeruginosa. *Journal of Plankton Research*, *40*(1), 16–28.

Yu, B., & Diao, X. (2011). Cambodia's agricultural strategy: Future development options for the rice sector. *Cambodia Development Resource Institute (CDRI), Council for Agricultural and Rural Development (CARD), and IFPRI Special Report. Phnom Penh, Cambodia: CDRI*, *1284*(1283), 1282.

Yuan, L. L., & Jones, J. R. (2020). Rethinking phosphorus–chlorophyll relationships in lakes. *Limnology and Oceanography*, *65*(8), 1847–1857.

Zhang, F., Li, J., Shen, Q., Zhang, B., Tian, L., Ye, H., Wang, S., & Lu, Z. (2019). A soft-classification-based chlorophyll-a estimation method using MERIS data in the highly turbid and eutrophic Taihu Lake. *International Journal of Applied Earth Observation and Geoinformation*, *74*, 138–149.

Zhang, You, Cheng, L., Li, K., Zhang, L., Cai, Y., Wang, X., & Heino, J. (2019). Nutrient enrichment homogenizes taxonomic and functional diversity of benthic macroinvertebrate assemblages in shallow lakes. *Limnology and Oceanography*, *64*(3), 1047–1058.

List of References

Zhang, Yuanzhi, Pulliainen, J., Koponen, S., & Hallikainen, M. (2003). Water quality retrievals from combined Landsat TM data and ERS-2 SAR data in the Gulf of Finland. *IEEE Transactions on Geoscience and Remote Sensing*, *41*(3), 622–629.

Zhao, J., Ramin, M., Cheng, V., & Arhonditsis, G. B. (2008). Competition patterns among phytoplankton functional groups: How useful are the complex mathematical models? *Acta Oecologica*, *33*(3), 324–344.

Zheng, Y., Han, F., Tian, Y., Wu, B., & Lin, Z. (2014). Addressing the uncertainty in modeling watershed nonpoint source pollution. In *Developments in Environmental Modelling* (Vol. 26, pp. 113–159). Elsevier.

Zhu, L., Shi, W., Zhou, J., Yu, J., Kong, L., & Qin, B. (2021). Strong turbulence accelerates sediment nitrification-denitrification for nitrogen loss in shallow lakes. *Science of The Total Environment*, *761*, 143210.

Zhu, M., Paerl, H. W., Zhu, G., Wu, T., Li, W., Shi, K., Zhao, L., Zhang, Y., Qin, B., & Caruso, A. M. (2014). The role of tropical cyclones in stimulating cyanobacterial (Microcystis spp.) blooms in hypertrophic Lake Taihu, China. *Harmful Algae*, *39*, 310–321.

# Appendix A    Interpolation of Water Level Data at Kampong Luong Gauging Station

Throughout this thesis, water levels from the Kampong Luong gauging station is used. However, this station has missing data in the periods from January 1990 to June 1996, August to December 1997, January to July 1998, December 1998 and January to April 2009.

In this study, to create patches for the missing water level data, a linear regression between all the available water level data at Kampong Luong and the closest gauging station on the Mekong River (at Phnom Penh port) was calculated (Figure B-1). This regression equation was used to estimate the missing data for Kampong Luong based on the continuous water level data records at Phnom Penh Port. Figure B-2 shows the original and interpolated water level data.
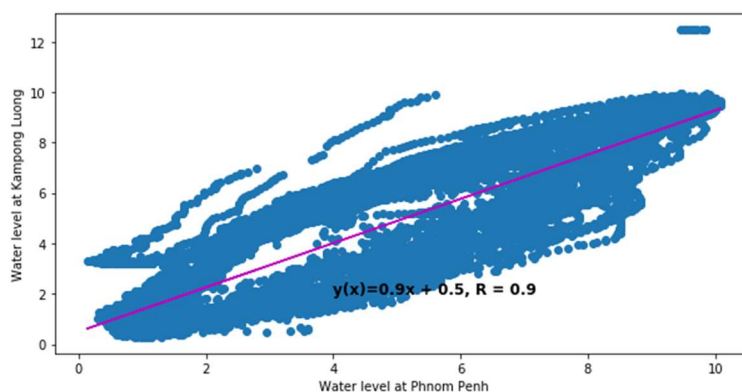


Figure B-1 Water levels as measured at Kampong Luong gauging station and Phnom Penh Port gauging station, and the associated linear regression equation linking the data
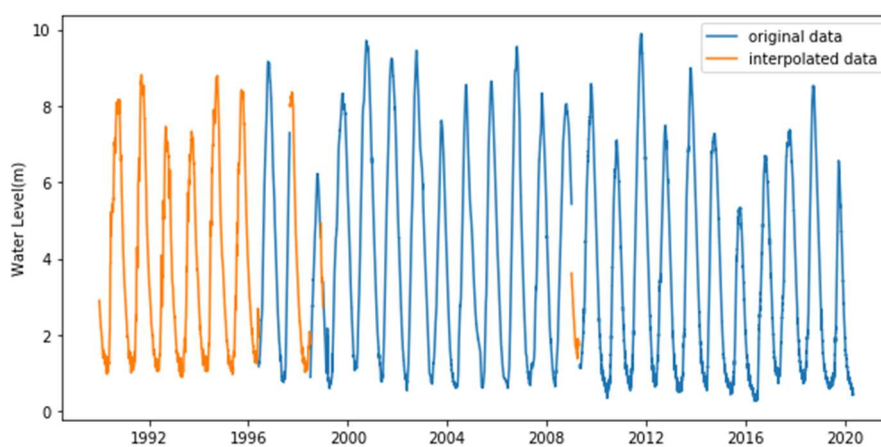


Figure B-2 Water levels at Kampong Luong, based on original (blue line) and interpolated (orange line) data

## Appendix B    Tonle Sap Lake's Phytoplankton Species

| Study | Wet Season | Dry Season |
|---|---|---|
| J Blache, 1951; (in Campbell et al., 2006 and Ohtaka et al., 2010) | Dominated by *Aulacoseira granulata* (diatom) followed by cyanobacteriaand green algae. | Cyanobacteria (consisting of *Anabaena*, *Lyngbia* and *Microcystis)* exceeded diatom |
| Mizuno & MORI, 1970 (in Ohtaka et al., 2010) | Information not available | *Microcystis flos-aquae* abundantly occurred in the south and north basins, making an algal scum (other cyanobacteria, such as *Oscillatoria* and *Anabaena*, and a diatom, *Aulacoseira granulata* subdominantly occurred. |
| (Sarkkula et al., 2003) | diatom i.e. *Aulocoseira* | *Anabaena* |
| (I. C. Campbell et al., 2006) | Green algae (61%), cyanobacteria (35%), diatom (4%) | |
| (Ohtaka et al., 2010) | In the open water of North basin, diatoms, especially *Aulacoseira granulata*, and cyanobacteria *Anabaena spp* in the open water.  In the South basin, diatoms (mostly *Aulacoseira granulata*) and  cyanobacteria (*Anabaena* and *Microcystis*) | Cyanobacteria, composed of mostly *Microcystis* with a small part of Anabaena, surpassed other algae in all the stations except for open-water of North basin where the diatom Aulacoseira granulata dominated. |

List of References

| Study | Wet Season | Dry Season |
|---|---|---|
| Tudesque et al., 2019 (study on diatom only) | 60% of the abundance is Aulacoseira Thawaites, fairly stable over time. | |
| Figure 6 in Ung et al., 2019 (study on bacteria only) | In North basin, cyanobacteria concentrations in the lake water increased in the dry season and reached a peak in the transition from dry to rainy season.<br><br>In the south basin, cyanobacteria concentrations in the lake water increased in the dry season then decreased in the transition from dry to rainy season before increased again in the rainy season. | |

# Appendix C    **Estimation of Water Residence Time of Tonle Sap Lake**

Water residence time of Tonle Sap Lake is estimated from the water level data, which is measured at Kampong Luong by the Mekong River Commission. Water residence time for one particular day $WRT_{day\_x}$ is calculated by dividing the volume of the lake for that day $V_{day\_x}$ with the water flow rate for that day $F_{day\_x}$:

$$WRT_{day\_x}[day] = \frac{V_{day\_x}}{F_{day\_x}}$$

The volume of the lake for one particular day is calculated with estimation used by M Kummu et al. (2014), which is:

$$V_{day\_x}[km^3] = 0.7307 * wl_{day_x}^2 - 0.3554 * wl_{day\_x} + 0.9127$$

Here, $wl$ is water level. The flow rate for one particular day is acquired by taking the difference between the volume of the lake on that day and the volume of the lake on the next day:

$$F_{day\_x}\left[\frac{km^3}{day}\right] = |V_{day_{x+1}} - V_{da\ x}|$$

The table below shows the average water residence time of Tonle Sap Lake in the drought, flood, and normal year, during the late outflow, low water, inflow and early outflow period.

| Year Type | Water Residence Time (days) | | | |
|---|---|---|---|---|
| | Late Outflow | Low Water | Inflow | Early Outflow |
| Drought Year | 53 | 107 | 59 | 88 |
| Flood Year | 47 | 59 | 65 | 102 |
| Normal Year | 47 | 55 | 74 | 103 |

# Appendix D   TSS Concentrations Measured from the

# Field Campaign

| Date/Time | Latitude (deg N) | Longitude (deg E) | TSS Concentrations (mg/L) |
|---|---|---|---|
| 3-Feb-2019 10:51 | 13.065 | 104.063 | 33.58209 |
| 3-Feb-2019 11:07 | 13.060 | 104.044 | 51.02041 |
| 3-Feb-2019 11:27 | 13.051 | 104.025 | 57.16667 |
| 3-Feb-2019 11:49 | 13.039 | 104.001 | 58.10345 |
| 3-Feb-2019 12:07 | 13.032 | 103.981 | 43.58209 |
| 3-Feb-2019 12:34 | 13.018 | 103.945 | 42.34375 |
| 3-Feb-2019 12:53 | 13.009 | 103.925 | 29.11392 |
| 3-Feb-2019 13:06 | 12.994 | 103.932 | 26.02273 |
| 3-Feb-2019 13:18 | 12.983 | 103.943 | 25.81081 |
| 3-Feb-2019 14:02 | 13.010 | 103.985 | 40.31746 |
| 3-Feb-2019 14:12 | 13.021 | 104.008 | 50.72464 |
| 3-Feb-2019 14:36 | 13.034 | 104.030 | 45.29412 |
| 3-Feb-2019 14:54 | 13.049 | 104.056 | 33.83562 |
| 3-Feb-2019 15:07 | 13.058 | 104.071 | 31.23457 |
| 3-Feb-2019 15:23 | 13.073 | 104.084 | 20.69767 |
| 4-Feb-2019 10:46 | 13.077 | 104.105 | 314.2647 |
| 4-Feb-2019 11:16 | 13.056 | 104.075 | 45.15152 |
| 4-Feb-2019 11:31 | 13.046 | 104.061 | 44.92537 |
| 4-Feb-2019 11:45 | 13.034 | 104.048 | 44.375 |
| 4-Feb-2019 12:06 | 13.024 | 104.035 | 47.33333 |
| 4-Feb-2019 12:23 | 12.998 | 104.032 | 50 |
| 4-Feb-2019 12:43 | 13.008 | 104.023 | 52.22222 |
| 4-Feb-2019 12:58 | 12.997 | 104.031 | 51.93548 |
| 4-Feb-2019 13:45 | 13.000 | 104.063 | 20.77778 |
| 4-Feb-2019 14:10 | 13.018 | 104.068 | 18.47059 |
| 4-Feb-2019 14:17 | 13.034 | 104.074 | 23.875 |
| 4-Feb-2019 14:28 | 13.046 | 104.073 | 25.625 |
| 9-Feb-2019 08:16:13 | 13.228 | 103.724 | 205.8824 |
| 9-Feb-2019 08:32:30 | 13.229 | 103.808 | 137.963 |
| 9-Feb-2019 08:40:00 | 13.228 | 103.798 | 121.1538 |
| 9-Feb-2019 08:52:50 | 13.225 | 103.790 | 112.2222 |
| 9-Feb-2019 09:30:47 | 13.225 | 103.781 | 95.18519 |
| 9-Feb-2019 09:13:57 | 13.222 | 103.771 | 74.22222 |
| 9-Feb-2019 09:23:10 | 13.221 | 103.762 | 50.5 |
| 9-Feb-2019 09:31:20 | 13.220 | 103.753 | 31.15385 |
| 9-Feb-2019 09:43:15 | 13.218 | 103.744 | 27.79412 |
| 9-Feb-2019 09:52:51 | 13.216 | 103.735 | 22.93333 |
| 9-Feb-2019 10:01:40 | 13.214 | 103.725 | 16.73684 |
| 9-Feb-2019 10:10:33 | 13.212 | 103.717 | 14.21965 |
| 9-Feb-2019 06:19:22 | 13.211 | 103.708 | 4.891304 |
| 9-Feb-2019 10:26:50 | 13.211 | 103.701 | 7.654321 |
| 9-Feb-2019 10:36:23 | 13.219 | 103.704 | 6.746988 |

| | | | |
|---|---|---|---|
| 9-Feb-2019 10:47:48 | 13.229 | 103.707 | 3.529412 |
| 9-Feb-2019 10:59:13 | 13.238 | 103.706 | 2.9 |
| 9-Feb-2019 11:18:09 | 13.247 | 103.711 | 4.497041 |
| 9-Feb-2019 11:39:50 | 13.252 | 103.715 | 18.53333 |
| 9-Feb-2019 11:58:30 | 13.258 | 103.709 | 27.14286 |
| 11-Feb-2019 08:12:40 | 13.230 | 103.827 | 235.9223 |
| 11-Feb-2019 08:31:40 | 13.223 | 103.830 | 140.8065 |
| 11-Feb-2019 08:49:50 | 13.211 | 103.831 | 131.9565 |
| 11-Feb-2019 08:57:40 | 13.199 | 103.834 | 182.5926 |
| 11-Feb-2019 09:23:50 | 13.177 | 103.840 | 174.0909 |
| 11-Feb-2019 10:31:10 | 13.221 | 103.886 | 141.2308 |
| 11-Feb-2019 11:04:50 | 13.225 | 103.851 | 123.4783 |
| 11-Feb-2019 11:15:16 | 13.221 | 103.842 | 123.2967 |
| 11-Feb-2019 11:25:20 | 13.226 | 103.833 | 154.9091 |
| 15-Feb-2019 08:31:18 | 13.187 | 103.967 | 80.3125 |
| 15-Feb-2019 08:46:19 | 13.176 | 103.969 | 115.3731 |
| 15-Feb-2019 09:01:48 | 13.185 | 103.973 | 98.04878 |
| 15-Feb-2019 09:13:30 | 13.192 | 103.973 | 125.1923 |
| 15-Feb-2019 09:23:24 | 13.194 | 103.964 | 106.9767 |
| 15-Feb-2019 09:39:15 | 13.198 | 103.948 | 95.57377 |
| 15-Feb-2019 09:50:31 | 13.200 | 103.937 | 109.8361 |
| 15-Feb-2019 09:58:30 | 13.203 | 103.930 | 112.5 |
| 15-Feb-2019 10:10:15 | 13.205 | 103.921 | 121.6667 |
| 15-Feb-2019 10:21:42 | 13.193 | 103.919 | 141.8367 |
| 15-Feb-2019 10:32:50 | 13.188 | 103.925 | 156.1404 |
| 15-Feb-2019 10:44:45 | 13.181 | 103.932 | 130.5 |
| 15-Feb-2019 10:51:50 | 13.175 | 103.938 | 154.955 |
| 16-Feb-2019 09:12:10 | 13.164 | 103.933 | 98.88889 |
| 16-Feb-2019 09:29:50 | 13.155 | 103.922 | 113.6765 |
| 16-Feb-2019 09:43:13 | 13.150 | 103.911 | 123.7705 |
| 16-Feb-2019 09:55:10 | 13.143 | 103.903 | 126.3077 |
| 16-Feb-2019 10:10:25 | 13.136 | 103.893 | 119.1935 |
| 16-Feb-2019 10:24:36 | 13.129 | 103.882 | 109.697 |
| 16-Feb-2019 10:37:06 | 13.122 | 103.874 | 98.16667 |
| 16-Feb-2019 10:51:00 | 13.115 | 103.862 | 116.2963 |
| 16-Feb-2019 11:01:08 | 13.106 | 103.865 | 112.6667 |
| 16-Feb-2019 11:11:50 | 13.098 | 103.871 | 111.9355 |
| 16-Feb-2019 11:23:00 | 13.092 | 103.878 | 103.7778 |
| 16-Feb-2019 11:33:50 | 13.085 | 103.883 | 79.85075 |
| 16-Feb-2019 11:44:20 | 13.078 | 103.890 | 97.61905 |
| 16-Feb-2019 11:55:56 | 13.071 | 103.896 | 93.90625 |
| 16-Feb-2019 12:06:10 | 13.064 | 103.900 | 82.24 |
| 16-Feb-2019 13:20:43 | 13.188 | 103.967 | 88.73016 |

# Glossary of Terms

**aerobic**    relating to, involving, or requiring free oxygen.

**autotroph**  An organism that can produce its own food using light, water, carbon dioxide, or other chemicals. Also called primary producers.

**benthic**    Anything associated with or occurring on the bottom of a body of water.

**diagenesis** The process that describes physical and chemical changes in sediments caused by increasing temperature and pressure as they get buried in the Earth's crust

**diatom**     Photosynthesising algae, found in almost every aquatic environment including fresh and marine waters, soils (almost anywhere moist).

**diazotroph**    Bacteria and archaea that fix atmospheric nitrogen gas into a more usable form such as ammonia.

**diazotrophic**    Has the ability to fix $N_2$.

**eukaryote**    Cell or organism that possesses a clearly defined nucleus. The eukaryotic cell has a nuclear membrane that surrounds the nucleus. See prokaryotes for comparison.

**hypoxic**    $O_2$ concentration in the water is below 2 mg/L (compared with anoxic which is near zero)

**heterocyst**    Also called heterocyte, are specialized nitrogen-fixing cells formed during nitrogen starvation by some filamentous cyanobacteria

**mineralization**    A process through which organic nutrient is converted into inorganic form with the help of microbes

**prokaryotes**Organisms that consist of a single prokaryotic cell, lacks an envelope-enclosed nucleus. See eucaryotes for comparison